Quantum backflow in the presence of defects

Alexandre Hefren de Vasconcelos Junior

Doctor of Philosophy

University of York
Mathematics

August 2021

Abstract

A physical quantity that is positive in classical physics can become negative in quantum physics, but it may be bounded. Quantum inequalities are lower bounds on averages of these physical quantities. In the case of energy densities of a quantum field, it is called a quantum energy inequality. In the case of the probability current density of right-moving states, it is called the quantum backflow effect.

This thesis is concerned with various aspects of the quantum backflow effect in the presence of defects. The backflow effect states that a particle moving towards a reference point with positive momentum may have the probability of being found at the right of the reference point decreased with time. Defects represent a way of implementing generalised point interactions without necessarily having an explicit potential function to be added to the Hamiltonian of a physical system and are described by sewing conditions defined at the defect location. Starting from the Dirac δ-distribution, which can be regarded as a potential function but also as a point defect, we extend the analysis to the jump-defect, a discontinuous and purely transmitting integrable defect allowing conservation of total energy and momentum. In this thesis, we will examine how the backflow is affected in the presence of different defects giving special focus on the jump-defect, which does not have a backscattering contribution to the backflow constant and makes our analysis compatible with conservation laws. Beyond the Schrödinger equation, we will introduce and analyse backflow with defects in the Dirac equation, which takes into account the spin contribution to the probability current. The existence of bound states are shown to be relevant for the bounds on backflow, and numerical results will support that. Furthermore, we will investigate how the backflow constant in the presence of defects differs from the interaction-free situation.

Contents

List of Figures

Acknowledgments

Let me begin by expressing how I am grateful to my supervisor, Ed Corrigan, who made possible the completion of this thesis with his exceptional guidance, patience, positive feedback and limpid thoughts. I am sure I would have benefited even more from his expertise and encouragement to progress on my research if we had more face to face meetings. However, even over Zoom meetings (because of the pandemic), I had the pleasure to discuss with him not only physics and mathematics but also generalities about life, politics, British culture (including the weather in Britain) and more. During very difficult times, his support was crucial to cheer me up, and I found out that Ed is a great professor and also a great human being.

I thank Henning Bostelmann for introducing me to the quantum backflow effect, giving guidance on analytic perturbation theory and having many instructive discussions with me in his office. I wish to thank Kasia Rejzner who contributed to the improvement of my seminars in York as well for my training in the early stages of my PhD. I also would like to thank Chris Fewster and Bernard Kay for some mini-lectures given and for their time answering some of my questions either in the corridors of the Department of Mathematics, during coffee breaks or anywhere else. My gratitude to Bert Schroer, who I first met in Brazil and completely influenced the way I see mathematical physics, for suggesting a PhD in York and for inspiring me with his depth of thought.

I thank Petrus Yuri for the help with FORTRAN and members of the IT Services at York who facilitated my understanding of how to operate the York Viking cluster.

I would then like to thank my parents for their unconditional love, support and patience during all these years. To my relatives who contributed as well towards my academic achievements: Heloísa, Egídio, Luciene and Lastênia.

I thank the friends I made in York (from different parts of the world) who shared good moments together making life easier and also taught me something about their culture and views on different matters. It was an enriching and pleasant experience.

I am thankful to the people who helped me in the process of learning during all my time as a student before starting a PhD at York and going back to my A-levels. That includes (but not limited to) previous supervisors, José Helayël-Neto and Carlos Alberto, and lecturers, Jorge Herbert, José Ramos, Evaldo Curado, Josué Mendes (in memoriam). To Sousa Nunes, the best Portuguese grammar teacher I had and whose words are roughly translated here: "the supreme purpose of education is to set man free of his own ignorance. From this emancipation results a more fair and fraternal world because self knowledge yields alterity, respect and love for the others. It is the illusion of being an island that divide us and impoverish society, because that alienates mankind in face of themselves, expanding hate in the world. Only genuine education, in its noblest acceptation, unite and make us stronger". I hope that genuine education will expand its boundaries to reach more members of our society, and it is my sincere commitment to be part of that process.

Finally, I gratefully acknowledge the financial support received from the University of York with an Overseas Research Scholarship and from the Department of Mathematics with a Departmental Teaching Studentship.

Author's declaration

I declare that the work presented in this thesis, except where otherwise stated, is based on my own research carried out at the University of York and has not been submitted previously for any degree at this or any other university. Sources are acknowledged by explicit references. The thesis includes work previously published as an arXiv pre-print: 2007.07393 [1].

— 1 —

Introduction

Quantum theory certainly has different mathematical formulations, and there are significant conceptual differences between quantum mechanics and quantum field theory that go beyond a mere relativistic extension [2]. Nevertheless, quantum theory shares some basic ideas such as Heisenberg's uncertainty principle among any of its formulations or extensions. Effects related to the uncertainty principle may arise as inequalities. For example, the "quantum energy inequalities" in quantum field theory [3, 4], which are lower bound restrictions on the fluxes and energy densities of physical systems, and the quantum backflow phenomenon [5] for the probability current in quantum mechanics. A more extensive list of references to backflow will be provided in section 2.1. The general picture of a quantum inequality is the statement that a positive physical quantity in classical physics can be negative in quantum physics, but it is bounded below.

Backflow happens by the superposition of states with only positive momentum. In particular, a quantum particle moving in one dimension and described by this superposition of right-moving states has a positive expectation value of its momentum operator. However, locally, the probability flux can assume negative values. This leads to the immediate question on the existence of limitations on the magnitude and duration of negative probability fluxes. In interaction-free situations, the limitations do exist, and its temporal extent is characterized by a dimensionless constant that was first numerically calculated [6] to be $\Delta_{BM} \approx 0.038$. For that, Bracken and Melloy concentrated on the problem of a quantum mechanical particle in one dimension with a normalized state ψ and corresponding probability flux j_ψ. Then they showed that the increase in the probability $P(t)$ of finding a right-moving particle in the negative

half-line $(-\infty, 0)$, during a time interval $[0, T]$, obeys the inequality

$$P(T) - P(0) = -\int_0^T j_\psi(0,t)dt \leq \Delta_{BM}. \tag{1.1}$$

That constant was numerically calculated subsequently [7, 8] with more accuracy to be $\Delta_{BM} \approx 0.0384517$. Similarly to the quantum energy inequalities, which are limitations on the magnitude and duration of negative energy densities (obtained from expectation values of a stress-energy tensor), the backflow inequality can be stated in its time-averaged or spatial-averaged version. The total energy of a physical system being bounded below is a fact related to the existence of a stable ground state. Nonetheless, there is an incompatibility between positive energy density conditions and local quantum fields [9]. The lower bound on the backflow effect, however, does not seem to have an immediately clear physical interpretation. Consideration of both effects in a common framework such as a free relativistic theory may provide some insight on their relationship. In fact, whilst most of the work on quantum backflow considered only the non-relativistic situation without any internal degree of freedom, the case of a free Dirac particle with spin-$\frac{1}{2}$ was studied in [10], for instance. Moreover, as the energy is usually considered in connection with a conservation law, it is reasonable to do the same for the backflow analysis and associate a conservation law with it when possible.

Interaction-free situations present a playground for numerous discussions, but more realistically one has to consider the effect of interaction. In [11], the backflow effect was extended to scattering situations in short-range potentials. It reinforced the universality of quantum backflow beyond a free theory and also stated that the existence of a lower bound, the constraint on how negative it can be, is stable under the inclusion of interaction. Although their work has proved the existence of lower bound estimates for a particular class of short-range potentials, they also noticed that a very short-range δ potential, although formally outside the validity of their theorem, has a backflow effect of finite magnitude. A special particularity of the δ is that it can be seen as a potential function, but it can also be seen as a point defect that is characterised by some sewing conditions at the defect location. Knowing that, we ask ourselves about the possibility of including other type of point defect described by a set of sewing conditions in the discussion of the quantum backflow effect.

This thesis will be particularly concerned with the backflow effect in the presence of defects. We extend the quantum backflow effect to this less restrictive situation,

in which the interaction is represented by a set of sewing conditions describing some discontinuity rather than having to specify an explicitly known potential function. Defects were previously considered in scattering situations [12], and integrable defects are generally categorised as purely transmitting [13]. In an integrable field theory, the introduction of boundaries and defects can, in general, spoil the integrability of the theory. As integrability is related to the existence of conservation laws, we shall look for the possibility of introducing an integrable defect in order to have both total energy and momentum conserved. In fact, general point interactions constructed by means of self-adjoint extensions of the Hamiltonian operator have the probability conserved, but the momentum, for instance, is not guaranteed to be conserved, and that is exactly the case of the δ-defect. As with a non-constant potential function, a defect also breaks space translation invariance since it has a specific location. Surprisingly, it is possible that the defect conditions compensate for the lack of translation invariance, and momentum is conserved. Note that the reflection coefficient in the case of the δ depends (with a phase factor) on the position where it is placed on the real line, and it does not seem possible to conserve momentum. Nonetheless, there is a specific defect with the attributes we would like to analyse in connection with the backflow effect. In particular, we consider a jump-defect [14, 15] that is purely transmitting in the context of non-relativistic quantum mechanics in one spatial dimension. In this respect, the jump-defect is similar to the Pöschl-Teller potential [16] given by

$$V(x) = -\frac{\mu(\mu+1)}{2\cosh^2 x}, \quad \mu > 0. \tag{1.2}$$

However, the latter is only reflectionless when the parameter μ is taken to be an integer, while the jump-defect is always purely transmitting. The jump-defect is 'halfway' between the Pöschl-Teller and the δ potential, but there are two relevant features that make it very different from the δ. Because it is purely transmitting, all contributions towards the negative probability fluxes come solely from the superposition of positive momentum states rather than a mixture of backscattering and the superposition of positive momentum states. It also allows us to keep conserved quantities that were conserved in the free case, such as the total energy, momentum (related to probability flux) and probability. As point defects, both of them involve some kind of discontinuity. But while the δ has a discontinuous first derivative of the wavefunction, the jump-defect has a discontinuous wavefunction describing it. Specifically, the wavefunction

discontinuity requires a treatment that involves distinct pair of domains rather than a single domain. More generally, these can involve multiple one-dimensional domains when several defects are placed at junctions of a network [17]. We remark that the jump-defect has the form of a Bäcklund transformation applied to a particular point in space rather than the entire real line, a 'frozen' Bäcklund transformation.

We will analyse the backflow for the discontinuous and transparent jump-defect, considering both the non-conserved probability current and the conserved probability current, and show that the backflow effect has a finite spatial extent, or a lower bound. In considering the adjusted conservation of momentum, the need for an extra contribution term to the backflow will be remarked. We will also extend the previous analysis [11] for the δ-case by scanning different values of the parameters and unveiling some structure in the attractive case. It is known that the δ-impurity can be, in some situations, used to model various different interactions in condensed matter, many-body theory and atomic physics, for instance. In particular, we mention the band theory of metals with Dirac comb potential or Dirac-Kronig-Penney model, one-dimensional version of the hydrogen atom and hydrogen molecule ion, a Bose gas and a gas of electrons; see [18, 19, 20, 21, 22] and references therein. Beyond one single δ-defect, a double δ-defect, described by a pair of deltas, will also be considered and have its backflow compared to the results of the single δ-defect. Although the double δ-defect has some structure not supported in a single δ-defect such as the existence of scattering resonances, for example, the presence of reflection is an almost unavoidable feature of this interaction. In fact, the double δ-defect can be transparent but in very limited circumstances that are energy-dependent. The situation in which there is total transmission and, therefore, no backscattering contribution mixing with the backflow effect is not possible for an interaction described by a δ potential function, but a jump-defect provides us with that possibility. Furthermore, their bound states seem to be relevant for the backflow and will be investigated.

Quantum inequalities can be formulated as an eigenvalue problem that has to be solved for the lowest eigenvalue of a given operator. In fact, this is not only the case of the probability current in the backflow effect but also of the energy density in energy inequalities. In [23], Fewster and Teo reformulated the quantum energy inequalities, for free massless scalar fields in even dimensional Minkowski space, in terms of finding the

lowest eigenvalue of a self-adjoint operator $\mathbb{H}$. Specifically, the inequality reads

$$\langle g|\mathbb{H}g\rangle \geq 0, \quad \forall g \in C_0^\infty(I) \tag{1.3}$$

with test function g supported on the interval $I \subset \mathbb{R}$, and $\mathbb{H}$ is a generalized Schrödinger operator on $L^2(I)$ that has its potential term replaced by a given energy density ρ. Hence, the positivity of $\mathbb{H}$ can be equivalently formulated as the problem of finding the lowest eigenvalue of $\mathbb{H}$. This formulation provides a test as to whether a given energy density is compatible with the quantum energy inequalities and an intuitive understanding of the so-called quantum interest conjecture [24] by an analogy with the quantum mechanics of a particle moving on the real line: negative energy densities (loans) become potential wells and positive energy densities (repayments) become potential barriers. It is very interesting that similar formulation works in the backflow for a spatially smeared probability current density in the free case [7]. In particular, the equivalent positive Schrödinger operator has its potential term replaced by the probability current density of a given right-moving state. Despite the formulation as an eigenvalue problem, an optimal analytical bound on the backflow effect is not known in the interaction-free case. When interaction is taken into account, an eigenvalue problem is generally unlikely to be solved analytically, but perturbation theory can be used to attempt to solve the given problem in terms of the simpler problem, namely, the free case. Thus, the backflow constant in the presence of interaction could be treated as a deviation from the constant in the free case. Analytic perturbation theory may be useful to study the behaviour of the backflow constant, but it might be difficult to know whether the approximations converge for a given set of parameters and estimate the error involved by neglecting higher orders of approximation. This thesis will, at least for the lowest order, look into the numerical results of perturbation theory applied to the cases where the interaction is described by a δ-defect or a jump-defect in the Schrödinger equation. These are exactly solvable models, and resorting to approximation methods is not required. In spite of that, these models can be used to check the plausibility of the perturbation results in comparison with the exact backflow results.

While the maximum amount of spatially averaged backflow is bounded in one dimension, that is unlikely to be generally true in three-dimensional Euclidean space. This expectation comes from results of quantum energy inequalities although backflow in three dimensions was not defined or even considered in previous works. Energy densities

can be made arbitrarily negative at a point. While timelike smearing yields averaged energy densities that are bounded below, spatial smearing is, in general, not enough to produce a state-independent quantum energy inequality [25]. Backflow was not analysed in higher dimensions yet, but we can similarly expect that the probability current has to be averaged in space and time (or time) in order to obtain a state-independent lower bound that restricts the backflow phenomenon. Incidentally, the form taken by the probability current for a charged particle, with mass m and charge q, in an electromagnetic field and described by the Schrödinger equation with wavefunction Ψ in three dimensions

$$\mathbf{J} = \frac{\hbar}{2mi}\left(\Psi^\star\nabla\Psi - \Psi\nabla\Psi^\star\right) - \frac{q}{m}\mathbf{A}\Psi^\star\Psi, \tag{1.4}$$

with vector potential $\mathbf{A}$, is very common in physics and is also present in the conserved current expression for particles with spin. Let us just mention the particular examples of the current for a spin-0 scalar particle in the Klein-Gordon equation and a spin-$\frac{1}{2}$ particle in the Dirac equation (Gordon decomposition [26]), respectively, given by

$$J^\mu = i\left(\phi^\star\partial^\mu\phi - \phi\partial^\mu\phi^\star\right) - 2q\phi^\star\phi A^\mu, \tag{1.5}$$

$$J^\mu = \frac{i}{2m}\left(\bar{\psi}\partial^\mu\psi - (\partial^\mu\bar{\psi})\psi\right) + \frac{1}{m}\partial_\alpha\left(\bar{\psi}\Sigma^{\mu\alpha}\psi\right) - \frac{q}{m}\bar{\psi}\psi A^\mu, \tag{1.6}$$

where, in quantum field theory, the spatial components of these expressions are interpreted as the electromagnetic current associated with the particles in the presence of the vector-potential A^μ, $\Sigma^{\mu\alpha}$ are generators of Lorentz transformations and ϕ and ψ are a scalar field and a Dirac spinor, respectively. Although they are not probability currents, the first term in each expression above is the convective part of the flux, responsible for the movement of charges. Evidently, while a negative movement of charges can be interpreted as the positive flux of particles with negative charge, the same interpretation applied to a negative probability flux would imply the existence of negative probability, a concept first introduced by Dirac, who believed that negative energy and negative probability always occur together and suggested that, "like a negative sum of money", should not be considered as nonsense [27]. Perhaps this financial analogy motivated the quantum interest conjecture about local negative energy densities. Feynman [28] also suggested possible interpretations for making sense of negative probabilities. Nevertheless, we will not discuss negative probabilities but take the view of backflow as

the existence of negative probability fluxes for right-moving states. Motivated by this relation in which the electric current density for a charged particle is proportional to the probability current density, Bracken and Melloy [6] suggested a possible experimental setup where the existence of backflow could be confirmed by measuring the electric current of that particle initially prepared in right-moving states.

Similarly to the electromagnetic current that has not only influence from the mass of the particle but also from the spin, the probability current can be affected [29, 30] by orbital angular momentum and spin (e.g., spin-orbit interaction). As the relativistic Dirac equation takes the spin of the particle into account, we will analyze the backflow effect for a spin-$\frac{1}{2}$ particle in the presence of δ-defects described by the Dirac equation. It is worth noting that the consideration of a δ-defect in the Dirac equation does not lead to a unique possibility but rather to different sets of sewing conditions. In particular, we will look into the case of an electrostatic δ_e-defect as well the case of a mass-like δ_m-defect and make a comparison with the results of a δ-defect in the Schrödinger equation. Moreover, a δ-defect in the Dirac equation causes a discontinuity in the wavefunction solution and, consequently, is already a type of jump condition. It cannot, however, be considered a jump-defect, since it does not classify as an integrable defect. Then, a natural further step would be including a jump-defect in the (one-dimensional) Dirac equation. The first-order nature of the Dirac equation requires the sewing conditions to involve its two spinor components ψ_1 and ψ_2 instead of derivatives of the wavefunction as it happens for general point interactions in the Schrödinger equation. The possibility of including a jump-defect will be considered as we reflect on the use of a suitable Bäcklund transformations in order to find the required sewing conditions.

Thesis Outline

This thesis is composed of seven chapters and two appendices. In chapter 2, we present the quantum backflow effect in the interaction-free case and in the case of scattering for short-range potentials. Then, we extend the discussion of the backflow to situations where the interactions are described by defects. Chapter 3 considers the quantum backflow effect in the presence of a δ-defect as well a double δ-defect and a δ'-defect obtained from the double δ-defect in the zero-range limit where the distance between the pair of deltas tends to zero. Chapter 4 focuses attention on the backflow effect in

the presence of the purely transmitting jump-defect in the linear Schrödinger equation. The main purpose of the chapter is to examine the possibility and the consequences of considering the backflow effect in the presence of a defect that is, at the same time, a point defect and transparent. Additionally, it aims at exploring the similarities and differences between the δ and the jump-defect with regard to the backflow. Chapter 5 considers the analytical perturbation theory of the probability current operator in order to expand the backflow constant in power series of the interaction strength. In Chapter 6, we examine the relativistic backflow effect in the setting of the first-order Dirac equation for a particle of spin-$\frac{1}{2}$. More specifically, we consider the relativistic backflow in the presence of an electrostatic δ_e-defect and in the presence of a mass-like δ_m-defect. Chapter 7 has a final discussion and summarises the results presented in the thesis as well possible directions for further investigation in the future. Numerical results are provided alongside the discussion presented in each chapter and are composed of two-dimensional and three-dimensional plots displaying the lowest eigenvalue of the probability current operator against the position of measurement x_0, which is the center of a positive test function, and against the strength of the different interactions, or defect coupling, considered in this work. With the exception of the appendices, all numerical results are averaged with the same Gaussian function that has a fixed width. Appendix A shows results of the backflow constant in the Pöschl-Teller potential for various values of the parameter μ. These provide some further evidence to make a conjecture about bound states in chapter 7. Finally, Appendix B considers the calculation of the backflow constant spatially averaged with different choices of weight functions in the case of a jump-defect.

— 2 —

Quantum backflow

2.1 NEGATIVE FLOW OF PROBABILITY

In non-relativistic quantum mechanics, the continuity equation for the probability density in one space dimension is

$$\partial_t \rho = -\partial_x j \,, \tag{2.1}$$

where $\rho = |\psi|^2$ is the probability density, j is the probability current density [30] (or probability flux) and ψ the square-integrable wavefunction of the system. The Schrödinger equation for the wavefunction of a quantum system is simply

$$i\hbar \partial_t \psi = H\psi \,, \tag{2.2}$$

where H is the self-adjoint Hamiltonian operator associated with the system. The state vector is commonly denoted by $|\psi\rangle \in \mathcal{H}$, as an abstract vector in the Hilbert space $\mathcal{H}$ of the physical system. Not all solutions of this equation are elements of the space of (equivalence classes of) square-integrable functions $L^2(\mathbb{R})$, but these solutions are crucial for scattering theory. As a consequence of the Schrödinger equation for a particle of mass m, in the free case, one has the probability flux at position x given by

$$j_\psi(x) = \frac{i\hbar}{2m} \left(\partial_x \psi^\star(x)\psi(x) - \psi^\star(x)\partial_x \psi(x)\right) := \langle \psi,\, J(x)\psi \rangle, \tag{2.3}$$

where now the ψ-dependence is explicitly indicated, and $j_\psi(x)$ can be expressed in terms of the associated quadratic form $J(x)$. The space average of (2.3) with a test function, generally $f \in \mathcal{S}(\mathbb{R})$ in Schwartz-class [1] is given by

[1] Such functions are nice for having a Fourier transform and they include the space of smooth functions of compact support i.e. $C_0^\infty \subset \mathcal{S}$.

$$j_\psi(f) = \langle \psi,\, J(f)\psi \rangle = \int dx\, f(x)\, j_\psi(x)\,, \tag{2.4}$$

and is understood as the spatial-averaged probability current measured by a spatially extended apparatus. The corresponding smeared operator is the integration $J(f) = \int f(x)J(x)dx$, understood in the sense of quadratic forms. This operator is Hermitian for a real function f and is written as

$$J(f) = \frac{1}{2m}\left(\hat{P} f(\hat{X}) + f(\hat{X})\hat{P}\right), \tag{2.5}$$

with position operator $\hat{X}$ and momentum operator $\hat{P} = -i\hbar\partial_x$. Similarly, in particular, it is common to write $J(x)$ in terms of the generalized position eigenvector $|x\rangle$, and it has the following symmetric form

$$J(x) = \frac{1}{2m}\left(|x\rangle\langle x|\,\hat{P} + \hat{P}\,|x\rangle\langle x|\right). \tag{2.6}$$

From a square-integrable wavefunction, the probability density can then be defined in terms of position probability density $|\psi(x)|^2$ or momentum probability density $|\tilde{\psi}(k)|^2$ by means of the Fourier transform [2] $(\mathcal{F}\psi)(k) = \tilde{\psi}(k) = (2\pi)^{-1/2}\int dx\; e^{-ikx}\psi(x)$.

The effect that, for a particle with positive momentum ($k > 0$), the probability of finding it to the right of some reference point may decrease with time is called quantum backflow effect. This means that given a wavefunction $\tilde{\psi}$ with support in momentum space restricted by $\mathrm{supp}(\tilde{\psi}) \subset \mathbb{R}_+$, right-moving wavefunction, it is not guaranteed at all that the probability current density fulfills the positivity condition $j_\psi(x) > 0$ with $x \in \mathbb{R}$. That effect was initially discovered and studied in the context of the time of arrival in quantum mechanics by Allcock [5]. Later on, Bracken and Melloy [6] investigated the effect in greater detail analysing the temporal extent of the effect as an eigenvalue problem for a free quantum particle. Their results were also extended to the case where the particle is moving under a constant force [31], and again the probability flows, for a finite period of time, in the opposite direction to the momentum. It is important to highlight the fact that quantum backflow has no classical analogue effect and it is not a spreading of a Gaussian wave packet as previously suggested [32], and subsequently clarified in [33] by showing that the Wigner function associated with this Gaussian

[2] Omitted limits of integration are assumed to be the full real line $\mathbb{R}$.

wave packet is positive at all times. That the effect can be reproduced by a simple superposition of two plane waves was illustrated in [6] and similarly for a superposition of two Gaussians wave packets [34], where the authors show that, despite Gaussian wave packets having support on both positive and negative momentum, the negativity of the current cannot be explained by the very small probability of having negative momentum which comes from the Gaussian state. Quantum backflow was also related, in the phase-space, to another interference effect called quantum reentry where position rather than momentum is constrained [35, 36]. Following that interesting relation, a particle escaping through a Dirac δ barrier was analysed in [37] and compared to the evolution of a free particle. The backflow was also considered in the case of a system with spin-orbit coupling in [38], in the rotational motion of a particle in a ring [39]. Relativistic effects on the backflow of a free particle were examined in [10, 40, 41]. Being a quantum phenomenon augmented by certain "backflow states" (states in which backflow occurs) [42], its level of non-classicality can be compared to the required negativity of the Wigner function, as was done in [43], where it was stated that the negativity of the Wigner function is only a necessary prerequisite for the occurrence of backflow. After Allcock, the effect was shown to be relevant for the discussion of quantum events and the meaning of arrival-time distribution [44, 45]. However, not only the temporal extent, as originally discovered, of backflow has attracted attention in the literature. In fact, by focusing on the shape of backflowing regions, therefore considering its position dependence, backflow was shown to be closely related to superoscillations [46]. It was also considered for the case of an electrically charged particle in a constant magnetic field [47, 48]. An analogue optical effect was observed in [49]. Furthermore, the spatial extent of backflow was analysed considering the spatial-averaged probability current [7, 11] rather than its temporal-averaged version. In its spatially averaged version, the backflow has similarities to the quantum energy inequalities [7, 4] in quantum field theory. This thesis will focus on the spatially averaged version of the backflow effect.

2.2 FREE CASE

In interaction-free situations, the maximal amount of backflow, spatially averaged with a positive test function f, i.e. the lowest bound, is defined [11] by

$$\beta_0(f) := \inf \langle E_+ J(f) E_+ \rangle_\psi \ , \tag{2.7}$$

where the infimum is understood as

$$\inf \langle A \rangle := \inf_{\|E_+\psi\|=1} \langle \psi,\, A\psi \rangle \in (-\infty, \infty)\,,$$

for all $\psi \in D(A)$, the domain of an operator A, with square-integrable $\psi \in L^2(\mathbb{R})$. According to the minimax principle [50], $\beta_0(f)$ is the minimum eigenvalue of the averaged current evaluated in right-moving states, $E_+ J(f) E_+$. The orthogonal projection E_+ of the momentum operator makes sure that the momentum is positive ($k > 0$). In particular, if ψ is a right-mover, $E_+\psi = \psi$. The question of how negative this quantity $\beta_0(f)$ can be, and if it is actually bounded below, was answered by Eveson, Fewster and Verch in the following theorem [7]

Theorem 1. *For every positive test function $f \in \mathcal{S}(\mathbb{R})$, $\exists\, C_f \geqslant 0$ such that the inequality $\langle J(f) \rangle_\psi \geqslant -C_f$ holds true, where ψ is taken to be normalised and right-moving, i.e. $\psi \in R = \{\psi \in L^2(\mathbb{R}) |\ \tilde{\psi}(k) = 0$ for $k < 0$ and ψ' continuous and square-integrable$\}$.*

Thus, $\beta_0(f) > -\infty$, as C_f is a finite constant. More precisely,

$$\int dx\ f(x) j_\psi(x) \geq -\frac{\hbar}{8\pi m} \int dx\ |g'(x)|^2 > -\infty, \tag{2.8}$$

where $f = g^2$ for some real $g \in \mathcal{S}(\mathbb{R})$, and prime denotes derivative with respect to position variable. The inequality (2.8) has origin in the following estimations. Define a multiplication operator by $(M_f\psi)(x) = f(x)\psi(x)$, and write the spatial average as

$$\begin{aligned} \int dx\ f(x) j_\psi(x) &= \frac{\mathrm{Re}\langle \psi,\, M_f \hat{P}\psi \rangle}{m} = \frac{\mathrm{Re}\langle \psi,\, M_g \hat{P} M_g \psi \rangle}{m} \\ &= \frac{\hbar}{m} \int \frac{dk}{2\pi} k\ \left| (\widetilde{M_g\psi})(k) \right|^2, \end{aligned} \tag{2.9}$$

where $M_f\hat{P}$ was substituted in terms of the commutator $[M_g, M_g\hat{P}]$. The Fourier transform of the product $(\widetilde{M_g\psi})(k)$ is given by the convolution theorem

$$(\widetilde{M_g\psi})(k) = \int_0^\infty \frac{dk'}{\sqrt{2\pi}} \tilde{g}(k-k')\tilde{\psi}(k') \tag{2.10}$$

which has the integration limits restricted to $k' > 0$ because ψ is a right-moving state. Then, there are two estimations used in the derivation of the theorem. The first, and

more important, is a bound by comparing the integral with its part arising from $k < 0$

$$\int dx\ f(x)j_\psi(x) \geq \frac{\hbar}{m}\int_{-\infty}^{0}\frac{dk}{2\pi}k\ \left|(\widetilde{M_g\psi})(k)\right|^2 = -\frac{\hbar}{m}\int_{0}^{\infty}\frac{dk}{2\pi}k\ \left|(\widetilde{M_g\psi})(-k)\right|^2, \quad (2.11)$$

and the second estimation comes from applying the Cauchy-Schwarz inequality to the expression $\left|(\widetilde{M_g\psi})(k)\right|^2$ that is given by means of (2.10). Then, it follows that

$$\left|(\widetilde{M_g\psi})(-k)\right|^2 \leq \int_0^\infty \frac{dk'}{2\pi}\left|\tilde{g}(k+k')\right|^2, \quad (2.12)$$

using also the fact that $\|\psi\| = 1$ and that $|\tilde{g}(-k)|^2 = |\tilde{g}(k)|^2$ because g is a real function. Combining that with the previous estimation (2.11) gives

$$\begin{aligned}\int dx\ f(x)j_\psi(x) &\geq -\frac{\hbar}{m}\int_0^\infty\frac{dk}{2\pi}\int_0^\infty\frac{dk'}{2\pi}k\left|\tilde{g}(k+k')\right|^2\\ &= -\frac{\hbar}{m}\int_0^\infty\frac{d\xi}{4\pi^2}\left|\tilde{g}(\xi)\right|^2\int_0^\xi dk\ k\\ &= -\frac{\hbar}{m}\int_{-\infty}^\infty\frac{d\xi}{16\pi^2}\xi^2\left|\tilde{g}(\xi)\right|^2\\ &= -\frac{\hbar}{8\pi m}\int dx\left|g'(x)\right|^2,\end{aligned} \quad (2.13)$$

which is obtained by making a change of variables such that $\xi = k + k'$, using the evenness property of the integrand $|\tilde{g}(\xi)|$ and and the Parseval-Plancherel identity.

Theorem 1 describes a quantum inequality that is state-vector independent. Moreover, whilst the operator $E_+J(f)E_+$ is bounded below it is unbounded above, for positive f, exactly as the corresponding non-smeared version $E_+J(x)E_+$. Note, however, that the lower bound depends on the choice of test function f that is related to the measurement apparatus. Effectively, the unboundedness is a high momentum effect [11]. In the context of the Weyl-Wigner quantisation, it was also shown in [7] that the backflow effect for the spatially smeared flux $j_\psi(f)$, as a quantum inequality, can be seen as a direct consequence of the sharp Gårding inequalities [51] in the theory of pseudo-differential operators, although it is not possible to determine the magnitude of the bound C_f from that. Interestingly, a strong improvement of the Gårding inequality was derived from considering the consequences of the uncertainty principle for the theory of pseudo-differential operators [52, 53].

2.3 INTERACTION IN SCATTERING SITUATIONS

For scattering situations, we consider the effect of an interaction with a potential term V, external and time-independent for simplicity, added to the free Hamiltonian so that

$$H = \frac{\hat{P}^2}{2m} + V(\hat{X}). \tag{2.14}$$

As a physical requirement, the potential is Hermitian. While the concept of right-movers is clear in a free case, the time evolution associated with an interacting Hamiltonian does not commute with the projector E_+, meaning that the space of right-movers $E_+L^2(\mathbb{R})$ is not invariant under time evolution transformations. As an alternative equivalent concept, we adopt the asymptotic right-movers in the sense of scattering theory, as used before in [11]. In this way, we consider a state such that its incoming asymptote is a right-mover. The incoming Møller operator is given by

$$\Omega^{(\mathrm{IN})} = \Omega_V := \underset{t\to-\infty}{\text{s-lim}}\, e^{+iHt}e^{-iH_0t}\,, \tag{2.15}$$

with s-lim denoting the strong operator limit and H_0 the free Hamiltonian. Our quantity of interest is now dependent on the potential and defined as

$$\beta_V(f) := \inf \left\langle E_+\Omega_V^\dagger J(f)\Omega_V E_+ \right\rangle_\psi\,, \tag{2.16}$$

which is called the "asymptotic backflow constant" [11] and it is the lowest eigenvalue of the operator $E_+\Omega_V^\dagger J(f)\Omega_V E_+$. In general, $\beta_V(f)$ has a contribution from scattering as a result of the interaction, with the exception of special cases in which there is no reflection. Moreover, it has physical units of $\hbar/(m\ell^2)$, with a length scale ℓ as the unit of length. In the future, we will refer to this operator as the "(asymptotic) probability current operator" or simply the "interacting current".

To ensure the applicability of the scattering theory, we usually work with potentials that vanish sufficiently fast at spatial infinity. This is based on the fact that the fall-off properties of the potential are related to smoothness properties of the scattering data. Specifically, it is usual to require the fulfillment of the condition [54]

$$\|V\|_1^1 := \int_{-\infty}^{+\infty} dx\,(1+|x|)\,|\,V(x)\,| < \infty\,, \tag{2.17}$$

and we say that $V \in L^1_1(\mathbb{R})$. In the stationary scattering theory, one has the time-independent Schrödinger equation (TISE) for a wavefunction $\varphi(x)$

$$\left(-\frac{\hbar^2}{2m}\frac{\partial^2}{\partial x^2} + V(x)\right)\varphi(x) = \frac{(\hbar k)^2}{2m}\varphi(x), \tag{2.18}$$

for which the scattering solutions $x \to \varphi_k(x)$ with $k > 0$ have asymptotics of the form

$$\varphi_k(x) = \begin{cases} T_V(k)e^{ikx} + o(1) & \text{as } x \to \infty, \\ e^{ikx} + R_V(k)e^{-ikx} + o(1) & \text{as } x \to -\infty\,, \end{cases} \tag{2.19}$$

with transmission $T_V(k)$ and reflection $R_V(k)$ coefficients. In the scattering context, the Schrödinger equation together with boundary conditions (2.19) is equivalent to a Lippmann-Schwinger equation [55]

$$\varphi_k(x) = T_V(k)e^{ikx} + \int dy\, G_k(x-y)U(y)\varphi_k(y), \tag{2.20}$$

with $U = (2m/\hbar^2)\,V$. For this choice of complementary function (the inhomogeneous term of the integral equation), the Green's function for the free TISE, which is a solution of the equation $G_k''(x) + k^2 G_k(x) = \delta(x)$, is

$$G_k(x) = -\frac{\sin(kx)}{k}\theta(-x), \tag{2.21}$$

where θ is the Heaviside function: $\theta(x) = 0$ for $x < 0$ and $\theta(x) = 1$ for $x > 0$.

For situations where the interaction is exactly solvable, we do not need to make use of Green's functions in the Lippmann-Schwinger equation. Later in our discussion, chapter 5, we will consider and apply some analytic perturbation theory for the probability current operator, and Green's function will be essential in our analysis. Either working with perturbation approximations or the exact solution, a key ingredient for analysing the backflow effect in scattering situations is the expansion of the Møller wave operator in the following integral form; see, for example, [56] for the Lemma below.

Lemma 1. *Let $V \in L^1_1(\mathbb{R})$. Then the operator Ω_V defined in* (2.15) *exists. Further, the solution $x \mapsto \varphi_k(x)$ ($k > 0$) of* (2.18) *with the asymptotics* (2.19) *exists and is unique, and for any $\tilde{\psi} \in C_0^\infty(\mathbb{R})$,*

$$\langle x|\,\Omega_V E_+\,|\psi\rangle = (\Omega_V E_+\psi)(x) = \frac{1}{\sqrt{2\pi}}\int_0^\infty dk\,\varphi_k(x)\tilde{\psi}(k)\,. \tag{2.22}$$

By the use of some estimates, e.g., [54, 57], the following theorem [11] is a result on the existence of backflow in scattering situations and also on its lower bound.

Theorem 2. *Let the potential function V be a $L^1_1(\mathbb{R})$-class potential, i.e. $\|V\|^1_1 < \infty$. For any $f \in C^\infty_0(\mathbb{R})$, with $f \geqslant 0$, $\exists\, C_{V,f} > 0$ such that*

$$\langle\psi|E_+\Omega_V^\dagger J(f)\Omega_V E_+|\psi\rangle \geqslant -C_{V,f} \quad \textit{for } \|\psi\| = 1. \tag{2.23}$$

Hence, the asymptotic backflow constant is finite, $\beta_V(f) > -\infty$. The existence of backflow and the boundness (below) of backflow are stable under the addition of a scattering potential to the Hamiltonian. This means that, even in the presence of reflection, the effect is bounded below. Henceforth, we denote the expectation value of the interacting operator in a general (normalized) state vector $|\psi\rangle$ by

$$\langle J_V(f)\rangle_\psi \coloneqq \langle\psi|\, E_+\Omega_V^\dagger J(f)\Omega_V E_+\,|\psi\rangle\,. \tag{2.24}$$

Moreover, the expansion of this expectation value with respect to scattering states φ_k in position space relies on the use[3] of the Lemma 1.

As is the case for the Hamiltonian, we expect that the asymptotic current operator has a spectrum composed of pure point and absolutely continuous parts. Thus, we have some eigenvalues, with the lowest one denoted by $\beta_V(f)$, and at some point a continuum of generalized eigenvalues. That is justified on the basis of the evidences provided by the numerical calculations, which will be explained in section 4.5. It is important to stress our interest in this lowest eigenvalue in the context of quantum inequalities.

2.4 BACKFLOW IN THE PRESENCE OF A DEFECT

In the next two subsequent chapters of the present work, Chapter 3 and Chapter 4, we will, in more details, address the concept of defects by introducing some particular defects into the Schrödinger equation. Following that, the backflow effect will then be analysed in the presence of these defects. More specifically, the single δ-defect, the double δ-defect and the jump-defect, respectively. Moreover, Chapter 6 will also consider the

[3]The Lemma 1 requires $\tilde{\psi}$ to be smooth of compact support $\tilde{\psi} \in C^\infty_0$. However, $C^\infty_0(\mathbb{R})$ is dense in $L^2(\mathbb{R})$ and through the use of Friedrichs extensions [58] the discussion applies to a general ψ in the domain $D(J_V(f))$ of our operator.

presence of defects but in the Dirac equation instead. Before the backflow calculations that will be carried out later once the interactions are explicitly particularised, we need to set out the general structure of our quantities of interest, namely the probability current operator and its lowest eigenvalue taking interaction into account.

A mathematically oriented discussion on the introduction of singular perturbations of partial differential operator, particularly in the context of Hilbert spaces and the Schrödinger equation, started in [59]. These authors considered the perturbation of a Hamiltonian with a delta potential function using the extension theory of symmetric operators. The theory of self-adjoint extensions of symmetric operators, based on the fact that a symmetric operator can be extended to a self-adjoint operator when its deficiency indices are equal, was very important in the development of exactly solvable models in quantum mechanics specially because of the Laplacian operator or kinetic energy operator. The literature is vast but some of the earliest references can be mentioned [60, 61, 62, 63, 64, 65, 66, 67]. Since the deficiency indices play an important role in the existence of self-adjoint extensions, let us recall the following result [58]

Definition 1. *Let A be a symmetric operator with domain $D(A)$ and adjoint $A^\dagger$. Its deficiency indices are the pair of numbers n_+, n_-, given by*

$$\begin{aligned} n_+ &:= \dim\left(\ker(A^\dagger - i)\right), \\ n_- &:= \dim\left(\ker(A^\dagger + i)\right). \end{aligned} \tag{2.25}$$

Then, there are three possibilities

(i) If $n_+ = n_- = 0$, A is either self-adjoint or has a unique self-adjoint extension and is said to be essentially self-adjoint.

(ii) If $n+ = n_- = n \geq 1$, there exist self-adjoint extensions of A, which are parametrized by a unitary $n \times n$ matrix, a n^2-parameter family of such extensions.

(iii) If $n_+ \neq n_-$, then A has no self-adjoint extension.

These self-adjoint extensions can be described in terms of matching conditions relating the value of a wavefunction and its derivatives. In particular, for point interactions, the conditions are defined at these interaction sites. Physically, point interactions, or zero-range potentials, are understood as sharply localised potentials

but they are mathematically special in the sense that they are singular perturbations with support of zero measure of the free Hamiltonian $H_0 = -\frac{\hbar^2}{2m}\partial_x^2$ for a free particle of mass m. Thus, for the Hamiltonian with a point interaction (located at the origin, for convenience), its self-adjoint extension differs from H_0 just by including the appropriate matching conditions describing the particular interaction of interest. To consider a simple case, let us denote the densely defined operator $L = -\partial_x^2$, $D(L) = C_0^\infty(\mathbb{R}\setminus\{0\})$, all $C_0^\infty(\mathbb{R})$ functions having compact support separated from the origin, and, from that, we have $\langle\phi,\, L\psi\rangle = \langle L^\dagger\phi,\, \psi\rangle$ for $\phi \in D(L^\dagger)$ and $\psi \in D(L)$ where $L^\dagger$ is the adjoint of L. In addition, L has deficiency indices $(2,2)$. The self-adjointness conditions on L, for square-integrable functions ϕ and ψ without support at the origin[4], require that the operator and its adjoint have the same domain and L is a symmetric operator, $\int_{-\infty}^{\infty}\phi^\star(x)(L\psi)(x)\,dx = \int_{-\infty}^{\infty}(L\phi^\star)(x)\psi(x)\,dx$, that can be expressed in the form

$$-\int_{-\infty}^{\infty}\left(\phi^\star\partial_x^2\psi - \left(\partial_x^2\phi^\star\right)\psi\right)dx = \Big[\,\phi^\star\partial_x\psi - (\partial_x\phi^\star)\psi\Big]_{0^-}^{0^+} = 0, \tag{2.26}$$

which can hold true in the simplest case where the functions and their derivatives are continuous at the origin. Nevertheless, there are other possibilities and the case of a δ interaction is the known example where the function is continuous at the origin but its derivative is not. That is described by the following conditions: $\psi(0^+) = \psi(0^-) = \psi(0)$ and $\partial_x\psi(0^+) - \partial_x\psi(0^-) = 2\lambda\psi(0)$ with $\lambda \in \mathbb{R}$, see (3.1) in Chapter 3. Equally conceivable, a discontinuous function can also hold (2.26) true. An example of such more severe discontinuity is obtained in the case the interaction is represented by the derivative of a delta, known as the $\delta'(x)$. Unfortunately, it seems that the admissibility of discontinuities in the wavefunction is not well explored in the textbook literature on quantum mechanics. There are, however, numerous physical situations or models where these discontinuities are realizable. Some examples in the literature include the mass jump, which describes a physical system with an abrupt discontinuity of the mass at one point that happens for a quantum particle moving in a media formed up by two different materials, the problem of the connection rules in semiconductor heterostructures, junctions and the short-range limit of a two-body interaction [69, 70, 71, 72, 73, 74]. While the existence of a self-adjoint Hamiltonian operator and a finite average kinetic energy for a quantum particle are physical requirements, there is

[4]In particular, ψ belongs to the Sobolev space $W_2^2(\mathbb{R}\setminus\{0\})$ [68].

no physical reason to rule out the presence of discontinuities in the wavefunction. In Chapter 4, we will present the jump-defect as another special example of a discontinuous wavefunction that is associated with a finite kinetic energy. Defects or impurities on the real line are modeled by point interactions, and we will make interchangeable use of these terms in this thesis. Because of the singular nature of these interactions, it is not always convenient or possible to have an analytical expression for a potential function representing them. In that sense, defects provide us with more possibilities that go beyond the addition of a zero-range potential function to the Hamiltonian of a physical system. Furthermore, the self-adjoint extensions of the Hamiltonian can be used to construct general point interactions [75, 76, 77, 78, 79] that, in the case of a single interaction center in one dimension, are characterized by a four-parameter family matching conditions as follows [80]

$$\begin{pmatrix} \varphi_k(0^+) \\ \varphi_k'(0^+) \end{pmatrix} = e^{i\theta} \begin{pmatrix} a & b \\ c & d \end{pmatrix} \begin{pmatrix} \varphi_k(0^-) \\ \varphi_k'(0^-) \end{pmatrix}, \tag{2.27}$$

where φ_k' denotes the spatial derivative, the coefficients $a, b, c, d \in \mathbb{R}$ and $\theta \in [0, \pi)$ are restricted by the condition $ad - bc = 1$, which is called the non-separated condition because the regions $x < 0$ and $x > 0$ are connected. The case where there is no transmission, effectively an infinite wall, is called separated type and its matching conditions are called separated conditions. The case of a single δ-defect can be reproduced by taking $a = 1$, $b = 0$, $c = 2\lambda$, $d = 1$ and $\theta = 0$. Interestingly, self-adjoint extensions of the Hamiltonian operator are equivalent to enforcing probability conservation or that probability current is continuous across the discontinuity, that is at the defect position [81, 82, 83]. Specifically, for stationary solutions φ_k, the condition requires that $\partial_x j_{\varphi_k} = 0$, where j_{φ_k} is obtained from (2.3) by the substitution of ψ for φ_k. Taking into account the real line excluding the origin, this means that

$$j_{\varphi_k}(0^+) = j_{\varphi_k}(0^-), \tag{2.28}$$

to be understood in the limiting sense. We remark that, although the wavefunction might be discontinuous, the Hamiltonian operator can be self-adjoint and probability conserved. These general point defects described by self-adjoint extensions, however, do not exhaust all possible point interactions. In fact, the case of a δ' interaction, see Chapter 3, shows that we may have to use additional assumptions such as symmetry

properties of the interaction, and different assumptions can result in different point interactions. All that discussion is not limited to the one-dimensional case or even to the Schrödinger equation only and it can be extended [84, 85]. The conservation of probability was also used to create different matching conditions including the case of a particle moving on the circle with a point interaction [86, 87]. For that inclusion, the matching conditions characterizing the self-adjoint extensions of the Hamiltonian (which has deficiency indices $(2,2)$) relate the family of point interactions conserving probability to a 2 x 2 unitary matrix $U \in U(2)$ as follows

$$(U-I)\begin{pmatrix}\varphi_k(0^+)\\ \varphi_k(0^-)\end{pmatrix} + iL_0(U+I)\begin{pmatrix}\varphi_k'(0^+)\\ -\varphi_k'(0^-)\end{pmatrix} = 0, \tag{2.29}$$

where $L_0 \neq 0$ is an arbitrary constant and I is the identity matrix in $U(2)$.

A defect in one-dimensional configuration space, therefore, can be viewed as a type of point interaction implemented into the physical system with sewing conditions connecting the pair of regions separated by the defect position on the real line. Thus, we consider here the effect of a generic interaction in the context of the Schrödinger equation. It is also convenient here to set $\hbar = m = 1$ by a suitable re-scaling of the length and time units. In the presence of a general non-trivial interaction term, at least of short-range type, we can write the expectation value (2.24) of the interacting probability current, in position space, as follows

$$\langle\psi|\, J_V(f)\,|\psi\rangle = \int dx \int dx' (\Omega_V E_+\psi)^\star(x')\,[J(f)(x',x)]\,(\Omega_V E_+\psi)(x), \tag{2.30}$$

with the kernel $J(f)(x',x)$ in position space. In order to simplify this equation, we need a general expression for $J(f)(x',x)$, which can be obtained from the expectation value $\langle\psi|\, J(f)\,|\psi\rangle$ substituting the unbounded operator $J(f)$ in terms of position and momentum operators using (2.5) as

$$\begin{aligned}\langle\psi|\, J(f)\,|\psi\rangle &= \frac{1}{2}\,\langle\psi|\,\hat{P}f(\hat{X}) + f(\hat{X})\hat{P}\,|\psi\rangle \\ &= -\frac{i}{2}\int dy\,\psi^\star(y)\left(f(y)\frac{\partial\psi(y)}{\partial y} + \frac{\partial}{\partial y}(f(y)\psi(y))\right),\end{aligned} \tag{2.31}$$

which can be rewritten in the form

$$\begin{aligned}\langle\psi|\, J(f)\,|\psi\rangle = -\frac{i}{2}\int dy\,\psi^\star(y)\Bigg[\int dy'\, f(y)\frac{\partial\delta(y-y')}{\partial y}\psi(y') \\ + \frac{\partial f(y)}{\partial y}\delta(y-y')\psi(y') + f(y)\frac{\partial\delta(y-y')}{\partial y}\psi(y')\Bigg],\end{aligned}$$

where we have used the trick of rewriting the wavefunction $\psi(y) = \int \delta(y-y')\psi(y')dy'$. Hence, since $\langle\psi| J(f) |\psi\rangle = \int dy \int dy' \psi^\star(y') \left[J(f)(y',y)\right] \psi(y')$, we obtain

$$J(f)(y,y') = -\frac{i}{2}\left[2f(y)\frac{\partial\delta(y-y')}{\partial y} + \frac{\partial f(y)}{\partial y}\delta(y-y')\right]. \tag{2.32}$$

In abstract Dirac notation, we write the general structure of the interacting operator current $J_V(f)$. From (2.22), it follows that the resolution of the operator Ω_V can be written in the abstract form

$$\Omega_V = \int_{-\infty}^{\infty} dk \, |\varphi_k\rangle \langle k| \,, \tag{2.33}$$

where $|k\rangle$ is the generalized momentum eigenvector (in the sense of rigged Hilbert spaces), and the dual eigenvector (linear functional) $\langle q|$ is such that $\delta(q-k) = \langle q|k\rangle$. In particular, a plane wave has the normalization convention given by $\langle x|k\rangle = e^{ikx}/\sqrt{2\pi}$. It is not difficult to derive, by comparison with (2.30), the abstract operator

$$J_V(f) = E_+\Omega_V^\dagger J(f)\Omega_V E_+ = \left[E_+ \int dq' \, |q'\rangle \langle\varphi_{q'}| \, J(f) \int dq \, |\varphi_q\rangle \langle q| \, E_+\right]. \tag{2.34}$$

The expression (2.34) is the interacting operator expanded in terms of the interacting state vector and it highlights how $J_V(f)$ differs from the free operator $E_+J(f)E_+$. Obtaining an expression for that linear operator is also the starting point from where some analytical perturbation theory can be applied to the analysis of the backflow constant in Chapter 5. For a practical calculation such as obtaining the lowest eigenvalue of the operator $J_V(f)$, we will work with stationary scattering states and momentum space wavefunctions of the Hilbert space. Back to the expectation value expression (2.24), it can, therefore, be written in terms of φ_k as

$$\langle\psi| J_V(f) |\psi\rangle = \frac{1}{2\pi}\int_0^\infty dk \int_0^\infty dk' \tilde{\psi}^\star(k')\tilde{\psi}(k) \int dx \int dx' \varphi_{k'}^\star(x') J(f)(x',x)\varphi_k(x), \tag{2.35}$$

where we will denote the spatial inner integrals by

$$L(k',k) = \int dx \int dx' \varphi_{k'}^\star(x') J(f)(x',x)\varphi_k(x). \tag{2.36}$$

Having a defect located at the origin ($x = 0$) of the real line, the line is split into two regions, left of the defect ($x < 0$) and right of the defect ($x > 0$). In the presence

of defects, we will clearly distinguish solutions by denoting the stationary scattering solution u_k for the left region and v_k for the right region. As for the square-integrable wavefunctions solutions of the time-dependent Schrödinger equation, they are denoted u and v, respectively. Because φ_k is in general discontinuous at the origin, it is necessary to split the spatial integrals in (2.36) accordingly. Alternatively, the stationary solution φ_k can be expressed as

$$\varphi_k(x) = \theta(-x)\ u_k(x) + \theta(x)\ v_k(x), \tag{2.37}$$

where, for solutions continuous at the origin, the Heaviside function can take the value at the origin given by $\theta(0) = 1/2$. For φ_k discontinuous at the origin, that is not a possible choice and the value at the origin $\varphi_k(0)$ is not specified, but always understood in the limiting sense through the use of the sewing conditions only.

As a matter of finding the lowest backflow eigenvalue expression, we need to take the minimum of the expression (2.35) obtained from

$$\beta_V(f) = \frac{1}{2\pi}\int_0^\infty dk \int_0^\infty dk'\ \tilde{\jmath}^*(k')\tilde{\jmath}(k)L(k',k), \tag{2.38}$$

where we tacitly assume the existence of the lowest eigenvector $|J_{min}\rangle$ of the operator $J_V(f)$, for which the associated wavefunction, in momentum space, is denoted by $\tilde{\jmath}(k)$. That assumption is supported by the numerical analysis, which is explained in section 4.5. At the present moment, however, an explicit analytical solution for the lowest eigenvector is not known even in the free case. That is also the case for the temporal version of the backflow [8, 34].

— 3 —

Backflow in the presence of δ-defects

3.1 BACKFLOW IN THE PRESENCE OF A δ-DEFECT

We first review the backflow calculation in the presence of a δ-defect [11] because of its importance and as a stepping stone towards the jump-defect case that is the topic of discussion in the next Chapter 4. It shall be said that the δ can be seen as a Dirac delta potential term $V(x) = \lambda\delta(x)$, with $\lambda \in \mathbb{R}$ the strength of the potential, but also as an impurity or a point defect in the real line that is implemented by a set of matching or sewing conditions and is denominated δ-defect. After considering a single δ-defect, we take a further step and analyse the backflow in the presence of the double δ-defect. The latter is an interaction of physical interest and will be discussed in section 3.3. An important and direct consequence of that discussion will be the inclusion of the singular δ'-defect that has a discontinuity similar to that of the purely transmitting jump-defect. The δ'-defect will be obtained from the double δ-defect in the zero-range limit.

Although the δ potential function is not a $L_1^1(\mathbb{R})$-class potential (it is not a locally integrable function), it was shown in [11] that one can have a (rough) estimate of the lowest backflow eigenvalue, and the numerical results show that the δ potential is indeed a special case that also has a lower bound for its $\beta_V(f)$. Here we add to the numerical results and the analytical expression for (2.36) of the work contained in [11]. The aims for this are twofold: the lowest backflow eigenvalue displays a different behaviour for defect parameter values $|\lambda| < 1$ and the analytical calculation of (2.36), in the δ-defect case, highlights the differences with respect to the discontinuous jump-defect case. For the moment, let us introduce the following notation without further justification as

it will be further discussed in Chapter 4. The delta impurity (as a local defect) has matching conditions defined at a point, and its wavefunction in one spatial dimension can be split into left part ($x < 0$), denoted u, and right part ($x > 0$), denoted v, such that

$$u(0) = v(0) = \psi(0), \quad v_x(0) - u_x(0) = 2\lambda\psi(0), \tag{3.1}$$

where the evaluation of the wavefunction ψ, solution of the time-dependent Schrödinger equation, at zero is understood in the right and left limit sense. These are well-known consequences from the continuity of the wavefunction at the defect's location and the discontinuity of its spatial derivatives or slopes. More precisely, without focusing on issues of self-adjoint extensions, we shall mention that $V(x) = \lambda\delta(x)$ is a point interaction with wavefunction ψ, as a function in the domain of a self-adjoint Hamiltonian H, that belongs to the Sobolev space $W^{2,2}(\mathbb{R}\setminus\{0\}) = H^2(\mathbb{R}\setminus\{0\})$, the space of all $\psi \in L^2(\mathbb{R})$ whose first and second order (distribution) derivatives belong to $L^2(\mathbb{R})$, where

$$H^m(\mathbb{R}\setminus\{0\}) = \left\{\psi \in L^2(\mathbb{R}) |\ \partial^\alpha\psi \in L^2(\mathbb{R}),\ \forall\alpha,\ |\alpha| \le m\right\} \tag{3.2}$$

is the Sobolev space of order m, and m is a nonnegative integer. Note that the distributions and their derivatives are to be understood here with respect to test functions in $C_0^\infty(\mathbb{R}\setminus\{0\})$. We are interested in the Sobolev space $H^2(\mathbb{R}\setminus\{0\})$ of functions that admits a finite jump at the origin because defects discontinuities can be accommodated in this space. For that, we remark that an alternative definition of Sobolev spaces can be used on $\mathbb{R}\setminus\{0\}$ in which $H^2(\mathbb{R}\setminus\{0\})$ is the completion of $\{\psi \in C^2(\mathbb{R}\setminus\{0\}) \mid \|\psi\|_{2,2} < \infty\}$ with respect to the appropriate Sobolev norm, which is $\|\psi\|_{2,2} = \left(\sum_{|\alpha|\le 2}\|\partial^\alpha\psi\|_2^2\right)^{1/2}$, and $\|.\|_2$ is the usual L^2-norm. Moreover, as the origin is removed from the domain, the conditions (3.1) are the set of conditions connecting the value of the wavefunction ψ and its derivatives at the origin.

Let φ_k denote the solution for the TISE in the presence of a δ-defect. We can work with derivatives in the weak sense as both φ_k and its derivative $\partial_x\varphi_k$ are both locally integrable functions $\varphi_k \in L^1_{\text{loc}}(\mathbb{R})$, $\partial_x\varphi_k \in L^1_{\text{loc}}(\mathbb{R})$. The full square-integrable time-dependent solution to the Schrödinger equation is denoted by

$$\begin{aligned}\varphi(x,t) =& \frac{1}{\sqrt{2\pi}}\int_0^\infty dk\,\tilde{g}(k)\exp(-iwt)\varphi_k(x)\\ =& \frac{1}{\sqrt{2\pi}}\int_0^\infty dk\,\tilde{g}(k)\exp(-iwt)\left(\theta(-x)u_k(x) + \theta(x)v_k(x)\right),\end{aligned} \tag{3.3}$$

where $\tilde{g} \in C_0^\infty(\mathbb{R})$ is an arbitrary not identically zero and smoothly varying function used for producing the wave packet as a proper square-integrable $L^2(\mathbb{R})$-solution. As we established before, we denote the solution at the left of the defect by u and at the right by v. The time-independent scattering (from the left) states in position basis (2.19), compatible with the sewing conditions (3.1), are

$$\begin{aligned} u_k(x) &= \exp(ikx) + \frac{\lambda}{ik-\lambda}\exp(-ikx) \quad x<0, \\ v_k(x) &= \left(\frac{ik}{ik-\lambda}\right)\exp(ikx) \quad x>0, \end{aligned} \tag{3.4}$$

where the reflection coefficient $R(k)$ and the transmission coefficient $T(k)$ for the δ-defect are explicitly written. In particular, for the δ-defect, $\varphi \in H^1(\mathbb{R}) \cap H^2(\mathbb{R}\setminus\{0\})$ as it is continuous at the origin. We want to concentrate our attention on the time-independent part $\varphi_k(x)$ composed of (3.4) and, for that, the inner integral (2.36) reads

$$L(k',k) = \int dx \int dx' \left[(\theta(-x')u^\star_{k'} + \theta(x')v^\star_{k'})\, J(f)(x',x)\, (\theta(-x)u_k + \theta(x)v_k)\right]. \tag{3.5}$$

Since the expression (2.32) for $J(f)(x',x)$ has a factor of $-i/2$, we absorb it by working with $2iL(k',k)$ instead. Each term is expanded by the insertion of the $J(f)(x',x)$ and simplified after integration. Let us focus only on the spatial integrals, namely the kernel $2iL(k',k)$. First, we recall that a locally integrable function $\varphi \in L^1_{\text{loc}}(\mathbb{R})$ can be associated with a linear functional, a distribution, by $\langle\varphi,\phi\rangle = \int dx\, \varphi(x)\phi(x)$ with $\phi \in C_0^\infty(\mathbb{R})$. The derivative of that distribution is defined by $\langle\partial\varphi,\phi\rangle = -\langle\varphi,\partial\phi\rangle$. In this weak sense, the derivative (with respect to test functions in $C_0^\infty(\mathbb{R})$) of of our function φ_k is

$$\partial\varphi_k = (v_k(0) - u_k(0))\,\delta_0 + \varphi_k' \,, \tag{3.6}$$

where φ_k' denotes the (piecewise defined) strong derivative of φ_k that is undefined at the origin, and δ_0 is the Dirac delta distribution concentrated at the origin $x=0$, $\langle\delta_0,\phi\rangle = \phi(0)$. Also, the values of the functions u_k and v_k at the origin are understood in the limiting sense, $u_k(0) = \lim_{\varepsilon\to 0^-} u_k(\varepsilon)$ and $v_k(0) = \lim_{\varepsilon\to 0^+} v_k(\varepsilon)$. Because we know that the gap $v_k(0) - u_k(0)$ is actually zero for the δ-defect, the weak and the strong derivatives coincide outside the origin with the strong derivative undefined at the origin. The kernel can be written as the smearing with the test function f of the following

quantity involving φ_k and its first derivative

$$2iL(k',k) = \int dx' f(x') \left(\varphi^\star_{k'}(x') \frac{\partial \varphi_k(x')}{\partial x'} - \frac{\partial \varphi^\star_{k'}(x')}{\partial x'} \varphi_k(x') \right), \tag{3.7}$$

and the derivatives of φ_k are understood in the strong sense. It follows immediately that the integral can be split in two parts in terms of the functions u_k and v_k as

$$\begin{aligned} 2iL(k',k) = & \int_{-\infty}^{0} dx' f(x') \left(u^\star_{k'}(x') \frac{\partial u_k(x')}{\partial x'} - \frac{\partial u^\star_{k'}(x')}{\partial x'} u_k(x') \right) \\ & + \int_{0}^{\infty} dx' f(x') \left(v^\star_{k'}(x') \frac{\partial v_k(x')}{\partial x'} - \frac{\partial v^\star_{k'}(x')}{\partial x'} v_k(x') \right), \end{aligned} \tag{3.8}$$

where the derivatives are understood in the strong sense.

Finally, we can write down the lowest backflow eigenvalue as

$$\beta_V(f) = \frac{1}{2\pi} \int_0^\infty dk \int_0^\infty dk' \tilde{\mathcal{J}}^*(k') \tilde{\mathcal{J}}(k) L(k',k),$$

with the Hermitian kernel

$$\begin{aligned} 2L(k',k) &= (k+k') \int_{-\infty}^{0} dx' f(x') \exp(ix'(k-k')) \\ &+ \frac{\lambda(k'-k)}{(ik-\lambda)} \int_{-\infty}^{0} dx' f(x') \exp(-ix'(k+k')) \\ &- \frac{\lambda(k-k')}{(ik'+\lambda)} \int_{-\infty}^{0} dx' f(x') \exp(ix'(k+k')) \\ &+ \frac{\lambda^2(k+k')}{(ik'+\lambda)(ik-\lambda)} \int_{-\infty}^{0} dx' f(x') \exp(-ix'(k-k')) \\ &- \frac{kk'(k+k')}{(ik'+\lambda)(ik-\lambda)} \int_{0}^{\infty} dx' f(x') \exp(ix'(k-k')), \end{aligned} \tag{3.9}$$

which is obtained by the use of equation (3.4). Thus, the kernel is composed of contributions located at either the left $(-\infty, 0)$ of the defect or the right $(0, \infty)$ of the defect, and there is no contribution purely supported at the defect position.

In section 4.1.2, we will check conservation of energy, momentum and probability in the presence of a δ-defect and compare with the equivalent analysis applied to a situation described by a jump-defect. Then, the possibility of finding contributions to these physical quantities that are located precisely at the defect position will be

investigated. Such extra terms are regarded as contributions coming purely from the defect. Particularly, we will find that, provided they exist, these terms are finite and do not cause, for example, undesirable infinite energies despite the defect discontinuities. For the calculation of the lowest backflow eigenvalue $\beta_V(f)$, as the eigenfunction $\tilde{\mathcal{J}}(k)$ is not analytically known, we need to rely upon numerical calculations in order to plot the result. Some graphs for the δ-defect case can be found in section 3.2 along with a discussion of the results.

3.2 NUMERICAL RESULTS

Details on the numerical analysis can be found in section 4.5, including the definition of all parameters involved in the calculations. The backflow calculation in the presence of a δ-defect was analysed in section 3.1, and the corresponding kernel was analytically simplified to expression (3.9). Here, we present additional numerical results to those reported in [11], where the defect parameter was restricted to $|\lambda| = 1$. All the graphs refer to the probability current operator smeared with a Gaussian test function. Specifically, the graphs show the lowest backflow eigenvalue $\beta_V(f)$ against the center x_0 of the averaging Gaussian function f. Attractive refers to the case $\lambda < 0$, and repulsive to the case $\lambda > 0$. See the following figure 3.2 and figure 3.3 where we vary the parameter λ for displaying its behaviour under the strengthening or weakening of the interaction. In particular, in the limit $\lambda \to \pm\infty$, it becomes a purely reflecting situation, equivalent to a boundary theory. Naturally, when $\lambda \to 0$ the interaction-free case is obtained. For the free case, the lowest eigenvalue is represented by the line $\beta_0(f) \approx -0.241$. As shown by figure 3.2, there is a maximum of the lowest eigenvalue, in the attractive case, close to the defect's location when $|\lambda| < 1$. Moreover, the maximum seems to peak when the defect parameter is $\lambda = -1/2$. Despite not being included in this thesis, a few of other parameters around $\lambda = -1/2$ ($\lambda = -0.40, -0.45, -0.55, -0.60$) were explored and suggested that the maximum indeed peaks at $\lambda = -1/2$. This is a new observation. We do not have a physical explanation for it, but it is worth exploring in the future. Changing the width of the Gaussian causes the maximum to peak at different values of λ, but that is somehow expected as different widths also modify the backflow eigenvalue even in the interaction-free situation. Finally, sufficiently increasing its absolute value ($|\lambda| > 1$) causes the attractive and repulsive cases to approach each other.

Classically, the intuition underlying the different behaviours between $\lambda > 0$ (repulsive) and $\lambda < 0$ (attractive) is that the particle velocity is lower in the former case and higher in the latter case when compared with the free case. Hence, in the attractive case the backflow effect is weaker than in the repulsive case. From the point of view of quantum mechanics, the difference is more subtle. Note that the pole of the transmission and reflection coefficients in (3.4) is at $k = -i\lambda$. In the complex energy plane, bound states have imaginary part Im $k > 0$ and virtual states (or antibound states) have Im $k < 0$. Then, in the case of the δ-defect, while positive values of λ yield virtual states, negatives values of λ yield physical bound states. There are, therefore, two important factors determining the behaviour of the backflow constant at the left of the defect: backscattering and bound states. In the transmission region at the right of the defect, the situation in both cases is similar to the free case. In contrast to the left region, the right region has no superposition of incoming and reflected waves but only transmitted wave, which can shift away the backflow lowest eigenvalue from the free case, but $\beta_V(f)$ is still represented by a constant line. That is why the two curves, blue ($\lambda > 0$) and red ($\lambda < 0$), merge at the right of the defect.

Additionally to the two-dimensional plots, we have varied the parameter λ over a wide range for displaying three-dimensional pictures, figure 3.4 and figure 3.5, to illustrate how the lowest backflow eigenvalue $\beta_V(f)$ is affected in the presence of the δ-defect. This can be compared to the results of the double δ-defect in section 3.4 and to the results of Chapter 4 where the jump-defect parameter α varies, figures 4.9, 4.10, 4.12 and 4.13 in section 4.4. The only difference between figure 3.4 and figure 3.5 is that the former is plotted over a larger range of λ to show global aspects and the latter covers a smaller range of the parameter in order to exhibit local features around the defect's location. In particular, figure 3.5 shows very clearly that the peak at $\lambda = -1/2$ where $\beta_V(f) \approx -0.081$. All these results are stable against increasing the number N of discretization steps and the momentum cutoff P_{cutoff}.

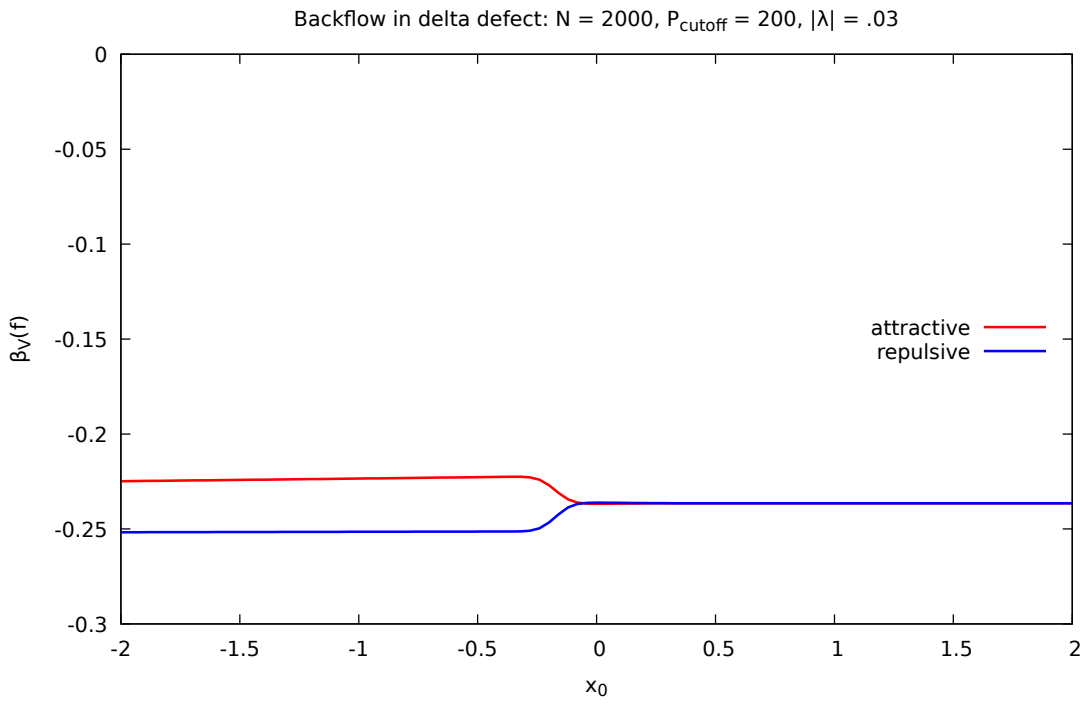

(a)

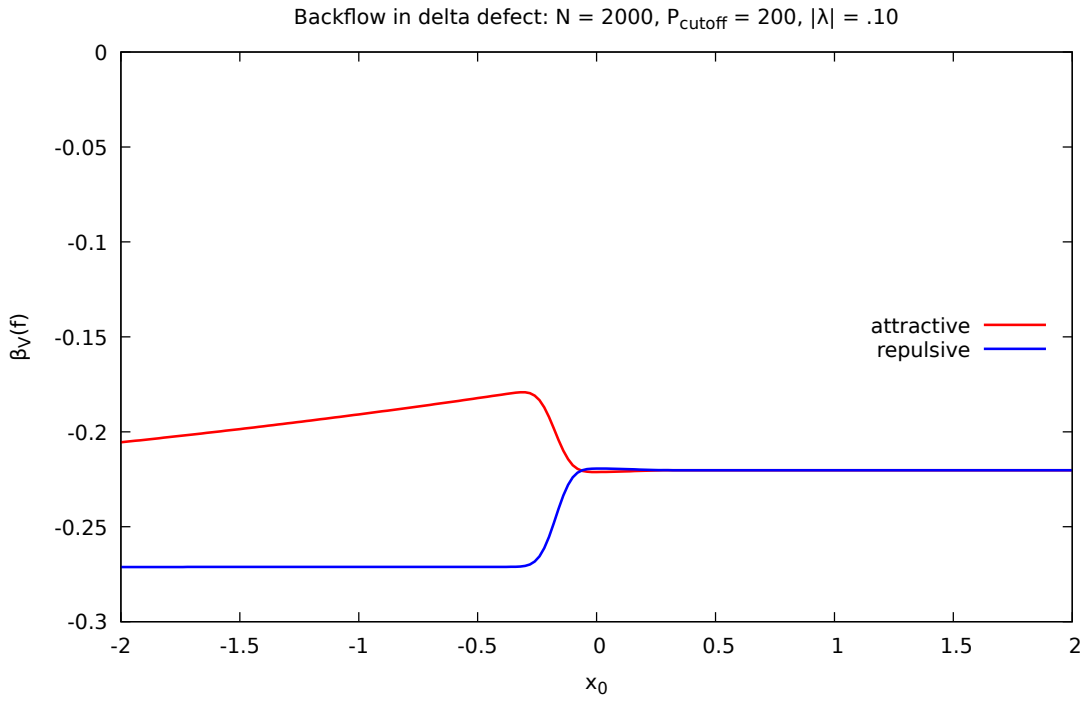

(b)

Figure 3.1: Lowest backflow eigenvalue of the current operator, for which (a) $|\lambda| = 0.03$ (b) $|\lambda| = 0.1$.

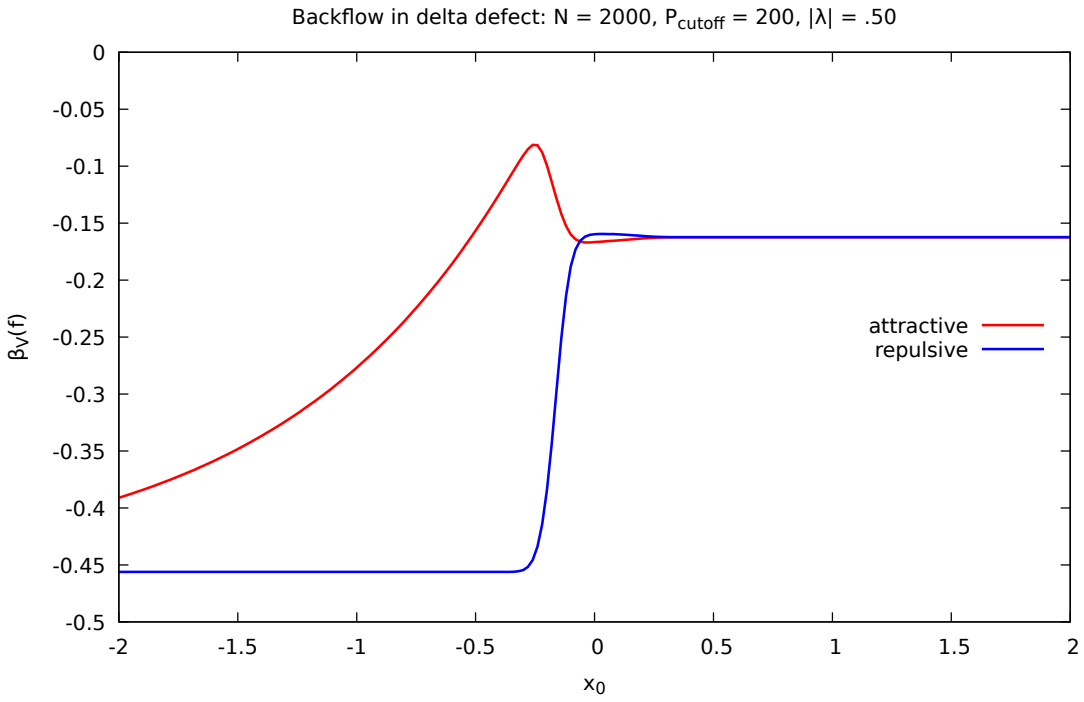

(a)

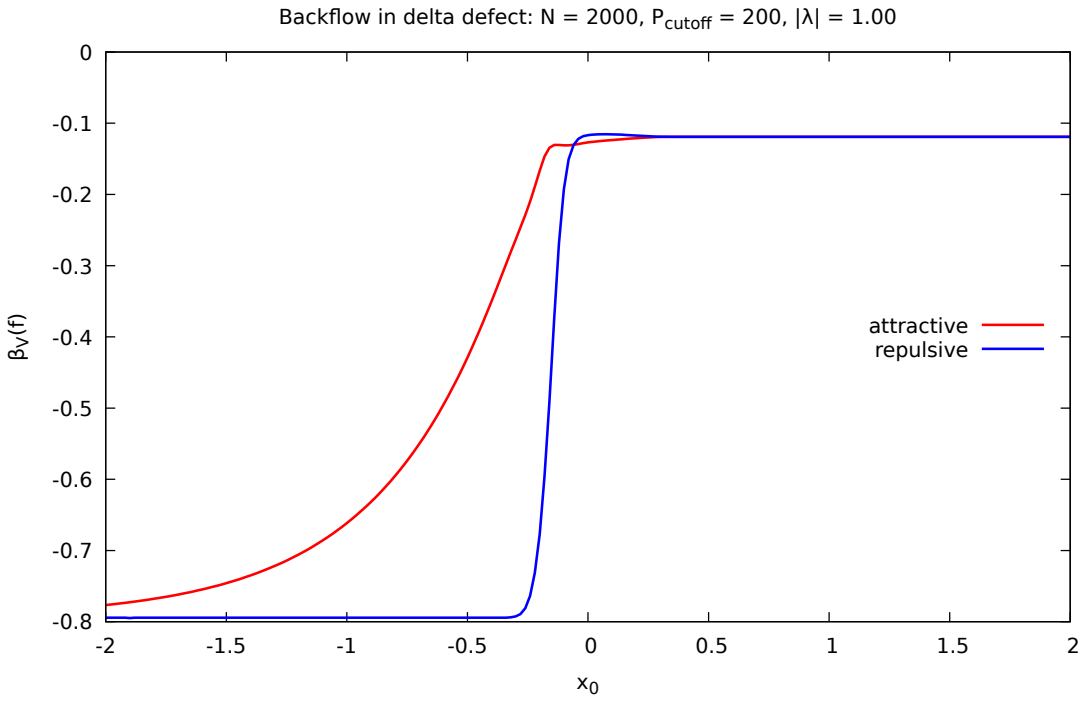

(b)

Figure 3.2: Lowest backflow eigenvalue of the current operator, for which (a) $|\lambda| = 0.5$ (b) $|\lambda| = 1.0$.

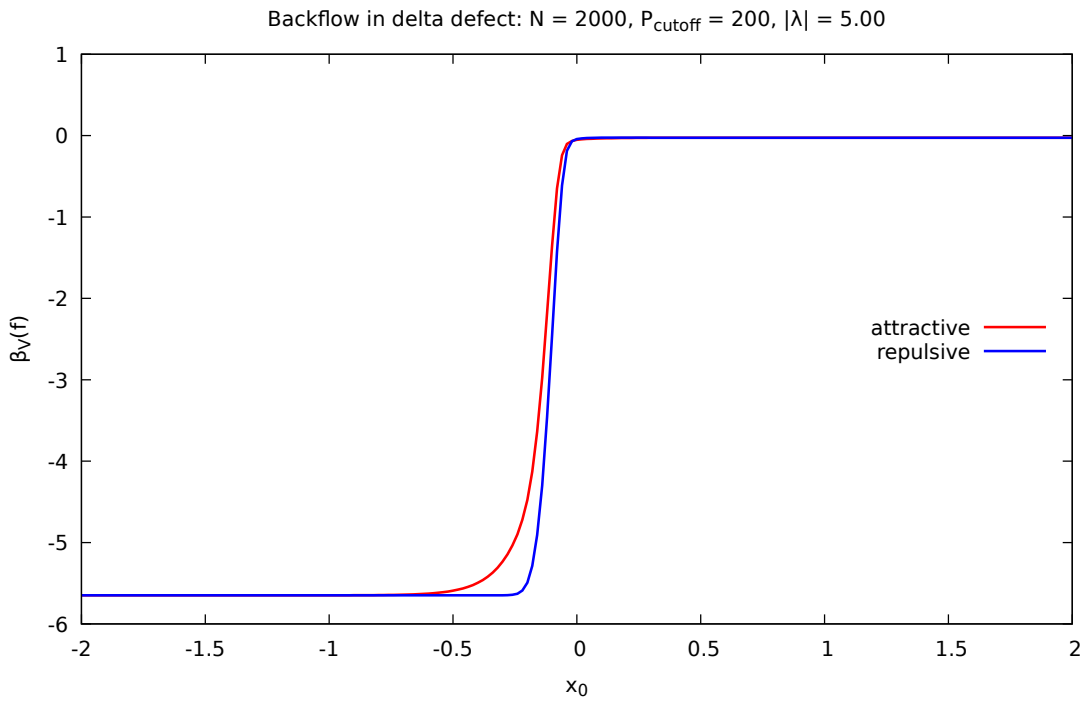

(a)

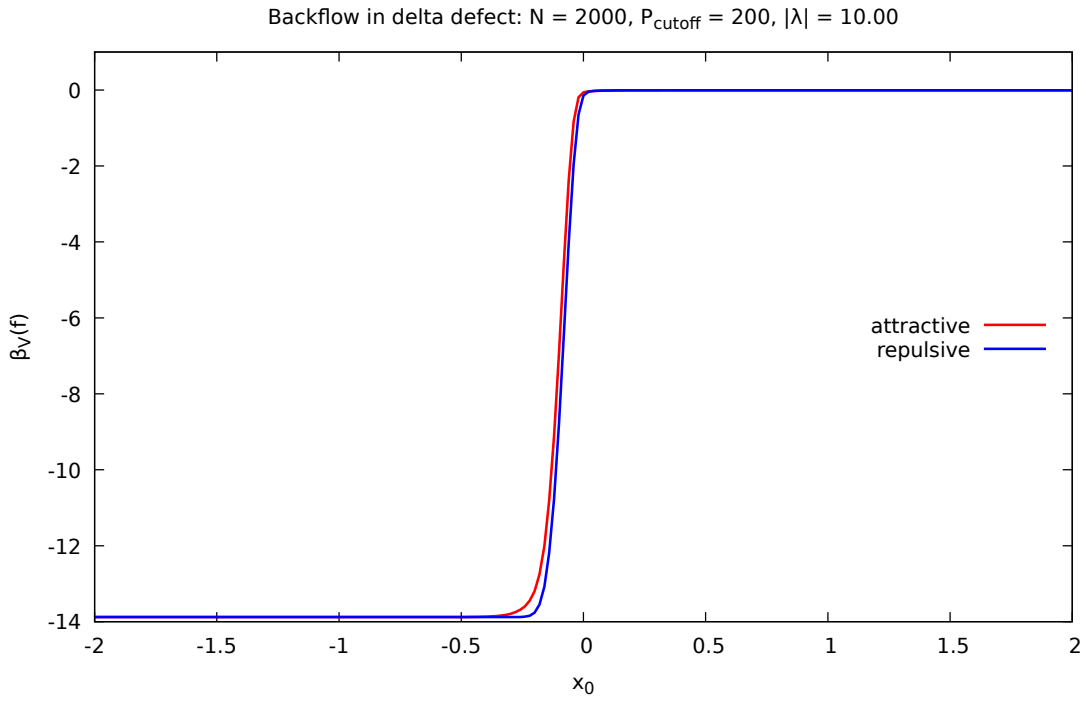

(b)

Figure 3.3: Lowest backflow eigenvalue of the current operator, for which (a) $|\lambda| = 5.0$ (b) $|\lambda| = 10.0$.

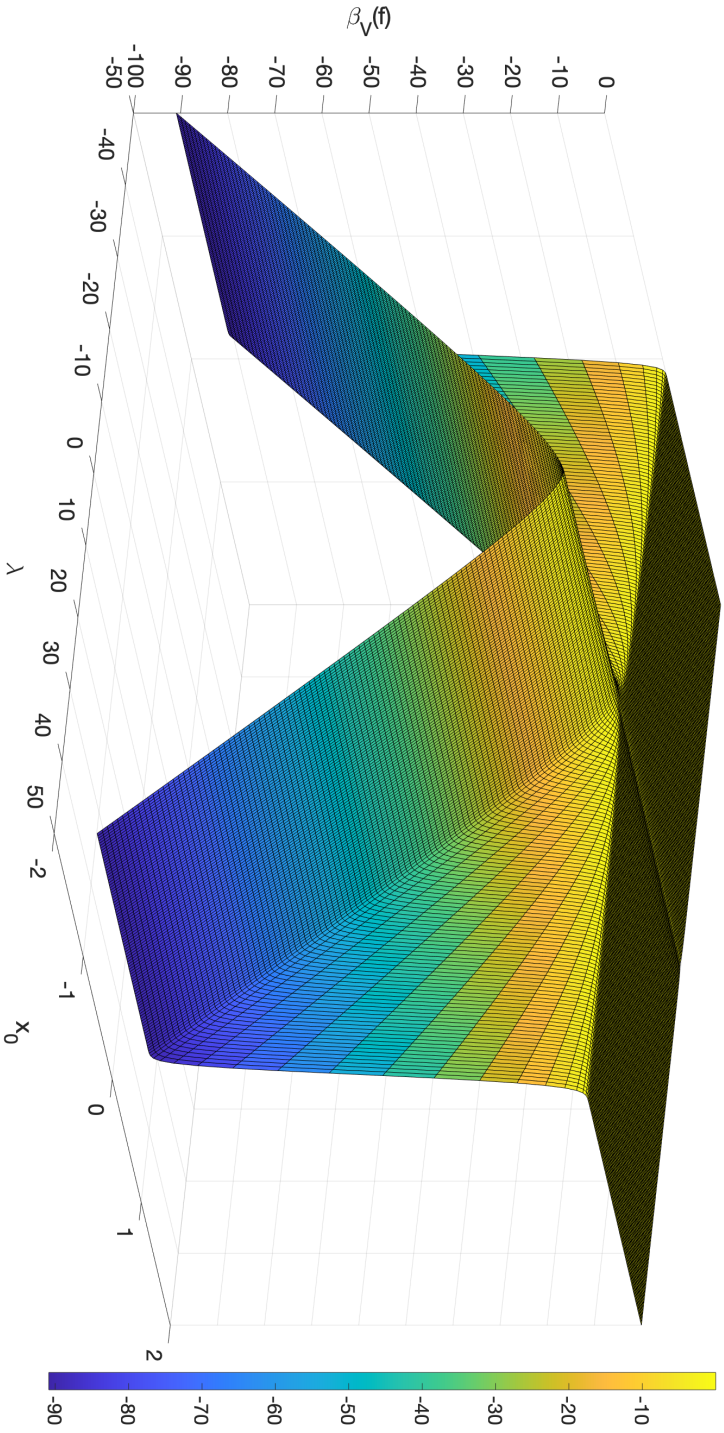

Figure 3.4: Probability current lowest eigenvalue for the δ-defect, $P_{\text{cutoff}} = 200$, $N = 2000$.

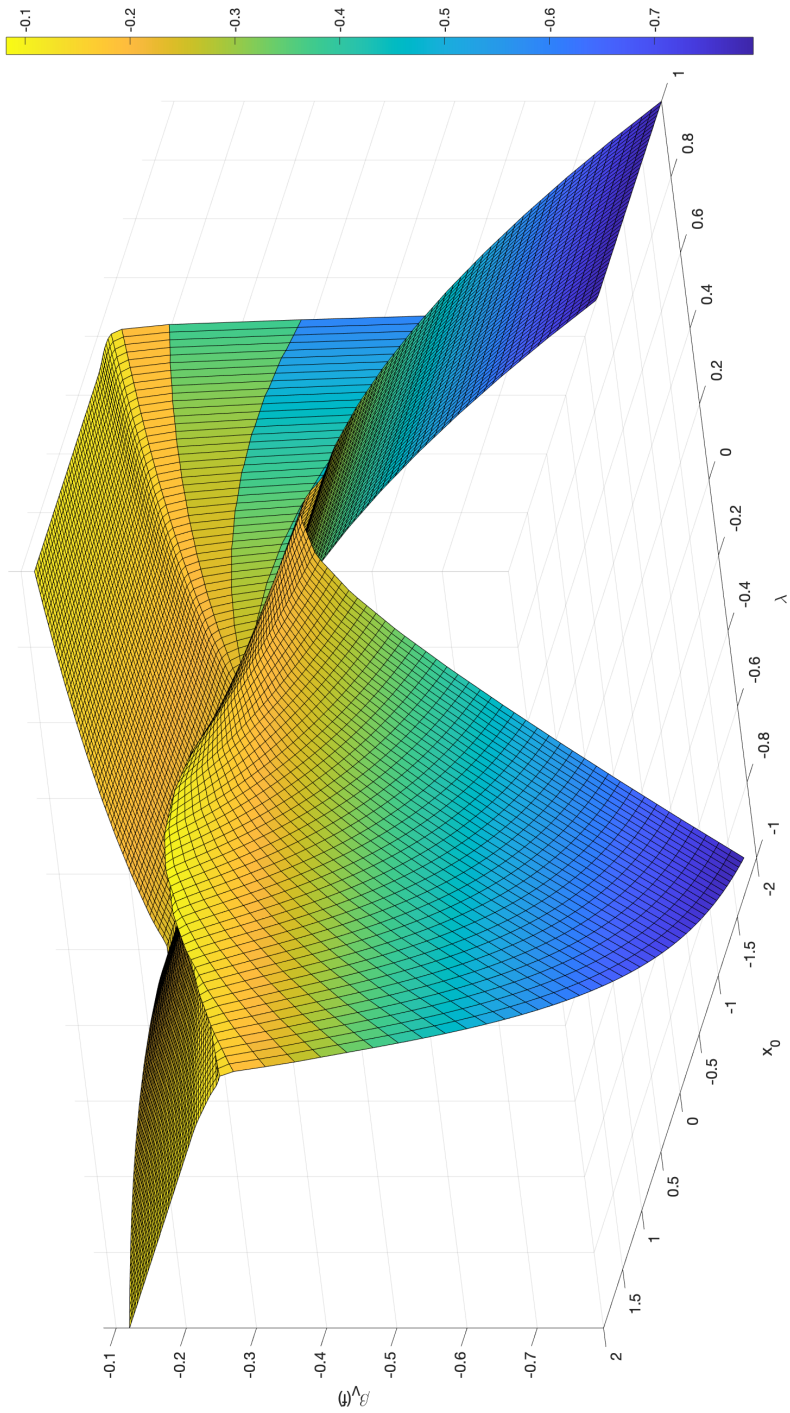

Figure 3.5: Probability current lowest eigenvalue for the δ-defect, $P_{\text{cutoff}} = 200$, $N = 2000$.

3.3 THE DOUBLE δ-DEFECT

While the δ-defect always describe a situation where the reflection coefficient $R(k)$ is non-zero, it can also be seen as a particular case from the more general double δ-defect. Given two δ impurities, each one located at a different point in the real line, the single δ-defect is obtained in the limit that these two defect's positions are the same. In that sense, the double delta case is more general and has additional features that are not present in the single delta case. For instance, the number of bound states can change up to two instead of a single bound state, the presence of resonances and the possibility of having a zero reflection coefficient, in other words a situation where the defect is transparent. In terms of applications in physical situations, the double delta can model, for example, the diatomic hydrogen gas molecule [21, 88] or the pair of plates in the Casimir effect [89, 90, 91]. Moreover, what would describe the derivative of a Dirac-δ as a quantum mechanical potential, or as a defect called δ'-defect, can be obtained from the double δ-defect in a limiting process where the deltas approach each other. Consequently, other more general situations as the double δ-δ'-defect can also be explored in the context of the Casimir effect and nuclear physics [92, 93]. Here we are interested in how the double δ-defect defers from the single δ-defect in regard to the quantum backflow effect. Most of the calculations related to the double delta are similar to those in the case of a single delta. Hence, we will rely on previous sections to present the results of this sections not in a detailed and lengthy exposition but highlighting some important points without significant losses.

For that purpose, the potential is now considered in its general form as $V(x) = \lambda_1\delta(x-a_1)+\lambda_2\delta(x-a_2)$, with real parameters λ_1 and λ_2, the potential strengths, and a_1 and a_2 the positions where the impurities are located in the real line such that $a_1 < a_2$. Exactly as before, the sewing conditions are defined only at the defect's location, a_1 and a_2, expressing the fact that the wavefunction is continuous at these two points and that there is a discontinuity of the slopes at the same points. Thus, in evident similarity to (3.1), the sewing conditions are

$$\begin{aligned} u(a_1) = w(a_1) = \psi(a_1), \quad w_x - u_x = 2\lambda_1 w(a_1), \\ w(a_2) = v(a_2) = \psi(a_2), \quad v_x - w_x = 2\lambda_2 v(a_2), \end{aligned} \tag{3.10}$$

where u, w, v correspond to the pieces of the wavefunction located at the left of the

first delta, $(x < a_1)$, in the middle between the two deltas $(a_1 < x < a_2)$, and at the left of the second delta $(x > a_2)$, respectively. The time-independent scattering states compatible with (3.10) can be shown to have the following form

$$\begin{aligned} u_k(x) &= \exp(ikx) + R(k)\exp(-ikx) \qquad x < a_1, \\ w_k(x) &= A(k)\exp(ikx) + B(k)\exp(-ikx) \qquad a_1 < x < a_2, \\ v_k(x) &= T(k)\exp(ikx) \qquad x > a_2, \end{aligned} \tag{3.11}$$

with $k > 0$, and the corresponding coefficients given as follows

$$\begin{aligned} A(k) &= \frac{k^2 + ik\lambda_2}{k^2 + ik(\lambda_1+\lambda_2) - \lambda_1\lambda_2\left(1 - \frac{\beta^2}{\alpha^2}\right)} \\ B(k) &= \frac{-ik\beta^2\lambda_2}{k^2 + ik(\lambda_1+\lambda_2) - \lambda_1\lambda_2\left(1 - \frac{\beta^2}{\alpha^2}\right)} \\ T(k) &= \frac{k^2}{k^2 + ik(\lambda_1+\lambda_2) - \lambda_1\lambda_2\left(1 - \frac{\beta^2}{\alpha^2}\right)} \\ R(k) &= \frac{-ik\left(\alpha^2\lambda_1 + \beta^2\lambda_2\right) - \lambda_1\lambda_2(\beta^2 - \alpha^2)}{k^2 + ik(\lambda_1+\lambda_2) - \lambda_1\lambda_2\left(1 - \frac{\beta^2}{\alpha^2}\right)}, \end{aligned} \tag{3.12}$$

where $T(k)$ is the transmission coefficient and $R(k)$ is the reflection coefficient and we have set $\alpha := \exp(ika_1)$ and $\beta := \exp(ika_2)$. In particular, if $a_1 = -a$ and $a_2 = a$, with $a > 0$, the potential is symmetrical when $\lambda_1 = \lambda_2 = \lambda$, and the interaction is entirely repulsive or entirely attractive. Similarly, the particular case where $a_1 = -a$ and $a_2 = a$ with $\lambda_1 = -\lambda_2 = \lambda$ corresponds to the antisymmetric situation composed of a mixture of attractive and repulsive interactions.

Alternatively to the use of sewing conditions to obtain the coefficients (3.12), one can write the solution to the time-independent Schrödinger equation in terms of the Lippmann-Schwinger (2.20) in the form

$$\begin{aligned} \varphi_k(x) &= \exp(ikx) + 2\lambda_1 \int G_k(x-y)\delta(y-a_1)\varphi_k(y)dy \\ &\quad + 2\lambda_2 \int G_k(x-y)\delta(y-a_2)\varphi_k(y)dy \\ &= \exp(ikx) + 2\sum_J \lambda_J G_k(x-a_J)\varphi_k(a_J), \end{aligned} \tag{3.13}$$

with index $J = 1, 2$ corresponding to a_1 and a_2, respectively, and the integral kernel

$$G_k(x-y) = \frac{1}{2ik} e^{ik|x-y|} \,. \tag{3.14}$$

The evaluation of $\varphi_k(x)$ at $x = a_I$, with index $I = 1, 2$, is given as follows

$$\varphi_k(a_I)\left[1 - 2\lambda_I G_k(a_I - a_I)\right] - 2\lambda_J G_k(a_I - a_J)\varphi_k(a_J) = \exp(ika_I), \tag{3.15}$$

with $I \neq J$. That can, more generally, be written in the matrix form

$$\begin{pmatrix} M_{11} & M_{12} \\ M_{21} & M_{22} \end{pmatrix} \begin{pmatrix} \varphi_k(a_1) \\ \varphi_k(a_2) \end{pmatrix} = \begin{pmatrix} \exp(ika_1) \\ \exp(ika_2) \end{pmatrix}, \tag{3.16}$$

where the components of the complex matrix M are expressed by

$$M_{IJ} = \begin{cases} 1 - 2\lambda_I G_k(a_I - a_I) & I = J, \\ -2\lambda_J G_k(a_I - a_J) & I \neq J. \end{cases} \tag{3.17}$$

As a result, at the defect's location, $\varphi_k(a_J)$ is

$$\varphi_k(a_J) = \sum_I \left(M^{-1}\right)_{JI} \exp(ika_I), \tag{3.18}$$

and, the scattering solution $\varphi_k(x)$ can be expressed

$$\varphi_k(x) = \exp(ikx) + \sum_{J=1}^{2}\sum_{I=1}^{2} \lambda_J \frac{e^{ik|x-y|}}{ik} \left(M^{-1}\right)_{JI} \exp(ika_I). \tag{3.19}$$

In particular, the reflection coefficient $R(k)$, for example, can be obtained from that when we consider $x < a_1$, and the transmission $T(k)$ in the region $x > a_2$.

The backflow analysis in the presence of finitely many δ impurities follows very similarly from the simpler case in the presence of a single one. In particular, the expression (2.36) will split into three regions of integration determined by $(-\infty, a_1), (a_1, a_2)$ and (a_2, ∞) corresponding to u, w and v, respectively. The asymptotic backflow constant in the presence of a double delta defect interaction is given by equation (2.38) with a kernel expression, to be compared with (3.9) and that can be calculated in a similar

manner as was done in the single delta case, given by

$$\begin{aligned}
2L(k',k) &= (k+k')\int_{-\infty}^{a_1} dx' f(x')\exp(ix'(k-k')) \\
&+ (k'-k)R(k)\int_{-\infty}^{a_1} dx' f(x')\exp(-ix'(k+k')) \\
&+ (k-k')R^\star(k')\int_{-\infty}^{a_1} dx' f(x')\exp(ix'(k+k')) \\
&- (k+k')R^\star(k')R(k)\int_{-\infty}^{a_1} dx' f(x')\exp(-ix'(k-k')) \\
&+ (k+k')A^\star(k')A(k)\int_{a_1}^{a_2} dx' f(x')\exp(ix'(k-k')) \\
&+ (k'-k)A^\star(k')B(k)\int_{a_1}^{a_2} dx' f(x')\exp(-ix'(k+k')) \\
&+ (k-k')B^\star(k')A(k)\int_{a_1}^{a_2} dx' f(x')\exp(ix'(k+k')) \\
&- (k+k')B^\star(k')B(k)\int_{a_1}^{a_2} dx' f(x')\exp(-ix'(k-k')) \\
&+ (k+k')T^\star(k')T(k)\int_{a_2}^{\infty} dx' f(x')\exp(ix'(k-k')).
\end{aligned} \tag{3.20}$$

As previously executed, the same numerical calculations are used in order to obtain the lowest eigenvalue $\beta_V(f)$, from (2.38), with the only difference being the number of interaction centers considered. It is easy to check that the backflow analysis in the general case of finitely many δ-defects immediately follows from the particular case of the double δ-defect. Because each delta represents a zero-range interaction or a point-defect, the asymptotic behaviour of the solution to the Schrödinger equation is greatly simplified, although the calculations quickly become laborious with the increase of the number of impurities. The case of infinitely many delta interactions, also known as Dirac comb, will not be considered here, but it can be treated as a limiting case where the number of impurities tends to infinity. In particular, the expression (3.19) would involve infinite sums corresponding to the infinitely many interaction centers. Furthermore,the double δ-defect can already be quite singular. The zero-range limit $a_1 \to a_2 \to 0$ turns the interaction into a more severe discontinuity that represents what will be called a δ'-defect and discussed in the next section.

3.4 NUMERICAL RESULTS FOR THE DOUBLE δ-DEFECT

The numerical analysis for the backflow effect in the presence of a double δ-defect is presented here in the form of graphs displaying the lowest eigenvalue $\beta_V(f)$ of the probability current operator as a function of the position of measurement x_0 that is the center of the positive test function f, chosen to be a Gaussian function. The reader can find the relevant details on the numerical analysis in section 4.5. Additionally, some three-dimensional plots, in terms of $\beta_V(f)$, position x_0 and potential strength λ, are included in this section.

Some of the particular choices we make when computing the backflow constant are here described. The more known case, well-covered in the literature, is the special case when the the defect's locations in the real line are $-a_1 = a_2 = a$ and with strength $\lambda_1 = \lambda_2 = \lambda$, the symmetric case, or $\lambda_1 = -\lambda_2 = \lambda$, the antisymmetric case. The symmetric one will be referred as a pair of identical deltas and the antisymmetric one will be referred as a pair of opposite deltas. These were considered in the present work, and the respective results provided below. Keeping the positions fixed, $-a_1 = a_2 = a$, one can also consider the case in which the strengths are related as $\lambda_1 = c\lambda_2$, where $c \in \mathbb{Z}$ is a constant of proportionality between the impurities. That possibility was contemplated in the numerical calculations with some few values chosen as reference and depicted in the plots therein. In accordance to what was done in the previous case of a single δ-defect, λ assumes positive and negative values in this section. To cover the various possibilities regarding the choice of signs and magnitudes, the results are organized in subsections as follows: identical pair of deltas 3.4.1, opposite pair of deltas 3.4.2 and general pair of deltas 3.4.3.

3.4.1 The case of identical double δ-defect

The pair of identical deltas is specially characterized by the condition that $\lambda_1 = \lambda = \lambda_2$. The terms attractive and repulsive refer to the sign of the potential strengths corresponding to the first and the second deltas in the double δ-defect. Attractive, therefore, represents the situation where both deltas have negative strengths, $\lambda_1 < 0$ and $\lambda_2 < 0$. Repulsive represents the pair of deltas where both deltas have a positive strength, $\lambda_1 > 0$ and $\lambda_2 > 0$. Here we consider the positions of each delta fixed with

$-a_1 = a_2 = 0.5$. Because it is an identical pair of deltas, the limiting case where they approach each other, $a_1 \to a_2$, is trivial in the sense that the result is effectively a single δ-defect with total strength twice the value of the individual strengths. Although we did not include here the results when $a_1 \to a_2$, we can confirm that the previously mentioned maximum peak, at $\lambda = -1/2$, for the backflow constant $\beta_V(f)$ in the presence of a single delta is reproduced setting $-a_1 = a_2 = 0.01$ and $\lambda_1 = \lambda_2 = -0.25$, as we may have expected from the results of section 3.2.

In evident similarity to the case of a δ-defect, the pair of identical deltas for very small perturbations, figure 3.6, shows that the attractive case has a less negative backflow constant than the repulsive case of opposite strength for almost the entire region at the left of the interaction centers. As in the previous single δ-defect case, backscattering and bound states are important factors determining the behaviour of the backflow constant at the left of the defects. However, in the middle region between the defects ($a_1 < x_0 < a_2$), $\beta_V(f)$ depends critically on the coefficients $A(k)$ and $B(k)$ from (3.12) that are connecting both defects, and an intuitive description of how $\beta_V(f)$ changes is not straightforward in the general case. In contrast to the case of a single δ-defect, the red and blue curves do not merge anymore in the transmission region at the right of the defects ($x_0 > a_2$). To understand this behaviour, note that, although $\beta_V(f)$ is given by a constant line in that region, the transmission coefficient $T(k)$ has different magnitudes depending on whether the pair of defects is attractive or repulsive. In the absence of reflection, we can expect a symmetric situation in which the backflow constant is the same far away at the left and at the right of the defects. It is also expected that the presence of bound states becomes more relevant without the backscattering contribution to the backflow. In particular, points of maxima of $\beta_V(f)$ should appear exactly at the defect position. In fact, these expectations will be met in the case of a purely transmitting jump-defect.

With the increase of the potential strength, represented by figures 3.7 and 3.8, the appearance and development of two peaks of maximum for negative values of the strength occur until a certain point where the peaks start to contract. In particular, while the highest peak in the backflow constant does not seem to be achieved for $\lambda = -1/2$ with $a = 0.5$, the two distinct peaks in the attractive case are connected by a minimum in between. After that, as the interaction becomes much stronger, the second interaction center looks as a totally reflecting wall while the first center has partial

transmission, figure 3.9. For a three-dimensional graph displaying all these features, see figure 3.10 and compare with the previous δ-defect in figure 3.4. Because the local features corresponding to small values $|\lambda|$ are less noticeable when considering a large range of the parameter λ, figure 3.11 shows a better representation of what happens for when the interaction is limited to $|\lambda| \leq 1$. That can be compared to figure 3.5 noticing the difference on the peaks in the attractive region where $\lambda < 0$.

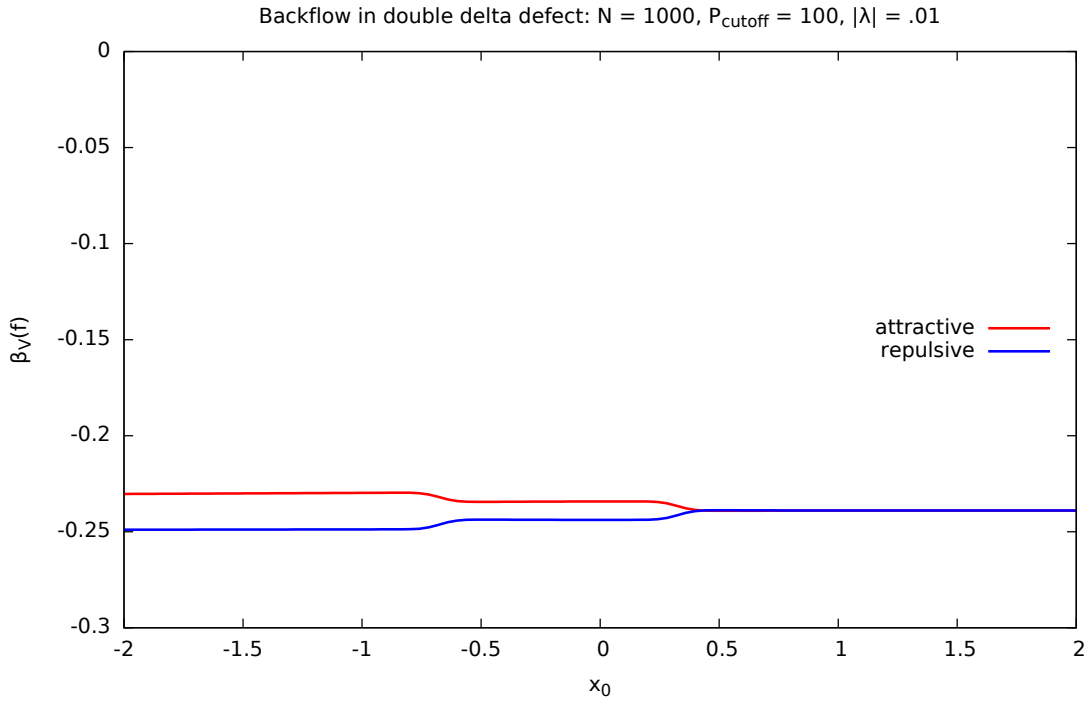

(a)

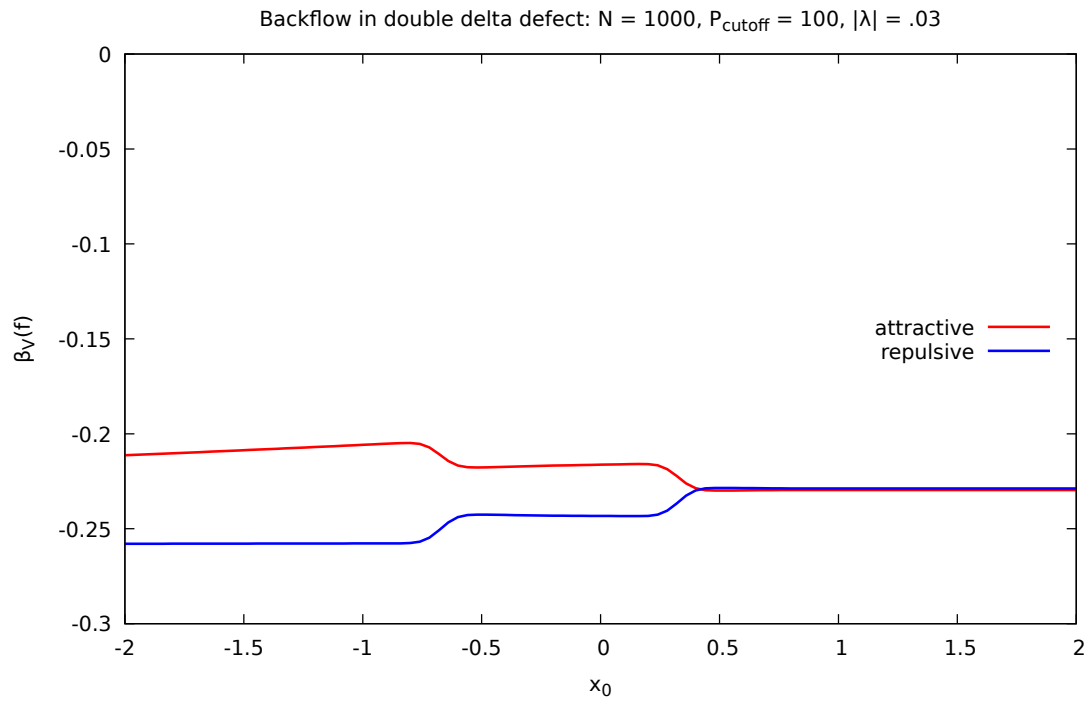

(b)

Figure 3.6: Lowest backflow eigenvalue of the current operator in the presence of a pair of identical deltas, $a_1 = -a_2 = -0.5$. (a) $|\lambda| = 0.01$ (b) $|\lambda| = 0.03$.

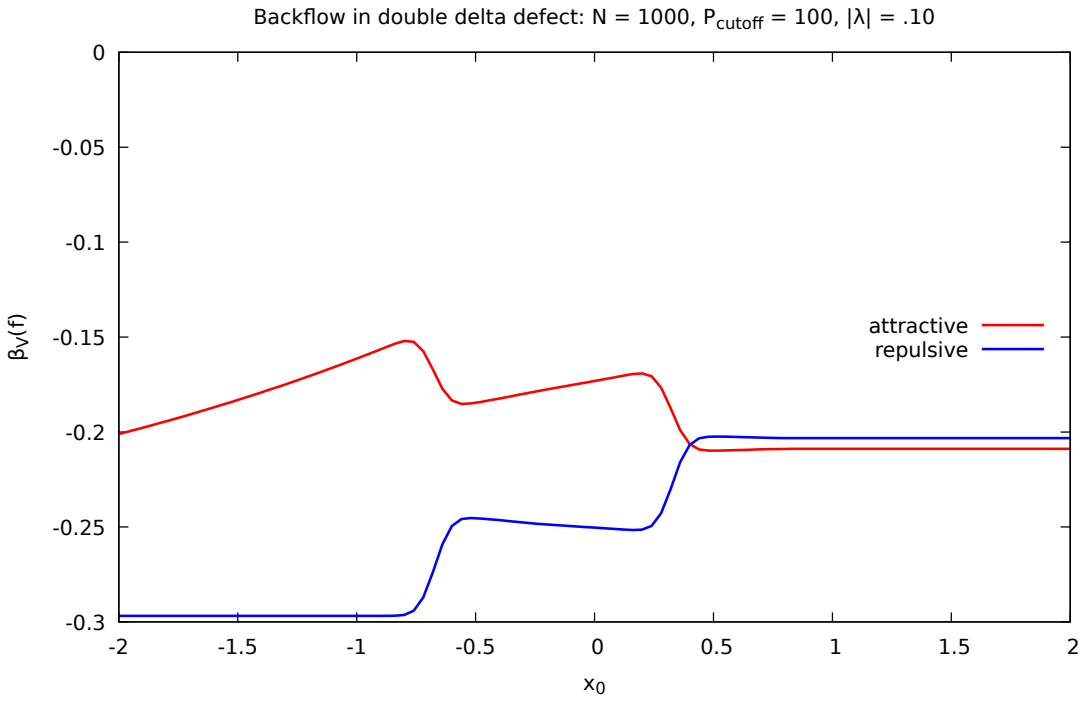

(a)

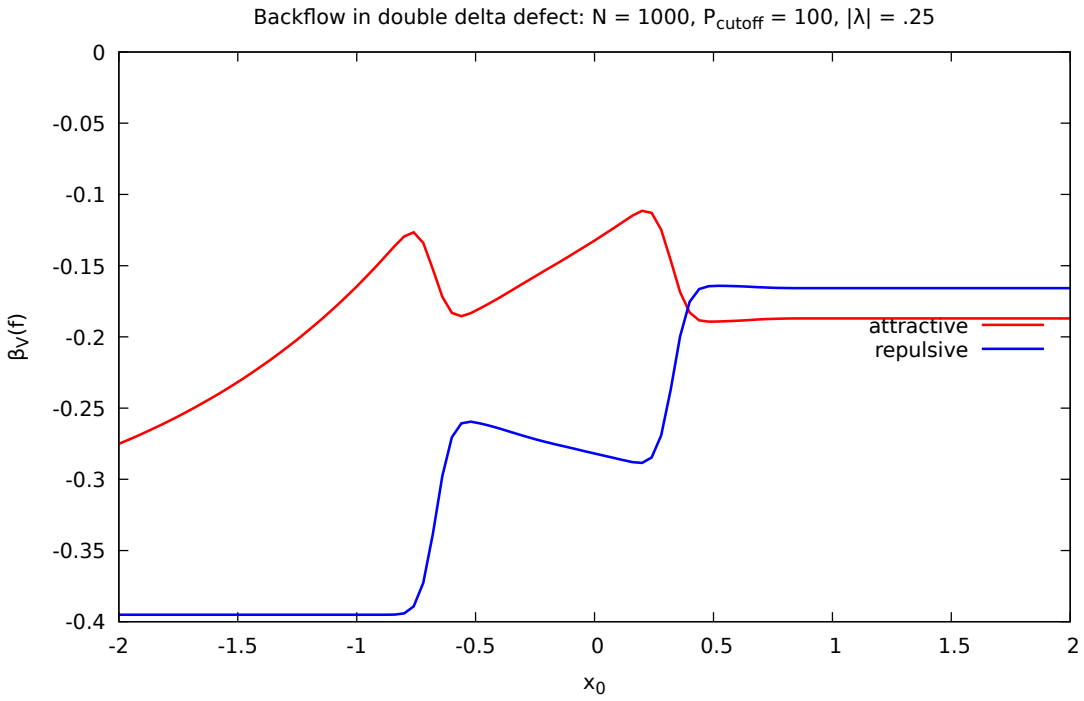

(b)

Figure 3.7: Lowest backflow eigenvalue of the current operator in the presence of a pair of identical deltas, $a_1 = -a_2 = -0.5$. (a) $|\lambda| = 0.1$ (b) $|\lambda| = 0.25$.

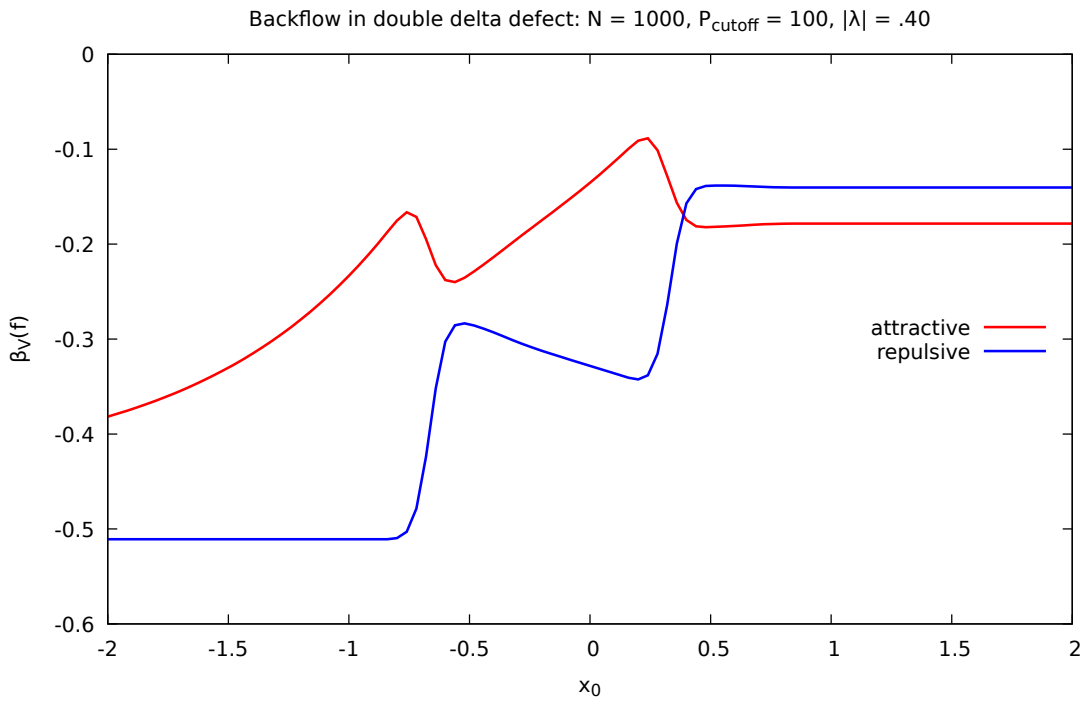

(a)

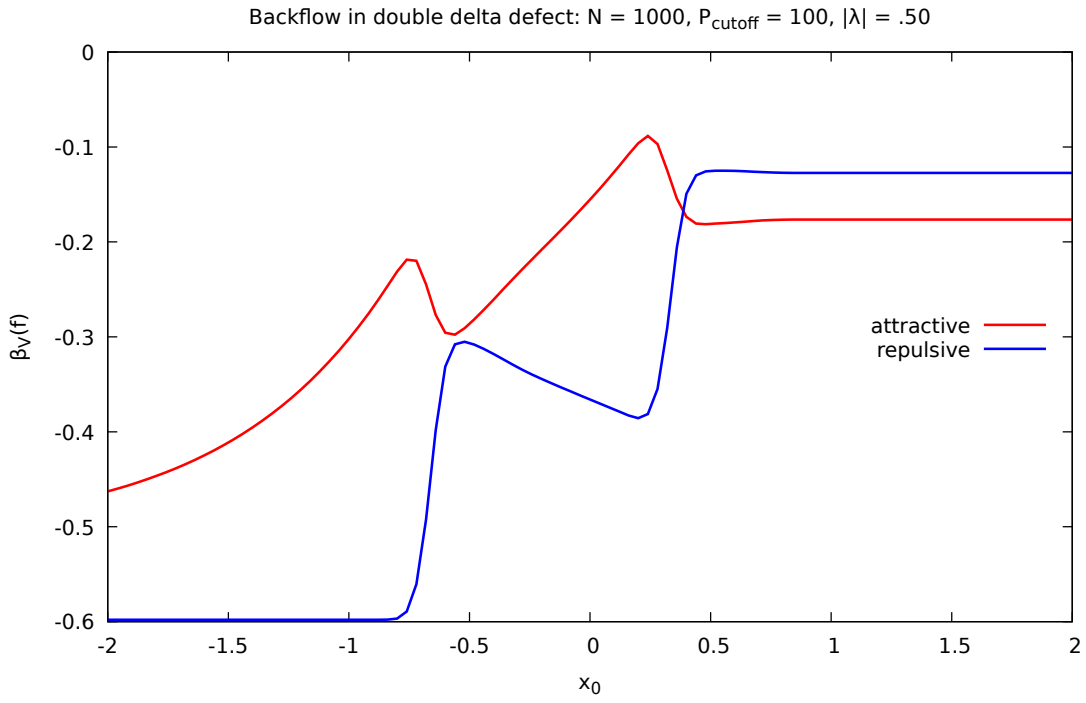

(b)

Figure 3.8: Lowest backflow eigenvalue of the current operator in the presence of a pair of identical deltas, $a_1 = -a_2 = -0.5$. (a) $|\lambda| = 0.4$ (b) $|\lambda| = 0.5$.

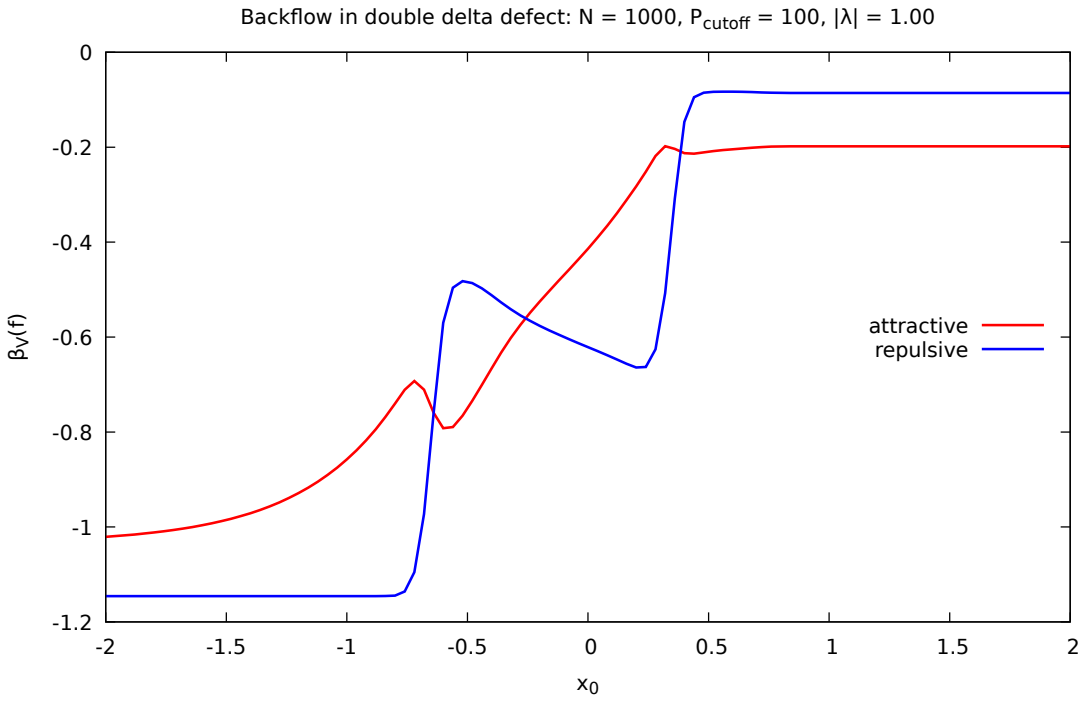

(a)

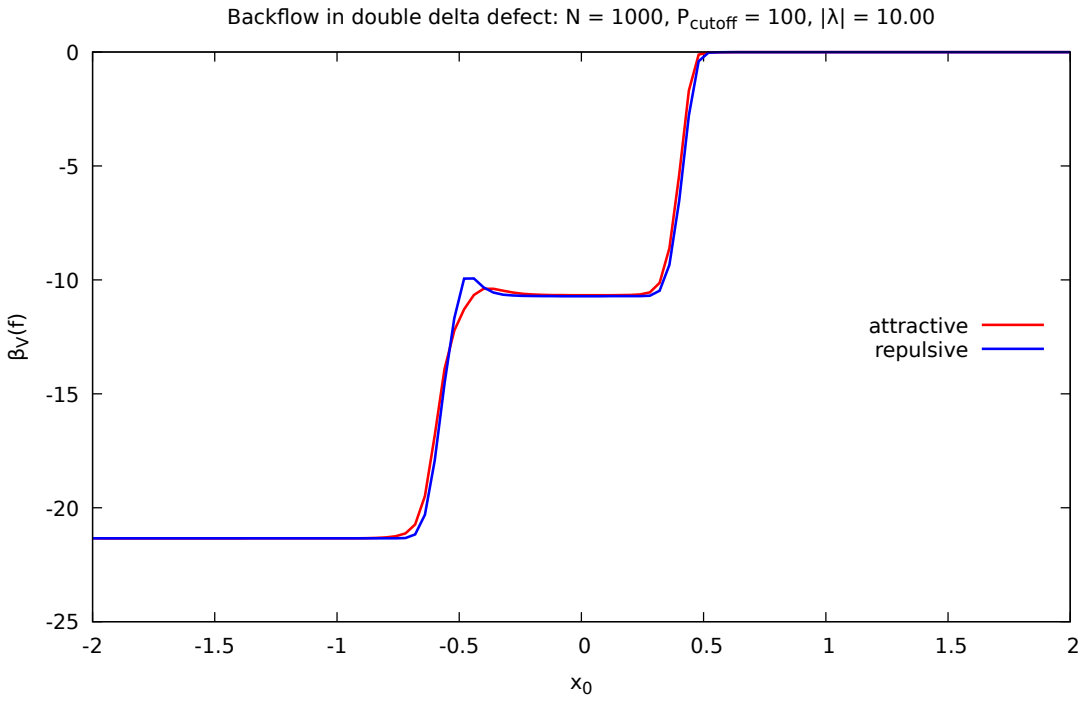

(b)

Figure 3.9: Lowest backflow eigenvalue of the current operator in the presence of a pair of identical deltas, $a_1 = -a_2 = -0.5$. (a) $|\lambda| = 1.0$ (b) $|\lambda| = 10.0$.

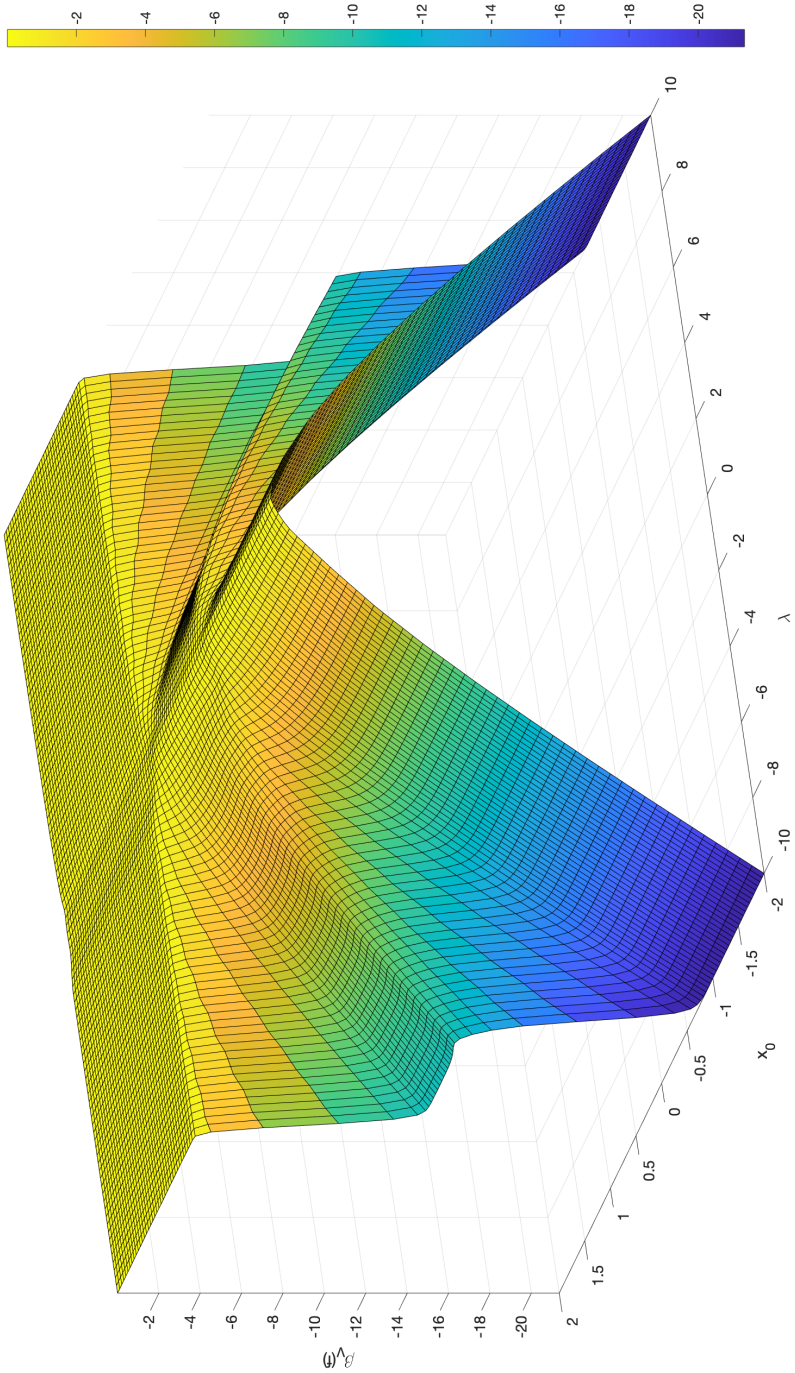

Figure 3.10: Probability current lowest eigenvalue for the double δ-defect with $a_1 = -a_2 = -0.5$ and $\lambda_1 = \lambda_2 = \lambda$, $P_{\text{cutoff}} = 200$, $N = 2000$.

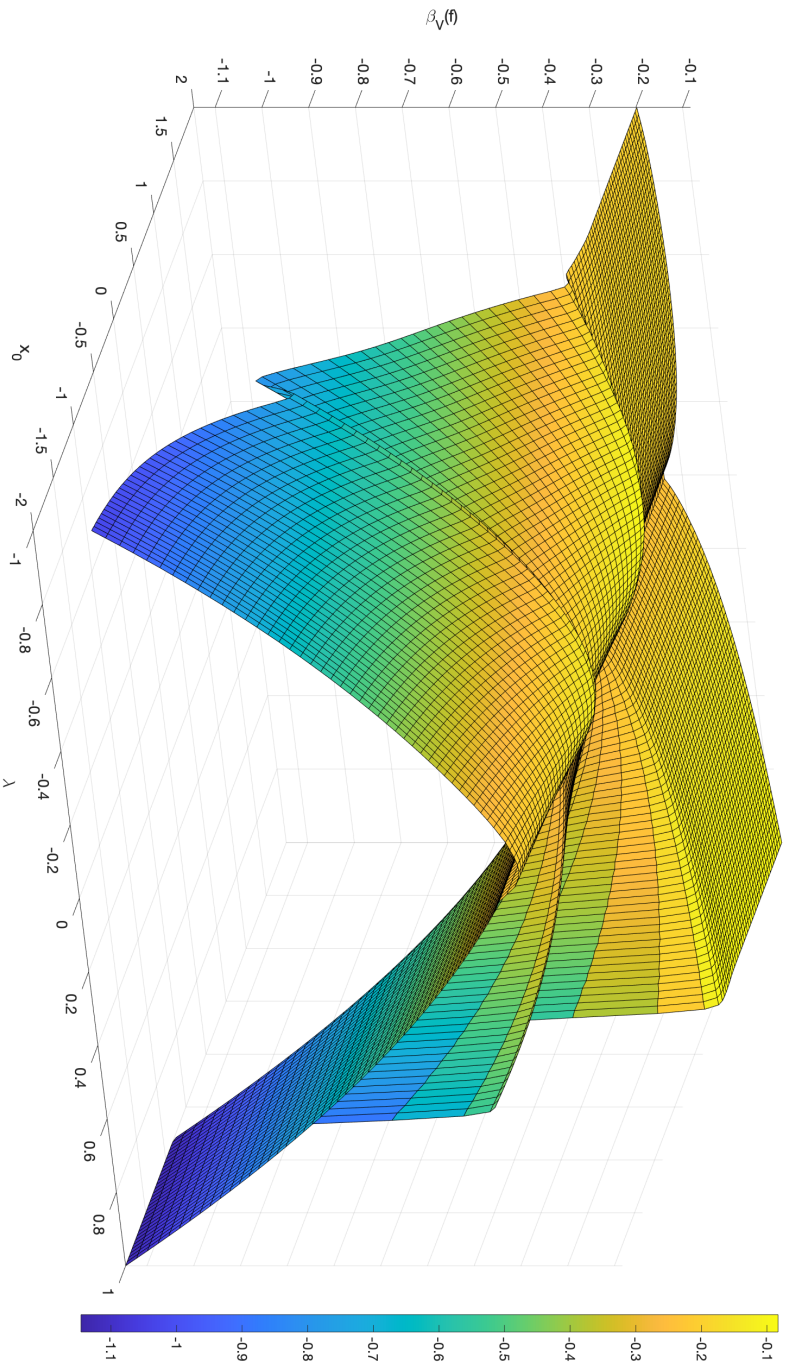

Figure 3.11: Probability current lowest eigenvalue for the double δ-defect with $a_1 = -a_2 = -0.5$ and $\lambda_1 = \lambda_2 = \lambda$, $P_{\text{cutoff}} = 200$, $N = 2000$.

3.4.2 The case of opposite double δ-defect

The pair of opposite deltas is specially characterized by the condition that $\lambda_1 = \lambda = -\lambda_2$. The terms "attractive-repulsive" and "repulsive-attractive" refer to the pair of signs of the strengths corresponding to the first and the second deltas in the double δ-defect. Attractive-repulsive, therefore, represents the situation where the first delta has strength $\lambda_1 < 0$ and the second has strength $\lambda_2 > 0$, and vice versa.

Differently from the identical pair of deltas, the opposite pair does not reduce to the case of a single delta when $a_1 \to a_2 \to 0$. In fact, that limit is interesting as it reproduces a different interaction, located at the origin, known as the derivative of the Dirac delta $\delta'(x) = d\delta(x)/dx$ with corresponding potential $V(x) = \mu\delta'(x)$, $\mu \in \mathbb{R}$. Due to the discontinuous nature of that interaction, there was a controversy as to what is the correct way of implementing it. More specifically, the product $\delta'(x)\psi(x)$ is ill-defined for a wavefunction ψ discontinuous at the origin. In summary, there are distinct interactions called δ' in the literature [94, 95, 96, 97, 98, 99, 80, 67, 100, 101, 102, 103, 104, 105, 106]. There are two distinct sets of sewing conditions called δ', and that caused confusion for some time. Although they both have a discontinuous wavefunction solution, one has continuous derivative at the defect's location and the other has in general a jump discontinuity in the derivative of its wavefunction. The former is characterized by the following pair of sewing conditions [95, 67]

$$\begin{aligned} v(0) - u(0) &= 2\mu\psi_x(0), \\ v_x(0) = u_x(0) &= \psi_x(0), \end{aligned} \tag{3.21}$$

which is invariant under a parity transformation ($x \mapsto -x$) and, therefore, incompatible with the $\delta'(x)$ that is an odd (generalized) function of x. Hence, the interaction represented by (3.21) does not describe a Hamiltonian perturbed by the derivative of a Dirac delta potential. The latter, differently, can be expressed by the pair of sewing conditions [98, 80]

$$\begin{aligned} v(0) &= \frac{1+\mu}{1-\mu}\, u(0), \\ v_x(0) &= \frac{1-\mu}{1+\mu}\, u_x(0), \end{aligned} \tag{3.22}$$

and is, in fact, a matching condition widely used in the literature to represent the interaction corresponding to the derivative of a Dirac delta potential. The respective

reflection and transmission coefficients are

$$\begin{aligned} R &= \frac{-2\mu}{1+\mu^2}, \\ T &= \frac{1-\mu^2}{1+\mu^2}, \end{aligned} \tag{3.23}$$

which are k-independent. Note that $\mu = \pm 1$ corresponds to a situation of zero transparency, purely reflecting, while $\mu \to \infty$ causes the reflection coefficient to approach zero, a purely transmitting case. For most values of the potential strength μ, there is a partial transmission. We remark that expressions (3.21) and (3.22) are matching conditions that do not explicitly refer to any regularization process of the singular δ'. Differently from that, however, Šeba's work [94] analysed the δ' potential function in terms of a pair of opposite deltas, also called a point dipole interaction. The δ' is obtained by the dipole interaction in the zero-range limit that

$$\delta'(x) = \lim_{\varepsilon \to 0} \left(\frac{1}{2\varepsilon} \right) \left[\delta(x+\varepsilon) - \delta(x-\varepsilon) \right], \quad \varepsilon > 0, \tag{3.24}$$

but Šeba proved some general results considering a family of regularized potentials $V_{\nu,\varepsilon,\mu}$ in the zero-range for the Hamiltonian [94]

$$H_{\nu,\varepsilon,\mu} = -\frac{1}{2}\frac{d^2}{dx^2} + \lim_{\varepsilon \to 0} \left(\frac{\mu}{2\varepsilon^\nu} \right) \left[\delta(x+\varepsilon) - \delta(x-\varepsilon) \right], \quad \nu > 0, \tag{3.25}$$

which can be achieved from our notation on the double δ-defect by effectively setting $\lambda_1 = \mu/(2\varepsilon^\nu)$ and $\lambda_2 = -\mu/(2\varepsilon^\nu)$ together with $a_1 = -\varepsilon$ and $a_2 = \varepsilon$. That interaction can be classified in three different situations depending upon the value of the parameter ν when $\varepsilon \to 0$. If $\nu < 1/2$, the interaction reduces to a purely transmitting case where the transmission coefficient $T(k) \to 0$. If $\nu = 1/2$, the interaction is equivalent to a single delta, which is partially transparent, with the relation $\lambda = -\mu^2/2$. Finally, for $\nu > 1/2$, the interaction becomes a totally reflecting wall causing the half-lines $(-\infty, 0)$ and $(0, \infty)$ to become completely disjoint. That result seems to show that the δ' interaction ($\nu = 1$) is not of a physical interest. However, changing the limiting process [102] in which that interaction (3.24) is obtained, specifically by considering a family of regularizing potentials with the inclusion of a second regularizing parameter in addition to the parameter ε, allows two distinct situations as a result. The first one is purely reflecting, in agreement with [94], and the other, depending on the value

of the parameter μ, can be either purely reflecting (for most values of μ) or partially transparent (for a countable resonance set $\Gamma = \left\{\mu \,|\, \tan\sqrt{\mu} = \tanh\sqrt{\mu}\right\}$). In terms of sewing conditions, these can be stated as [107]

$$\begin{aligned} v(0) &= \theta(\mu)u(0) \\ v_x(0) &= \theta^{-1}(\mu)u_x(0) \end{aligned} \tag{3.26}$$

with coupling function $\theta : \Gamma \to \mathbb{R}$ given

$$\theta(\mu) = \frac{\cosh\sqrt{|\mu|}}{\cos\sqrt{|\mu|}}, \quad \mu \in \Gamma. \tag{3.27}$$

Otherwise, when $\mu \notin \Gamma$, the totally reflecting wall is obtained with the Dirichlet boundary condition at the origin, $u(0) = v(0) = 0$. As a consequence, the corresponding reflection and transmission coefficients are

$$\begin{aligned} R &= \frac{1-\theta^2(\mu)}{1+\theta^2(\mu)} \quad \text{for } \mu \in \Gamma, \\ T &= \frac{2\theta(\mu)}{1+\theta^2(\mu)} \quad \text{for } \mu \in \Gamma. \end{aligned} \tag{3.28}$$

Alternatively, when $\mu \notin \Gamma$, the coefficients are $R = -1$ and $T = 0$, representing the totally reflecting wall. Note that again, similarly to (3.22), these do not depend on k. This result, in disagreement with [94], means that a model for the δ' interaction contains hidden parameters [108, 107]. In other words, the operator obtained in the zero-range limit from a family of short-range potentials depends on the choice of the regularization, and, therefore, different approximating families of potentials produce different results.

Taking together all the facts described in this section, there is a discrepancy between the results for a δ' interaction depending on whether the results are derived from the sewing conditions (3.22) or from a regularization process of this singular interaction. The problem is essentially related to the fact that the product $\delta'(x)\psi(x)$ is ill-defined for ψ discontinuous at the origin. Similar situation will be the main topic of the discussion of the backflow in the presence of a jump-defect in the next Chapter 4. The way in which we approximate our results to describe the backflow effect in the presence of a δ'-defect is by using the sewing conditions (3.10) for a pair of opposite deltas in the limit that $a \to 0$. The backflow results for a pair of opposite deltas in the zero-range limit are

results for a point dipole interaction. Physically, a point dipole interaction corresponds to a situation where a small region of large repulsive interaction is immediately followed by a small region of large attractive interaction. Possible technological applications where this interaction is explored include, for example, nanodevices in semiconductor physics [109]. Because of the numerical limitations in our analysis, we restricted the distance a to a few values: $a = (0.5, 0.1, 0.01)$.

Starting from the case where $a = 0.5$, the results show that, for small values of the potential strength λ, figure 3.12, there is not much difference between the cases attractive-repulsive and repulsive-attractive in positions sufficiently distant from the interaction centers. That is different from the previous subsection with an identical pair of deltas where attractive and repulsive are easily distinguished by their lowest backflow eigenvalue even for sufficiently distant positions x_0, as can be seen in figures 3.6 and 3.7. As the potential strength increase, that distinction starts to be noticeable, figure 3.13. In particular, the attractive-repulsive case starts to develop a peak before the first interaction center and the repulsive-attractive case develops its peak immediately before the second interaction center, as expected from our previous results describing the behaviour of the backflow constant for attractive and repulsive interactions; see figure 3.14. For very large values $|\lambda|$, figure 3.15, the totally reflecting wall is achieved but with an almost constant $\beta_V(f)$ in the region between the pair of deltas ($a_1 < x_0 < a_2$). In figure 3.16, with a smaller $a = 0.1$, the result shows small bell-shaped bumps near to the origin with a backflow constant $\beta_V(f) \approx \beta_0(f)$ for sufficiently far from the origin positions x_0. Interestingly, this is very similar to the case of the purely transmitting jump-defect for small values of $|\alpha|$, figure 4.2 in Chapter 4. As the potential strength increases, figure 3.18, the bumps distort into a situation of partial transmission where the previous apparent symmetry between far left ($x_0 << 0$) and far right ($x_0 >> 0$) positions is broken. Very strong potential strengths, shown in figure 3.19, cause the split of the real line into separate regions $(-\infty, 0)$ and $(0, \infty)$. Finally, for the smallest $a = 0.01$, the presence of bell-shaped bumps, starting from very weak non-zero potential strengths, figure 3.20, persists for a larger range of λ, see the case of $|\lambda| = 1$ in figure 3.21. As before, there seems to be some distortions implying a situation of partial transmission, but these happen in a smaller range of λ if compared to previous cases where $a = 0.5$ or $a = 0.1$. As the potential strength increases, the bumps swiftly disappear and become a wall with partial transmission until the point where there is no transmission,

corresponding to a total reflecting wall with Dirichlet boundary condition at the origin that effectively cause the probability current to be zero at the origin, figure 3.22.

The results presented in this section do not show an indication that there is a particular non-zero and finite value of the potential strength μ that will turn the interaction into a purely reflecting situation as implied by the set of sewing conditions (3.22). Moreover, for a fixed but small distance $a = \varepsilon$, successively increases of $|\lambda|$, which also implies the increase of μ, has the effect of approximating the interaction to a completely reflecting wall so that $R \to 0$. In that sense, the behaviour is more similar to what is predicted by the regularization process leading to (3.28), namely the complete separation of the regions $(-\infty, 0)$ and $(0, \infty)$ characterized by a zero probability current at the origin. Although our results show a partial transmission obtained from a continuous range of values of the parameter μ, rather than from a discrete range of values, this range seems to shrink as the distance a becomes smaller. Evidently, our analysis was restricted by the smallest distance considered that was $a = 0.01$, which may not be enough to simulate the limiting process in which the dipole interaction becomes a δ'-defect. Nevertheless, the presence of partial transmission indicates that, in contrast to [94], the δ'-defect is not simply equivalent to a totally reflecting potential wall.

In addition to the plots of the backflow constant against the position of measurement x_0, three-dimensional plots, including the variation on the potential strength λ, for the case where $a = 0.5$ and $a = 0.1$ are presented below. In figure 3.23, for $a = 0.5$, the region in between the pair of deltas ($a_1 < x_0 < a_2$) reveals some structure that does not appear to be present in figure 3.24 where the pair of deltas is much closer to each other, $a = 0.01$. The latter seems to glue together two different behaviours, as for the backflow constant, represented by the the regions $x_0 < 0$ and $x_0 > 0$. That difference can be highlighted when compared to the pair of identical deltas in figure 3.11. It is also worth comparing these results to the three-dimensional plots corresponding to the case of a single δ-defect, 3.5, which shares some similarities to figure 3.23 and figure 3.24 in terms of the shape of the graph, specially for points x_0 far from the origin and for larger values of $|\lambda|$. However, the single delta case connects the regions $x_0 < 0$ and $x_0 > 0$ in a smoother manner for $\lambda < 0$ where there is the presence of a maximum peak around $\lambda = -1/2$, as discussed before.

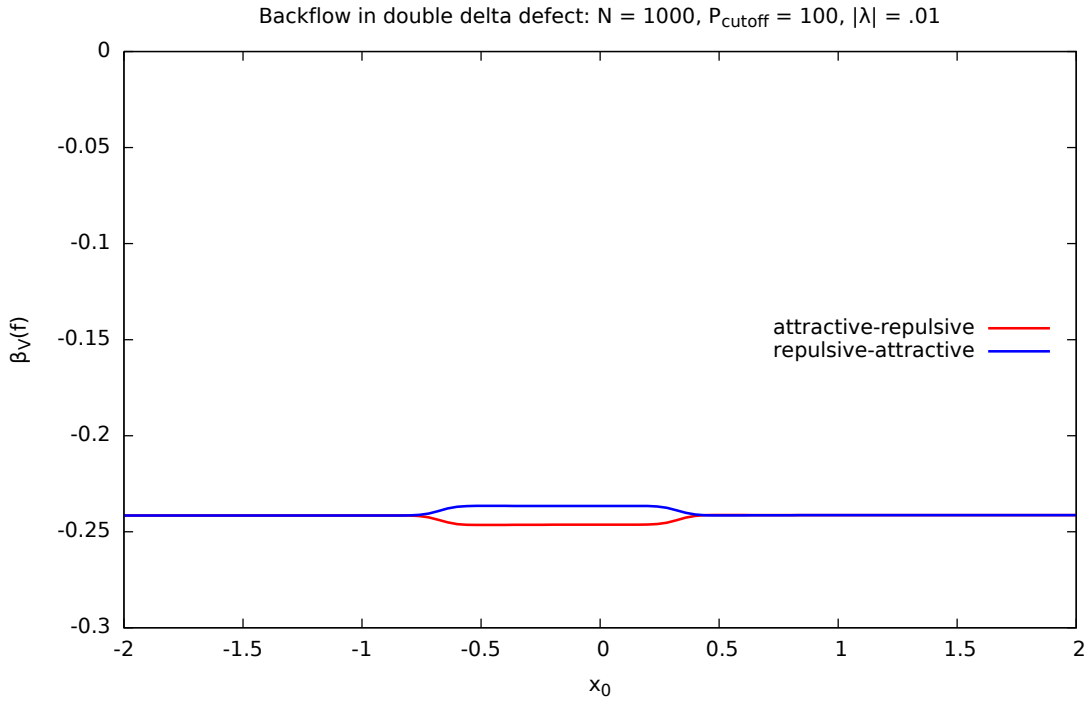

(a)

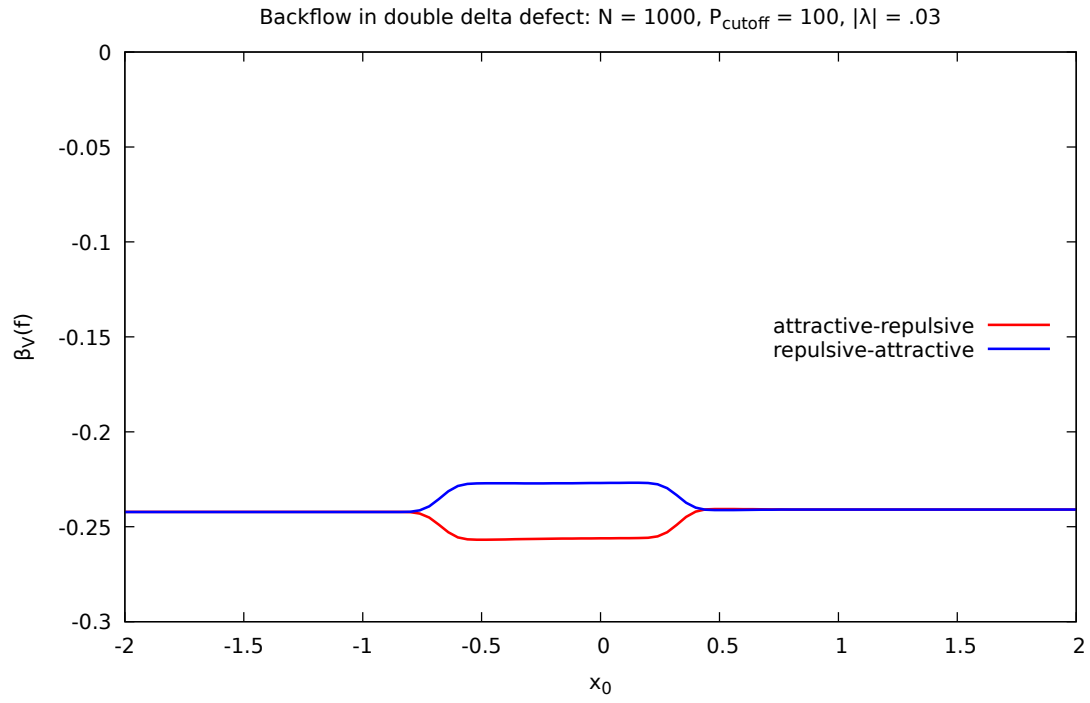

(b)

Figure 3.12: Lowest backflow eigenvalue of the current operator in the presence of a pair of opposite deltas, $a_1 = -a_2 = -0.5$. (a) $|\lambda| = 0.01$ (b) $|\lambda| = 0.03$.

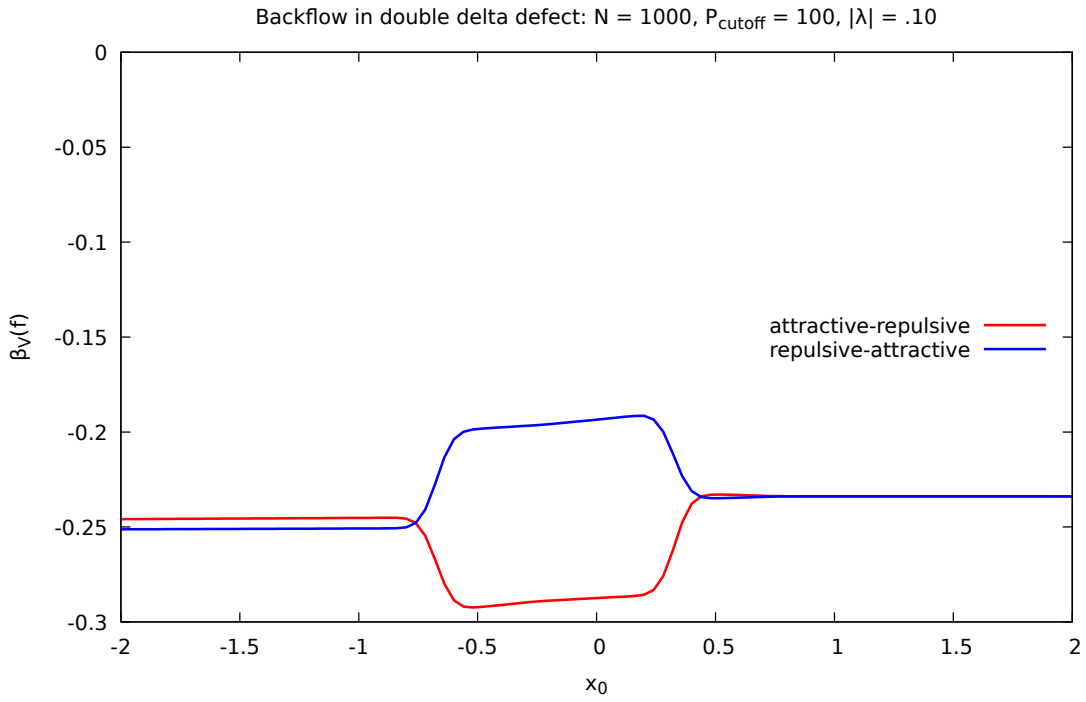

(a)

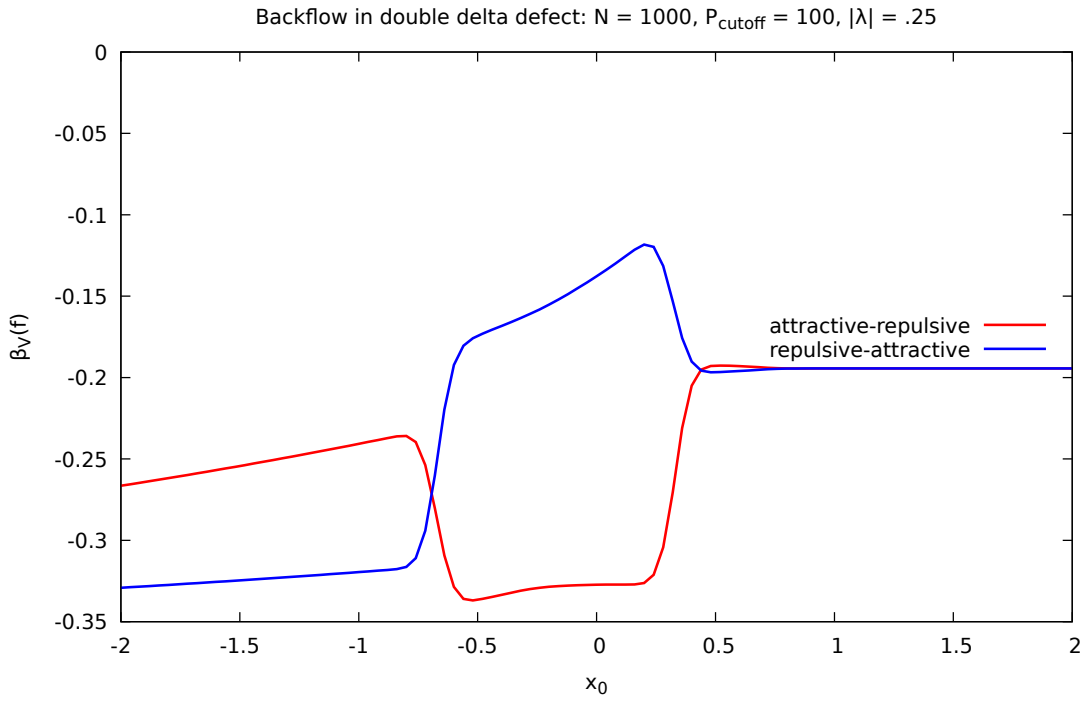

(b)

Figure 3.13: Lowest backflow eigenvalue of the current operator in the presence of a pair of opposite deltas, $a_1 = -a_2 = -0.5$. (a) $|\lambda| = 0.1$ (b) $|\lambda| = 0.25$.

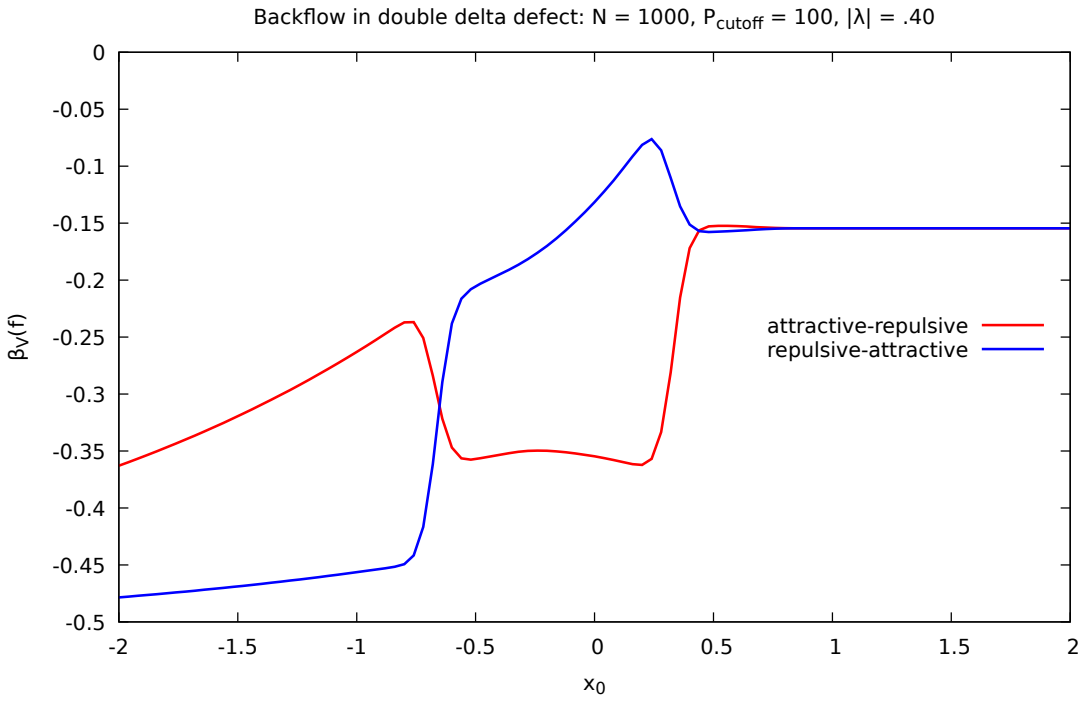

(a)

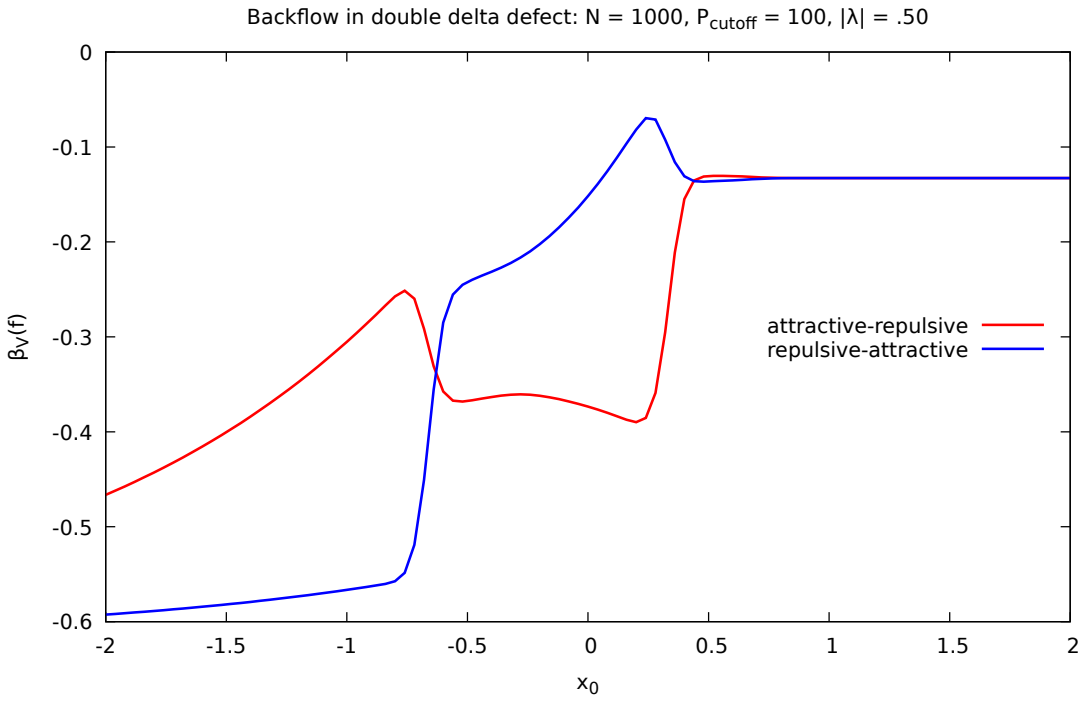

(b)

Figure 3.14: Lowest backflow eigenvalue of the current operator in the presence of a pair of opposite deltas, $a_1 = -a_2 = -0.5$. (a) $|\lambda| = 0.4$ (b) $|\lambda| = 0.5$.

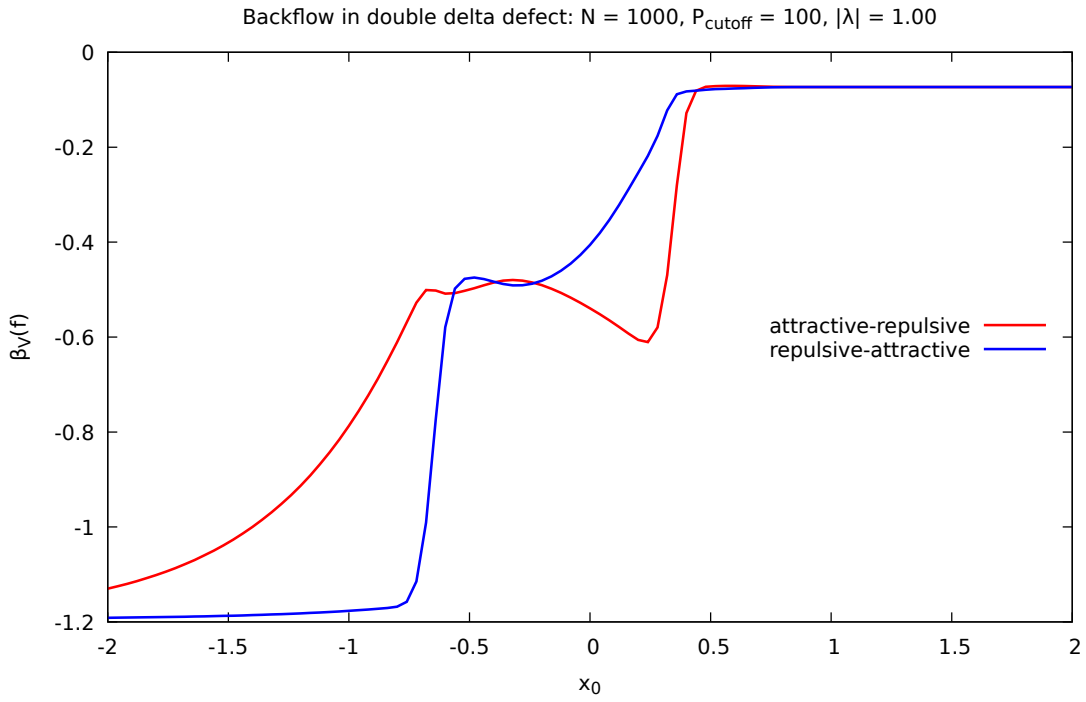

(a)

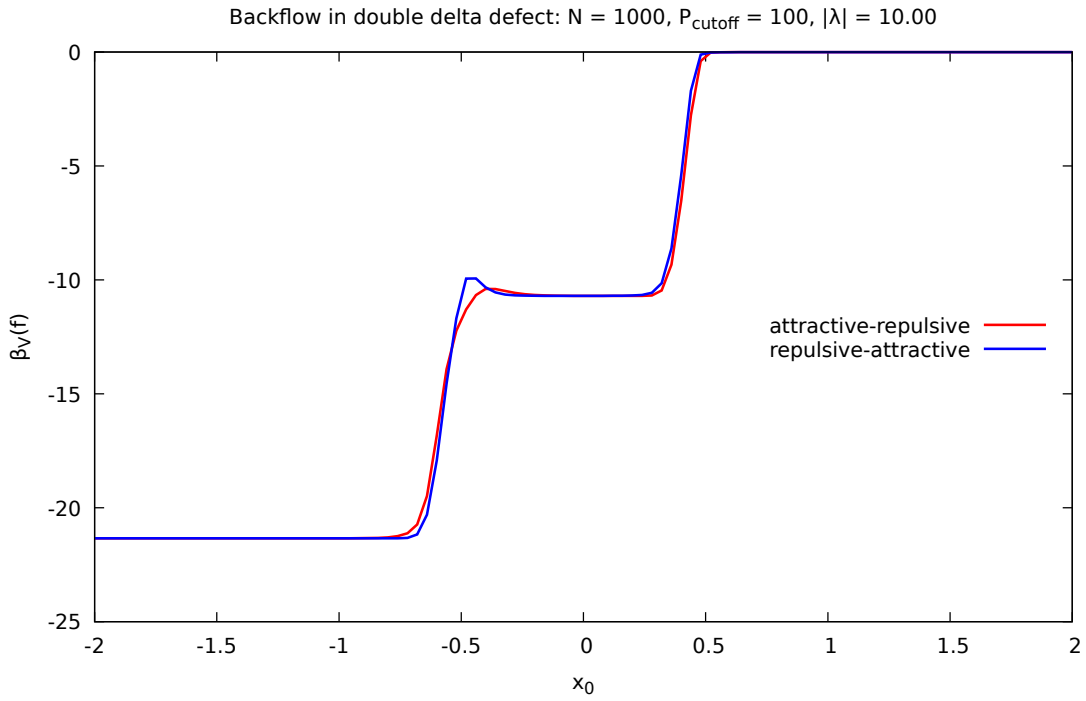

(b)

Figure 3.15: Lowest backflow eigenvalue of the current operator in the presence of a pair of opposite deltas, $a_1 = -a_2 = -0.5$. (a) $|\lambda| = 1.0$ (b) $|\lambda| = 10.0$.

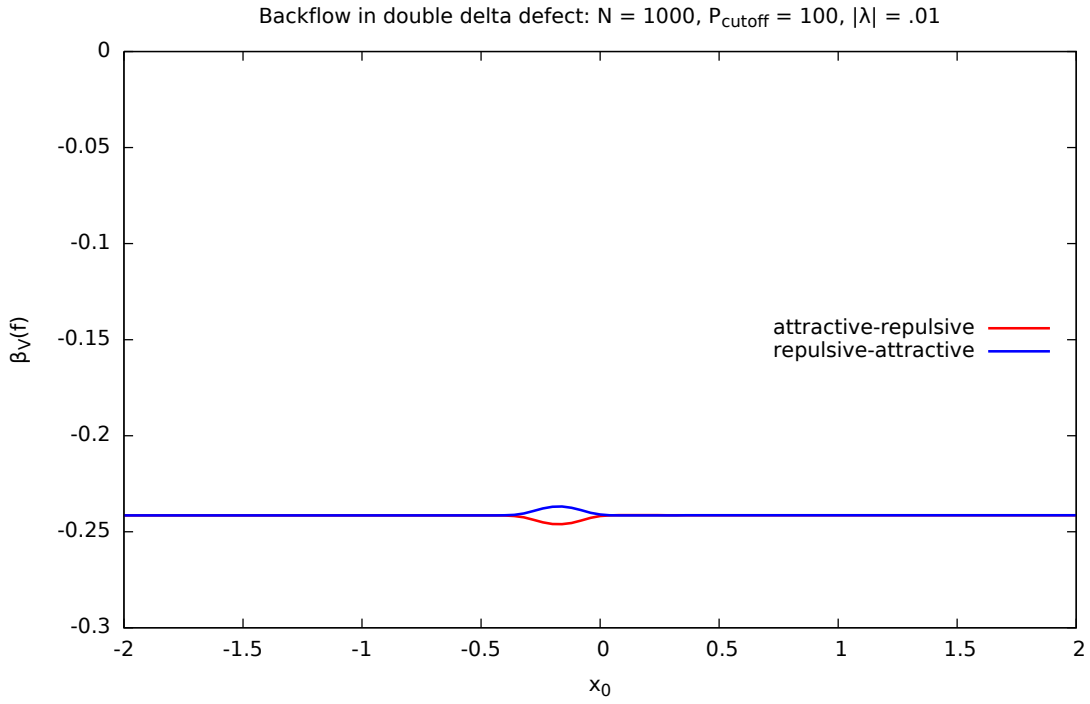

(a)

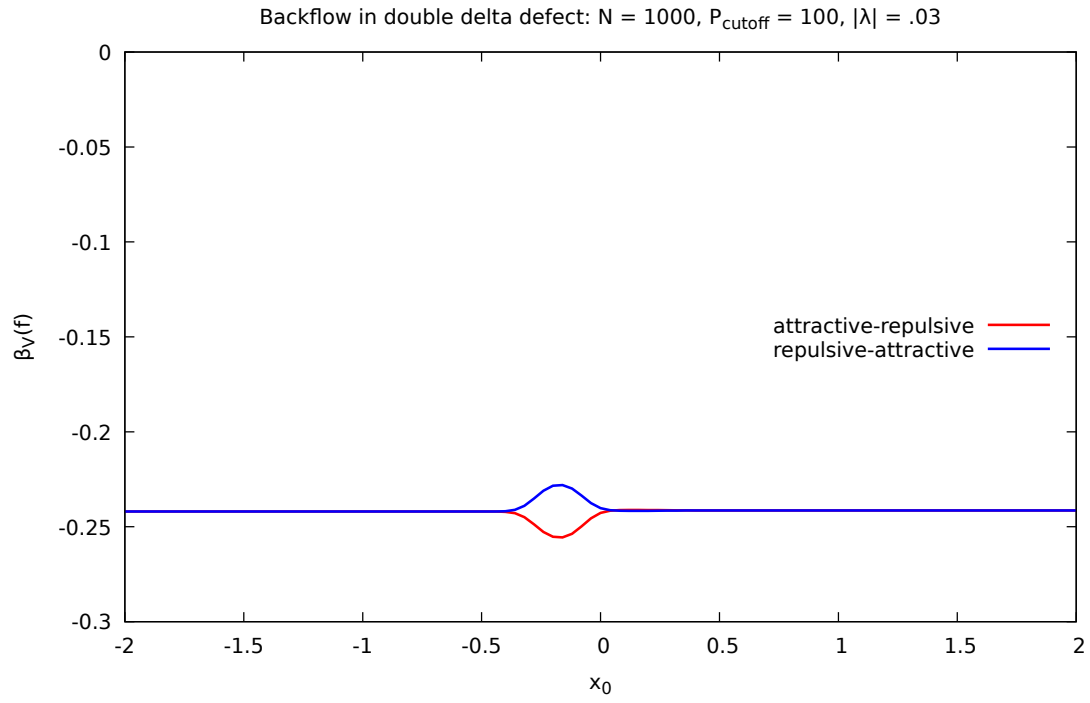

(b)

Figure 3.16: Lowest backflow eigenvalue of the current operator in the presence of a pair of opposite deltas, $a_1 = -a_2 = -0.1$. (a) $|\lambda| = 0.01$ (b) $|\lambda| = 0.03$.

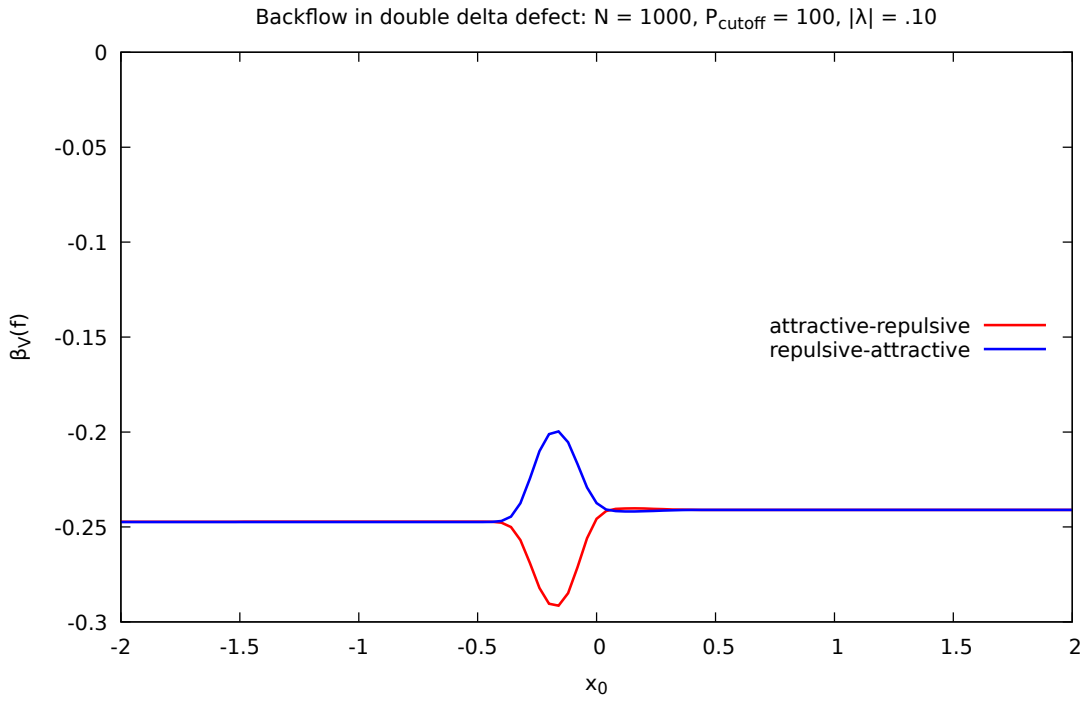

(a)

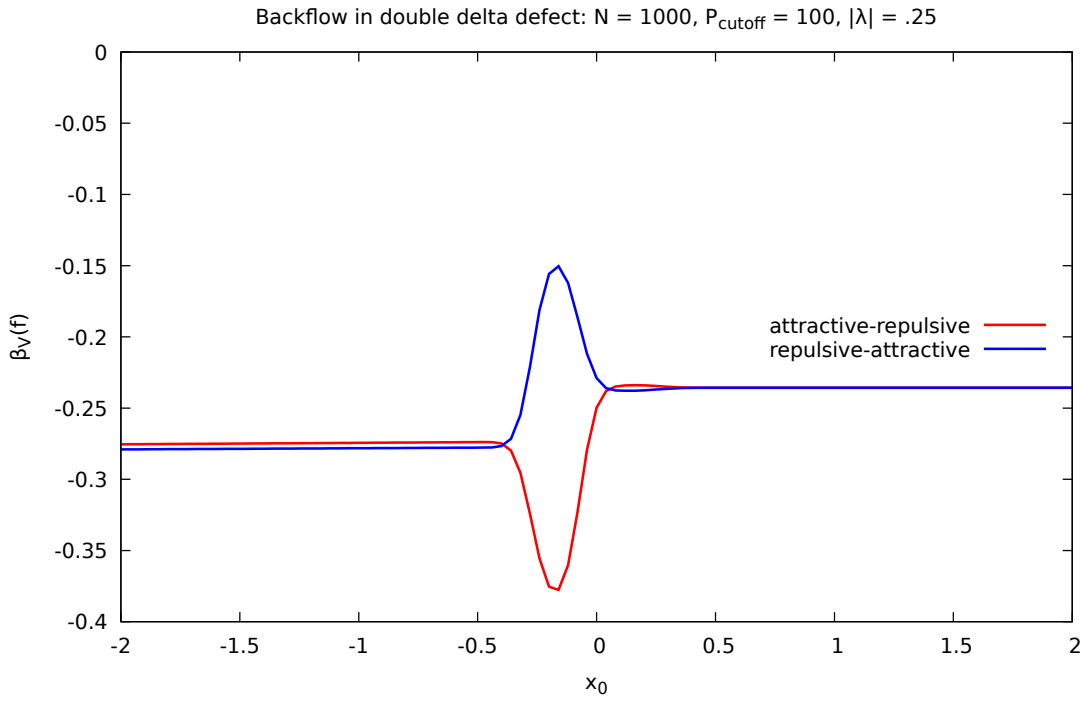

(b)

Figure 3.17: Lowest backflow eigenvalue of the current operator in the presence of a pair of opposite deltas, $a_1 = -a_2 = -0.1$. (a) $|\lambda| = 0.09$ (b) $|\lambda| = 0.25$.

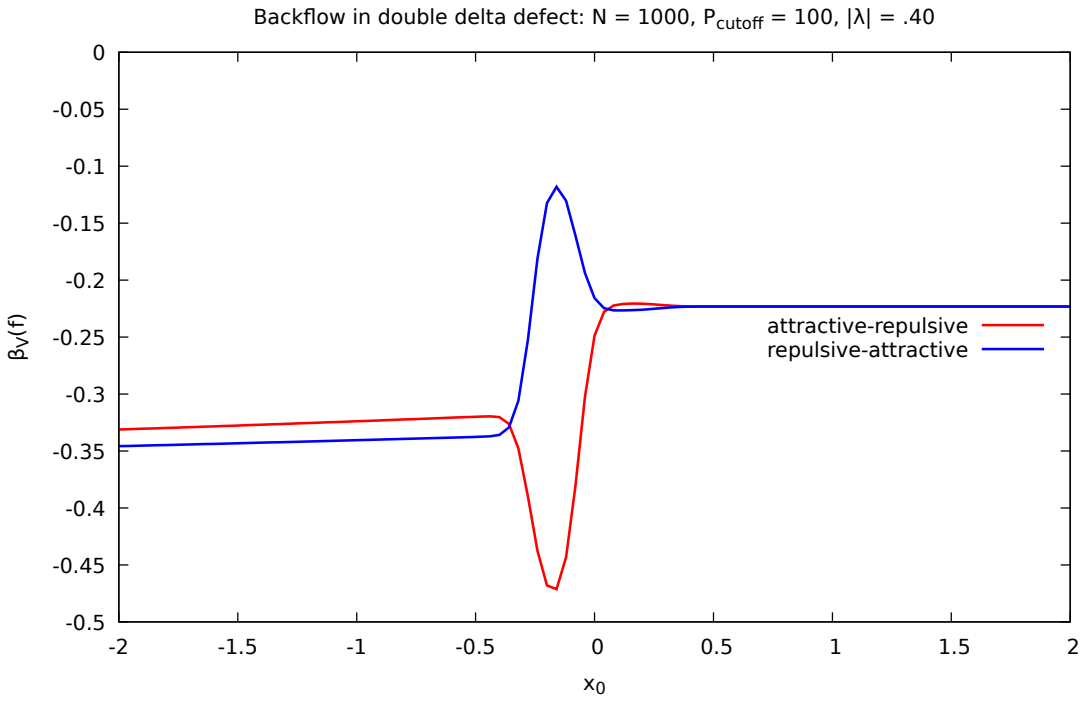

(a)

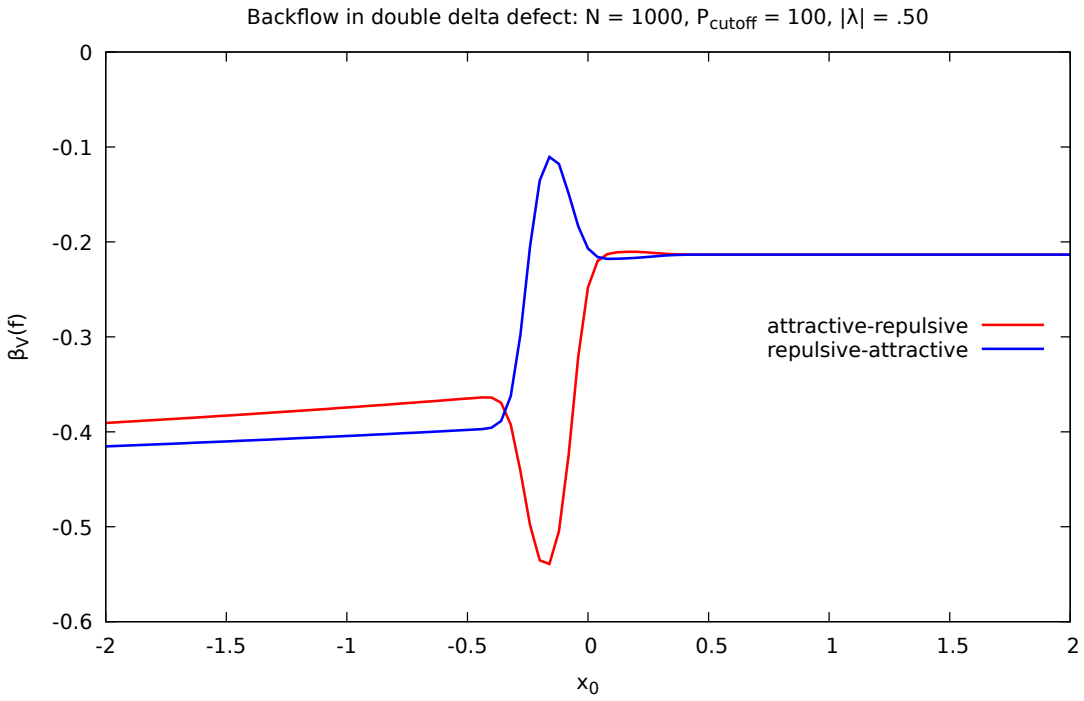

(b)

Figure 3.18: Lowest backflow eigenvalue of the current operator in the presence of a pair of opposite deltas, $a_1 = -a_2 = -0.1$. (a) $|\lambda| = 0.4$ (b) $|\lambda| = 0.5$.

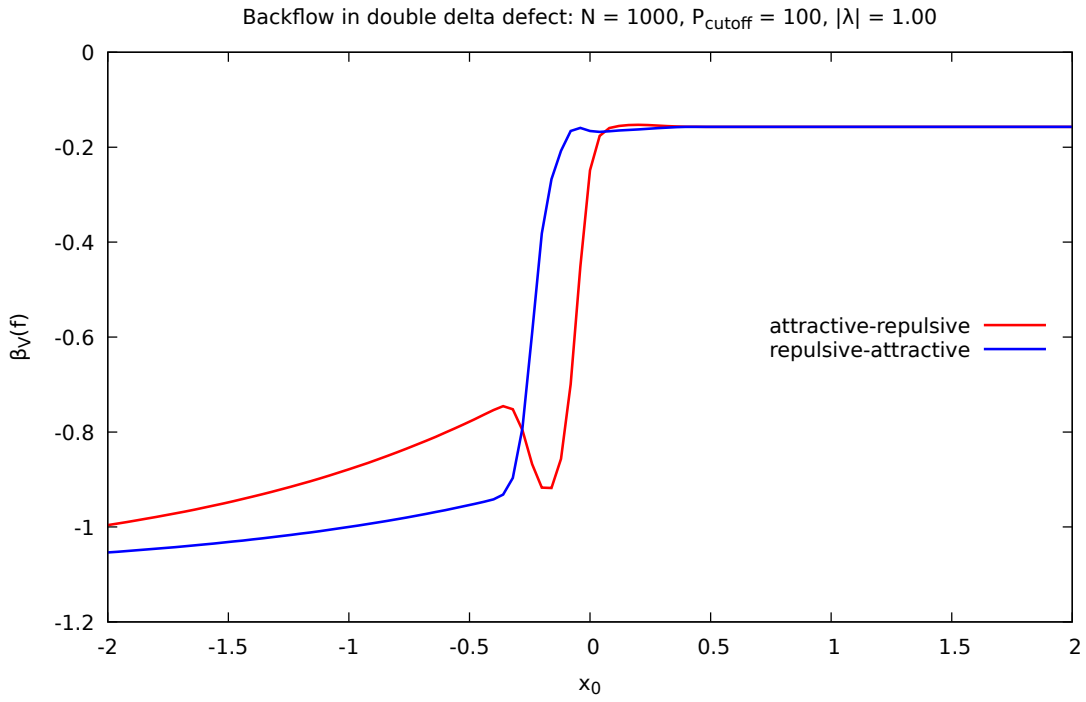

(a)

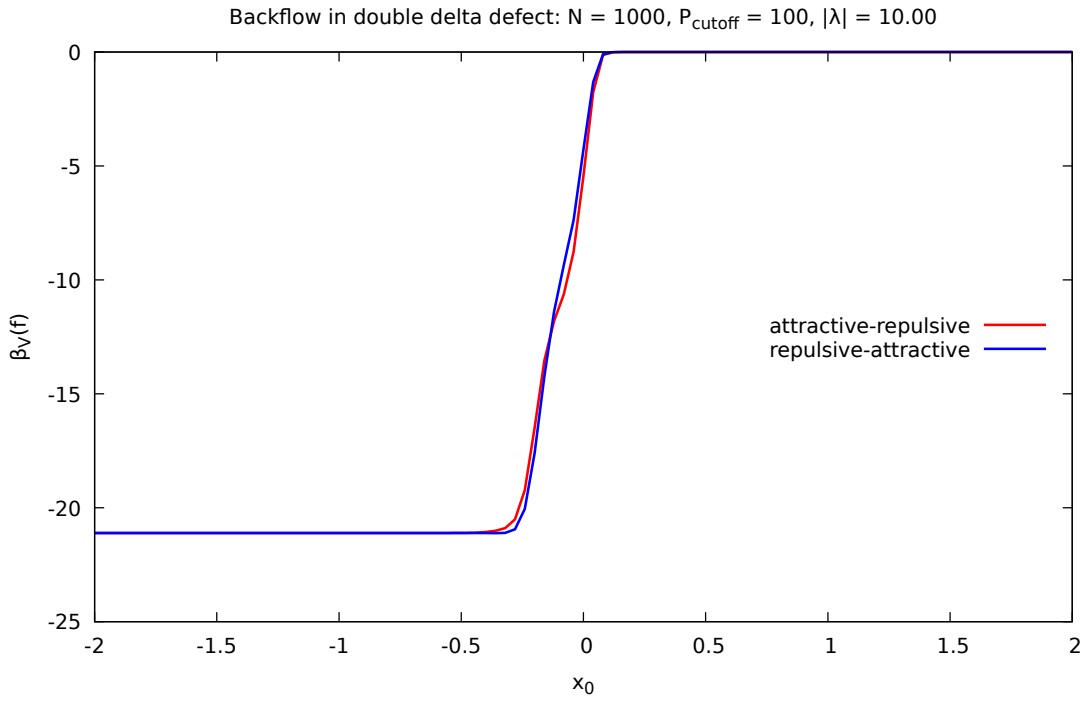

(b)

Figure 3.19: Lowest backflow eigenvalue of the current operator in the presence of a pair of opposite deltas, $a_1 = -a_2 = -0.1$, for which (a) $|\lambda| = 1.0$ (b) $|\lambda| = 10.0$.

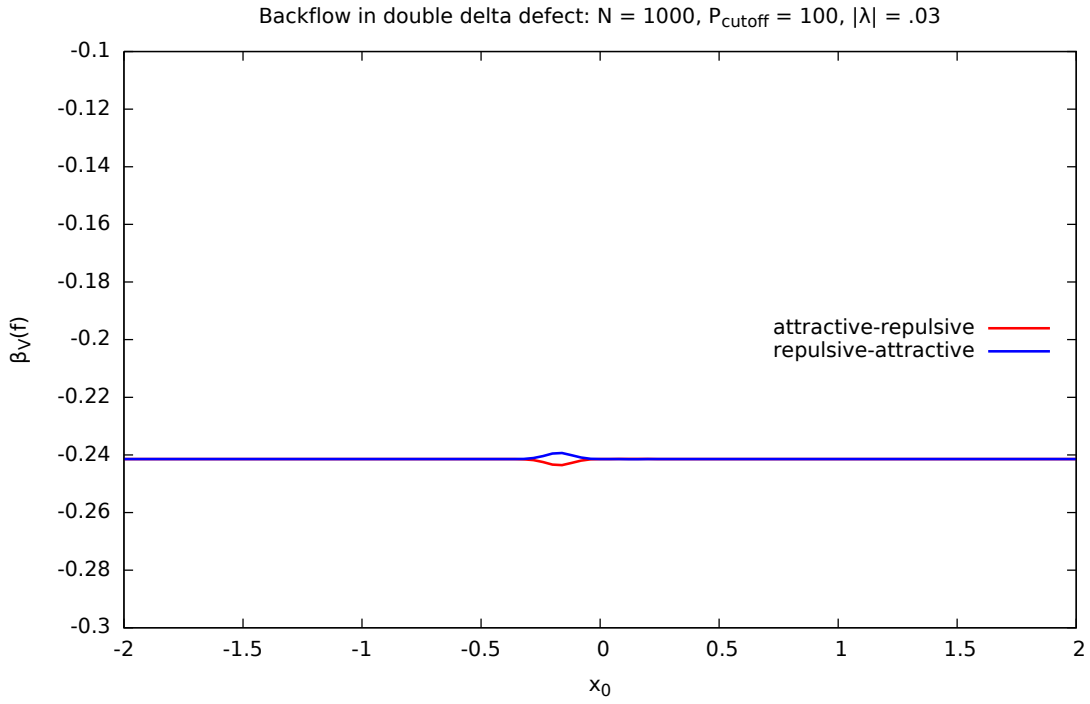

(a)

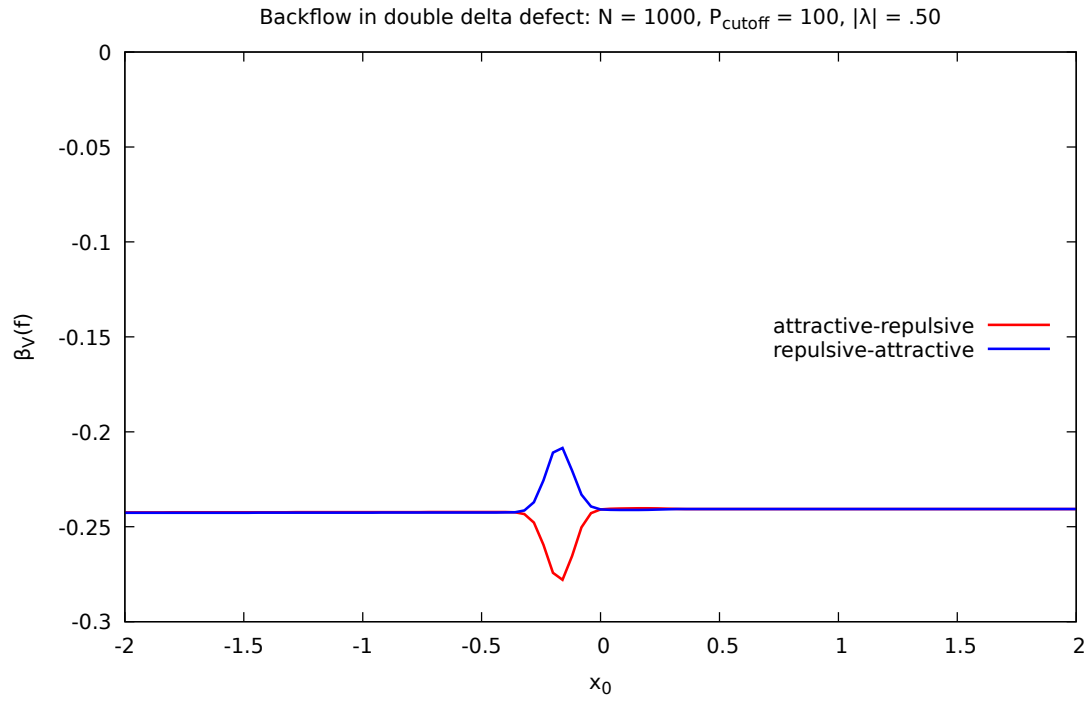

(b)

Figure 3.20: Lowest backflow eigenvalue of the current operator in the presence of a pair of opposite deltas, $a_1 = -a_2 = -0.01$, for which (a) $|\lambda| = 0.03$ (b) $|\lambda| = 0.5$.

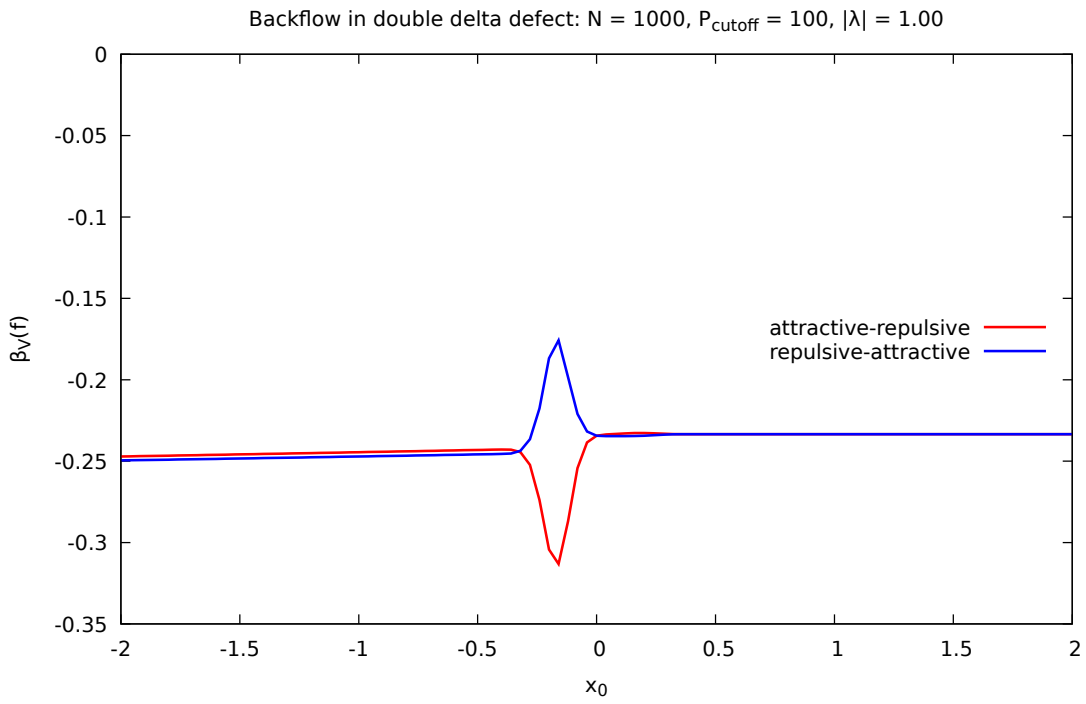

(a)

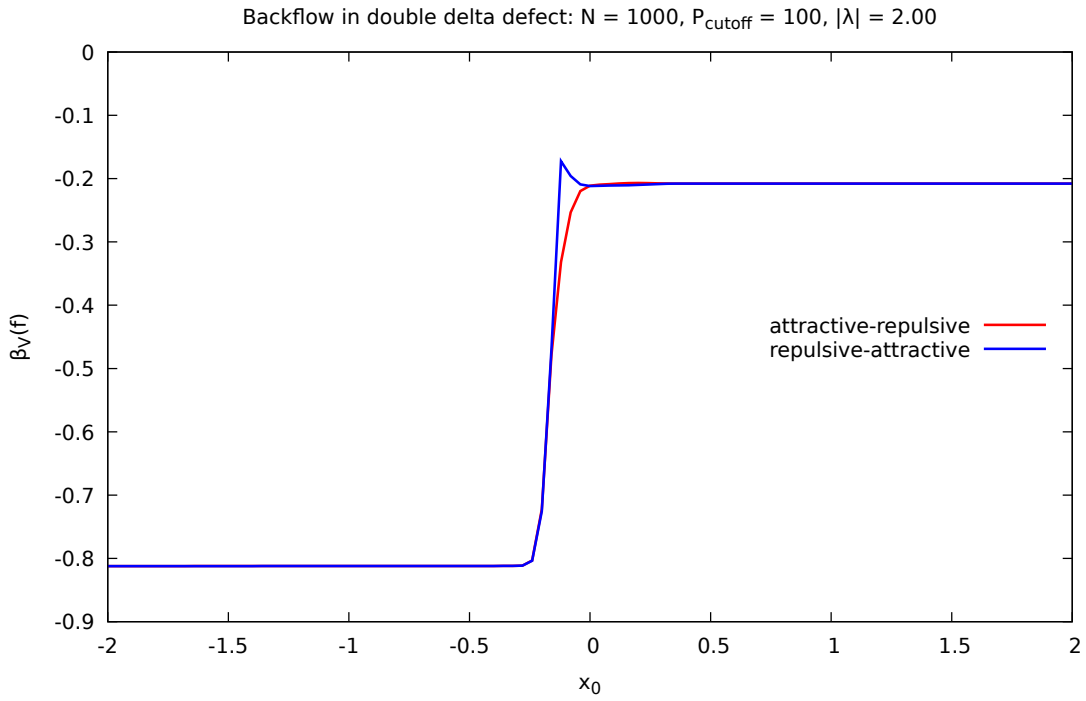

(b)

Figure 3.21: Lowest backflow eigenvalue of the current operator in the presence of a pair of opposite deltas, $a_1 = -a_2 = -0.01$, for which (a) $|\lambda| = 1.0$ (b) $|\lambda| = 2.0$.

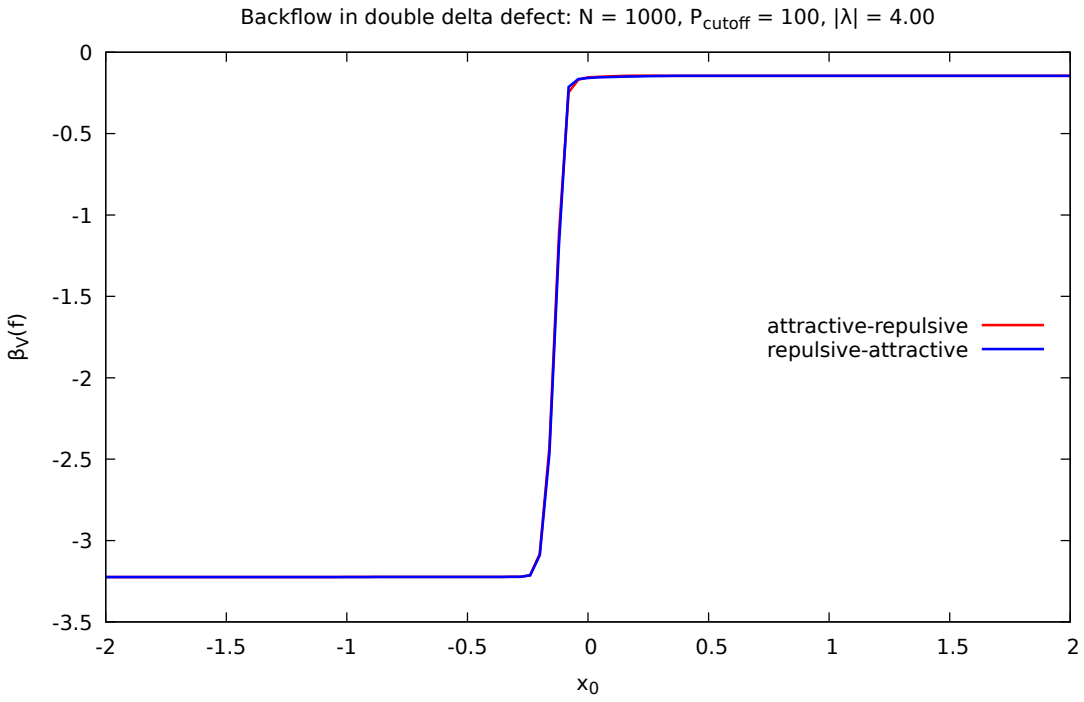

(a)

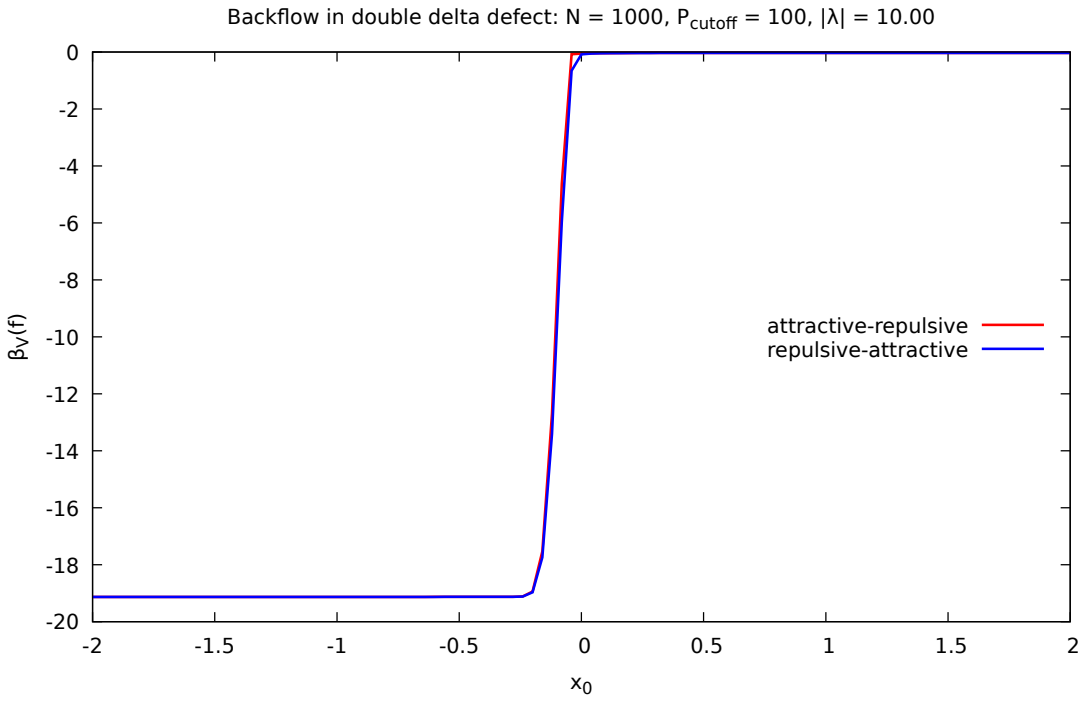

(b)

Figure 3.22: Lowest backflow eigenvalue of the current operator in the presence of a pair of opposite deltas, $a_1 = -a_2 = -0.01$, for which (a) $|\lambda| = 4.0$ (b) $|\lambda| = 10.0$.

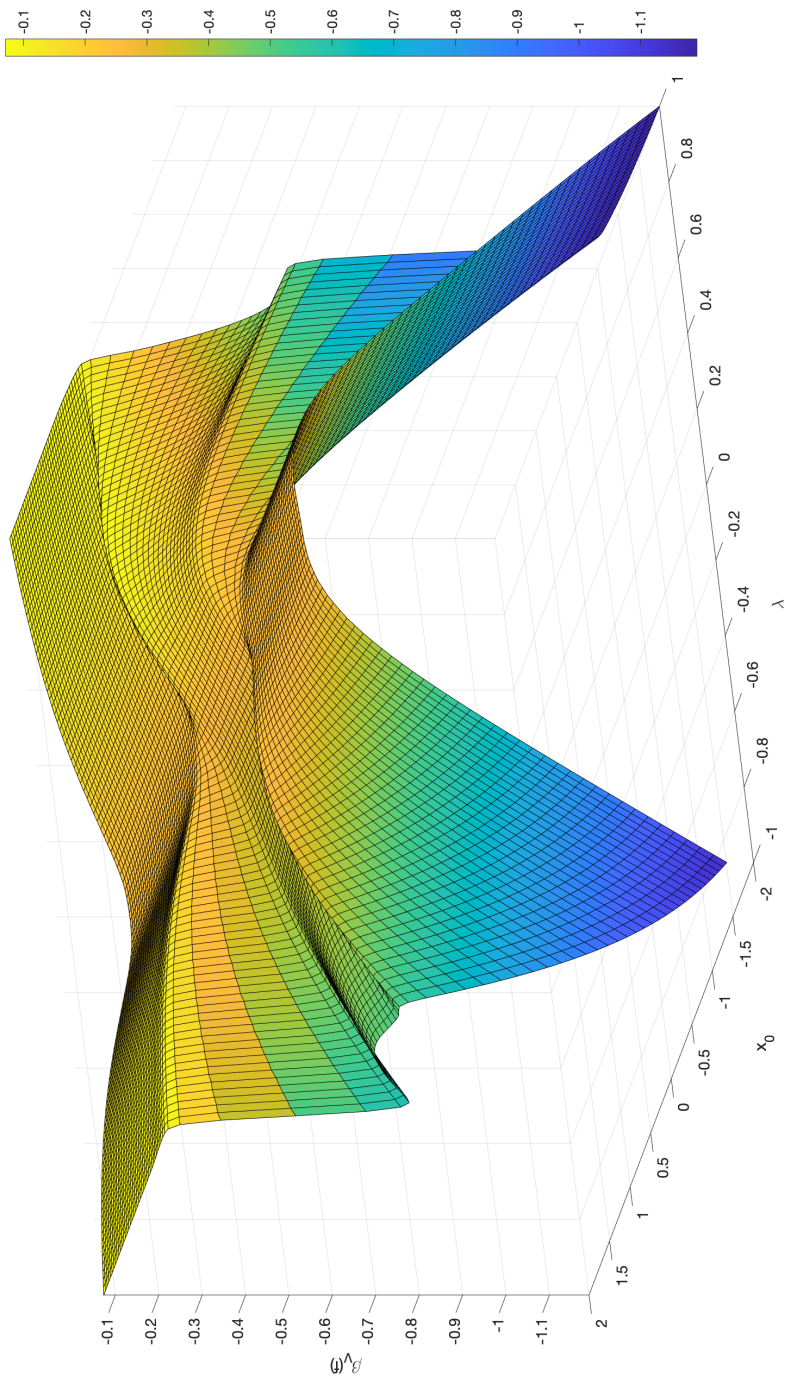

Figure 3.23: Probability current lowest eigenvalue for the double δ-defect with $a_1 = -a_2 = -0.5$ and $\lambda_1 = -\lambda_2 = \lambda$, $P_{\text{cutoff}} = 200$, $N = 2000$.

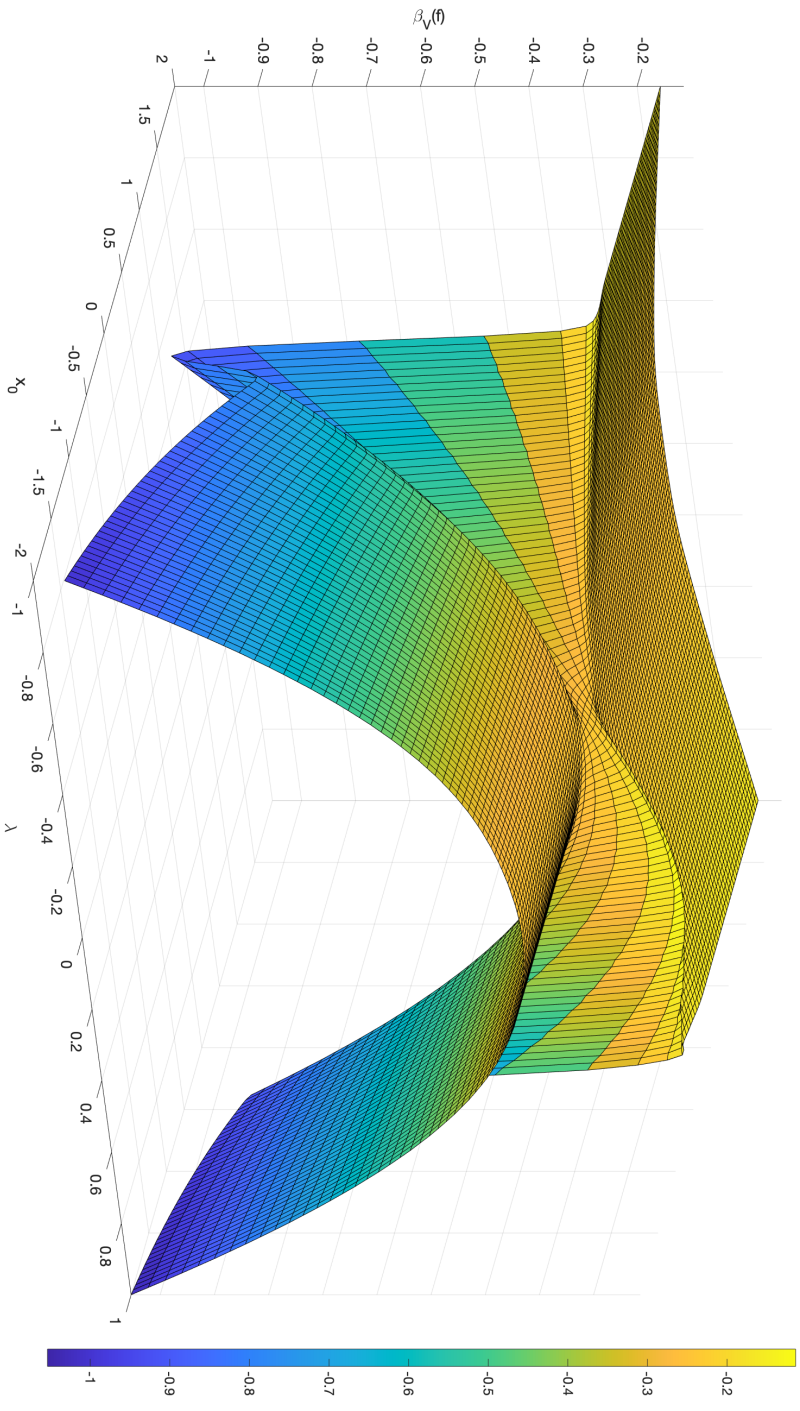

Figure 3.24: Probability current lowest eigenvalue for the double δ-defect with $a_1 = -a_2 = -0.1$ and $\lambda_1 = -\lambda_2 = \lambda$, $P_{\text{cutoff}} = 200$, $N = 2000$.

3.4.3 The case of general asymmetric double δ-defect

The pair of general asymmetric deltas is characterized by the extra freedom of allowing the condition that $|\lambda_1| \neq |\lambda_2|$. In particular, we consider the case where one strength is not much larger than the other ($|\lambda_2| = 2|\lambda_1|$) and the case where one of the strengths is much larger than the other ($|\lambda_2| = 10|\lambda_1|$). In the legends, the terms attractive and repulsive have the same meaning denoted in the previous subsections, namely the description of the pair of deltas as to whether the strengths have negative or positive value, respectively. Similarly, attractive-repulsive corresponds to the condition that $\lambda_1 < 0$ and $\lambda_2 > 0$, and repulsive-attractive corresponds to $\lambda_1 > 0$ and $\lambda_2 < 0$. As for the position of the impurities, we restrict to the case where $a = 0.5$.

When the asymmetric double δ-defect is composed of impurities which are not much stronger or much weaker relatively to each other, in a balanced mixture of strengths, $\beta_V(f)$ is not much perturbed from what one would expect after considering the results of the previous subsections. In contrasting difference, taking into account an imbalanced mixture of interaction strengths where the impurities are much weaker or much stronger to each other, the final result for the backflow constant is considerably affected by the strongest interaction center. These asymmetric cases share some features with previous case, as for the presence of peaks for certain negative values of the strength, for example, figures 3.25, 3.27, 3.29, 3.30 and 3.31. On the other hand, figures 3.26, 3.28 seem to sum up opposite (attraction and repulsion) effects leading to a combined total effect forming bumps in the neighbourhood of $x_0 = -0.5$. That is not possible with a single delta and is likely due the result of balance between strong and weak attraction and repulsion as well the appropriate distance between the interaction centers. When the interaction strength is very weak for the opposite pair of deltas, figures 3.27 (a) and 3.31 (a), it does not seem that the attractive-repulsive case has less backflow than the repulsive-attractive case in the regions before the first interaction site. However, that is not the case, and the reason is that our range $x_0 \in (-2, 2)$ is not enough to show that behaviour. In fact, subfigures (b) of the mentioned figures show that the red curve (attractive-repulsive) and the blue curve (repulsive-attractive) cross each other closer to the interaction centers for stronger strengths. Finally, figure 3.32 shows that the presence of a maximum for the attractive-repulsive case in the region immediately before the first impurity is retained, even for strong values such as $\lambda_1 = -1$, and the

behaviour in the middle region ($-0.5 < x_0 < 0.5$) can be quite intricate.

The main features presented here are the clear distinction between the behaviour of attractive and repulsive interactions, the existence of maxima, the number of them and their location with respect to the defect position. In the next chapter, where a purely transmitting defect is studied, there will be no backscattering affecting the backflow constant, and the analysis can be more precise (by comparison with what happens in a general scattering situation) in the sense that the backflow effect will be isolated.

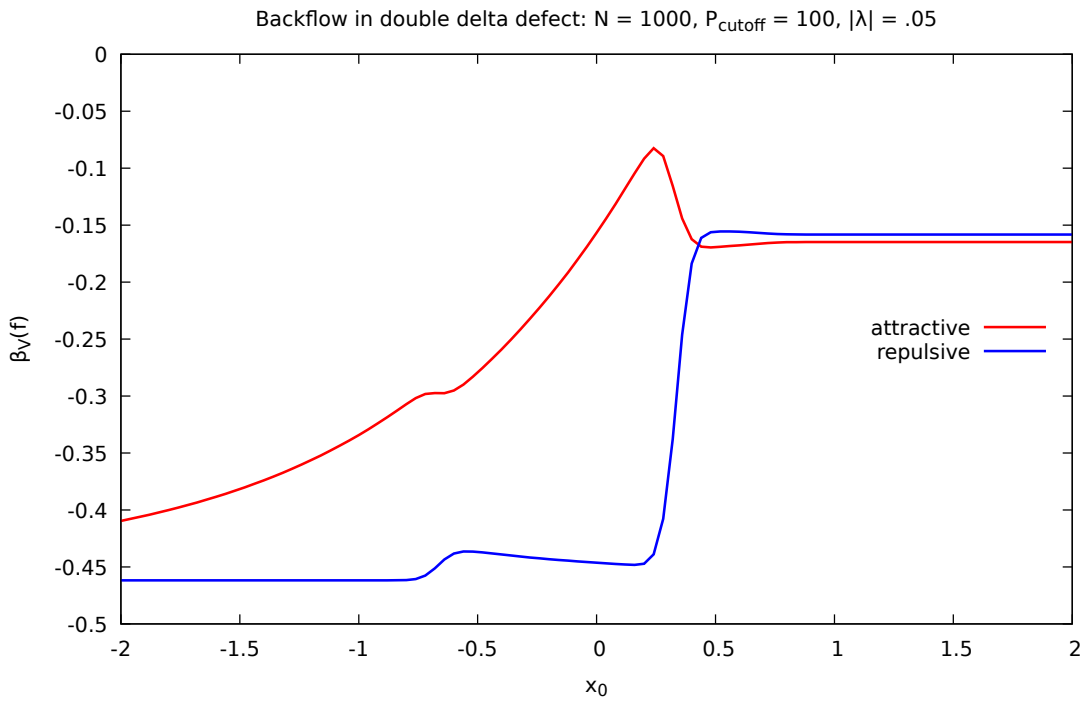

(a)

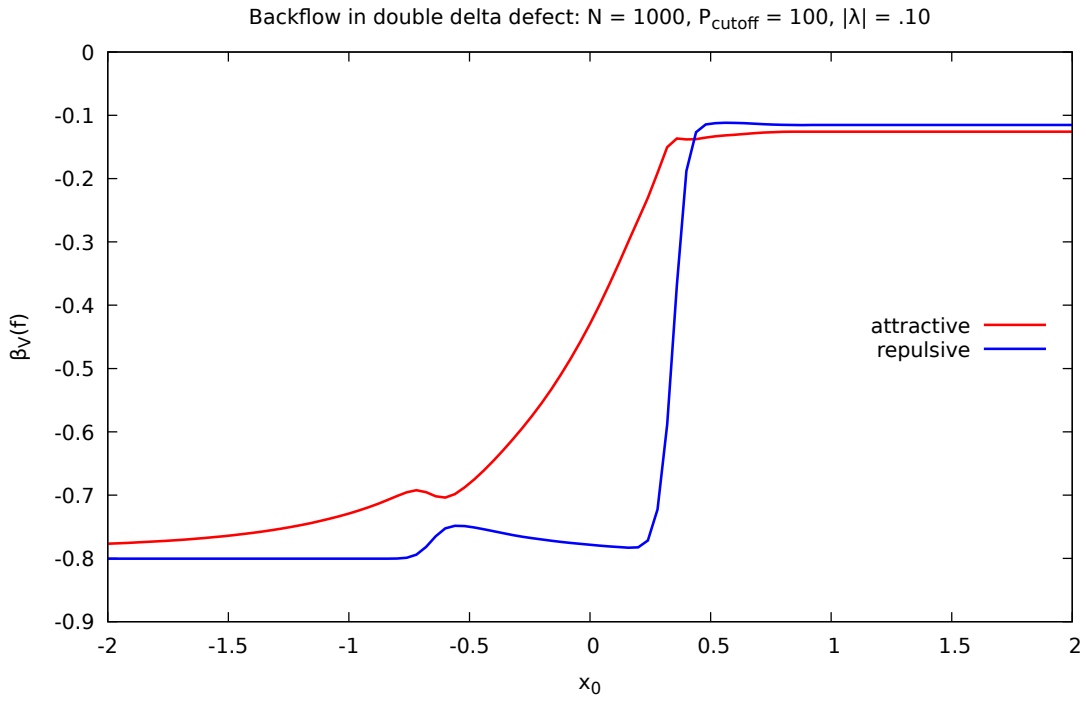

(b)

Figure 3.25: Lowest backflow eigenvalue of the current operator in the presence of a pair of deltas, $a_1 = -a_2 = -0.5$, $\lambda_1 = \lambda$ and $\lambda_2 = 10\lambda_1$, for which (a) $|\lambda| = 0.05$ (b) $|\lambda| = 0.1$.

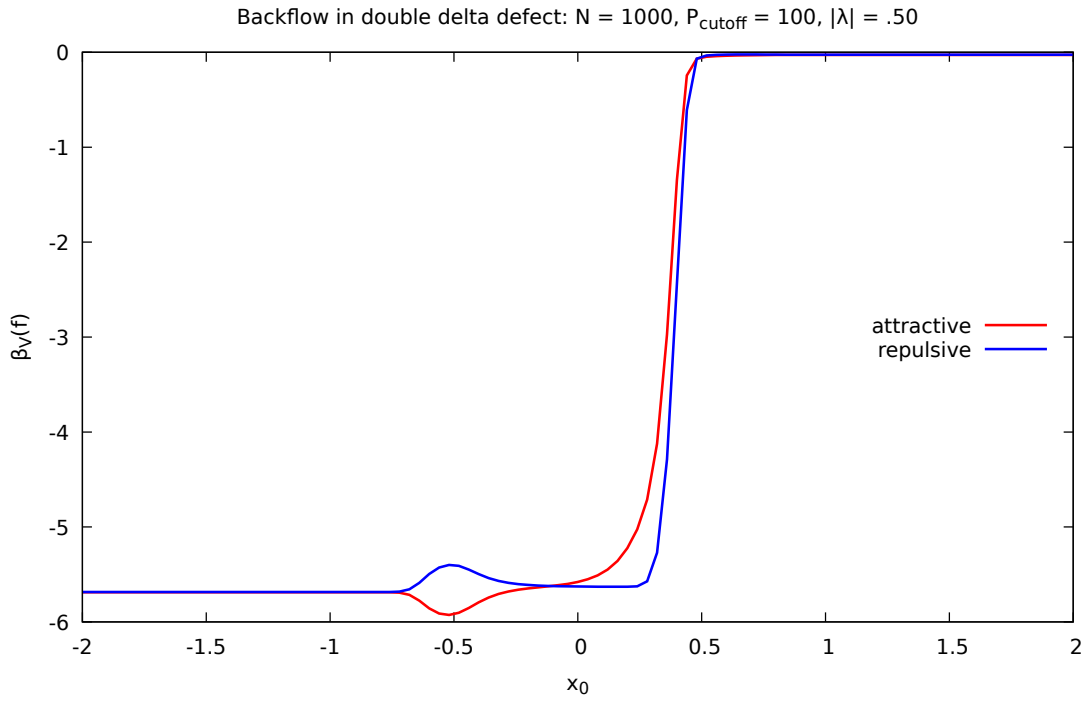

(a)

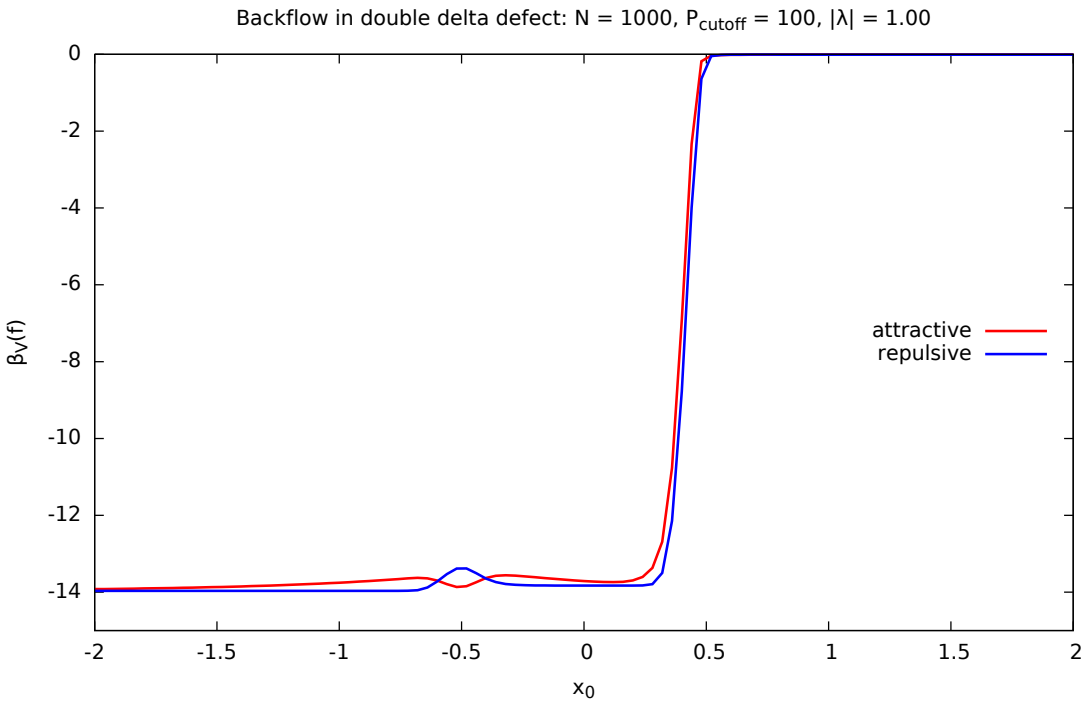

(b)

Figure 3.26: Lowest backflow eigenvalue of the current operator in the presence of a pair of deltas, $a_1 = -a_2 = -0.5$, $\lambda_1 = \lambda$ and $\lambda_2 = 10\lambda_1$, for which (a) $|\lambda| = 0.5$ (b) $|\lambda| = 1.0$.

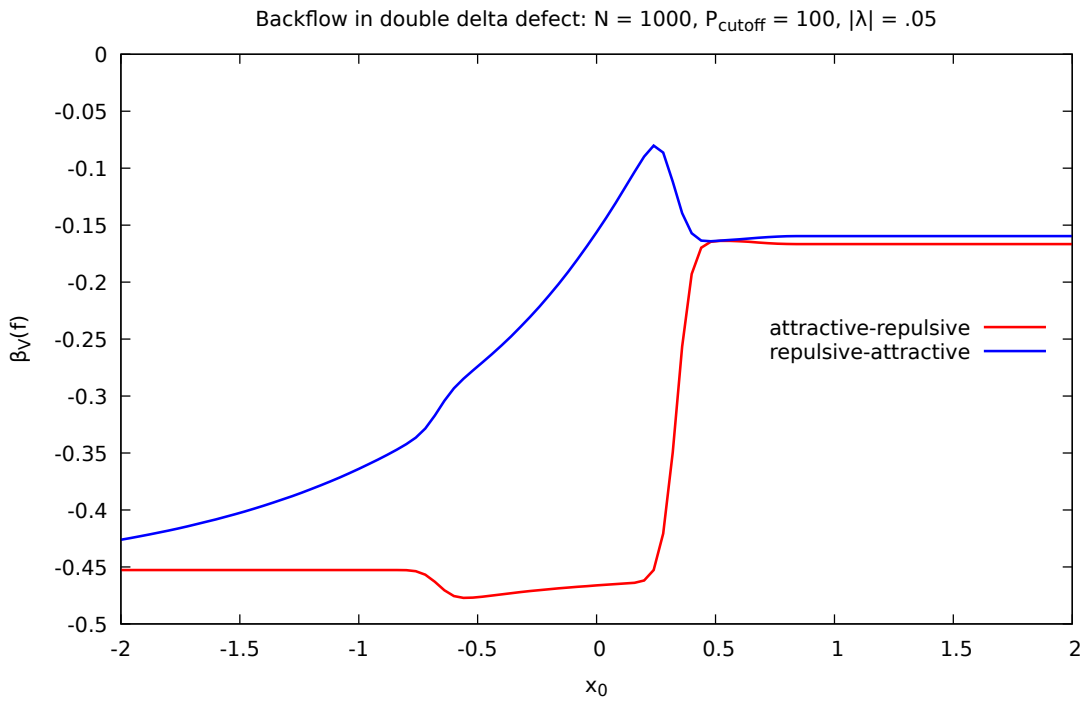

(a)

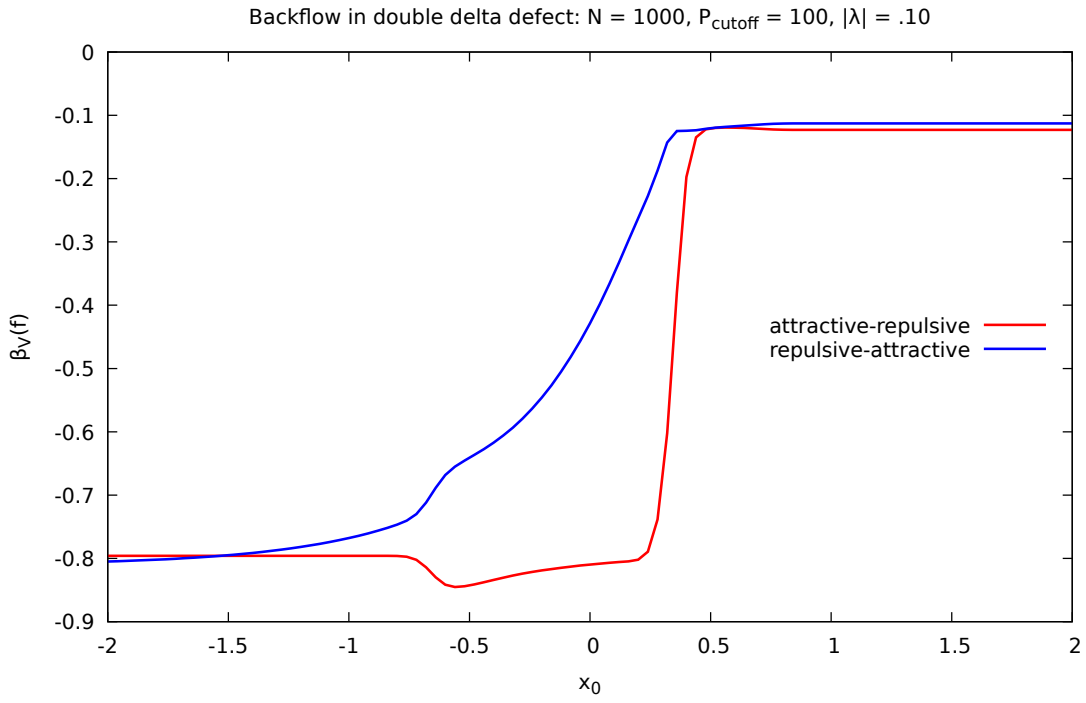

(b)

Figure 3.27: Lowest backflow eigenvalue of the current operator in the presence of a pair of deltas, $a_1 = -a_2 = -0.5$, $\lambda_1 = \lambda$ and $\lambda_2 = -10\lambda_1$, for which (a) $|\lambda| = 0.05$ (b) $|\lambda| = 0.1$.

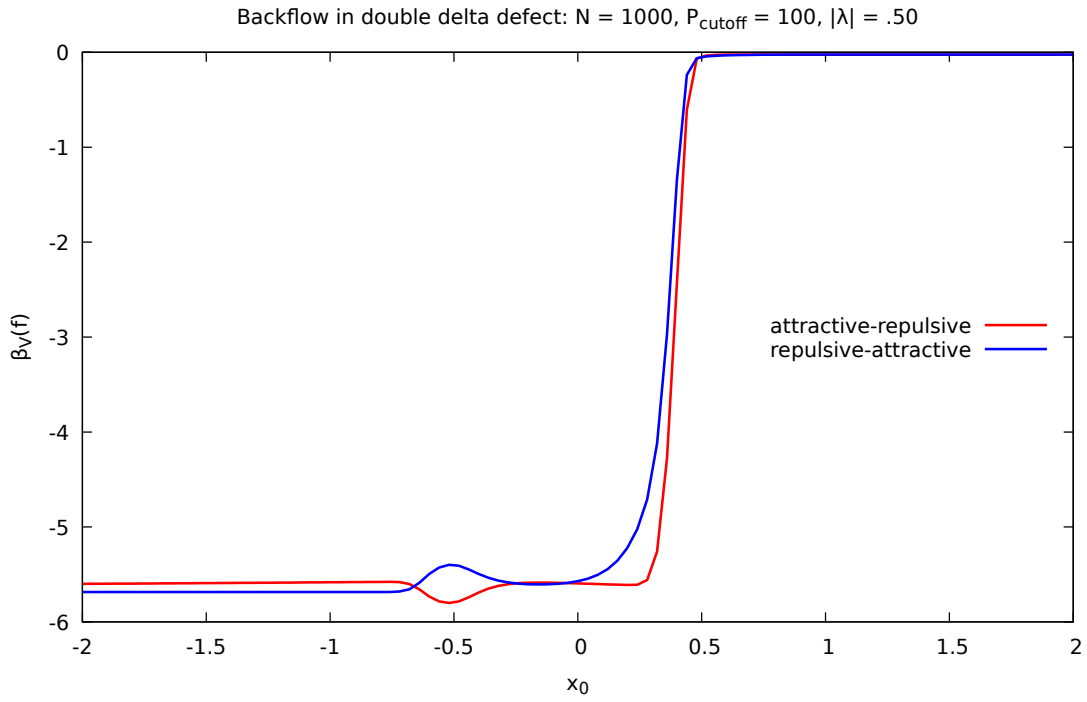

(a)

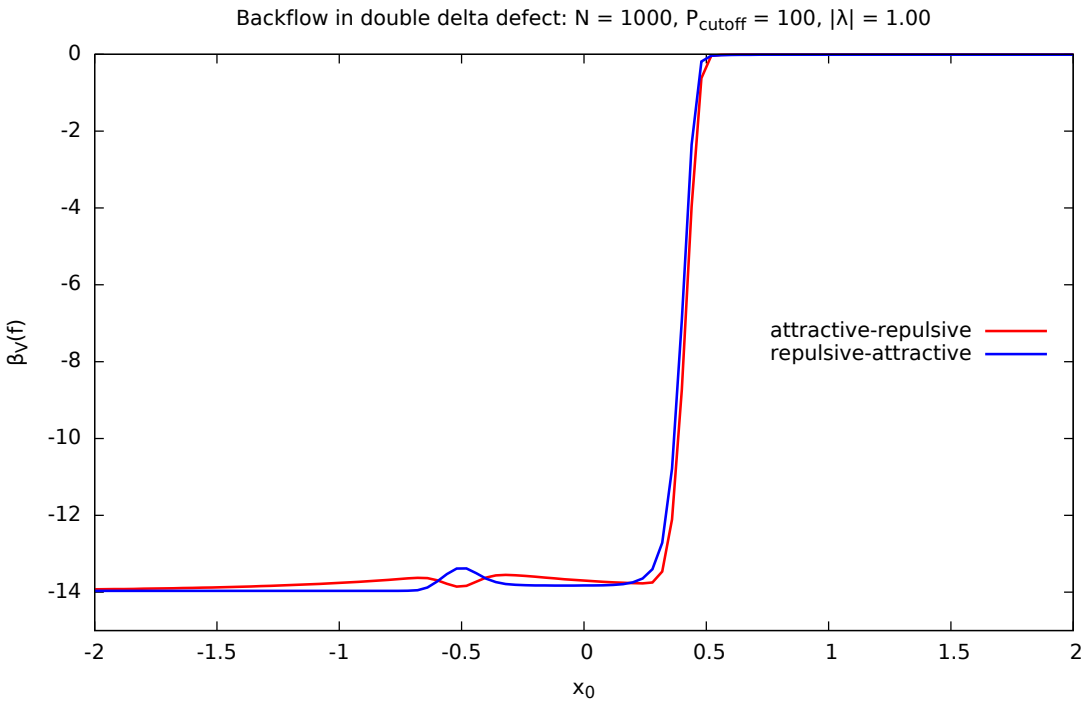

(b)

Figure 3.28: Lowest backflow eigenvalue of the current operator in the presence of a pair of deltas, $a_1 = -a_2 = -0.5$, $\lambda_1 = \lambda$ and $\lambda_2 = -10\lambda_1$, for which (a) $|\lambda| = 0.5$ (b) $|\lambda| = 1.0$.

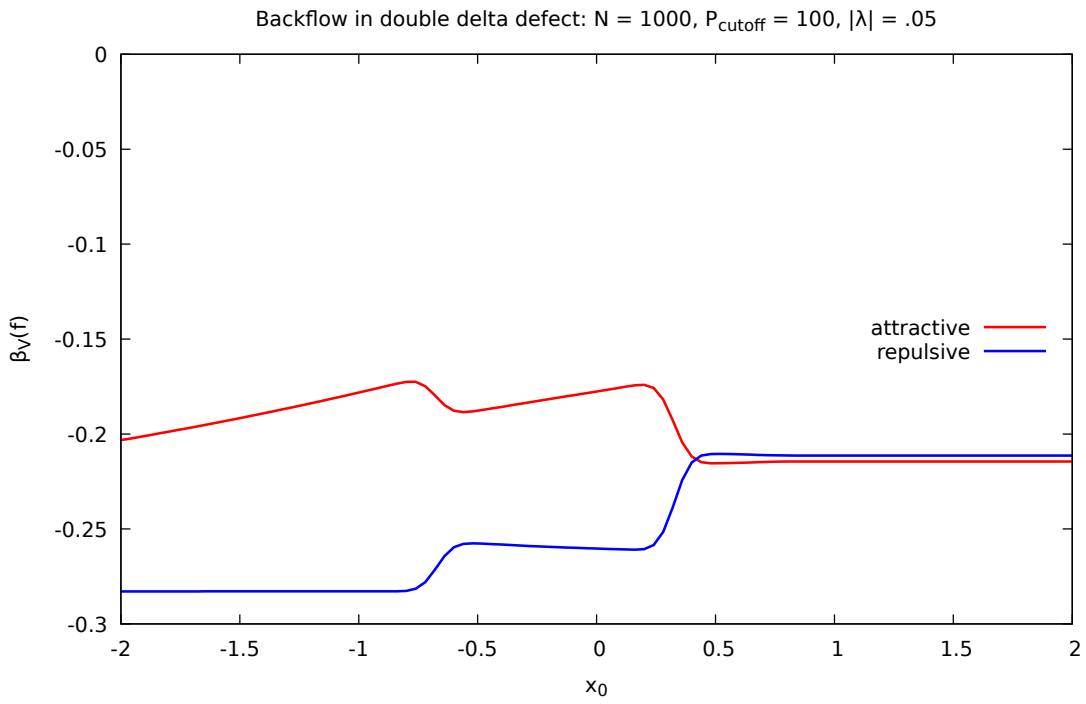

(a)

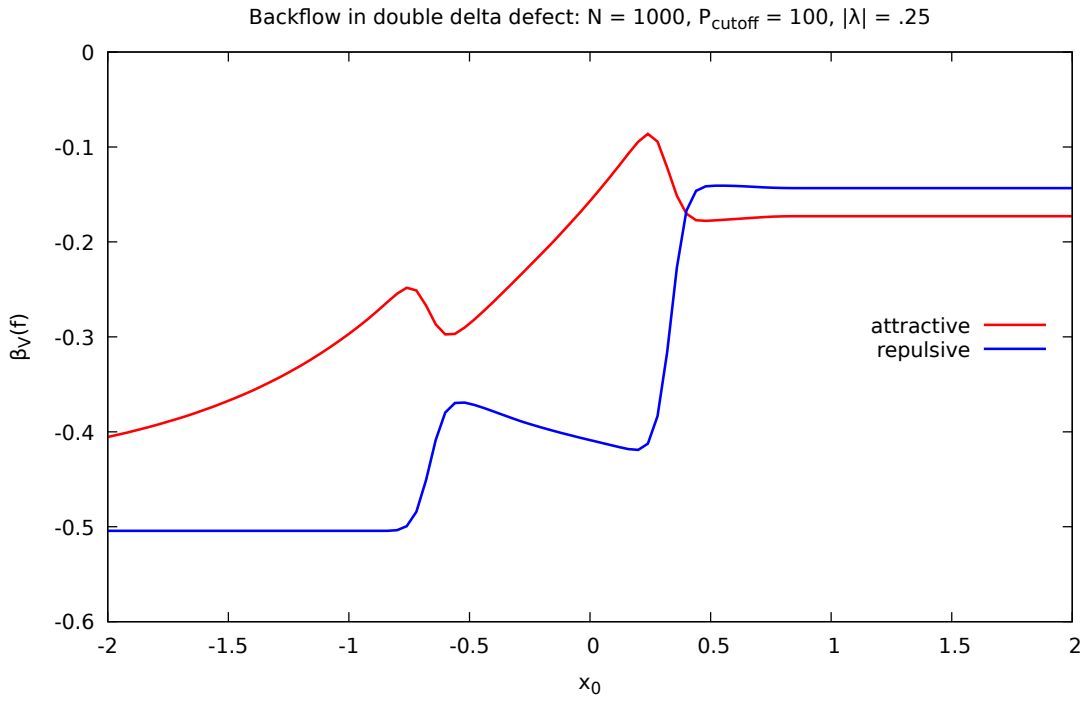

(b)

Figure 3.29: Lowest backflow eigenvalue of the current operator in the presence of a pair of deltas, $a_1 = -a_2 = -0.5$, $\lambda_1 = \lambda$ and $\lambda_2 = 2\lambda_1$, for which (a) $|\lambda| = 0.05$ (b) $|\lambda| = 0.25$.

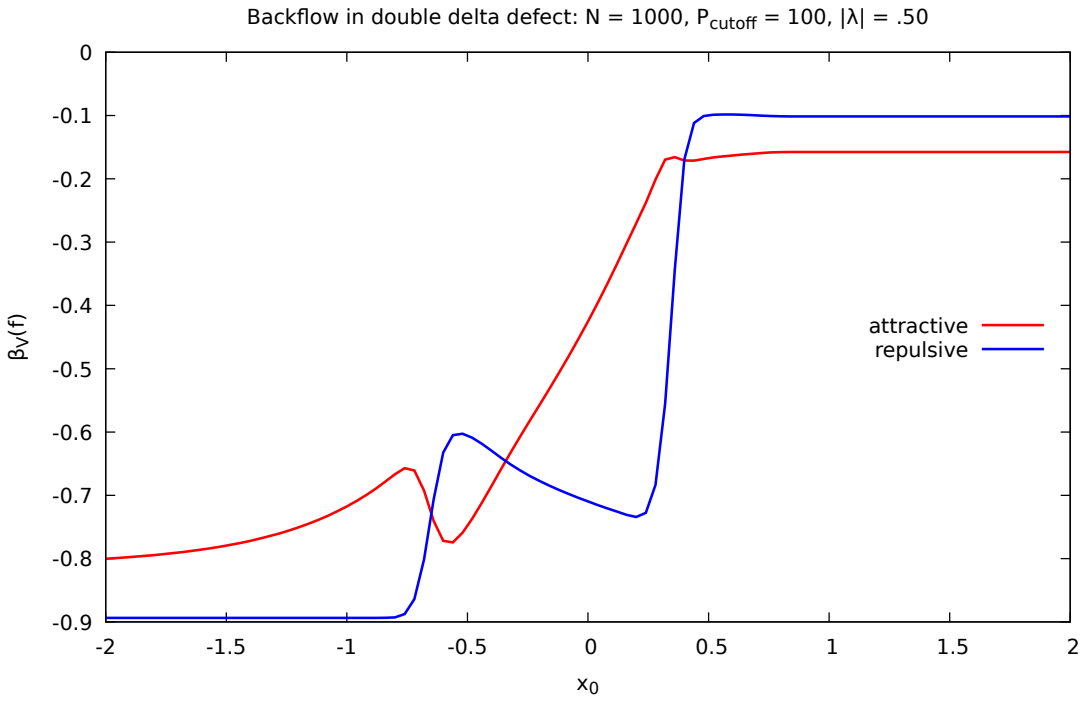

(a)

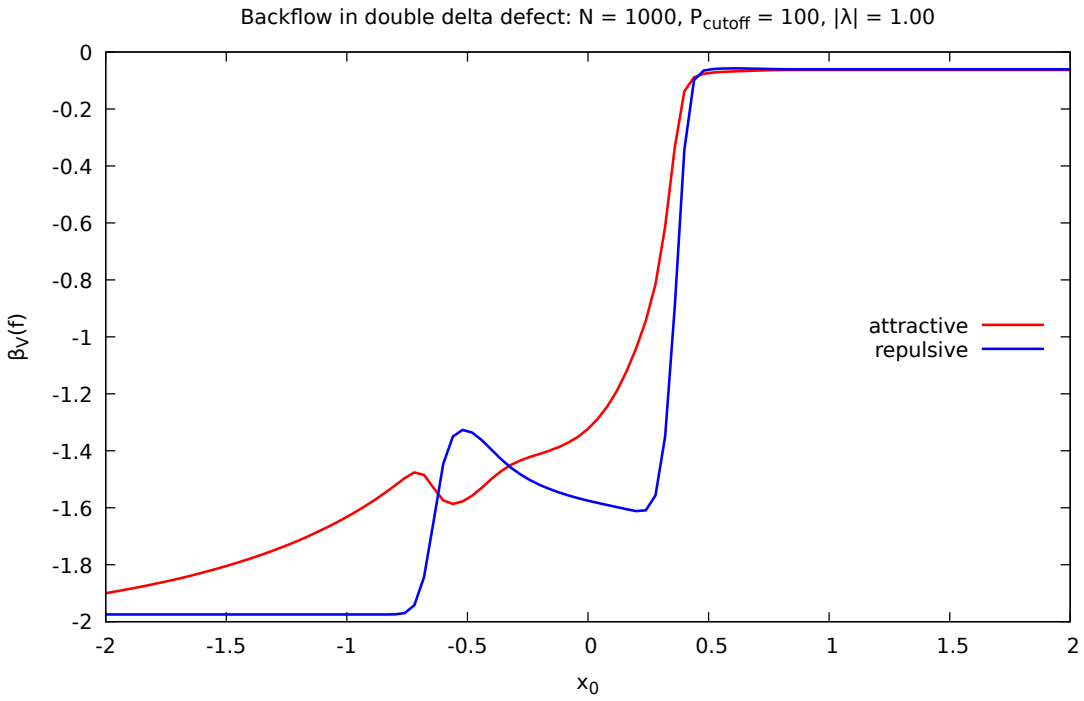

(b)

Figure 3.30: Lowest backflow eigenvalue of the current operator in the presence of a pair of deltas, $a_1 = -a_2 = -0.5$, $\lambda_1 = \lambda$ and $\lambda_2 = 2\lambda_1$, for which (a) $|\lambda| = 0.5$ (b) $|\lambda| = 1.0$.

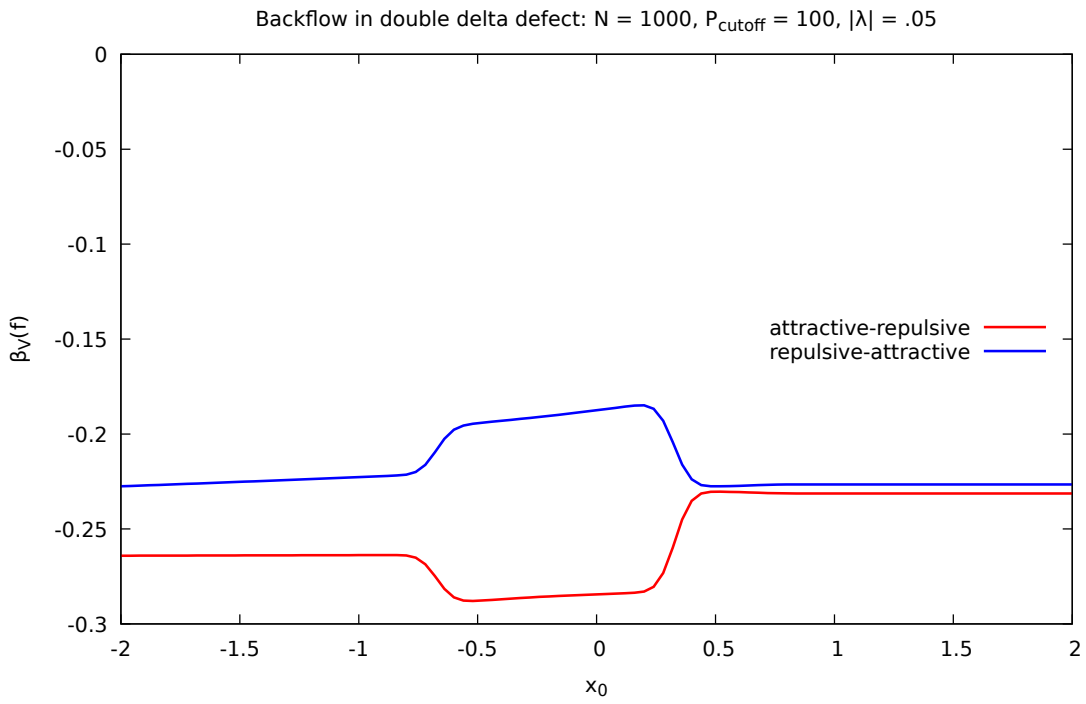

(a)

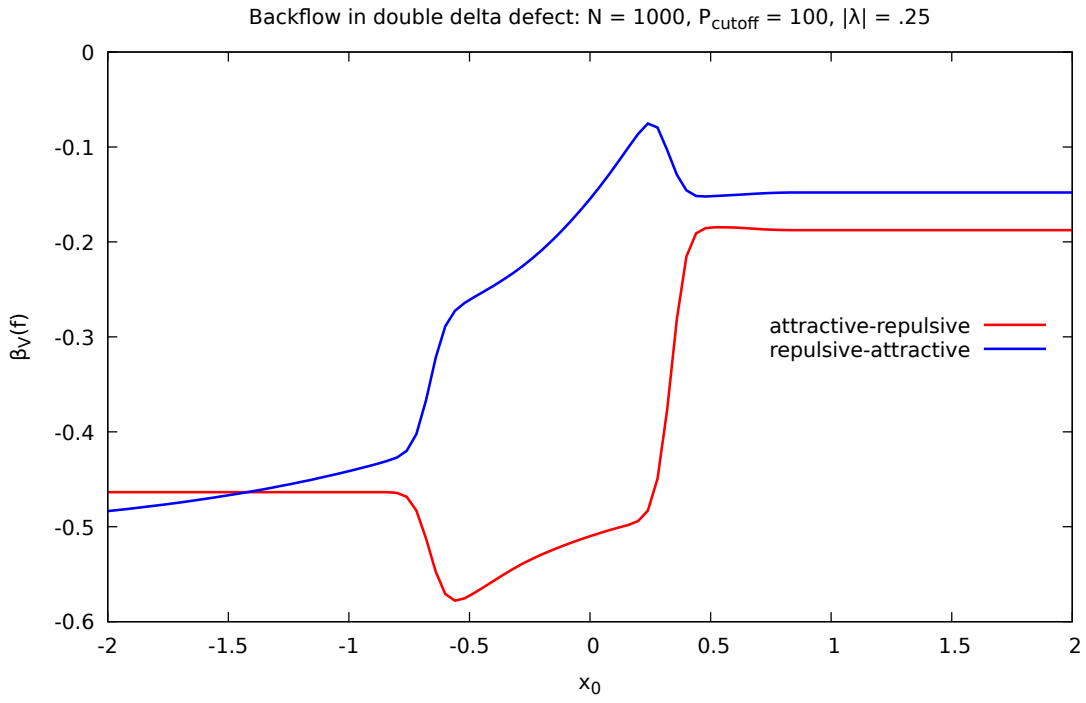

(b)

Figure 3.31: Lowest backflow eigenvalue of the current operator in the presence of a pair of deltas, $a_1 = -a_2 = -0.5$, $\lambda_1 = \lambda$ and $\lambda_2 = -2\lambda_1$, for which (a) $|\lambda| = 0.05$ (b) $|\lambda| = 0.25$.

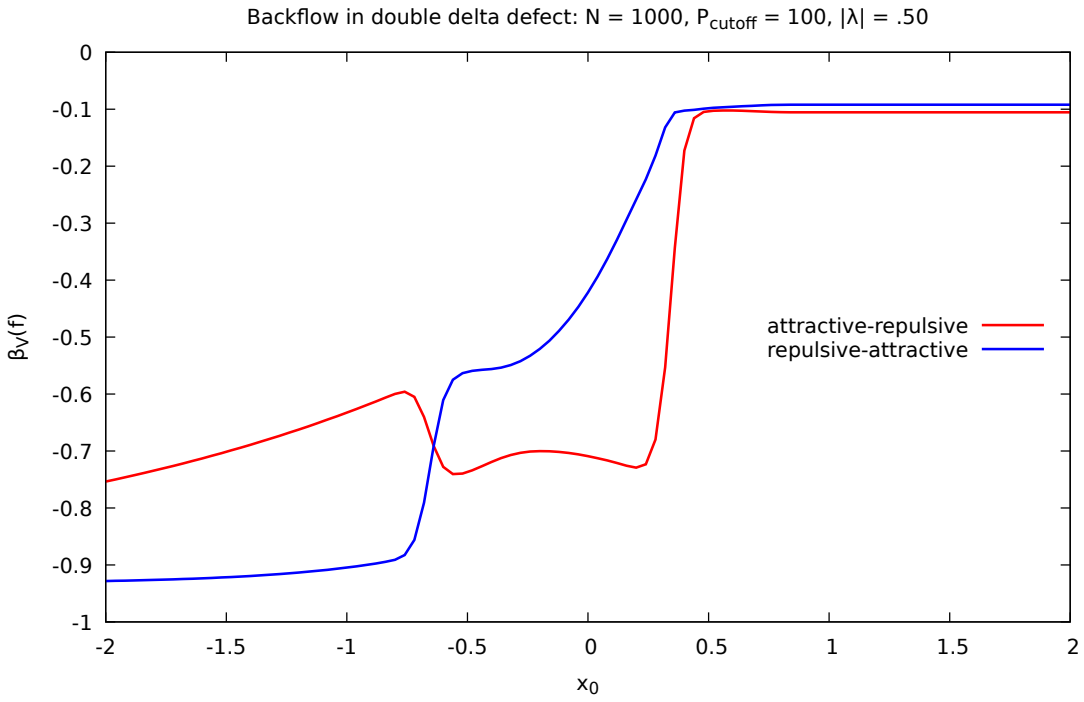

(a)

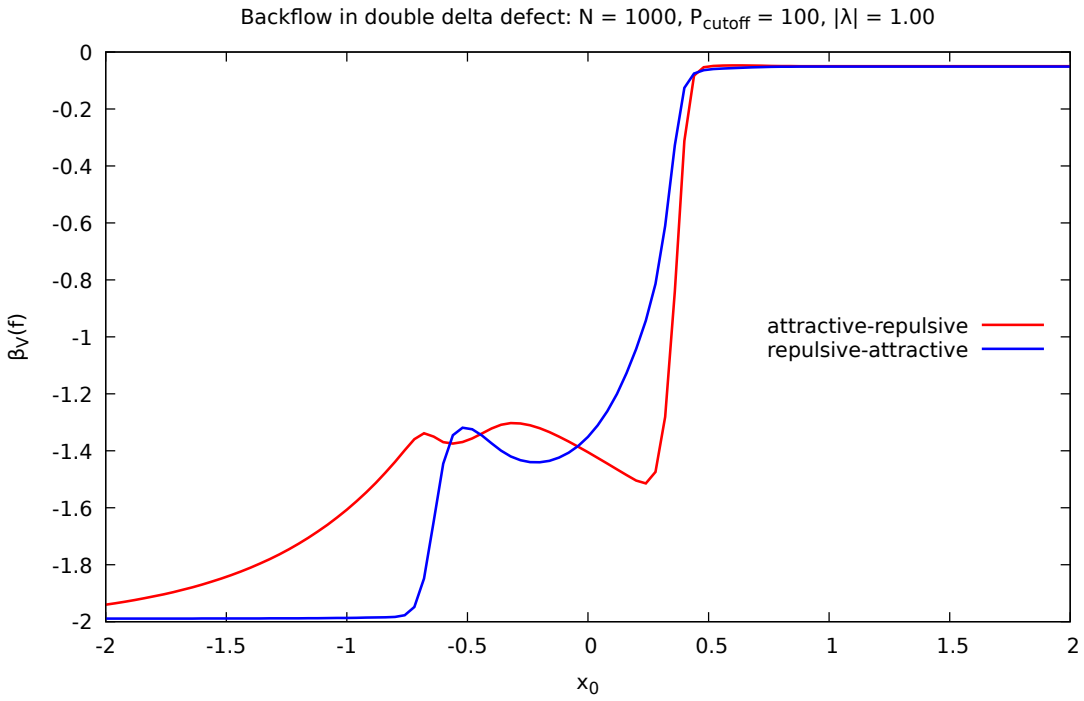

(b)

Figure 3.32: Lowest backflow eigenvalue of the current operator in the presence of a pair of deltas, $a_1 = -a_2 = -0.5$, $\lambda_1 = \lambda$ and $\lambda_2 = -2\lambda_1$, for which (a) $|\lambda| = 0.5$ (b) $|\lambda| = 1.0$.

— 4 —

Backflow in the presence of a jump-defect

4.1 INTEGRABLE DEFECTS

Either in classical or quantum theory, partial differential equations come in useful to describe the dynamics of the systems we want to study. The same physical idea can be implemented in different ways, depending on what one wants to describe. Integrable defects [12, 110, 13, 111, 112, 14, 113, 114, 115, 116] can be treated both in classical and quantum contexts in linear and nonlinear theories. In a linear theory, integrability is certainly redundant, but the underlying motivation is the same: to preserve conservation laws. Boundaries and defects are additional structures that can be added to the theory, but, generally, they spoil the integrability of the theory. Nevertheless, there are special types of defects that preserve integrability. This chapter will focus on one of such examples.

In the Schrödinger equation for a square-integrable wavefunction φ, one explicitly writes down a potential term, usually a function of the position, in the Hamiltonian of the system. In case the potential is only a function of the space coordinate (and possibly of time), but not of φ itself, the equation is still a linear partial differential equation. Additionally to working with an explicit potential term, there is another way of implementing interactions in the presence of point-like impurities or defects, a kind of internal boundary at a point. Rather than written as an external potential function, the defect can be described by a set of sewing conditions. In $1+1$ dimensions, these conditions relate the field and its derivatives on the left to the field and its derivatives on the right of the defect's location. The δ-type defect has the pedagogical advantage

of allowing both descriptions; it can be written as the usual delta potential $\delta(x)$ or as a set of two sewing conditions. In particular, for the δ-type defect, one condition is a statement of the continuity of the field at the defect location and the other one describes the discontinuity of the spatial derivative of the field, as discussed in the previous chapter. Although interesting and more familiar, the δ-type of impurity may spoil the integrability of a nonlinear integrable system. For instance, that is the case for the sine-Gordon equation [117]. However, some years ago it was shown that there exist two types of defects that are integrable, proved by constructing Lax pairs, and they were categorised as type I and type II [116, 118]. The former is simpler in the sense that only the field has dynamics, and the latter is a generalization with an extra function defined on the defect; it has an extra internal degree of freedom. Moreover, these defects can move with constant speed and are able to scatter [15].

In this thesis, we focus on the type I integrable defects. While the δ-type defect has continuous solutions at the defect location, we can have a defect that allows a discontinuity of the field at the same location. Such a defect, with a particular set of sewing conditions, is called a 'jump-defect'. In the context of fluid mechanics, such defects are very similar to shock waves, for example, which have sewing conditions expressed by the Rankine-Hugoniot conditions [119].

4.1.1 Jump-defect in a non-relativistic context

Although a Lagrangian description is not the only way for setting up the situation we are interested in, we can start from a Lagrangian in $1+1$ dimensions. By conveniently setting a length scale ℓ as the unit of length and $m\ell^2/\hbar$ as the unit of time, equivalently setting $\hbar = m = 1$, the Lagrangian density [120] is

$$\mathcal{L}[\psi] = \frac{i}{2}\left(\psi^\star\psi_t - \psi_t^\star\psi\right) - \frac{|\psi_x|^2}{2}\,, \tag{4.1}$$

and the Euler-Lagrange equation gives the linear Schrödinger equation

$$2i\psi_t + \psi_{xx} = 0, \tag{4.2}$$

with time and spatial derivatives of function ψ denoted by ψ_t and ψ_x, respectively. The defect can be placed at the position $x_D = 0$ on the real line, for example. This means that the bulk region, $-\infty < x < \infty$, will effectively split in two parts, as in figure 4.1.

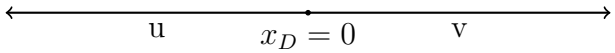

Figure 4.1: Locating a defect on the real line.

The field on the left of the defect ($x < 0$) will be denoted $u = u(x,t)$ and the field on the right ($x > 0$) will be denoted $v = v(x,t)$. The values of the fields at $x = x_D$ do not match and $v(x_D,t) - u(x_D,t) \neq 0$, representing a jump discontinuity. Specifically, the fields are evaluated at x_D in the following limiting sense

$$\begin{aligned} u(x_D,t) &= \lim_{\varepsilon\to 0} u(x_D-\varepsilon,t), \quad v(x_D,t) = \lim_{\varepsilon\to 0} v(x_D+\varepsilon,t), \\ u_x(x_D,t) &= \lim_{\varepsilon\to 0} u_x(x_D-\varepsilon,t), \quad v_x(x_D,t) = \lim_{\varepsilon\to 0} v_x(x_D+\varepsilon,t), \end{aligned} \tag{4.3}$$

with $\varepsilon > 0$. From the nonlinear Schrödinger model considered in [114], we particularise to the linear case, where u and v obey the linear Schrödinger equation, with a Lagrangian density composed of three contributions coming from u, v and the defect

$$\mathcal{L} = \theta(x_D - x)\mathcal{L}[u] + \theta(x - x_D)\mathcal{L}[v] + \delta(x - x_D)B[u,v]\,, \tag{4.4}$$

where the Heaviside function is $\theta(x) = 0$ for $x < 0$ or $\theta(x) = 1$ for $x > 0$ and

$$B[u,v] = \alpha\left[\frac{i}{4\alpha^2}\left((u-v)(u^\star - v^\star)_t - (u-v)_t(u^\star - v^\star)\right) + \frac{1}{4}(u+v)(u^\star + v^\star)\right] \tag{4.5}$$

with a real parameter α. That particular choice will ensure conservation of the quantities discussed in section 4.1.2. The full action taking into account the contributions from the bulk and from the defect itself has the following form

$$\mathcal{A} = \int dt\left[\int_{-\infty}^{x_D} dx\,\mathcal{L}[u] + B[u,v]\Big|_{x=x_D} + \int_{x_D}^{\infty} dx\,\mathcal{L}[v]\right], \tag{4.6}$$

from where the defect conditions follow from the variation of the action, accordingly to the stationary action principle, and are given by

$$\begin{aligned} u_x &= -\frac{i}{\alpha}(u-v)_t + \frac{\alpha}{2}(u+v)\Big|_{x=x_D}\,, \\ v_x &= -\frac{i}{\alpha}(u-v)_t - \frac{\alpha}{2}(u+v)\Big|_{x=x_D}\,, \end{aligned} \tag{4.7}$$

which can immediately be rearranged as

$$\begin{aligned} u_x - v_x &= \alpha(u+v)\big|_{x=x_D} \ , \\ v_x + u_x &= -\frac{2i}{\alpha}(u-v)_t\Big|_{x=x_D} \ , \end{aligned} \tag{4.8}$$

both valid at the defect's position $x = x_D = 0$. The first thing to notice is that the difference of the spatial derivatives is proportional to the average (arithmetic mean) value of the fields meeting at the defect's location, and the parameter α works as a strength of that difference. The second is the discontinuity at the defect, namely we can have $u \neq v$. For reference and comparison, we shall refer to the matching conditions (3.1), called sewing conditions for the δ-defect, simply as

$$u = v, \quad (v_x - u_x) = 2\lambda u, \tag{4.9}$$

both evaluated at the defect's position $x = x_D = 0$, and with λ the associated defect parameter. Note also the similarity to the Bäcklund transformations [121] for the linear Schrödinger equation. More specifically, suppose that the sewing conditions (4.7) are valid everywhere on the full real line and take the second order space derivatives as follows

$$\begin{aligned} u_{xx} + v_{xx} &= -\frac{2i}{\alpha}(u_x - v_x)_t \ , \\ u_x - v_x &= \alpha(u+v) \ , \end{aligned}$$

resulting in the Schrödinger equation for their sum $u + v$ in the form

$$2i(u+v)_t + (u+v)_{xx} = 0. \tag{4.10}$$

Doing similar calculations to their difference $u - v$, we obtain

$$2i(u-v)_t + (u-v)_{xx} = 0, \tag{4.11}$$

hence both u and v obey the Schrödinger equation independently, as expected for a Bäcklund transformation. The sewing conditions (4.7) would, therefore, be a Bäcklund transformation if the relations were valid for all positions instead of being defined only at the defect's location. In that sense, conditions (4.7) are 'frozen' Bäcklund transformations. When discussing general point interactions in section 2.4, we mention

that the δ-defect can be represented by a more general set of conditions (2.27) in consequence of the theory of self-adjoint extensions for the Hamiltonian operator or, equivalently, the conservation of probability implying the continuity of the probability current density at the defect's location. The case of the potential described by the derivative of a delta, namely, the δ' interaction is not that simple; one needs to take into consideration other factors such as its symmetry under parity transformations, for instance, in order to properly specify the interaction as previously discussed. We may ask if the jump-defect can also be completely characterized by this set of conditions. If we apply (4.8) to the square-integrable wavefunctions u and v constructed as wave packets from stationary scattering states u_k and v_k, the sewing conditions are shown to be energy-dependent, meaning that the constants a, b, c and d of (2.27) would have to depend on k. Alternatively, starting from conditions of the form (2.27) for the stationary scattering solution, the corresponding square-integrable solution would not have exactly the same form because the relation between these two involves the integration in k of an arbitrary function $\tilde{g} \in C_0^\infty(\mathbb{R})$, similar to the previous expression (3.3) in the δ-defect case. More specifically, the conditions upon the square-integrable solution would involve not only space derivatives but also time derivatives. In fact, the four-parameter family of defects described by (2.27) can accommodate sewing conditions in the same form as (4.8) for scattering solutions u_k and v_k, but then the square-integrable solutions u and v would not have the same set of sewing conditions. We remark that, in order to keep conserved total momentum, energy and probability, the set of sewing conditions is really about the square-integrable functions evaluated at the defect's position. Physically, it is clear that defects constructed from self-adjoint extensions enforce only probability conservation while the jump-defect enforces the conservation of three physical quantities, including the probability. Therefore, conditions such as (2.27) do not automatically provide a model of the jump-defect that we propose to examine in this chapter and they are not energy-dependent conditions.

At the moment, it is unknown if there is a physical system (approximately) described by these sewing conditions (4.7). However, they have a physical motivation based on energy, momentum and probability conservation, which will be discussed in the next section, and on the fact that discontinuities are ubiquitous in natural processes. As mentioned before in section 2.4 and at the beginning of this chapter, there are numerous situations where a defect, as a discontinuity, is a common phenomenon. Hydraulic

jumps, shock waves, a dislocation within a crystal and a mass jump are particular examples. In all cases, there is a discontinuous physical quantity while others remain continuous, and that is determined by some conservation laws. In the case of a defect with discontinuous wavefunction, conservation of probability imposes a continuous probability flux across the defect position as exactly expressed before in equation (2.28). In particular, the presence of a defect located at a particular position $x = x_D$ breaks space-translation invariance, and the conservation of momentum is a surprise. Before that discussion, we shall mention that the sewing conditions (4.7) allow the following pair of traveling wave solutions [114]

$$u_k(x) = u_0 \exp(-i\omega t + ikx), \quad v_k(x) = v_0 \exp(-i\omega t + ikx), \quad v_0 = \frac{k + i\alpha}{k - i\alpha} u_0, \quad (4.12)$$

where k is real, u_0 is a constant amplitude, and the frequency $\omega = k^2/2$ obeys the usual quadratic dispersion relation from the non-relativistic theory. These stationary scattering states do not span the entire Hilbert space as bound states are not taken into account. In the particular case of a δ-defect, it is possible to construct a complete set of (generalized) energy eigenfunctions [122]. More generally, the self-adjoint property of the Hamiltonian operator is not enough to guarantee asymptotic completeness, and the Hamiltonian cannot have a continuous singular spectrum. The spectral properties of the Hamiltonian critically depend on the type of interaction considered, and there are important theorems to that effect of asymptotic completeness that are relevant to the case of general point interactions, see [123], Theorem XI.9. A general study of the scattering theory for finite rank perturbations can be found in [124].

As our analysis will be restricted to the linear case, we directly look at conservation laws as our guiding principle for the construction of the jump-defect. Specifically, the jump-defect is designed in order to keep valid some conservation laws that are true in the free case. In other words, we ask that the implementation of the jump-defect does not cause a breakdown of the conservation laws we have in the free Schrödinger theory.

4.1.2 Conservation laws

In the free Schrödinger case, we know that quantities such as energy, probability and momentum are conserved. For that, we check how a point-defect may affect these conservation laws, and how (if possible) the sewing conditions can modify the quantity

so that it remains conserved in the presence of the defect. A similar analysis [114] was applied to a nonlinear model in the presence of defects. In particular, we compare the δ-defect to the jump-defect and analyse energy, momentum and total probability.

Taking only the u contribution defined at the left region $x < 0$, the energy density derived from the Lagrangian density given by (4.1) is

$$\mathcal{E} = \frac{|u_x|^2}{2}, \tag{4.13}$$

and similarly for v that is defined at the right region $x > 0$. The total energy carried by the fields u and v, either calculated as the expectation value of the Hamiltonian or as the spatial integral of the energy density, has to be split up into contributions from two domains when we have one single point-defect. Each domain is separately described by a Schrödinger equation, and the defect glues together these two regions by the sewing conditions at the defect's location. In fact, for cases where the wavefunction and its derivatives are continuous over the whole domain, breaking the full real line into disjoint halves does not make a difference to the dynamics at the middle point, but we want to include the jump-defect, and discontinuities can make a difference to the dynamics coupling the left half-line with the right half-line. That coupling is exactly determined by the set of sewing conditions. For instance, the discontinuity of the wavefunction derivative in the case of a δ-defect can be severe enough (Dirichlet boundary condition) to produce a totally reflecting wall disconnecting the left region from the right one. The same applies for all other physical quantities of interest, such as the total contribution from the fields u and v to the momentum density and to the probability density. The total contribution of the fields to the energy is therefore

$$E = \frac{1}{2}\int_{-\infty}^{0} u_x^\star u_x dx + \frac{1}{2}\int_{0}^{\infty} v_x^\star v_x dx, \tag{4.14}$$

where we have split up the integral taking into consideration that the defect is located at the origin $x = 0$. For checking conservation, we calculate the time derivative

$$\begin{aligned} E_t &= \frac{1}{2}\int_{-\infty}^{0} (u_{xt}^\star u_x + u_x^\star u_{xt}) dx + \frac{1}{2}\int_{0}^{\infty} (v_{xt}^\star v_x + v_x^\star v_{xt}) dx \\ &= \frac{1}{2}\left(u_t^\star u_x + u_x^\star u_t\right)|_{x=0} - \frac{1}{2}\left(v_t^\star v_x + v_x^\star v_t\right)|_{x=0}, \end{aligned}$$

where we used the Schrödinger equation and ignored the zero contributions at ± infinity as usual. For the δ-defect, using (4.9) we obtain

$$\begin{aligned} E_t &= -\lambda u_t^\star u + \lambda u^\star u_t \\ &= -\lambda \frac{\partial}{\partial t}(u^\star u)\Big|_{x=0} , \end{aligned}$$

which may not be zero, but we can guarantee the total energy (including a contribution from the defect itself) is conserved when suitably modified. That means the adjusted conserved energy is

$$E_c := E + \lambda u^\star u|_{x=0} . \tag{4.15}$$

Note that the total energy carried by the fields is slightly modified so that the revised total energy E_c is conserved, as expected. Furthermore, note that (4.15) is equivalent to the quadratic form of the Hamiltonian operator with a δ potential function; see [125]. For the jump-defect, we can check that the choice (4.7) produces

$$\begin{aligned} E_t = \frac{1}{2}\left[u_t^\star\left(\frac{-i}{\alpha}(u-v)_t + \frac{\alpha}{2}(u+v)\right) + u_t\left(\frac{i}{\alpha}(u^\star - v^\star)_t + \frac{\alpha}{2}(u^\star + v^\star)\right)\right]_{x=0} \\ - \frac{1}{2}\left[v_t^\star\left(\frac{-i}{\alpha}(u-v)_t - \frac{\alpha}{2}(u+v)\right) + v_t\left(\frac{i}{\alpha}(u^\star - v^\star)_t - \frac{\alpha}{2}(u^\star + v^\star)\right)\right]_{x=0} \\ = \quad \frac{\alpha}{4}\frac{\partial}{\partial t}\left((u+v)(u^\star + v^\star)\right)\Big|_{x=0} , \end{aligned}$$

which depends on the parameter α and may not be zero, but we can guarantee the conservation by modifying it with the following redefinition of the energy

$$E_c := E - \frac{\alpha}{4}|u+v|^2\Big|_{x=0} . \tag{4.16}$$

As already remarked, expressions evaluated at the origin have to be understood in the limiting sense of (4.3). Hence, the energy E_c is conserved. The time-translation invariance in both cases was preserved because the total conserved energy is composed of contributions coming from the bulk and also from the defect. Different from the case of a δ-defect, where one could directly calculate the quadratic form of the full Hamiltonian by means of the corresponding potential function, there is no explicitly known potential function to describe the jump-defect. Quadratic forms of the Hamiltonian (or energy forms) can also be used to work with singular interactions [126, 127, 128]. Recall that a

quadratic form q is a mapping $Q(q) \times Q(q) \to \mathbb{C} : (\varphi, \psi) \to \langle\varphi| H |\psi\rangle$, where $Q(q)$ is a dense subspace of the Hilbert space $\mathcal{H}$ known as the form domain that is the largest domain on which q can be defined [129]. In particular, the quadratic form q associated with a Hamiltonian H has domain $Q(q) = Q(H)$, where $Q(H)$ is called the the form domain of H. It is worth remarking that the form domain $Q(H)$ in the case of a δ-defect is the Sobolev space $H^1(\mathbb{R})$, but it is given by the direct sum $H^1(\mathbb{R}_-) \bigoplus H^1(\mathbb{R}_+)$ in the case of a jump-defect, with $\mathbb{R}_- = (-\infty, 0)$ and $\mathbb{R}_+ = (0, \infty)$. It is also worth noting that the defect contribution to the conserved energy E_c appears on-shell in the sense that the Schrödinger equation has to be used. Note that a discontinuity at the origin does not automatically imply that there is an unphysical infinite kinetic energy. That will be more clear in the next section 4.2 with a discussion of the jump-defect discontinuity.

Now, let us analyse the momentum. It is worth recalling the well-known fact that the momentum operator $\hat{P}$ has no self-adjoint extension over $L^2(0, \infty)$ [130], that is, on the semi-infinite line, because $\hat{P}$ has deficiency indices $(1, 0)$. In spite of that, it is possible to have self-adjoint extensions of the momentum operator on $L^2(\mathbb{R}_-) \bigoplus L^2(\mathbb{R}_+)$, see, for example, the account of [131]. In fact, for the case of a defect at the origin, $\hat{P}$ has deficiency indices $(1, 1)$, and its self-adjoint extensions are parametrized by $U(1)$. This means that the field on the left of the defect is related, at the origin, to the field on the right of it by a phase factor $e^{i\theta}$, where $\theta \in \mathbb{R}$. Indeed, the sewing conditions at the defect location represent a choice of self-adjoint extension. The momentum density associated with the field u is given by

$$\mathcal{P}(u) = \frac{i}{2} \left(u_x^\star u - u^\star u_x\right), \tag{4.17}$$

so that the total contribution of the fields to the momentum is

$$P = \frac{1}{2} \int_{-\infty}^{0} i \left(u_x^\star u - u^\star u_x\right) dx + \frac{1}{2} \int_{0}^{\infty} i \left(v_x^\star v - v^\star v_x\right) dx. \tag{4.18}$$

We take the time derivative

$$\begin{aligned} P_t =& \frac{1}{2} \int_{-\infty}^{0} i(u_{xt}^\star u + u_x^\star u_t - u_t^\star u_x - u^\star u_{xt}) dx + \frac{1}{2} \int_{0}^{\infty} i(v_{xt}^\star v + v_x^\star v_t - v_t^\star v_x - v^\star v_{xt}) dx \\ =& \quad \frac{1}{4} \left[-(2u_x^\star u_x) + (u^\star u_{xx} + u u_{xx}^\star)\right]_{x=0} - \frac{1}{4} \left[-(2v_x^\star v_x) + (v^\star v_{xx} + v v_{xx}^\star)\right]_{x=0} , \end{aligned}$$

where we used the Schrödinger equation and ignored the zero contributions at ± infinity. For the δ-defect, with (4.9),

$$\begin{aligned} P_t &= \frac{1}{4}\left[(-2(v_x^\star - 2\lambda v^\star)(v_x - 2\lambda v) + (-2iv^\star v_t + 2ivv_t^\star)) + (2v_x^\star v_x) - (v^\star v_{xx} + vv_{xx}^\star)\right]_{x=0} \\ &= \left(\lambda(vv^\star)_x - 2\lambda^2 vv^\star\right)\Big|_{x=0}\,, \end{aligned}$$

which cannot be written as a time derivative by the use of the sewing conditions. Hence, we are not able to fix this conservation law without any other extra considerations. The momentum P highlights the difference between the δ and the jump-defect because the same calculation applied to the jump-defect, using (4.7), yields

$$\begin{aligned} P_t = &-\frac{1}{4}\left[2\left(+\frac{i}{\alpha}(u^\star - v^\star)_t + \frac{\alpha}{2}(u^\star + v^\star)\right)\left(-\frac{i}{\alpha}(u-v)_t + \frac{\alpha}{2}(u+v)\right)\right. \\ &\left. - \left(u^\star\left(-\frac{i}{\alpha}(u-v)_{xt} + \frac{\alpha}{2}(u+v)_x\right) + u\left(+\frac{i}{\alpha}(u^\star - v^\star)_{xt} + \frac{\alpha}{2}(u^\star + v^\star)_x\right)\right)\right]_{x=0} \\ &+\frac{1}{4}\left[2\left(+\frac{i}{\alpha}(u^\star - v^\star)_t - \frac{\alpha}{2}(u^\star + v^\star)\right)\left(-\frac{i}{\alpha}(u-v)_t - \frac{\alpha}{2}(u+v)\right)\right. \\ &\left. - \left(v^\star\left(-\frac{i}{\alpha}(u-v)_{xt} - \frac{\alpha}{2}(u+v)_x\right) + v\left(+\frac{i}{\alpha}(u^\star - v^\star)_{xt} - \frac{\alpha}{2}(u^\star + v^\star)_x\right)\right)\right]_{x=0}, \end{aligned}$$

which can be simplified to

$$P_t = -\frac{i}{2}\left[\frac{\partial}{\partial t}\left(u^\star v - v^\star u\right)\right]_{x=0},$$

which may not be zero, but we can guarantee conservation of the total momentum (including a contribution from the defect itself) with a suitably adjusted momentum defined by

$$P_c := P + \frac{i}{2}(u^\star v - v^\star u)\Big|_{x=0}. \tag{4.19}$$

Then, the total momentum P_c is conserved. While it is not surprising that the energy is conserved, since the Hamiltonian generates the dynamics of a physical system, conservation of momentum is surprising because it will not be generally conserved, as shown by the example of a δ-defect.

The probability density for the field u is given by

$$\mathcal{N}(u) = u^\star u, \tag{4.20}$$

so that the total contribution of the fields to the probability is

$$N = \int_{-\infty}^{0} \mathcal{N}(u)dx + \int_{0}^{\infty} \mathcal{N}(v)dx = \int_{-\infty}^{0} u^\star u dx + \int_{0}^{\infty} v^\star v dx. \tag{4.21}$$

To examine its conservation, we consider

$$\begin{aligned} N_t &= \int_{-\infty}^{0} (u_t^\star u + u^\star u_t)dx + \int_{0}^{\infty} (v_t^\star v + v^\star v_t)dx \\ &= \frac{1}{2}\left(-iu_x^\star u + iu^\star u_x\right)|_{x=0} - \frac{1}{2}\left(-iv_x^\star v + iv^\star v_x\right)|_{x=0}, \end{aligned}$$

where we used the Schrödinger equation and ignored the zero contributions at infinities. For the δ-defect, using (4.9),

$$\begin{aligned} N_t &= \frac{1}{2}\left(-iu(v_x^\star - \lambda u^\star)|_{x=0} + iu^\star(v_x - \lambda u)|_{x=0} - \left(-iv_x^\star v + iv^\star v_x\right)|_{x=0}\right) \\ &= \frac{1}{2}\left(-iv_x^\star(u-v) + i(u^\star - v^\star)v_x)\right)\Big|_{x=0} = 0, \end{aligned}$$

which means this is automatically conserved. For the jump-defect, with the choice (4.7)

$$\begin{aligned} N_t &= \frac{1}{2}\left[\frac{u(u^\star - v^\star)_t + u^\star(u-v)_t)}{\alpha} + \frac{i\alpha}{2}\left(u^\star(u+v) - u(u^\star + v^\star)\right)\right]_{x=0} \\ &\quad - \frac{1}{2}\left[\frac{v(u^\star - v^\star)_t + v^\star(u-v)_t)}{\alpha} - \frac{i\alpha}{2}\left(v^\star(u+v) - v(u^\star + v^\star)\right)\right]_{x=0} \\ &= \frac{1}{2\alpha}\left[\frac{\partial}{\partial t}((u-v)(u^\star - v^\star))\right]_{x=0}, \end{aligned}$$

which depends on the parameter α and may not be zero. However, we can guarantee conservation of the total probability (including a contribution from the defect itself) with the following suitably modified total probability

$$N_c := N - \frac{1}{2\alpha}|u-v|^2\Big|_{x=0}. \tag{4.22}$$

Hence, the total probability N_c is conserved.

According to the textbook's definition of quantum observables, one can associate any physical quantity A with an observable $\hat{A}$ that is a self-adjoint operator in the Hilbert space. In the interaction-free situation, a particle on the real line has a self-adjoint momentum operator and self-adjoint Hamiltonian. The presence of a defect may affect

the self-adjointness property of some operators, although it is possible that there are self-adjoint extensions. The way we introduce a defect is by adjusting the free operators with a contribution from the defect itself, and that is found by means of the sewing conditions, which represent a choice of self-adjoint extension. Moreover, the existence of different self-adjoint extensions corresponds to the existence of different physics, see, for instance, [58], page 143. From a physical point of view, conservation laws relate to physical quantities. In particular, it is expected that the energy and probability of a physical system are conserved. Depending on the model under consideration, it is often the case that momentum is not conserved.

We have shown how both the δ and the jump-defect affect some conservation laws and we have seen how we can fix these conservation laws by redefining quantities with an extra contribution which comes from the defect. However, it is clear that the jump-defect can exchange both energy and momentum with the fields u and v to either side of it in a way that is compatible with their conservation, but the δ-defect does not have this compatibility. When we treat these defects in the context of quantum mechanics, the momentum P is actually related to the probability current. In particular, the momentum density $\mathcal{P}$ plays the role of the probability current density in natural units with $\hbar = m = 1$. The exact relation is appropriately expressed in the next section. Moreover, we will see how this extra term associated with the defect affects the calculation of the quantum backflow and how it significantly differs from the δ-defect case. Strikingly interesting, in the jump-case, is that the fixing term, to restore the conservation of P, has a substantial contribution to the lowest backflow eigenvalue $\beta_V(f)$.

4.2 BACKFLOW IN THE PRESENCE OF A JUMP-DEFECT

Now we consider the backflow calculation for the the jump-defect. However, we have to keep in mind that now our wavefunction φ_k has a jump discontinuity at the origin. Specifically, in the δ-defect case, the wavefunction and its derivative are locally integrable, that is $\varphi_k \in L^1_{\text{loc}}(\mathbb{R})$ and $\partial_x\varphi_k \in L^1_{\text{loc}}(\mathbb{R})$, with a wavefunction that is continuous on the full real line. In the jump-defect case, just the wavefunction is locally integrable $\varphi_k \in L^1_{\text{loc}}(\mathbb{R})$ but not its derivative because $\partial_x\varphi_k$ is given by (3.6), and the Dirac δ_0 is a singular distribution that is not represented by a locally integrable function.

Such discontinuities may cause the presence of undefined terms when multiplied by distributions. By avoiding the origin, we avoid this undesirable problem.

Given that now φ_k denotes the the scattering solution for the TISE in the presence of a jump-defect. Let us write the full square-integrable $\varphi \in L^2(\mathbb{R})$ and time-dependent jump solution to the Schrödinger equation as

$$\varphi(x,t) = \frac{1}{\sqrt{2\pi}} \int_0^\infty dk\, \tilde{g}(k) \exp(-iwt)\varphi_k(x) \tag{4.23}$$

with $\tilde{g} \in C_0^\infty(\mathbb{R})$ an arbitrary non-zero smoothly varying function, and the time-independent scattering (from the left) states in position basis are given by

$$\varphi_k(x) = \begin{cases} u_k(x) & = \exp(ikx), \quad x < 0 \\ \\ v_k(x) & = \left(\dfrac{k+i\alpha}{k-i\alpha}\right) \exp(ikx), \quad x > 0, \end{cases} \tag{4.24}$$

where the reflection coefficient $R(k) = 0$ and the transmission coefficient $T(k)$ for the jump-defect is explicit. From the theory of self-adjoint extensions of the Hamiltonian with a general point interaction at the origin, the free Hamiltonian is self-adjoint with domain $D(H) = H^2(\mathbb{R} \setminus \{0\})$ together with a a suitable set of sewing conditions defined at the origin. As mentioned before, a function in the Sobolev space $H^2(\mathbb{R} \setminus \{0\})$ is absolutely continuous except at the origin, where a finite jump discontinuity may be allowed. While the jump-defect connects the theory on the left of the origin ($x = 0$) with the theory on the right, we do not assign a definite value for the wavefunction at the defect's position because our wavefunction is $\varphi \in H^2(\mathbb{R} \setminus \{0\})$, although the right and left limits, in which u is evaluated at points approaching the origin from below and v from above, exist. From the definition of Sobolev spaces, it is not difficult to see that the weak derivative $\partial_x\varphi$ is such that $\partial_x\varphi \in H^1(\mathbb{R} \setminus \{0\})$ and it is defined with respect to test functions that are smooth functions ϕ of compact support separated from the origin, $\phi \in C_0^\infty(\mathbb{R} \setminus \{0\})$. Some of our physical quantities of interest, such as momentum and energy, involve derivatives of the wavefunction, and the first weak derivative in (3.6) has a term proportional to the Dirac distribution δ_0, which is not identified with a function in $L^1_{\text{loc}}(\mathbb{R})$, provided that $v_k(0) \neq u_k(0)$. However, because the distributional derivative $\partial_x\varphi \in H^1(\mathbb{R} \setminus \{0\})$ has to be defined in terms of $\phi \in C_0^\infty(\mathbb{R} \setminus \{0\})$, the weak and the strong derivatives coincide outside of the origin (noting that the strong derivative is

undefined at the origin) since ϕ is zero in the neighbourhood of $x = 0$. Hence, $\partial_x\varphi$ is locally integrable on $\mathbb{R} \setminus \{0\}$.

We concentrate our attention to the time-independent scattering state φ_k given by expression (4.24). A similar calculation to that of section 3.1, where we have to give a meaning to the derivatives in the inner kernel

$$L(k',k) = \int dx \int dx' \left[(\theta(-x')u^\star_{k'} + \theta(x')v^\star_{k'})\, J(f)(x',x)\, (\theta(-x)u_k + \theta(x)v_k)\right],$$

shows that the spatial integrals can be split into two regions of integration, a left part ($-\infty < x < 0$) and a right part ($0 < x < \infty$), corresponding to contributions purely from u and purely from v, respectively, as follows

$$\begin{aligned} 2iL(k',k) = &\int_{-\infty}^{0} dx' f(x') \left(u^\star_{k'}(x') \frac{\partial u_k(x')}{\partial x'} - \frac{\partial u^\star_{k'}(x')}{\partial x'} u_k(x') \right) \\ &+ \int_0^{\infty} dx' f(x') \left(v^\star_{k'}(x') \frac{\partial v_k(x')}{\partial x'} - \frac{\partial v^\star_{k'}(x')}{\partial x'} v_k(x') \right). \end{aligned}$$

Moreover, the derivatives can be understood in the strong sense, and there are no undefined terms that could appear from the product of singular distributions. In fact, the first contribution term gives

$$i(k+k') \int_{-\infty}^{0} dx' f(x') \exp(ix'(k-k')), \tag{4.25}$$

and the second contribution in terms of the transmission coefficient $T(k)$ is

$$i(k+k') \int_{0}^{\infty} dx' f(x') T^\star(k') T(k) \exp(ix'(k-k')). \tag{4.26}$$

Finally, we can write the lowest backflow eigenvalue of the operator $J_V(f)$ as

$$\beta_V(f) = \frac{1}{2\pi} \int_0^\infty dk \int_0^\infty dk' \tilde{\mathcal{J}}^*(k') \tilde{\mathcal{J}}(k) L(k',k),$$

with the kernel

$$\begin{aligned} 2L(k',k) = &(k+k') \int_{-\infty}^{0} dx' f(x') \exp(ix'(k-k')) \\ &+ \frac{(kk' + i\alpha(k'-k) + \alpha^2)}{(k'+i\alpha)(k-i\alpha)} (k+k') \int_0^\infty dx' f(x') \exp(ix'(k-k')), \end{aligned} \tag{4.27}$$

which is a Hermitian kernel, and $\tilde{\mathcal{J}}(k)$ is the normalised eigenfunction, in momentum space, associated with the lowest eigenvalue of the integral operator $J_V(f)$. This expression (4.27) was worked out for the non-conserved situation where we have not introduced any fixing term to conserve the probability current. In physical situations, we are interested in conserved quantities, and our jump-defect was specially devised for allowing conservation laws.

In section 4.1, we have established the condition for having a conserved total momentum P_c associated with a particular momentum density. The probability current is intimately related to the total momentum since

$$\int j_\psi(x)dx = \langle \hat{P} \rangle \,, \tag{4.28}$$

where we have set $\hbar = m = 1$, and $\hat{P}$ is the momentum operator. We can, therefore, interchangeably, refer to either momentum density or, equivalently, probability current density. In particular, Eq. (4.19) determines the adjusting term for obtaining a conserved probability current. The adjustment needs to be written in terms of a kernel, in momentum space, such that it can be added to the kernel $L(k', k)$ in (2.36). From (4.23), we can write the time-independent solution at the left of the defect as

$$\begin{aligned} u(x) &= \frac{1}{\sqrt{2\pi}} \int \tilde{g}(k) u_k(x) dk, \\ u^\star(x) &= \frac{1}{\sqrt{2\pi}} \int \tilde{g}^\star(k') u^\star_{k'}(x) dk', \end{aligned} \tag{4.29}$$

and similarly for the solution v at the right of the defect. Hence, after introducing the required projectors E_+ for right-movers, the adjustment expression is

$$\frac{i}{2} E_+ (u^\star v - v^\star u) E_+ \Big|_{x=0} = \frac{i}{4\pi} \int_0^\infty \int_0^\infty dk' dk \, \tilde{g}^\star(k') \tilde{g}(k) \left(\frac{2i\alpha(k+k')}{(k - i\alpha)(k' + i\alpha)} \right). \tag{4.30}$$

Note, section 4.1 has a discussion about conservation of physical quantities without making use of the smearing process with a positive test function f for producing spatial averaged quantities as introduced in our discussion of the quantum backflow in section 2.1. The test function has to be taken into account when considering the probability current operator. With our test function being a function only of the position, rather than time, the spatial averaged term corresponding to the defect contribution is

exactly what needs to be added to the expectation value $\langle J_V(f)\rangle_\psi$, from (2.24), to give the expectation value of the total adjusted probability current operator

$$\langle J_{cV}(f)\rangle_\psi = \langle J_V(f)\rangle_\psi + \frac{i}{4\pi}\int_0^\infty\int_0^\infty dk'dk\,\tilde{\psi}^\star(k')\tilde{\psi}(k)\left(\frac{2i\alpha(k+k')}{(k-i\alpha)(k'+i\alpha)}\right)f(0), \tag{4.31}$$

which is now actually related to the conserved probability current. Here the term $\langle J_V(f)\rangle_\psi$ only includes the kernel's contributions (4.27) which do not come from the defect. The defect's contribution is only taken into consideration when we impose the conservation of the probability current associated with the physical system we want to describe, which does not include the defect a priori. Finally, the expression (4.31) can be written as

$$\begin{aligned}\langle J_{cV}(f)\rangle_\psi \;=\; \frac{1}{2\pi}\int_0^\infty\int_0^\infty dk'dk\,\tilde{\psi}^\star(k')\tilde{\psi}(k)\Bigg[&(k+k')\int_{-\infty}^0 dx'f(x')\exp(ix'(k-k'))\\ &+\frac{(kk'+i\alpha(k'-k)+\alpha^2)}{(k'+i\alpha)(k-i\alpha)}(k+k')\int_0^\infty dx'f(x')\exp(ix'(k-k'))\\ &-\left(\frac{\alpha(k+k')}{(k-i\alpha)(k'+i\alpha)}\right)f(0)\Bigg].\end{aligned} \tag{4.32}$$

From this one only needs to take the infimum over the functions ψ, normalised with $\mathrm{supp}(\tilde{\psi}) \subset \mathbb{R}_+$ and suitably decaying as in (2.7), in order to obtain the lowest backflow eigenvalue $\beta_V(f) = \inf\langle J_{cV}(f)\rangle_\psi$ of the probability current operator $J_{cV}(f)$ in the presence of the jump-defect. Once we have simplified the kernel, we again need to rely upon the numerical calculations as the eigenfunction $\tilde{\mathcal{J}}(k)$ is not analytically known.

Clearly, the calculations in the previous section 4.1.2 are fully justified now that we emphasised the properties of the jump-defect wavefunction as an element of the appropriate Sobolev space, noting that the weak derivatives coincide with the strong ones. Particularly, given that $\varphi \in H^2(\mathbb{R}\setminus\{0\}) \cong H^2(\mathbb{R}_-)\bigoplus H^2(\mathbb{R}_+)$,

$$\begin{aligned} u &= \varphi|_{\mathbb{R}_-} \in H^2(\mathbb{R}_-) \subseteq C^1(\mathbb{R}_-),\\ v &= \varphi|_{\mathbb{R}_+} \in H^2(\mathbb{R}_+) \subseteq C^1(\mathbb{R}_+),\end{aligned} \tag{4.33}$$

where C^1 is the space of continuously differentiable functions. Also, as discussed in the previous section, the energy E is finite despite the wavefunction discontinuity. It follows from $\varphi \in H^2(\mathbb{R}\setminus\{0\})$ that the derivative $\partial_x\varphi \in H^1(\mathbb{R}\setminus\{0\}) \subset L^2(\mathbb{R})$. Thus,

the energy is given by the following finite L^2-norm

$$E = \frac{1}{2}\|\partial_x\varphi\|^2_{L^2(\mathbb{R})} = \frac{1}{2}\int |\partial_x\varphi(x)|^2\, dx, \tag{4.34}$$

where the integral is understood as the sum of the integrals in $(-\infty, 0)$ and $(0, \infty)$. To prove that $\varphi \in H^2(\mathbb{R}\setminus\{0\})$ is a true statement indeed, it is convenient to use an equivalent characterization of the Sobolev spaces H^m of order m, defined by the expression 3.2, in terms of the Fourier transform as follows

$$H^m(\mathbb{R}) = \left\{ \psi \in L^2(\mathbb{R}) \,\middle|\, \int \left(1+|\xi|^2\right)^m |\tilde{\psi}(\xi)|^2\, d\xi < \infty \right\}, \tag{4.35}$$

where $\tilde{\psi}$ is the Fourier transform of ψ, and $\xi \in \mathbb{R}$. From the equations (4.23) and (4.24), φ can be conveniently expressed as

$$\varphi(x,t) = \theta(-x)\varphi_-(x,t) + \theta(x)\varphi_+(x,t), \tag{4.36}$$

where φ_- and φ_+ are extensions of u and v, respectively, to the full real line. That is

$$\begin{aligned} \varphi_-(x,t) &= \frac{1}{\sqrt{2\pi}}\int \tilde{g}(k)\exp(-iwt+ikx)\, dk \quad \forall x \in \mathbb{R}, \\ \varphi_+(x,t) &= \frac{1}{\sqrt{2\pi}}\int \tilde{g}(k)T(k)\exp(-iwt+ikx)\, dk \quad \forall x \in \mathbb{R} \end{aligned} \tag{4.37}$$

are functions in $H^2(\mathbb{R})$, and the function $\tilde{g}$ is such that $\tilde{g}(k) = 0$ for $k < 0$ and an arbitrary compactly supported bounded function for $k \geq 0$. Thus, as an inverse Fourier transform, φ has the form

$$\varphi(x,t) = \begin{cases} \varphi_-(x,t) = \left(\mathcal{F}^{-1}\tilde{g}_t\right)(x), & x < 0 \\ \\ \varphi_+(x,t) = \left(\mathcal{F}^{-1}\left(T\tilde{g}_t\right)\right)(x), & x > 0, \end{cases} \tag{4.38}$$

with the time dependence rewritten in terms of $\tilde{g}_t := \tilde{g}\exp(-iwt)$. Note also that the Heaviside function is essentially bounded, particularly $|\theta(x)| \leq 1$, and the exponential $\exp(-iwt)$ and the reflection coefficient $T(k)$ are bounded as well. Finally, because $\tilde{g}$ is compactly supported and bounded, the products $\left(1+|\xi|^2\right)\tilde{g}_t$ and $\left(1+|\xi|^2\right)T\tilde{g}_t$ are square-integrable funcions, and, therefore, it is true that $\varphi \in H^2(\mathbb{R}\setminus\{0\})$. In summary,

the following inequalities hold true

$$\begin{aligned} \|\varphi\|^2_{L^2(\mathbb{R})} &\leq \|u\|^2_{L^2(\mathbb{R})} + \|v\|^2_{L^2(\mathbb{R})} < \infty, \\ \|\partial_x\varphi\|^2_{L^2(\mathbb{R})} &\leq \|\partial_x u\|^2_{L^2(\mathbb{R})} + \|\partial_x v\|^2_{L^2(\mathbb{R})} < \infty, \\ \left\|\partial_x^2\varphi\right\|^2_{L^2(\mathbb{R})} &\leq \left\|\partial_x^2 u\right\|^2_{L^2(\mathbb{R})} + \left\|\partial_x^2 v\right\|^2_{L^2(\mathbb{R})} < \infty, \end{aligned} \tag{4.39}$$

where the derivatives can be understood in the strong sense as discussed, and the kinetic energy E given by (4.34) is finite.

As we mentioned, non-removable discontinuities pose difficulties to the products with the Dirac measure δ, which is a Radon measure rather than a locally integrable function. In particular, a distributional product such as

$$\langle\varphi\delta, f\rangle = \langle\delta, \varphi f\rangle = \varphi(0)f(0),$$

with a function φ discontinuous at the origin and test function f, is undefined since there is no consistent way to define $\varphi(0)$. However, the wavefunctions of interest here are in Sobolev spaces separated from the origin, where a defect is placed. That is compatible with our physical picture in which the wavefunction φ does not assume a particular value at the origin. In the Lagrangian (4.4), we have made it clear that what is defined only at the defect's position is a contribution purely from the defect itself rather than the theory of the left or the theory of the right semi-infinite lines.

4.3 NUMERICAL RESULTS

For a purely-transmitting defect, for which the reflection coefficient $R(k)$ is identically zero at all energies, the solution φ_k with an asymptotic incoming right-mover maintains itself as a right-mover also after scattering off the defect. This is not the case for the δ-defect that has a mixture of right-movers and left-movers as a result of being scattered by the defect. In this sense, the reflectionless Pöschl-Teller potential is more similar to the jump-defect than the δ. However, for the Pöschl-Teller potential, the backflow effect is smaller inside the interaction region than in the free case [11]. That this is not true in the jump-case can be seen from the figures in this section. In fact, at the defect's location, the effect can be either smaller or bigger depending on the magnitude of the parameter α.

Several graphs of the backflow lowest eigenvalue in the presence of the jump-defect were plotted below. All the graphs refer to the probability current operator smeared with a Gaussian test function f. Specifically, as mentioned in the δ-defect case, the graphs show the lowest eigenvalue against the position of measurement x_0 where f is centered. Our main freedom to be tuned is the parameter α corresponding to the strength of the defect. Unlike the Dirac δ-defect, or other explicit potential functions, the jump-defect has a parameter that can not be clearly distinguished as attractive or repulsive according to its sign, being either positive or negative, respectively. As particular cases, $\alpha = 0$ gives the expected free case represented by a constant horizontal line $\beta_0(f) \approx -0.241$ and the limiting cases $\alpha \to \pm\infty$ also approach the free backflow eigenvalue $\beta_V(f) \to \beta_0(f)$. We already expected this as the solutions φ_k for the limiting cases $\alpha \to \pm\infty$ are related to the free case by only a global phase, but the probability current density has products of the solution wavefunction with its complex conjugated spatial derivative. Thus, in the limit, their lowest backflow eigenvalue is the same as the free case.

Initially, for small absolute values of the parameter α, the lowest backflow eigenvalue has some symmetry between the positive and negative parameter values, figure 4.2. Slightly increasing $|\alpha|$, $\beta_V(f)$ of the associated conserved probability current starts to show a distinctly different behaviour between the positive and the negative values of α, see figure 4.5. As its absolute value increases, the graphs become more similar in terms of the magnitudes of the lowest backflow eigenvalue. However, as indicated by the plots, both positive $\alpha > 0$ and negative $\alpha < 0$ seem to unveil some stationary points, and, in some cases, while a positive parameter shows three of these points, the corresponding negative parameter can show up to five stationary points, figure 4.6. With successive increases of the parameter's absolute value $|\alpha|$, the graphs tend to become more similar again. In particular, both positive and negative values show the same number of stationary points, though when one has a minimum the other one has a maximum and vice-versa, figure 4.7. Whilst the non-conserved current develops a persistent trough for both positive and negative parameters, the conserved one develops a mixture of troughs and bumps as shown by Figs. 4.5, 4.6 and 4.7. As numerical results for the rectangular potential in [11] suggest, bound states might contribute towards these bumps. It is worth mentioning that, from (4.12), it is possible to see the existence of bound states associated with the jump-defect for either $k = i\alpha$ or $k = -i\alpha$. The

respective bound states can then be described by the following solutions

$$\begin{aligned} u = 0, \quad v = v_0 \exp\big(i\alpha^2 t/2 - \alpha x\big), \quad (k = i\alpha), \\ u = u_0 \exp\big(i\alpha^2 t/2 + \alpha x\big), \quad v = 0, \qquad (k = -i\alpha), \end{aligned} \tag{4.40}$$

which are clearly square-integrable solutions (provided $\alpha > 0$) [114].

Additionally to the two-dimensional plots, we have varied the parameters to display a three-dimensional picture of how the lowest backflow eigenvalue $\beta_V(f)$ is affected in the presence of the jump-defect. For comparison, we have plotted both cases: $\beta_V(f)$ for the non-conserved probability current operator, figure 4.9 and figure 4.10, and for the conserved probability current operator, figure 4.12 and figure 4.13. All these can be found in section 4.4 below.

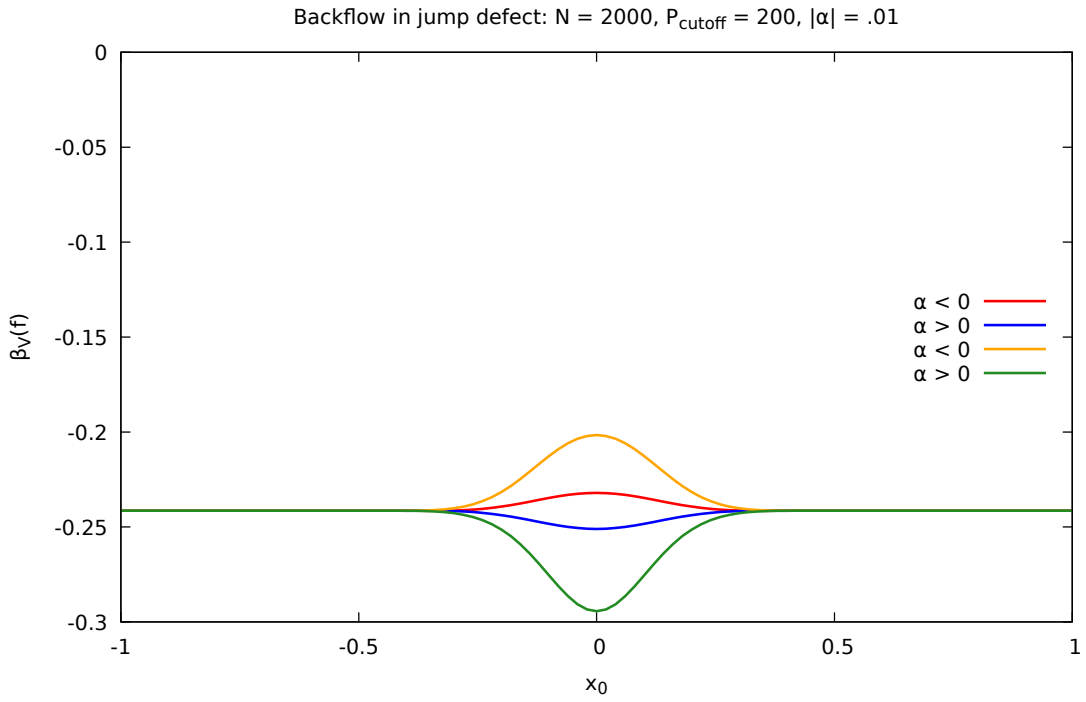

(a)

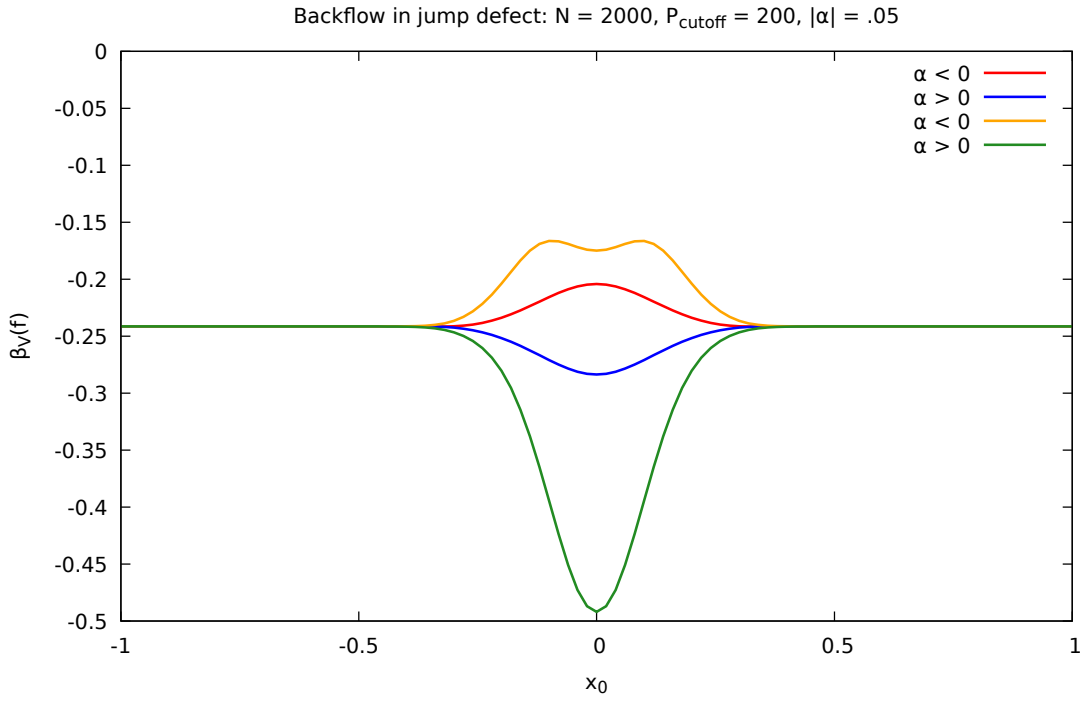

(b)

Figure 4.2: Lowest backflow eigenvalue of the current operator. **Red**/**blue** refer to the non-conserved probability current. **Yellow**/**green** refer to the conserved one. (a) $|\alpha| = 0.01$ (b) $|\alpha| = 0.05$.

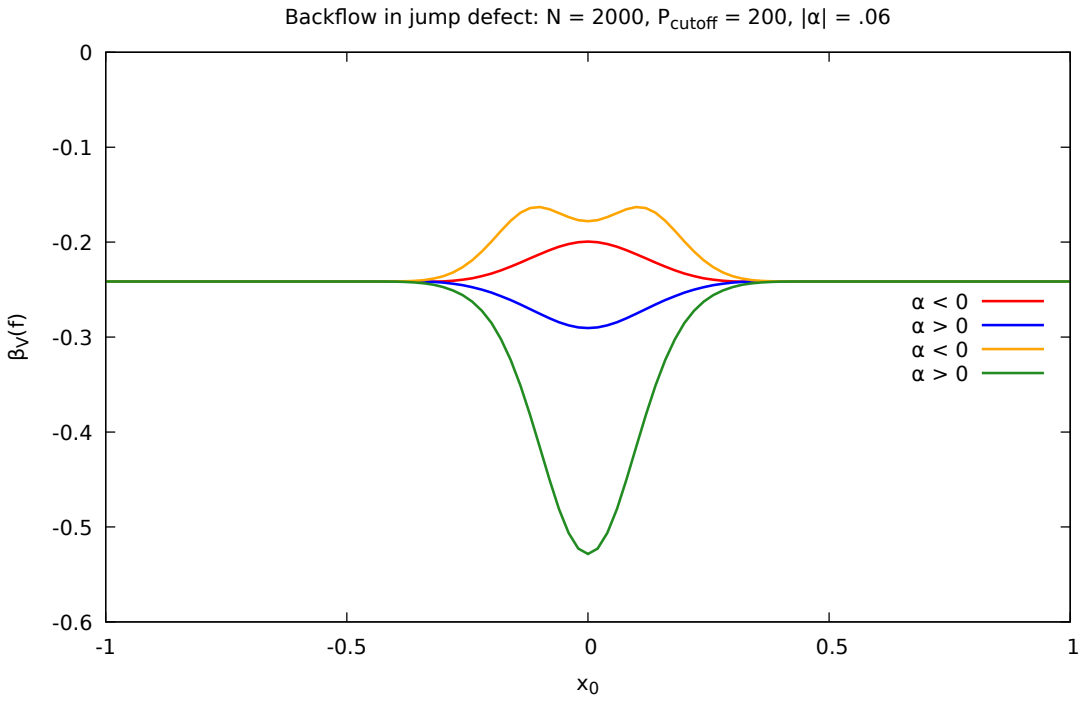

(a)

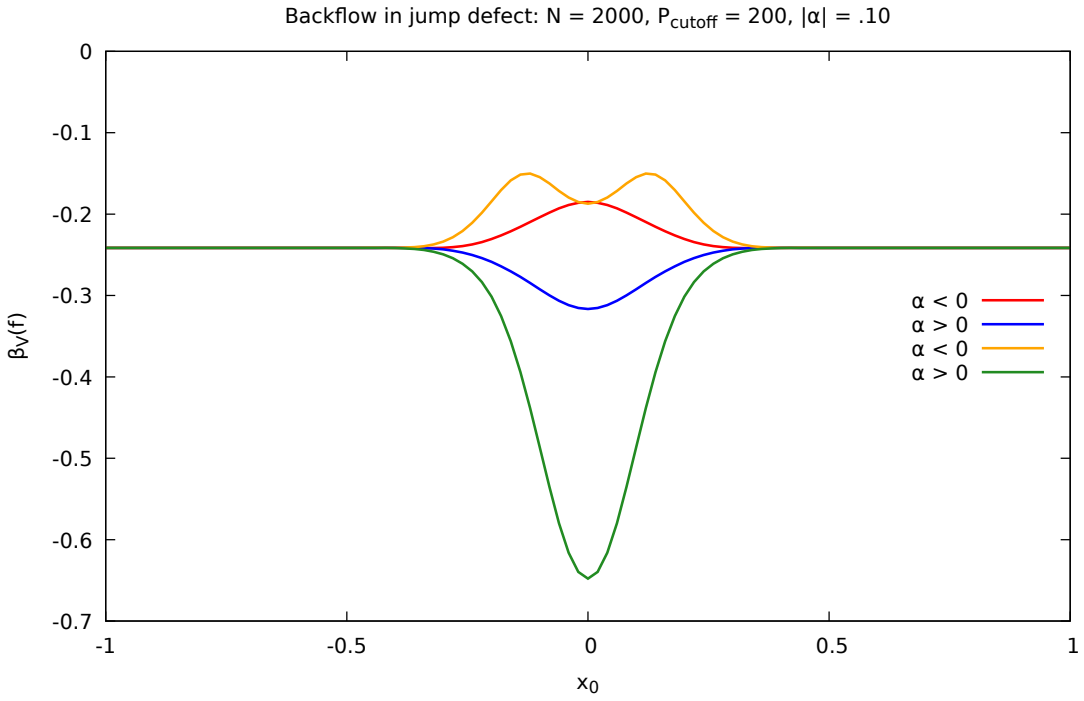

(b)

Figure 4.3: Lowest backflow eigenvalue of the current operator. **Red**/**blue** refer to the non-conserved probability current. **Yellow**/**green** refer to the conserved one. (a) $|\alpha| = 0.06$ (b) $|\alpha| = 0.1$.

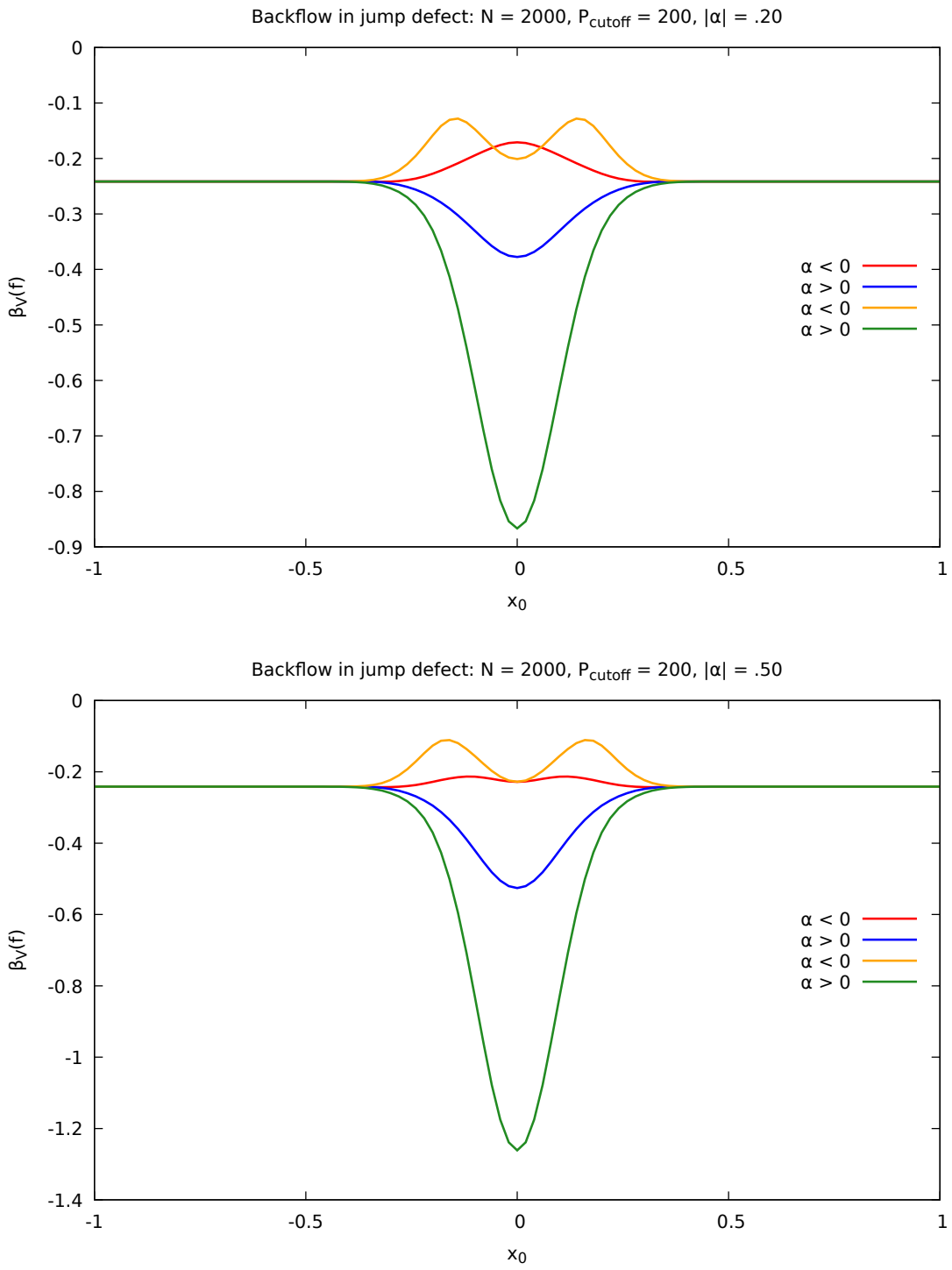

Figure 4.4: Lowest backflow eigenvalue of the current operator. **Red**/**blue** refer to the non-conserved probability current. **Yellow**/**green** refer to the conserved one. (a) $|\alpha| = 0.20$ (b) $|\alpha| = 0.50$.

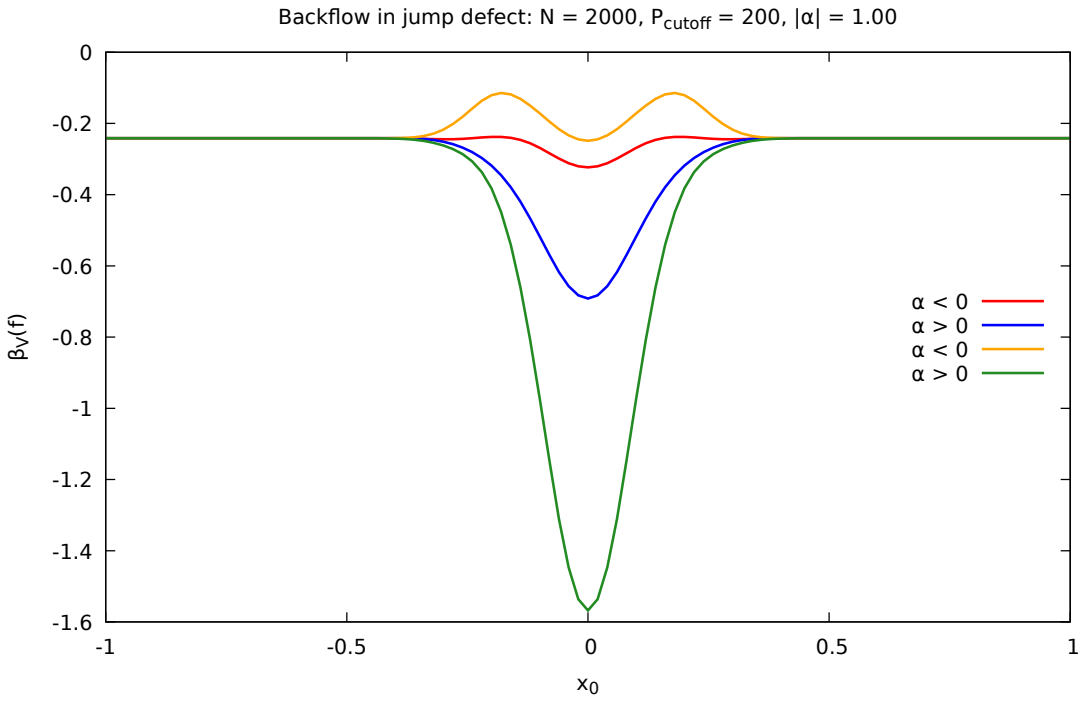

(a)

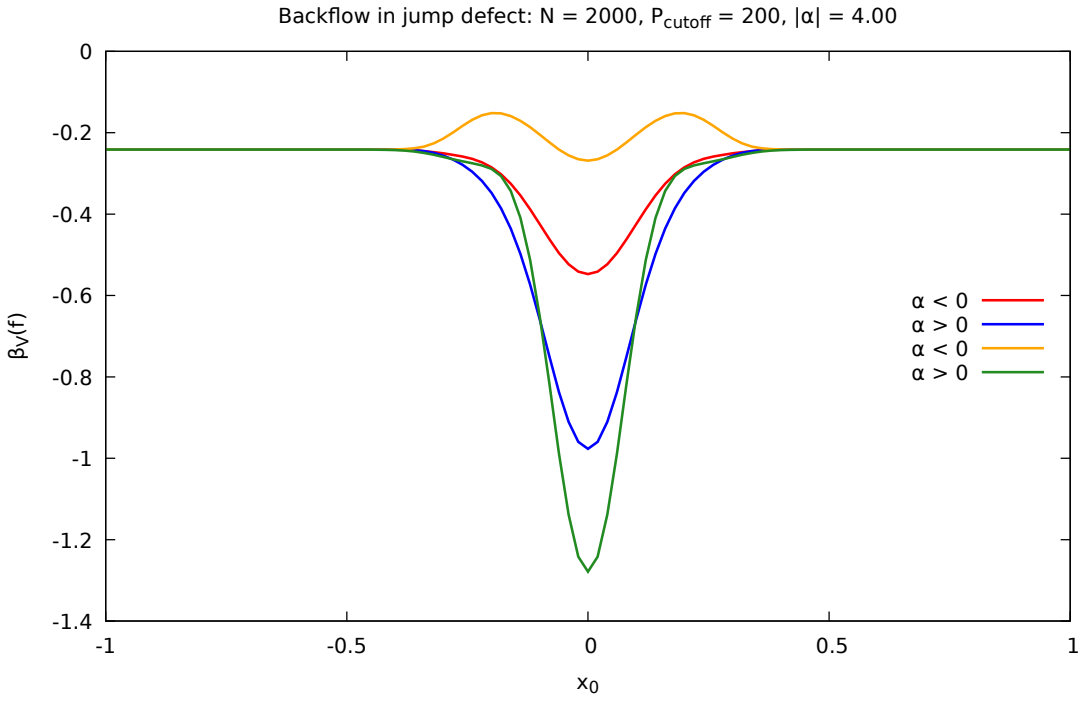

(b)

Figure 4.5: Lowest backflow eigenvalue of the current operator. **Red**/**blue** refer to the non-conserved probability current. **Yellow**/**green** refer to the conserved one. (a) $|\alpha| = 1.0$ (b) $|\alpha| = 4.0$.

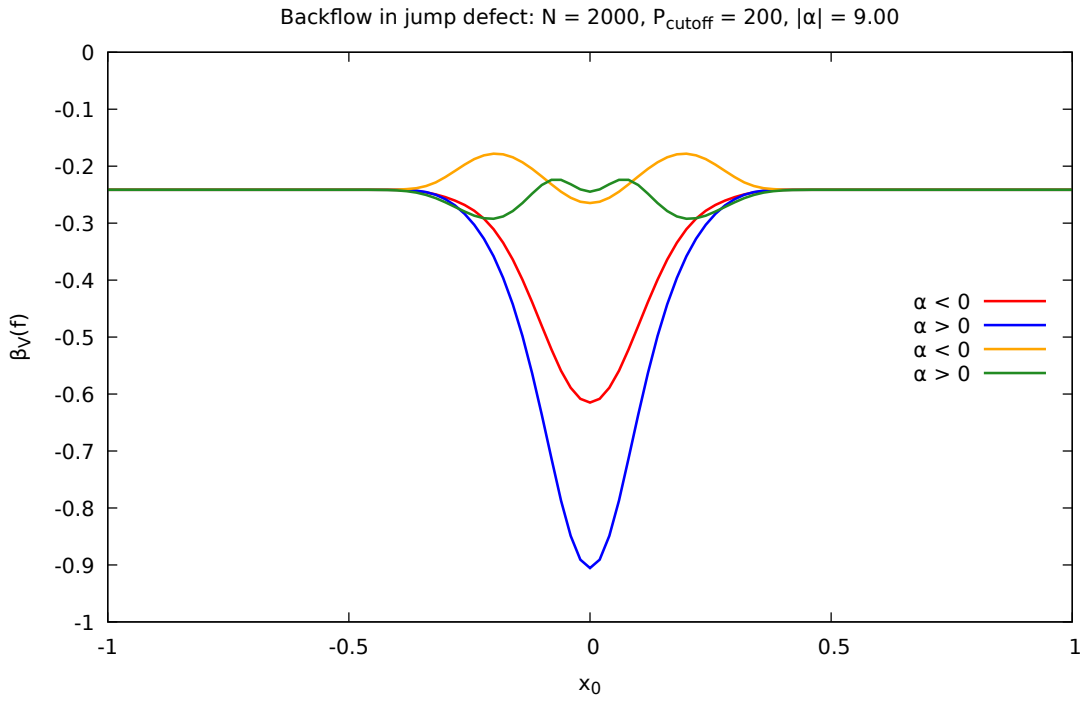

(a)

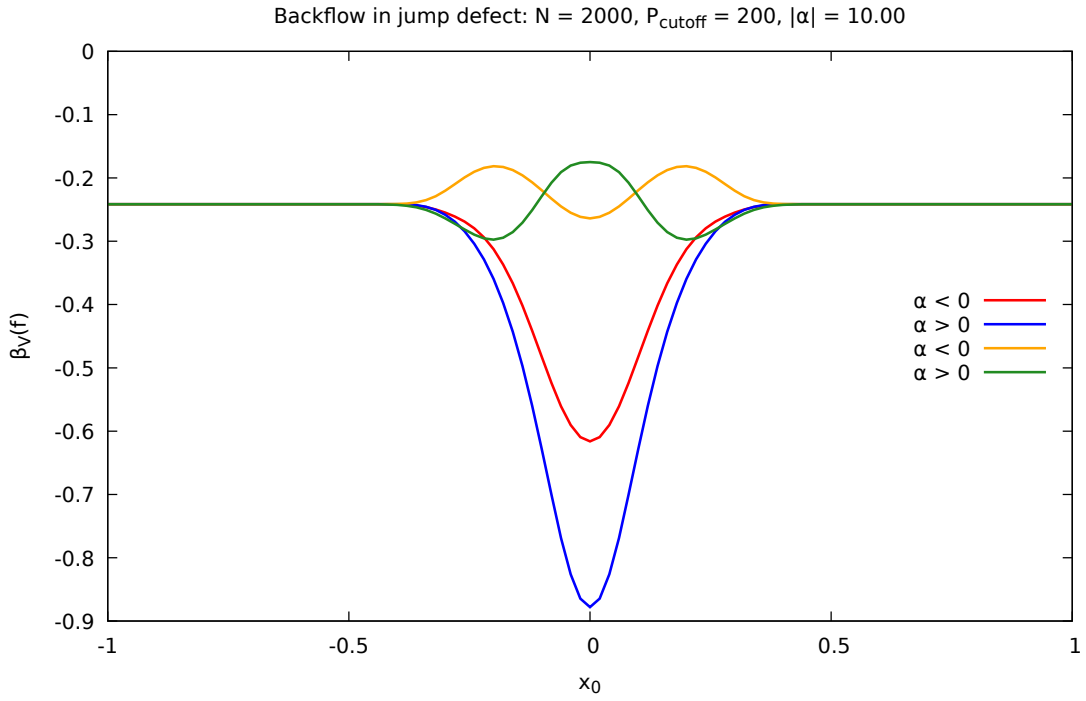

(b)

Figure 4.6: Lowest backflow eigenvalue of the current operator. **Red**/**blue** refer to the non-conserved probability current. **Yellow**/**green** refer to the conserved one. (a) $|\alpha| = 9.0$ (b) $|\alpha| = 10.0$.

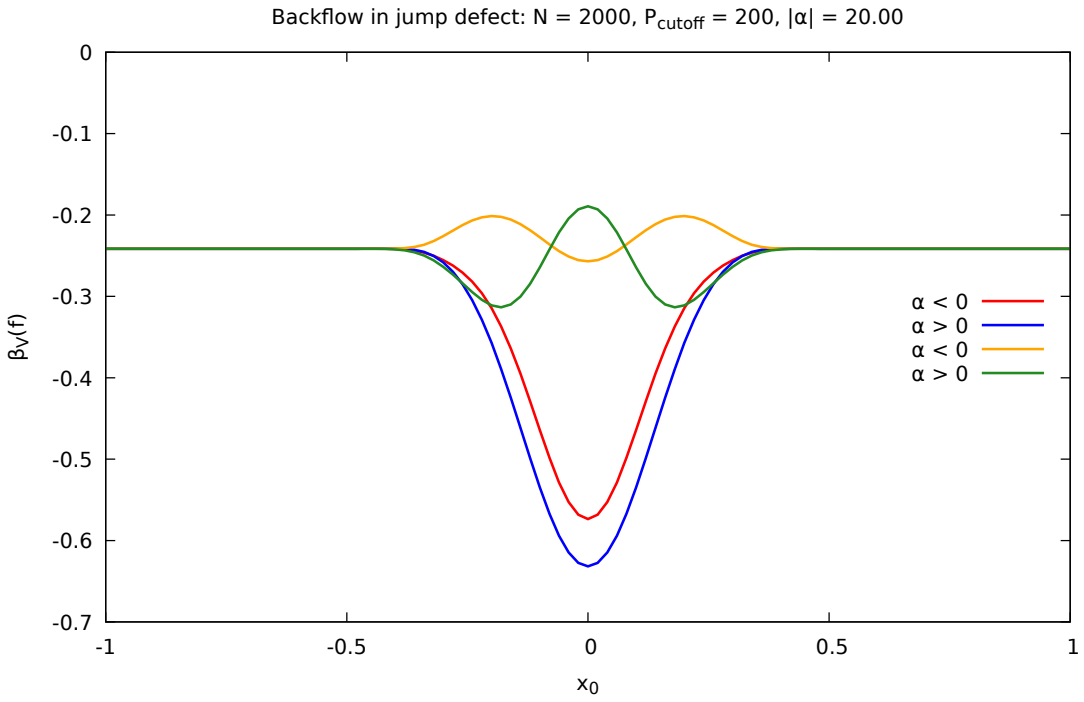

(a)

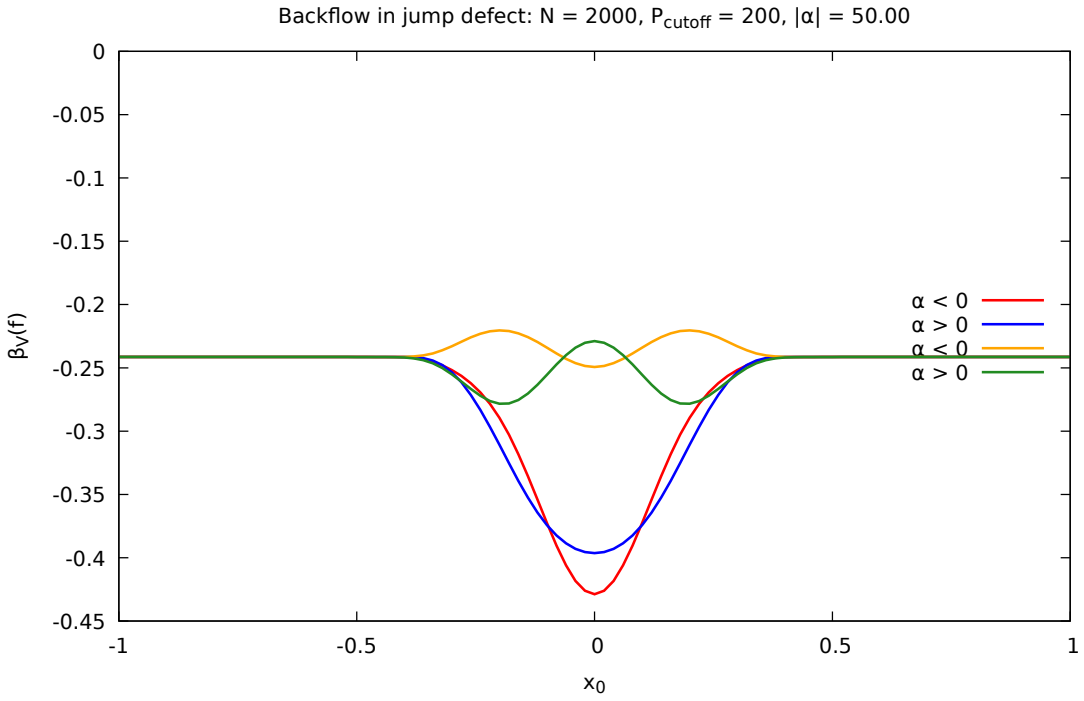

(b)

Figure 4.7: Lowest backflow eigenvalue of the current operator. **Red**/**blue** refer to the non-conserved probability current. **Yellow**/**green** refer to the conserved one. $|\alpha| = 20$ (b) $|\alpha| = 50$.

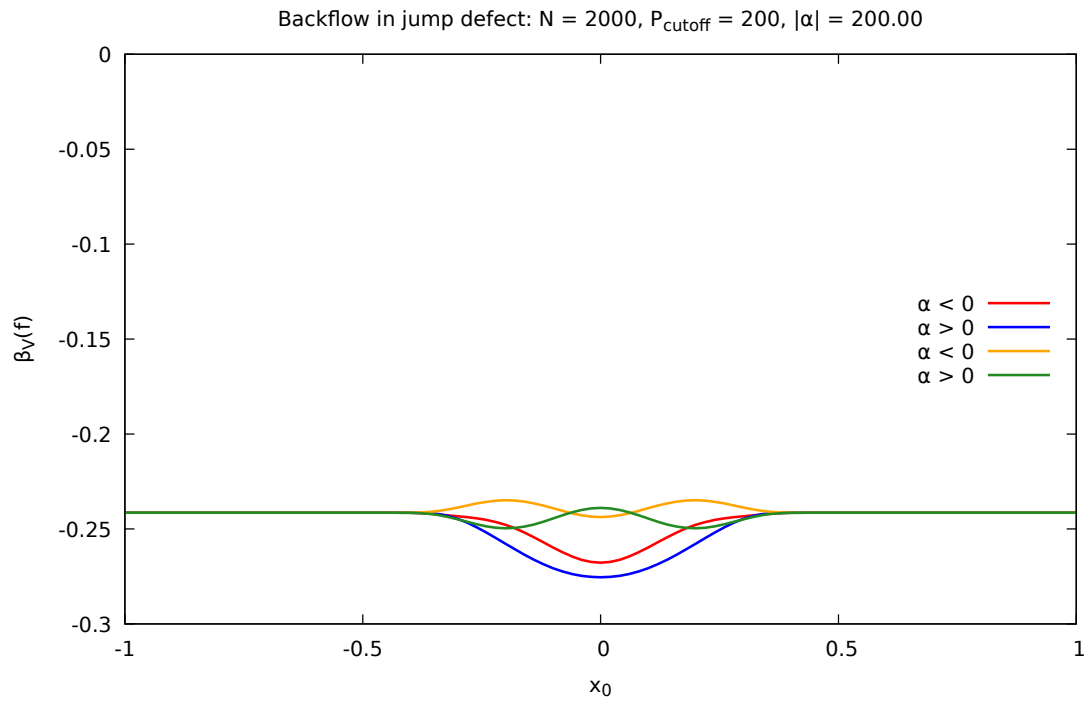

(a)

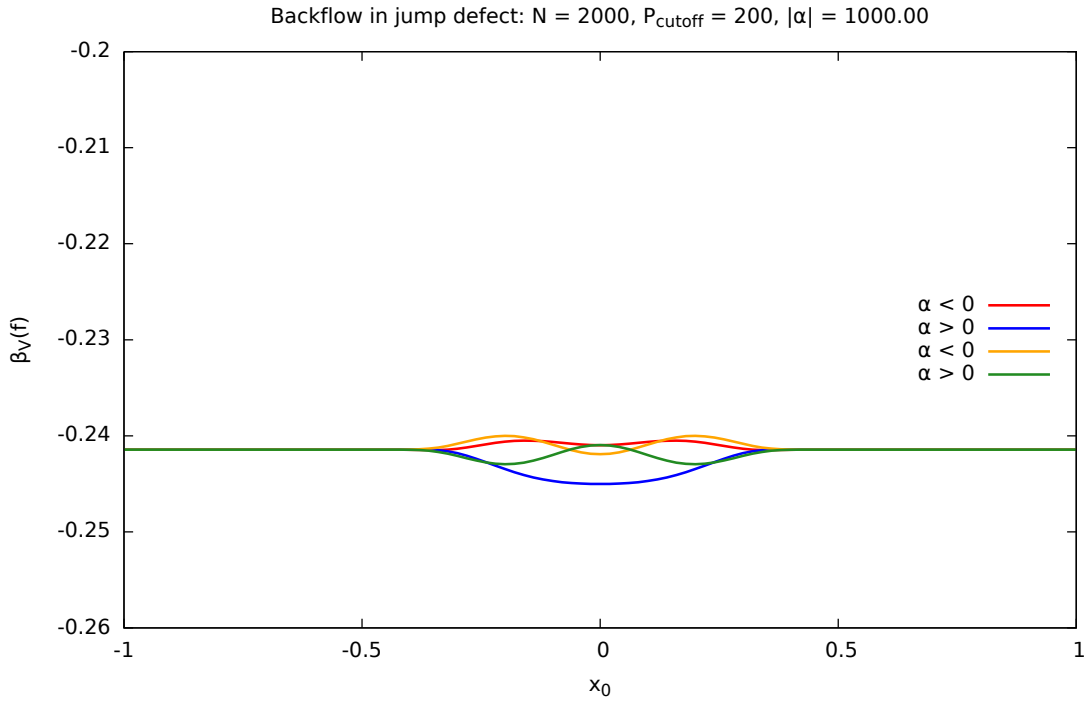

(b)

Figure 4.8: Lowest backflow eigenvalue of the current operator. **Red**/**blue** refer to the non-conserved probability current. **Yellow**/**green** refer to the conserved one. (a) $|\alpha| = 200$ (b) $|\alpha| = 1000$.

4.4 3D PLOTS

Here we present three-dimensional plots displaying the lowest eigenvalue $\beta_V(f)$ of the corresponding probability current operator as the defect parameter and the position of measurement x_0, which is the center of the averaging Gaussian function f, change. For the jump-defect, both the non-conserved, figures 4.9, 4.10 and 4.11, and the conserved probability current, figures 4.12, 4.13 and 4.14, were considered. In each case, we have plotted different versions that run over larger ranges of the defect parameter and another one that runs over a smaller range ($\alpha \in [-1, 1]$) for capturing some local details.

While the δ-defect inevitably embodies the presence of a reflection term as the result of an incoming right-moving asymptote being scattered at the origin, the jump-defect, which is a non-trivial interaction preserving integrability, provides a purely transmitting situation where the states are always right-movers and not only initially. Despite the evident loss of space-translation variance caused by its presence, the jump-defect is a topological defect in the sense that the corresponding sewing conditions do not explicitly depend upon where it is located. Thus, in the presence of a jump-defect, the backflow constant $\beta_V(f)$ for asymptotic regions far from it is approximately the value found in interaction-free situations, namely, $\beta_V(f) \approx \beta_0(f)$, see figures 4.9 and 4.12, in clear contrast to the δ-defect in figure 3.4. A similar effect occurs when $\alpha \to \pm\infty$ with $\beta_V(f) \approx \beta_0(f)$ while the δ-defect becomes a purely reflecting wall for $\lambda \to \pm\infty$. To compare some local features of the backflow constant in the jump-defect with those in the δ-defect, refer to figure 3.5 and figures 4.11 and 4.14. The jump-defect exchanges momentum and energy with the fields on either side of it and, in consequence, it is possible to conserve not only probability but also energy and momentum. Before imposing these conservation adjustments, as explained in section 4.1.2, the lowest eigenvalue of the probability current manifests the presence of two global minima, one for positive α and the other for negative α. After taking into account conservation, the lowest eigenvalue has a drastic change where the global minimum is manifested only for positive values of the parameter α. A curious fact is that regardless of which situation is being considered, whether the probability current is the non-conserved one or the conserved version, the lowest eigenvalue is symmetrical with respect to the position of measurement x_0 for all values of the parameter.

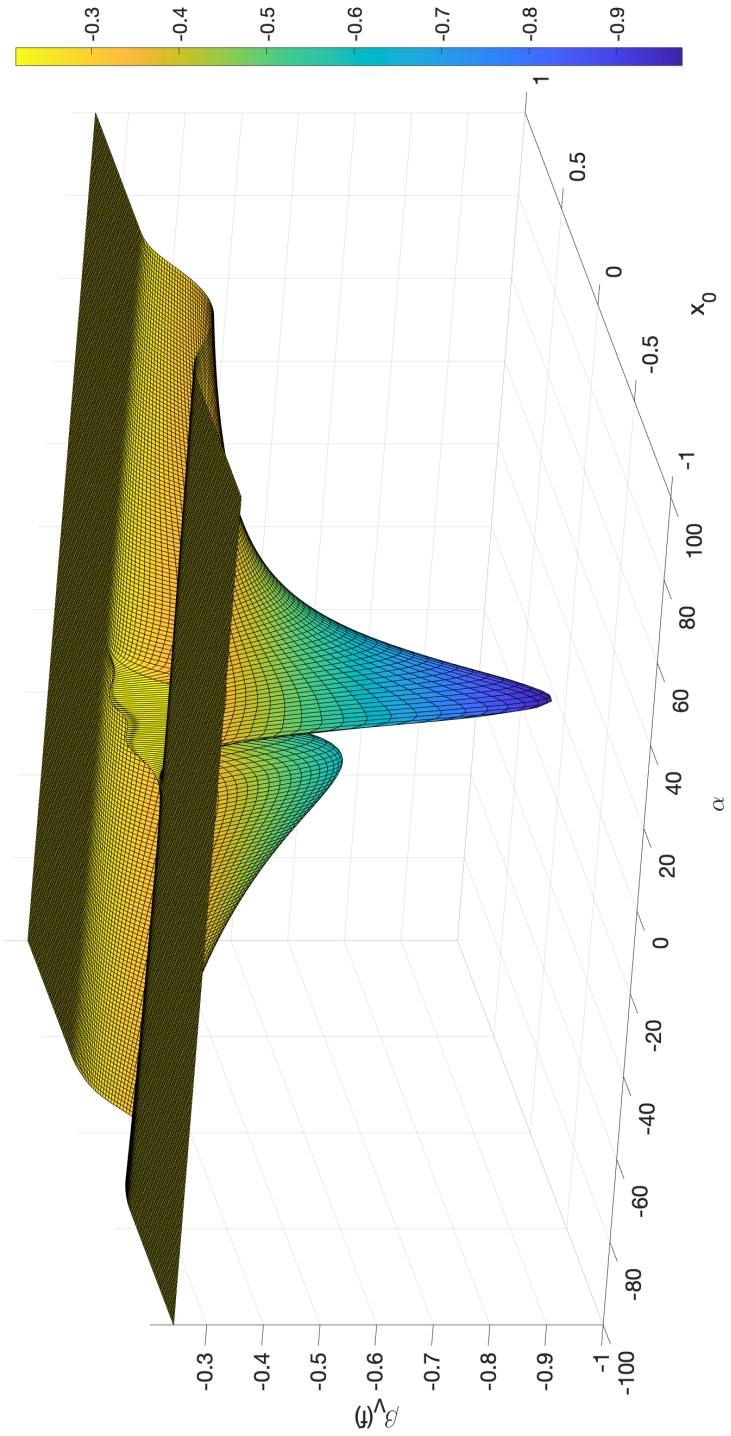

Figure 4.9: Probability current lowest eigenvalue, $P_{\text{cutoff}} = 200$, $N = 2000$.

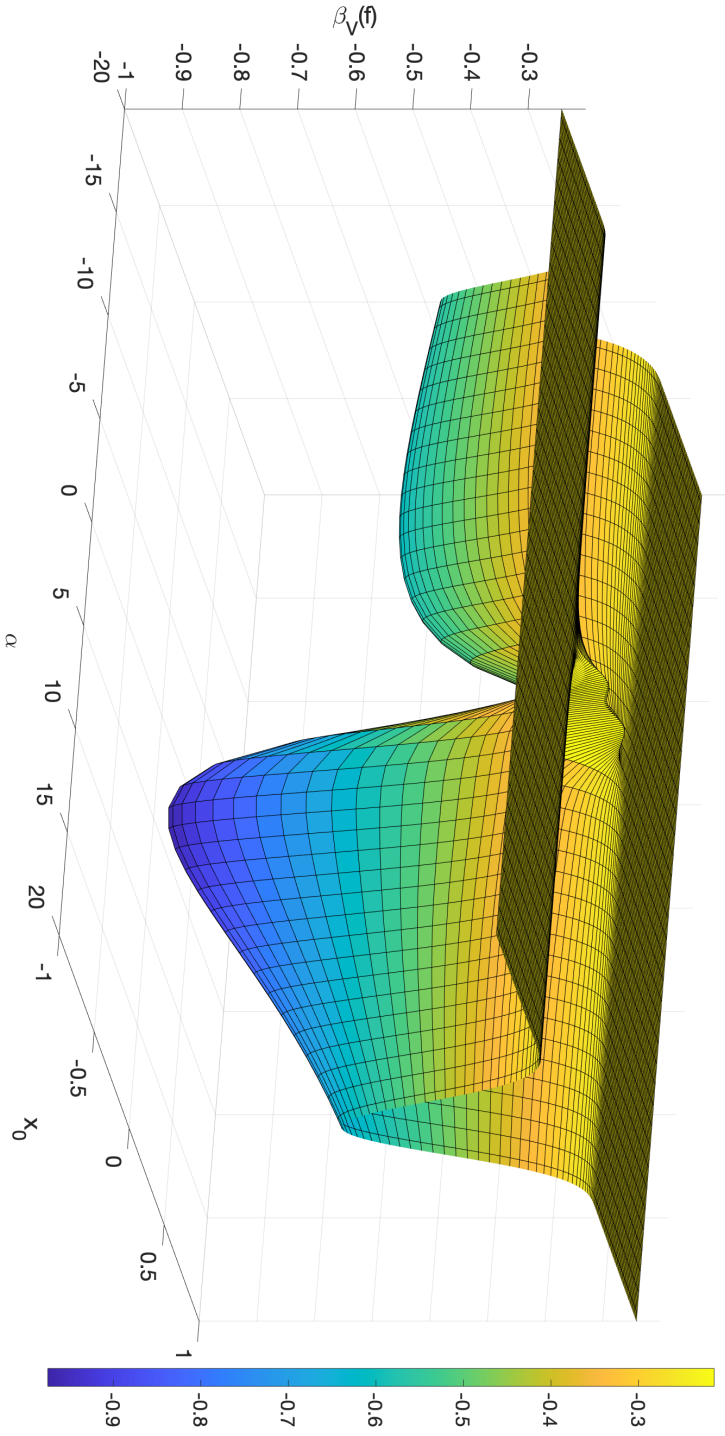

Figure 4.10: Probability current lowest eigenvalue, $P_{\text{cutoff}} = 200$, $N = 2000$.

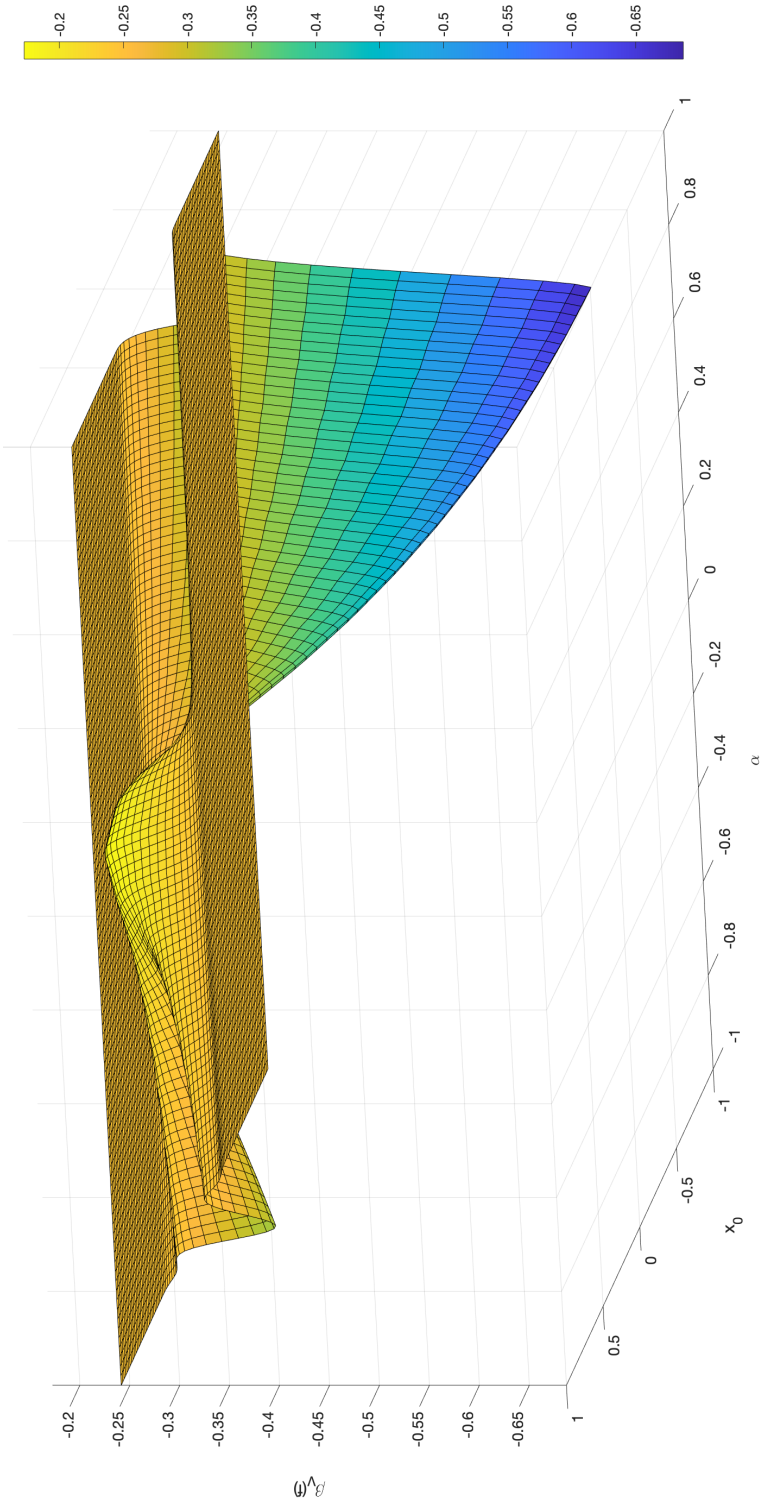

Figure 4.11: Probability current lowest eigenvalue, $P_{\text{cutoff}} = 200$, $N = 2000$.

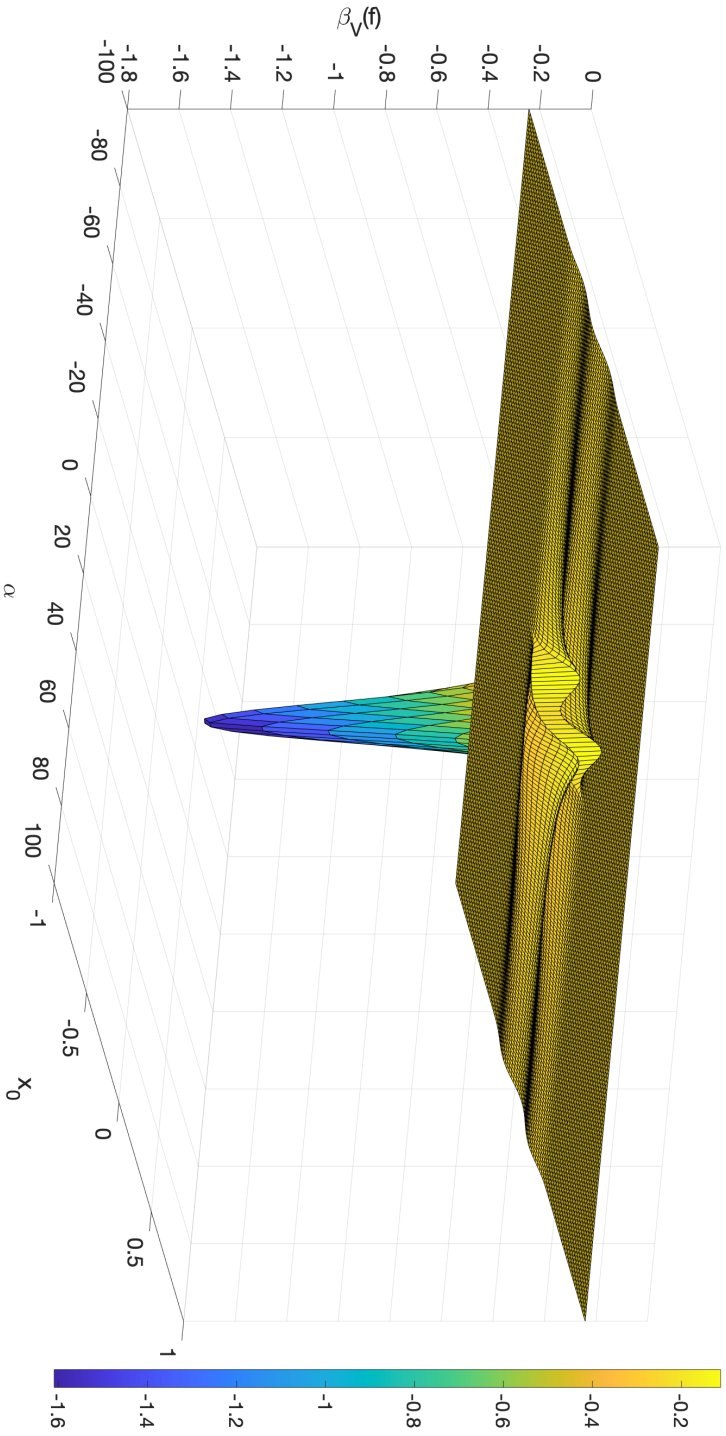

Figure 4.12: Conserved probability current lowest eigenvalue, $P_{\text{cutoff}} = 200$, $N = 2000$.

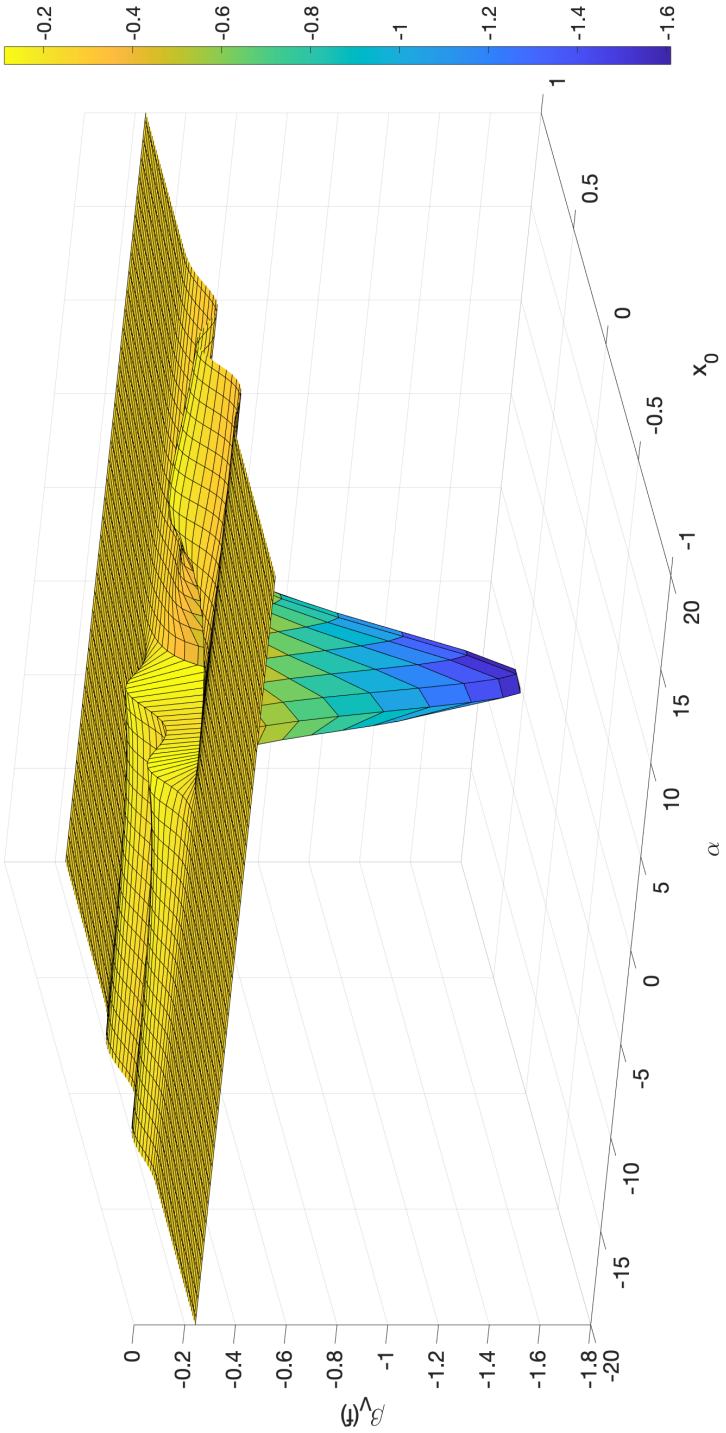

Figure 4.13: Conserved probability current lowest eigenvalue, $P_{\text{cutoff}} = 200$, $N = 2000$.

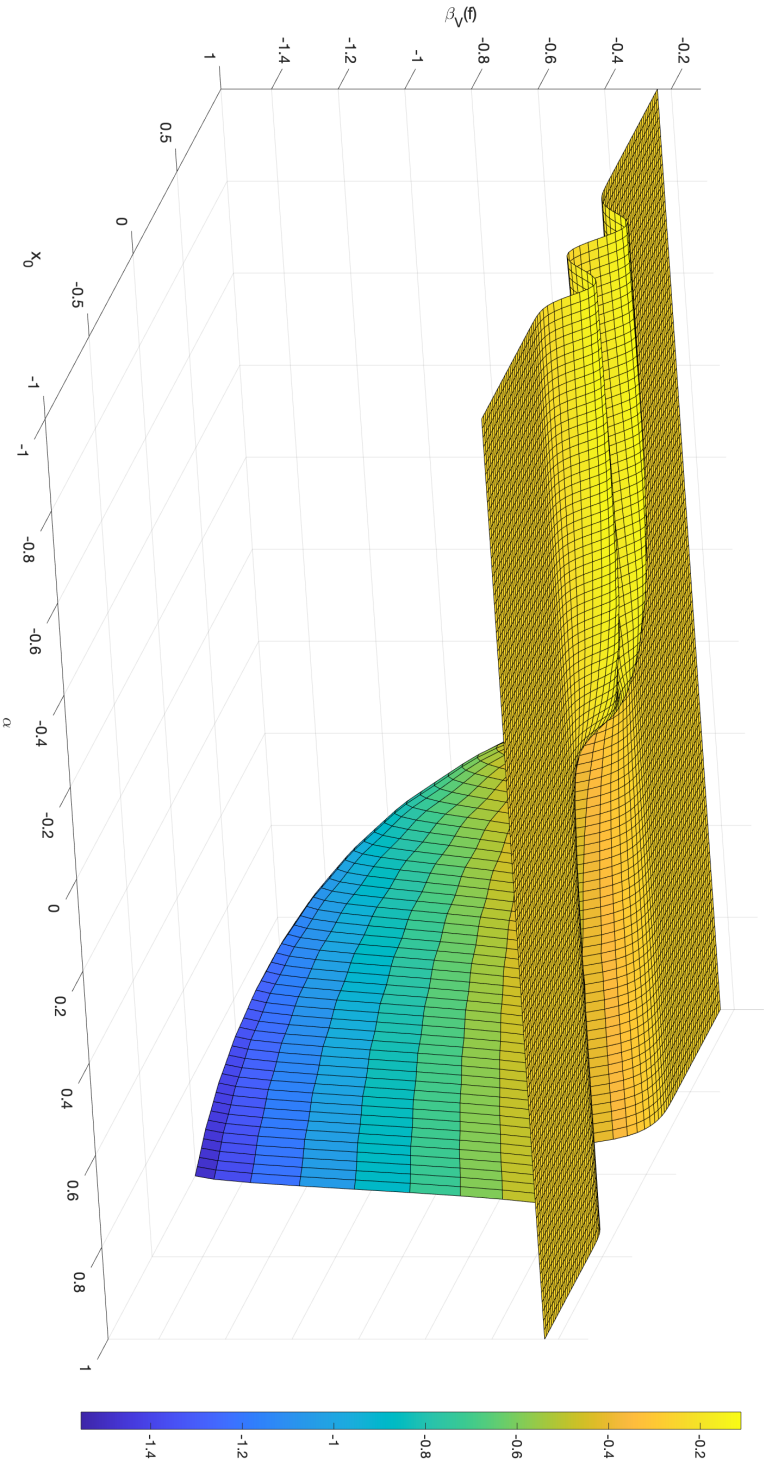

Figure 4.14: Conserved probability current lowest eigenvalue, $P_{\text{cutoff}} = 200$, $N = 2000$.

4.5 DETAILS ON THE NUMERICAL CALCULATIONS

We have adapted the basic numerical methods of [11] (where one can find the essential numerical description with a Java program) for a FORTRAN 90 program with some changes in regards to the method of integration and the calculation of the lowest eigenvalue of a complex Hermitian matrix M. The discontinuities due to the defects are also taken into account in the numerical integration. For that, the libraries used were QUADPACK [132] and EISPACK [133], respectively. In particular, the FORTRAN subroutine 'CH' [133] was used to find the lowest eigenvalue of interest, but this subroutine can be used to find all the eigenvalues and all the eigenvectors of M and, for that, it calls the recommended sequence of subroutines from EISPACK. The algorithm to find eigenvalues has two basic steps: it reduces a complex Hermitian matrix to a real symmetric tridiagonal matrix using unitary transformations and determines the eigenvalues of the original matrix from the real symmetric tridiagonal matrix [134].

Here is a summary of the meaning of each relevant variable to understand the plots presented in this work. For the numerical calculations, the discretization of an infinite-dimensional operator T on $L^2(\mathbb{R}_+, dk)$ with kernel K given by

$$K(k',k) = \frac{1}{2\pi} L(k',k) = \frac{i}{4\pi} \int dx f(x) \left(\partial_x \varphi^\star_{k'}(x) \varphi_k(x) - \varphi^\star_{k'}(x) \partial_x \varphi_k(x)\right) \tag{4.41}$$

into a N×N-matrix M is characterized by the parameter N, the number of equally spaced steps which divide the momentum interval $[0, P_{\text{cutoff}}]$, where the upper-limit cutoff of the integrations (2.35) in k and k' is denoted by P_{cutoff}. The components of such a matrix can be written as

$$M_{ij} = \langle \psi_i, T\psi_j \rangle = \int dk' \int dk\, \tilde{\psi}_i(k') K(k',k) \tilde{\psi}_j(k) \approx \frac{P_{\text{cutoff}}}{N} K(k_i, k_j), \tag{4.42}$$

where $\tilde{\psi}_i \, (i \in \mathbb{N} \mid i = (0, \ldots, N-1))$ are orthonormal step functions supported on the corresponding interval, and mid-points $k_i = (i + 1/2)\,(P_{\text{cutoff}}/N)$. The adoption of a cutoff P_{cutoff} is consistent with the fact that the lowest backflow eigenvector decays at large momentum.

The positive test function chosen for the spatial average of the probability current was a Gaussian

$$f(x) = \frac{1}{\sigma\sqrt{2\pi}} \exp\left(-\frac{(x-x_0)^2}{2\sigma^2}\right), \tag{4.43}$$

with width $\sigma = 0.1$ centered at the position x_0 of measurement where a spatially extended detector is located and cut off to the interval $x \in [x_0 - 8\sigma, x_0 + 8\sigma]$. Therefore, for each x_0 we have a matrix M for which the lowest eigenvalue needs to be calculated. We have restricted our position of measurement to $x_0 \in [-2, 2]$ in the case of the delta-defect and to $x_0 \in [-1, 1]$ in the jump-defect case because, as we move away from the jump-defect location, the lowest eigenvalue approaches the free case value $\beta_0(f) \approx -0.241$ for this particular choice of test function. That same Gaussian test function is used throughout this thesis to obtain the numerical results presented in the form of graphs, with the only exception of Appendix B that considers different choices of functions: the squared Lorentzian and the rectangular function.

Although essentially the same, the numerical analysis done for the conserved probability current involves an extra step, which is the addition of a fixing term to the non-conserved one such that the fixing term allows the conservation law to hold. Specifically, the fixing term in the presence of a jump-defect,

$$-\frac{1}{2\pi}\frac{\alpha(k+k')}{(k-i\alpha)(k'+i\alpha)}f(0), \tag{4.44}$$

is added to $K(k', k)$ to compose a new kernel denoted by $K_c(k', k)$, which is associated with a conserved quantity. The discretization process now involves that new kernel, and the FORTRAN program, with the same subroutines, is asked to calculate the lowest eigenvalue $\beta_V(f)$ of the corresponding N×N-matrix M.

The numerical results also suggest that the lowest eigenvalue is isolated at the bottom of the spectrum with the next eigenvalues (in ascending order) clustered about the zero and followed by a continuum of generalized positive eigenvalues. In fact, for $N = 1000$, $P_{\text{cutoff}} = 100$ in the free case, the second lowest eigenvalue denoted '$w(2)$' is $w(2) \approx -0.00012$. Same result was obtained for $N = 2000$, $P_{\text{cutoff}} = 200$.

— 5 —

Analytic perturbation theory for the probability current

Previously, we analysed the exact calculation of the backflow constant $\beta_V(f)$ in the presence of two distinct exactly solvable models, namely, the δ-defect and the jump-defect. Because these two interactions have known explicit solutions, it is worth comparing how satisfactory are the approximations provided by perturbation theory. In fact, perturbation theory may be the better alternative in other cases where the explicit solution is not known. Here we proceed by studying previous cases as a result of the analytic perturbation, a general treatment due to Kato [50] (especially chapters $2, 3, 5$ and 7), of the probability current operator. The results of this analysis will be presented at the end of the chapter.

5.1 ANALYTIC PERTURBATION THEORY

This section presents a brief summary of the case of operators defined on a finite-dimensional vector space. Let B be an operator defined on a finite-dimension space. The general perturbation of this operator, in powers of λ, is a formal power series. Let μ be one of the eigenvalues of B with algebraic multiplicity m, the perturbed weighted[1] mean $\hat{\mu}(\lambda)$ can also be written as a formal power series in the form

$$B(\lambda) = B + \sum_{n=1}^{\infty} \lambda^n B^{(n)} \,, \tag{5.1}$$

$$\hat{\mu}(\lambda) = \mu + \sum_{n=1}^{\infty} \lambda^n \mu^{(n)} \,, \tag{5.2}$$

[1]The weight is the multiplicity of the particularly chosen μ, which is also the sum of the multiplicities $m_1 + m_2 + \ldots + m_r$ for the μ-group eigenvalues $\mu_1(\lambda), \mu_2(\lambda), \ldots, \mu_r(\lambda)$.

where $B(\lambda)$ denotes the perturbed operator and $B = B(0)$ is the unperturbed operator. As a result of the perturbation, the eigenvalue μ will in general split into several eigenvalues of $B(\lambda)$, for $\lambda \neq 0$, namely, the μ-group (the totality of the eigenvalues of $B(\lambda)$ generated by splitting from the same unperturbed eigenvalue μ). We anticipate that for our case of interest, the lowest eigenvalue of the probability current operator, the algebraic multiplicity will be considered $m = 1$, leaving no chance for splitting such that the μ-group consists of a single eigenvalue $\mu(\lambda)$ and, consequently,

$$\hat{\mu}(\lambda) = \mu(\lambda). \tag{5.3}$$

That assumption is justified by the numerical analysis that indicates this is indeed the case. Given a linear operator $B \in \mathcal{L}(\mathbf{X})$, the space of all linear operators from a finite-dimensional vector space $\mathbf{X}$ of $\dim(\mathbf{X}) = N$ to itself, it can be represented by

$$B = S + D, \tag{5.4}$$

where S is a diagonalizable operator and D is a nilpotent commuting with S. Let $\mu_1, \ldots \mu_s$ be different eigenvalues of B, and $P_1 \ldots P_s$ its eigenprojections and $D_1 \ldots D_s$ the eigennilpotents. Then, the spectral representation of the operator B is written as

$$B = \sum_{h=1}^{s} \mu_h P_h + \sum_{h=1}^{s} D_h, \tag{5.5}$$

which leads to the Jordan canonical form (or normal form) of B.

Definition 2. *The eigenvalue μ_h of B is called semisimple if the associated eigennilpotent D_h is zero. The eigenvalue μ_h is called simple if $m_h = 1$ (algebraic multiplicity). In particular, $m_h = 1$ implies $D_h = 0$.*

Definition 3. *B is diagonalizable if and only if all of its eigenvalues μ_h are semisimple. B is called simple if all its eigenvalues μ_h are simple, in which case B has N eigenvalues.*

In quantum theory, a Hermitian operator is defined on a special vector space of interest, namely, the Hilbert space $\mathcal{H}$, in which is defined an inner product with a natural choice of norm defined in terms of the inner product, $(v, v)^{1/2} = \|v\|$, for any vector $v \in \mathcal{H}$. Because we are evidently interested in quantum theory, we will consider operator B to be Hermitian. The spectral representation is then simplified because

these eigennilpotents D_h are all zero. Additionally, we also reasonably consider that the perturbed operator $B(\lambda)$ is Hermitian. In that sense, we are restricting the discussion to Hermitian perturbations.

Theorem 3. *If the holomorphic family $B(\lambda)$ is Hermitian, the eigenvalues $\mu_h(\lambda)$ and the eigenprojections $P_h(\lambda)$ are holomorphic on the real axis, whereas the eigennilpotents $D_h(\lambda)$ vanish identically*[2]*.*

The basis of our analysis depends crucially on the properties of the unperturbed operator B that represents here a finite-dimensional version of the probability current operator. Following these initial considerations, we particularize the general method, which is based on the study of the resolvent of B, to our case of interest.

5.1.1 Analytic perturbation theory for Hermitian operators

Some references for this section can be found in [50, 135, 136]. Given a Hermitian operator B, ξ is an eigenvalue of B if there is a vector $u \neq 0$ such that

$$Bu = \xi u, \tag{5.6}$$

then ξ is a, generally complex, eigenvalue and $u \in \mathbf{X}$ is the associated eigenvector of B. The operator-valued function $R(\xi)$, called the resolvent of B, is given by

$$R(\xi) = R(\xi, B) = (B - \xi)^{-1} \tag{5.7}$$

and is defined for ξ in the resolvent set of B, that is $\xi \in \rho(B)$.

Definition 4. *The resolvent set of B, denoted by $\rho(B)$, is the set of complex values for which $R(\xi)$ exists and, therefore, $(B - \xi)$ is injective.*

From the resolvent set, immediately follows the definition of the spectrum set of B

Definition 5. *The complement of the resolvent set $\rho(B)$ is the spectrum $\sigma(B)$ of B*

$$\sigma(B) = \mathbb{C} \backslash \rho(B), \tag{5.8}$$

which contains all eigenvalues of B.

[2]However, this does not need to be the case if λ is an exceptional point, where the number of eigenvalues is not preserved [50].

In the finite-dimensional case, the spectrum set is called the point spectrum set, because there is no further decomposition of the spectrum. In fact, the continuous spectrum is quite different from the discrete spectrum. From the resolvent expression (5.7), given $\xi_1, \xi_2 \in \rho(B)$, one can write

$$\begin{aligned} R(\xi_1) &= R(\xi_1)(B-\xi_2)R(\xi_2) \\ R(\xi_2) &= R(\xi_1)(B-\xi_1)R(\xi_2), \end{aligned} \tag{5.9}$$

which can be subtracted one from the other to give the first resolvent equation or Hilbert's identity

$$R(\xi_1) - R(\xi_2) = (\xi_1 - \xi_2)R(\xi_1)R(\xi_2). \tag{5.10}$$

Two direct consequences of Hilbert's identity are first that

$$R(\xi_1)R(\xi_2) = R(\xi_2)R(\xi_1), \tag{5.11}$$

and second that the resolvent is holomorphic in the set $\rho(B)$ with the following properties

$$\frac{d}{d\xi}R(\xi) = R(\xi)^2, \tag{5.12}$$

$$\frac{d^n}{d\xi^n}R(\xi) = n!R(\xi)^{n+1} \quad n = 1, 2, 3\ldots \tag{5.13}$$

Hence, the Taylor expansion of the resolvent at $\xi_0 \in \rho(B)$ has the form

$$R(\xi) = \sum_{n=0}^{\infty}(\xi - \xi_0)^n R(\xi_0)^{n+1} = (1 - (\xi - \xi_0)R(\xi_0))^{-1} R(\xi_0), \tag{5.14}$$

which is convergent at least for $|\xi - \xi_0| < \|R(\xi_0)\|^{-1}$. That expression is called the first Neumann series of the resolvent. Additionally, for large values $|\xi|$, we can expand the resolvent expression $(B-\xi)^{-1}$ by writing

$$R(\xi) = (B-\xi)^{-1} = (1 - B\xi^{-1})^{-1}(-\xi^{-1}) = -\sum_{n=0}^{\infty}\frac{B^n}{\xi^{n+1}}, \tag{5.15}$$

which is convergent if and only if $|\xi| > \mathrm{spr}(B)$, thus $R(\xi)$ is holomorphic at $\xi = \infty$, and equal zero there. In particular, the spectral radius of an operator T, denoted by $\mathrm{spr}(T)$, is defined as

$$\mathrm{spr}(T) = \lim_{n\to\infty}\|T^n\|^{1/n}. \tag{5.16}$$

From the eigenvalue equation (5.6), if ξ is an eigenvalue the operator $(B-\xi)$ is singular. If, however, ξ is not an eigenvalue of B, then $\ker(\xi - B) = \{0\}$ with $(B-\xi)$ invertible. The condition for singularity is called the characteristic equation, namely, $\det(B-\xi) = 0$. The characteristic polynomial of B is $\chi(\xi, B) := \det(\xi - B)$ and has degree $N = \dim(\mathbf{X})$. The resolvent, as an inverse, is a rational operator-valued function of ξ that can be written as

$$R(\xi) = \frac{1}{\chi(\xi, B)} M_{N-1}(\xi), \tag{5.17}$$

where $M_{N-1}(\xi)$ is a polynomial operator-valued function of degree at most $(N-1)$. That can be seen from the use of Cramer's rule to calculate the inverse $(B-\xi)^{-1}$ in terms of the adjugate matrix of $(B-\xi)$, which is a polynomial in ξ of degree at most $(N-1)$. Hence, the eigenvalues of B, denoted by μ_h, are at most poles of the resolvent $R(\xi)$, rather than removable singularities that would imply a trivial $R(\xi) = 0$ by Liouville's theorem. The degeneracies of the eigenvalues are very important in the discussion of the perturbation analysis. There are two concepts, the algebraic and the geometric multiplicity of a given eigenvalue. The former is a multiplicity as a root of the characteristic polynomial and the latter is the number of linear independent (L.I) eigenvectors associated with that same eigenvalue. In general, the geometric one cannot exceed the algebraic, but B is diagonalizable if and only if these two different concepts of multiplicity coincide for all its eigenvalues. As in our case of interest B is diagonalizable, we can safely refer to 'multiplicity' without the need for being more specific. As our eigenvalue of interest (the lowest one) is considered to be nondegenerate, the associated projection is one-dimensional, and the resolvent has a pole of order one at this particular eigenvalue. It is possible, therefore, to write a Laurent expansion for the resolvent

$$R(\xi) = \sum_{n=-1}^{\infty} A_n (\xi - \mu_0)^n \tag{5.18}$$

in the neighbourhood of $\xi = \mu_0$, where μ_0 is an eigenvalue, and the coefficients are

$$A_n = \frac{1}{2\pi i} \int_{\Gamma} \frac{1}{(\xi - \mu_0)^{n+1}} R(\xi) d\xi, \tag{5.19}$$

with Γ a positively-oriented (counterclockwise) simple closed contour of integration sufficiently small and centred at μ_0 but excluding any other eigenvalue of B. An

important integral greatly used in this analysis is the Cauchy-Riesz integral from the holomorphic functional calculus. This calculus was applied and generalized to functions of infinite-dimensional linear operators by Dunford and Schwartz [137].

Definition 6. *Let f be a (complex) function holomorphic on $\sigma(B)$, holomorphic in small discs enclosing the eigenvalues. Since in general the spectrum has multiple connected components, $f(\xi)$ is only piecewise holomorphic. Let Γ be a system of positively-oriented simple closed contours that consists of regular points, not intersecting $\sigma(B)$, and lie inside the region where $f(\xi)$ is holomorphic with the eigenvalues inside theses countours. Then, the associated operator-valued function is*

$$f(B) = -\frac{1}{2\pi i}\int_{\Gamma} f(\xi)R(\xi, B)d\xi.$$

Particularly, the Riesz eigenprojection is one example of such integrals given by

$$f(B) := P_h = -\frac{1}{2\pi i}\int_{\Gamma_h} R(\xi, B)d\xi, \tag{5.20}$$

where P_h is called the (Riesz) projection associated with the μ_h-eigenvalue, the curve Γ_h encloses μ_h but no other eigenvalue of B and

$$f(\xi) = \begin{cases} 1 & |\xi - \mu_0| < \delta, \quad \delta > 0, \\ 0 & \text{otherwise.} \end{cases} \tag{5.21}$$

The basic property of eigenprojections that, for different eigenvalues μ_h, the summation

$$\sum_h P_h = 1$$

is obtained with the integration contour Γ enclosing all the eigenvalues of B. Now, back to the coefficients (5.19), in our Hermitian case, one has that for $n = -1$

$$A_{-1} = \frac{1}{2\pi i}\int_{\Gamma} R(\xi)\, d\xi = -P_0 \quad \text{(Riesz eigenprojection)}, \tag{5.22}$$

As a consequence of the properties from the product A_nA_m of these coefficients, one obtains in the case $m = n = -1$ that $A_{-1}^2 = -A_{-1}$, confirming that indeed $-A_{-1}$

satisfies an idempotent relation, and $A_{-1}A_m = A_m A_{-1} = 0$ for $m = 0, 1, 2, \ldots$ Let us denote the A_0 coefficient as

$$A_0 = \frac{1}{2\pi i} \int_{\Gamma} \frac{1}{(\xi - \mu_0)} R(\xi)\, d\xi = S_0. \tag{5.23}$$

It holds true then that $A_n = A_0^{n+1} = S_0^{n+1}$ for $n = 0, 1, 2, \ldots$ such that $P_0 S_0 = S_0 P_0 = 0$. Hence, the Laurent expansion of the resolvent around $\xi = \mu_0$ takes the form

$$R(\xi) = -\frac{P_0}{\xi - \mu_0} + \sum_{n=0}^{\infty} (\xi - \mu_0)^n S_0^{n+1}. \tag{5.24}$$

The principal part of this Laurent series is finite due to the fact that the degree of the pole does not exceed its multiplicity. Since $R(\xi)$ is meromorphic and holomorphic at infinity, it has a decomposition into a sum of partial fractions

$$R(\xi) = -\sum_{h=1}^{s} \left[(\xi - \mu_h)^{-1} P_h \right], \tag{5.25}$$

where μ_h denotes all the s eigenvalues of B, and P_h are the corresponding eigenprojections. Henceforth, we will omit the explicit μ_0-dependence of P_h by simply writing P as the the projection associated with the lowest eigenvalue μ of B, and similarly for all associated quantities. Note also that S_0 will be denoted by S. Considering that our eigenvalue of interest μ is not degenerate and has multiplicity $m = 1$, as mentioned before, the resolvent of B has a Laurent series in the neighbourhood of $\xi = \mu$ given by

$$R(\xi) = \sum_{n=-1}^{\infty} (\xi - \mu)^n S^{(n+1)}, \tag{5.26}$$

where $S^{(0)} = -P$, $S^{(n)} = S^n$, for $n \geq 1$. Additionally, these coefficients $S^{(n+1)}$ of the Laurent series obey the commutation relation: $PS = SP = 0$. The S in the expression (5.26) is simply the value at $\xi = \mu$ of the reduced resolvent of B, namely, $S(\mu)$.

Definition 7. *The holomorphic part of the the Laurent series (5.26) is called reduced resolvent of B with respect to μ and it has the form*

$$S(\xi) = \sum_{n=0}^{\infty} (-1)^n S^{n+1} (\xi - \mu)^n. \tag{5.27}$$

The name "reduced" resolvent for $S(\xi)$ is justified by the fact that the operator $(B-\xi)$ is invertible in $(1-P)\mathbf{X}$ and its true that

$$[(B-\xi) \restriction (1-P)\mathbf{X}]^{-1} = S(\xi) \restriction (1-P)\mathbf{X}, \tag{5.28}$$

where $\restriction (1-P)\mathbf{X}$ means restriction to the subspace $(1-P)\mathbf{X}$. Therefore,

$$S(\xi) \restriction (1-P)\mathbf{X} = R\left(\xi, B \restriction (1-P)\mathbf{X}\right), \tag{5.29}$$

the reduced resolvent of B can be seen as the resolvent of B restricted to the subspace $(1-P)\mathbf{X}$. This fact is important to understand that $S(\xi)$ may be written as a summation series involving all the others orthogonal projection operators P_h different from the projection P that is associated with our lowest eigenvalue μ. We remark that the reduced resolvent of B with respect to a general eigenvalue μ_h can be written as the summation over the eigenprojections of the others eigenvalues μ_l different from μ_h as

$$S_h(\xi) = -\sum_{l\neq h} \left[(\xi-\mu_l)^{-1} P_l\right]. \tag{5.30}$$

5.1.2 Eigenvalue expansion

As it happens that $B(\lambda)$ and $\mu(\lambda)$ are holomorphic at $\lambda = 0$, the total projection $P(\lambda)$ associated with μ is also holomorphic at $\lambda = 0$ and can be expanded in a formal power series of λ

$$P(\lambda) = \sum_{n=0}^{\infty} \lambda^n P^{(n)}, \quad P^{(0)} = P. \tag{5.31}$$

The eigenvalue problem is restricted to the subspace $P(\lambda)\mathbf{X}$ which contains the eigenvalue μ. In that particular subspace, the eigenvalue problem for $B(\lambda)$ is equivalent to the eigenvalue problem for the operator $P(\lambda)B(\lambda) = B(\lambda)P(\lambda) = P(\lambda)B(\lambda)P(\lambda)$, where we used the spectral representation and that $BP = PB$. The perturbed eigenvalue $\mu(\lambda)$ of the perturbed operator $B(\lambda)$, considering there is no splitting of μ, which is true for nondegenerate eigenvalue, is given by the trace

$$\mu(\lambda) = \mathrm{Tr}\left(B(\lambda)P(\lambda)\right) = \mu + \mathrm{Tr}\left((B(\lambda)-\mu)P(\lambda)\right). \tag{5.32}$$

Note that $\dim(P(\lambda)) = \dim(P)$, which is determined by the multiplicity of the eigenvalue μ, as a consequence of [50], Lemma I-4.10. As the numerical calculations on backflow

indicates and we consider that the lowest eigenvalue of the probability current operator is nondegenerate, we are interested in the case where the total projection is actually the projection for the single eigenvalue $\mu(\lambda)$ of $B(\lambda)$ that lies inside the the closed positively-oriented curve Γ. Thus, the projection

$$P(\lambda) = -\frac{1}{2\pi i}\int\limits_{\Gamma} R(\xi,\lambda)\, d\xi, \tag{5.33}$$

is the perturbed projection associated with $\mu(\lambda)$, and the existence of the resolvent $R(\xi,\lambda) = (B(\lambda)-\xi)^{-1}$ for $\xi \in \Gamma$ implies that the curve Γ does not cross any eigenvalue of $B(\lambda)$. In particular, the case $P(0) = P$, when we set $\lambda = 0$, represents the eigenprojection for the unperturbed eigenvalue μ of B.

In the calculation of (5.32), we need to work out the trace of the operator

$$(B(\lambda)-\mu)\,P(\lambda) = -\frac{1}{2\pi i}\int\limits_{\Gamma}(\xi-\mu)R(\xi,\lambda)\, d\xi \tag{5.34}$$

using properties of the resolvent as well the cyclic property of the trace. As a result, the following general expression, refer to Kato [50] for more details, establishes an explicit way of calculating the perturbation series, order by order in λ, for the perturbed eigenvalue $\mu(\lambda)$ taking into account our assumptions

$$\mu^{(n)} = \sum_{p=1}^{n}\frac{(-1)^p}{p}\sum_{\substack{\nu_1+\ldots\nu_p=n\\ \alpha_1+\ldots+\alpha_p=p-1\\ \alpha_j\geq 0;\,\nu_j\geq 1}} \mathrm{Tr}\left(B^{(\nu_1)}S^{(\alpha_1)}\ldots B^{(\nu_p)}S^{(\alpha_p)}\right), \tag{5.35}$$

where $S^{(\alpha_j)}$ with $\alpha_j > 1$ are powers of the value of the reduced resolvent (5.30) at $\xi = \mu$, and, in particular, $S^{(0)} = -P$, similarly as (5.26). Thus, for our (simple) lowest eigenvalue, the perturbation expressions up to the third order, for instance, can be found by taking the trace of operators as follows

$$\mu^{(1)} = \mathrm{Tr}\left(B^{(1)}P\right), \tag{5.36}$$

$$\mu^{(2)} = \mathrm{Tr}\left(B^{(2)}P - B^{(1)}SB^{(1)}P\right), \tag{5.37}$$

$$\begin{aligned}\mu^{(3)} = \mathrm{Tr}\big(&B^{(3)}P - B^{(1)}SB^{(2)}P - B^{(2)}SB^{(1)}P\\ &+ B^{(1)}SB^{(1)}SB^{(1)}P - B^{(1)}S^2B^{(1)}PB^{(1)}P\big),\end{aligned} \tag{5.38}$$

where $S^{(0)} = -P = -|B^{(0)}_{min}\rangle\langle B^{(0)}_{min}|$. Since our eigenvalue of interest is the lowest one, the associated eigenprojection P projects a vector onto the lowest eigenvector of the unperturbed operator B, namely, $|B^{(0)}_{min}\rangle$. For higher order perturbations, the number of possible combinations of operators, and consequently the number of terms, rapidly increases as can be seen from the expression of the fourth order perturbation

$$\begin{aligned}\mu^{(4)} = \mathrm{Tr}\big(&B^{(4)}P - B^{(1)}SB^{(3)}P - B^{(2)}SB^{(2)}P - B^{(3)}SB^{(1)}P \\ &+ B^{(1)}SB^{(1)}SB^{(2)}P + B^{(1)}SB^{(2)}SB^{(1)}P + B^{(2)}SB^{(1)}SB^{(1)}P \\ &- B^{(1)}S^2B^{(1)}PB^{(2)}P - B^{(1)}S^2B^{(2)}PB^{(1)}P - B^{(2)}S^2B^{(1)}PB^{(1)}P \\ &- B^{(1)}SB^{(1)}SB^{(1)}SB^{(1)}P + B^{(1)}S^2B^{(1)}SB^{(1)}PB^{(1)}P \\ &+ B^{(1)}SB^{(1)}S^2B^{(1)}PB^{(1)}P + B^{(1)}S^2B^{(1)}PB^{(1)}SB^{(1)}P \\ &- B^{(1)}S^3B^{(1)}PB^{(1)}PB^{(1)}P\big)\,.\end{aligned} \tag{5.39}$$

Note that the presence of of the projection P is shared among all these combinations of operators in the above expressions determining the different orders of the perturbations. In fact, that observation makes the calculations of the trace manageable, as the range of P is finite-dimensional. In particular, it is one-dimensional in our case.

5.2 INFINITE-DIMENSIONAL SETTING

In the previous section, we stated the most relevant results we need in the case of an operator B defined on a finite-dimensional vector space. Essentially the same machinery can be used in our case of interest that is the perturbation of the (unbounded) operator $J(f)$ defined on an infinite-dimensional Hilbert space. In particular, now the unperturbed operator is $E_+J(f)E_+$ (instead of B) and the perturbed operator $J(f)(\lambda)$ (instead of $B(\lambda)$) is the asymptotic current operator $E_+\Omega_V^\dagger J(f)\Omega_V E_+$. Similarly to the finite-dimensional case where the spectral theorem for Hermitian matrices simplifies the discussion, the probability current operator $J(f)$ is Hermitian $J(f) = J^\dagger(f)$, and the discussion is simplified in the sense that all nilpotent operators D are zero. We will focus on the interacting current $E_+\Omega_V^\dagger J(f)\Omega_V E_+$ that is also Hermitian, as long as we consider an Hermitian potential and a real parameter λ, and can be seen as the result of a perturbation to the interaction-free current. In particular, the spectral projection E_+ of the momentum operator is also Hermitian and was previously introduced in chapter 2. In that sense, we say this is an Hermitian perturbation.

When our perturbation analysis happens in a Banach space such as an infinite-dimensional Hilbert space, the analytic perturbation theory is more complicated than in finite-dimensional spaces, but the concepts of eigenvalue and resolvent are essentially the same. Let us, for convenience, omit in this chapter the f-dependence of our probability current operator such that we will denote it by J. The resolvent set of J, denoted by $\rho(J)$, is the set of complex values for which $R(\xi)$ exists with $(J-\xi)$ injective, is a bounded linear operator and is densely defined. In particular, if the domain of $R(\xi)$ is not dense in the space, ξ would be an element of the residual spectrum [55]. In regards to the spectrum, the spectrum set of an infinite-dimensional Hermitian operator can be decomposed into: pure point spectrum (eigenvalues), absolute continuous (crucial for scattering theory) and singular continuous, result that follows from a refinement of Lebesgue decomposition [129], Theorem I.13 and Theorem I.14. Despite some subtle differences between finite and infinite-dimensional cases, we consider the particular case of a perturbation theory applied to a single isolated eigenvalue μ of $\sigma(J)$ with finite multiplicity, and that makes possible to extend perturbation theory's results from finite-dimensional to infinite-dimensional cases. Hence, we now give emphasis to the concept of isolated eigenvalues.

Definition 8. *A point $\mu \in \sigma(J)$ is called discrete if μ is an isolated eigenvalue with eigenprojection P whose range is finite-dimensional.*

A useful theorem for the perturbation analysis, see [50, 138], states that, given a linear closed operator A in a general Banach space $\mathbf{X}$, assume that the set $\sigma(A)$ can be decomposed in two isolated parts σ_1 (bounded) and σ_2 such that the simple closed piecewise smooth curve Γ in the resolvent set $\rho(A)$ contains σ_1 in its interior, and σ_2 in the exterior. Then, it follows a decomposition of the Banach space given by

Theorem 4. *Let $\sigma(A) = \sigma_1 \cup \sigma_2$ and $\Gamma \subset \rho(A)$ be a simple closed piecewise smooth (positively oriented) curve separating the bounded part σ_1 from the unbounded one. If*

$$P = -\frac{1}{2\pi i}\int_{\Gamma}(A-\xi)^{-1}d\xi \ \in \mathcal{B}(\boldsymbol{X})\ , \tag{5.40}$$

then the decomposition $\boldsymbol{X} = M_1 \oplus M_2$, where $M_1 = P\boldsymbol{X}$ and $M_2 = (1-P)\boldsymbol{X}$, yields a decomposition of A into the associated parts $A_{M_1} \in \mathcal{B}(M_1)$ and A_{M_2} that can be

generally unbounded, with $\sigma(A_{M_1}) = \sigma_1$ *and* $\sigma(A_{M_2}) = \sigma_2$*. Furthemore,*

$$PA \subseteq AP = -\frac{1}{2\pi i}\int_{\Gamma} \xi(A-\xi)^{-1}d\xi \ \in \mathcal{B}(\boldsymbol{X}), \tag{5.41}$$

where $\mathcal{B}(\boldsymbol{X})$ *denotes the set of all bounded operators on* $\boldsymbol{X}$ *to itself.*

As a particular case of this theorem is when μ is the only point of the spectrum of the bounded operator A_{M_1}. For that, let σ_1 represent a single isolated eigenvalue μ of $\sigma(A)$, then $\sigma(A) = \{\mu\} \cup (\sigma(A)\backslash\{\mu\})$ is a decomposition into two isolated parts. Moreover, similar reasoning applies to the case of a finite system of eigenvalues, namely, the decomposition of the spectrum set into finitely many parts. Note that the theorem requires Γ to be a curve around μ with sufficiently small radius r, that is $0 < r < \epsilon$. The analytic perturbation theory for an isolated eigenvalue in the spectrum of a closed operator under a small perturbation is, therefore, handled very similarly for both finite and infinite-dimensional cases. In the next section, we shall find the perturbation for the backflow constant $\beta_V(f)$, the lowest eigenvalue of the probability current operator.

5.3 PERTURBATION OF THE INTERACTING CURRENT

It is often the case in quantum mechanics that the Hamiltonian H of a system is perturbed by an interaction such that H can be decomposed in the form $H = H_0 + \lambda V$, where H_0 is the free Hamiltonian operator and λ is a small real parameter that represents the strength of the potential V and, therefore, λV is treated as a small perturbation. Evidently, the free case is included by setting $\lambda = 0$. In this chapter, we will treat the potential strength as the parameter for the expansion of the formal power series in the perturbation analysis. Note that the Dirac delta potential function, for instance, will be denoted by $V(x) = \delta(x)$ instead of what we have previously considered, namely, $V(x) = \lambda\delta(x)$. That change is a suitable choice when we are thinking of the interaction as a perturbation. However, we are not interested in expanding the energy eigenvalues in powers of the perturbation parameter λ but the lowest eigenvalue of the interacting probability current operator. We remark that, while the perturbation to the Hamiltonian is represented by a single term linear in λ, the perturbation to the probability current operator will be described by an infinite series in a sense that will be made more precise later. For our purposes, it is enough to consider time-independent perturbations only.

The starting point of our analysis is the expectation value of the probability current operator in a general state vector $|\psi\rangle \in \mathcal{H}$ written in the following form

$$\langle J(\lambda)\rangle_{\psi} \coloneqq \langle\psi| E_{+}\Omega_{V}^{\dagger}J(f)\Omega_{V}E_{+} |\psi\rangle . \tag{5.42}$$

The expansion of the eigenvalues in power series of λ is obtained by expanding the Møller wave operator and relies on the use of the Lemma 1 making explicit use of a choice of asymptotics for the Lippmann-Schwinger equation (2.20). Let us modify our previous choice of Green's function and rewrite that equation as

$$\varphi_k(x) = g_k(x) + \lambda \int dy G_k(x-y)U(y)\varphi_k(y), \tag{5.43}$$

where $g_k(x) = \exp(ikx)$ is chosen as the complementary function, plane wave solution in the interaction-free situation ($\lambda = 0$), or simply the incident wave [139, 140]. This particular choice makes the analysis easier when we group together the power series terms corresponding to the same power in the potential strength λ in the iterative process described below. Given the boundary conditions (2.19), we employ a different Green's function from (2.21) such that

$$G_k(x-y) = \frac{e^{ik|x-y|}}{2ik}, \tag{5.44}$$

which gives the transmission amplitude

$$T_V = 1 + \lambda \int_{-\infty}^{+\infty} dy\ \frac{e^{-iky}}{2ik}U(y)\varphi_k(y),$$

and the corresponding reflection amplitude

$$R_V = \lambda \int_{-\infty}^{+\infty} dy\ \frac{e^{iky}}{2ik}U(y)\varphi_k(y).$$

More specifically, this choice of Green's function corresponds to the $+i\epsilon$ prescription on the poles of the resolvent of the free Hamiltonian, that is

$$\lim_{\epsilon\to 0}\left(H_0 - (E_k + i\epsilon)\right)^{-1} = G(E_k + i\epsilon) \equiv G_k\ , \tag{5.45}$$

where the Green's function is the kernel of the Green's operator. That is traditionally written as $\langle x| G_k |y\rangle = G_k(x,y)$ in the literature [141]. The Lippmann-Schwinger

equation is one example of an inhomogeneous Fredholm integral equation of the second kind. It provides an integral representation for the scattering solution $\varphi_k(x)$ of the Schrödinger equation in the presence of interaction rather than a closed-form solution. Through an iterative process in which $\varphi_k(y)$ in (5.43) is substituted by the entire expression represented by $\varphi_k(x)$ of that same equation, we can generate a series with successive higher power terms in λ. The iterative process will give rise to an infinite Neumann series for the integral equation. We describe the iterative process in abstract notation as follows. Given an inhomogeneous integral equation

$$f_k(x) = g_k(x) + \lambda \int dy K_k(x,y) f_k(y), \tag{5.46}$$

it has a formal solution in the form

$$|f_k\rangle = (\mathbb{1} - \lambda K_k)^{-1} |g_k\rangle . \tag{5.47}$$

The operator $(\mathbb{1} - \lambda K_k)^{-1}$ can be formally expanded as

$$(\mathbb{1} - \lambda K_k)^{-1} = \sum_{n=0}^{\infty} \lambda^n K_k^n, \tag{5.48}$$

for a linear bounded operator $K_k \in \mathcal{B}(\mathcal{H})$ provided that there exists a positive constant Λ with $|\lambda| < \Lambda$ to guarantee the convergence, in the sense of the operator norm, of this series. In fact, Λ is essentially given by $\Lambda = 1/|\gamma_{\max}|$, where $\gamma_{\max}$ is the eigenvalue of the operator K_k with the largest magnitude. For unbounded K_k, the series may not converge. The solution for $|f_k\rangle$ is, therefore, given by the formal power series

$$|f_k\rangle = \sum_{n=0}^{\infty} \lambda^n K_k^n |g_k\rangle . \tag{5.49}$$

K_k^n are integral operators whose corresponding kernels are denoted by $(K_k)_n(x,y) := \langle x| (K_k)^n |y\rangle$. For instance, taking $n = 2$ for the second order kernel in λ, we obtain

$$(K_k)_2(x,y) = \int dz K_k(x,z) K_k(z,y), \tag{5.50}$$

and similarly for higher orders in which $n > 2$. The power series for the scattering solution is called Neumann series and it has the form

$$f_k(x) = g_k(x) + \sum_{n=1}^{\infty} \lambda^n \int dy (K_k)_n(x,y) g_k(y). \tag{5.51}$$

Returning now to the average value of interest in regard to the backflow (5.42) and making use of (2.22) together with its corresponding adjoint, the expectation value of the interacting current operator for a general state vector $|\psi\rangle$ becomes

$$\langle\psi|\, E_+\Omega_V^\dagger J(f)\Omega_V E_+\,|\psi\rangle = \int dx \int dx'(\Omega_V E_+\psi)^\star(x')\,[J(f)(x',x)]\,(\Omega_V E_+\psi)(x). \tag{5.52}$$

That can be equivalently written in terms of Green's functions

$$\begin{aligned}\frac{1}{2\pi}\int_0^\infty dk \int_0^\infty dk'\tilde{\psi}^\star(k')\tilde{\psi}(k)\int dx\int dx'\left(g_{k'}^\star(x')+\lambda\int dy'\; U(y')G_{k'}^\dagger(x'-y')\varphi_{k'}^\star(y')\right)\\ \times J(f)(x',x)\left(g_k(x)+\lambda\int dy\; G_k(x-y)U(y)\varphi_k(y)\right).\end{aligned} \tag{5.53}$$

The expansion of this expression up to the first order is given by the Born approximation in which we approximate the $\varphi_k(y)$ (and similarly for $\varphi_k^\star(y')$) in the integrand by the incident plane wave $g_k(y)$ to obtain

$$\begin{aligned}\langle J(\lambda)\rangle_\psi = \frac{1}{2\pi}\int_0^\infty dk\int_0^\infty dk'\tilde{\psi}^\star(k')\tilde{\psi}(k)\Bigg[\int dx\int dx' g_{k'}^\star(x')J(f)(x',x)g_k(x)\\ +\lambda\int dx\int dx' g_{k'}^\star(x')J(f)(x',x)\int dy\; G_k(x-y)U(y)g_k(y)\\ +\lambda\int dx\int dx'\int dy'\; U(y')G_{k'}^\dagger(x'-y')g_{k'}^\star(y')J(f)(x',x)g_k(x)\Bigg]\\ +\mathcal{O}(\lambda^2),\end{aligned} \tag{5.54}$$

where the first term corresponds to the interaction-free case independent of λ. That expression will be useful for the approximation of the lowest eigenvalue perturbation up to first order. In abstract notation, we can find the general structure of these operators for all orders in λ in a more convenient manner. For that, let us first write the solution (5.43) in the form

$$|\varphi_q\rangle = |g_q\rangle + \lambda G_q U\,|\varphi_q\rangle \tag{5.55}$$

for an arbitrary momentum variable q, and use the resolution (2.33) of the Møller wave operator Ω_V to expand the expectation value of interest (5.52) as follows

$$\begin{aligned}\langle J(\lambda)\rangle_\psi = \int_0^\infty dq'\,\langle\psi|\,|q'\rangle\left(\;\langle g_{q'}| + \lambda\,\langle g_{q'}|\,K_{q'}^\dagger + \lambda^2\,\langle g_{q'}|\,(K_{q'}^\dagger)^2 + \dots\;\right)\\ \times J(f)\int_0^\infty dq\left(\;|g_q\rangle + \lambda K_q\,|g_q\rangle + \lambda^2(K_q)^2\,|g_q\rangle + \dots\;\right)\langle q|\,|\psi\rangle\,,\end{aligned} \tag{5.56}$$

where the infinite sum is being indicated by '...' for the moment, and we set the product $G_k U = K_k$. It is also known that the chosen complementary function g_q is an exponential such that $\langle x|q\rangle = e^{iqx}/\sqrt{2\pi} = \langle x|g_q\rangle / \sqrt{2\pi}$. Thus, in power series of λ, the operator $E_+\Omega_V^\dagger J(f)\Omega_V E_+$ has the form

$$J(\lambda) = \int dq' \, |q'\rangle \left(\langle q'| \sum_{n=0}^{\infty} \lambda^n (K_{q'}^\dagger)^n \right) J(f) \int dq \left(\sum_{n=0}^{\infty} \lambda^n K_q^n \, |q\rangle \right) \langle q| \, . \tag{5.57}$$

Particularly, the spectral projection of the momentum operator E_+ enforces that q and q' are positive, and, if we strictly consider only right-moving wavefunctions ($E_+\psi = \psi$), the projection E_+ acts simply as an identity operator. The first two terms of that infinite perturbation expansion, namely, the zero order, corresponding to the unperturbed probability current operator, and the first order perturbation $\lambda J^{(1)}$ are such that

$$J(\lambda) = J^{(0)} + \lambda J^{(1)} + \mathcal{O}(\lambda^2), \tag{5.58}$$

with $J^{(0)}$ and $J^{(1)}$ given by

$$J^{(0)} = E_+ J(f) E_+ \quad \text{(0th order)}, \tag{5.59}$$

$$\begin{aligned} J^{(1)} = &\int_0^\infty dq' \, |q'\rangle \langle q'| \, (G_{q'}U)^\dagger J(f) \int_0^\infty dq \;\; |q\rangle \langle q| \\ &+ \int_0^\infty dq' \, |q'\rangle \langle q'| \;\; J(f) \int_0^\infty dq (G_q U) \, |q\rangle \langle q| \quad \text{(1st order)}. \end{aligned} \tag{5.60}$$

Note that the operator $J^{(0)}$ is in agreement with the unperturbed current operator firstly mentioned in chapter 2, and $J^{(1)}$ is the operator read from the kernel expression (5.54) that contributes with a linear term of the form $\lambda J^{(1)}$, the first correction to the free case taking into account the Green's operator G_q. A single general power series expression for the probability current operator is obtained by combining the two power series as follows

$$\begin{aligned} J(\lambda) &= \int_0^\infty dq \int_0^\infty dq' \, |q'\rangle \langle q'| \left(\sum_{m=0}^{\infty} \left(\lambda K_{q'}^\dagger \right)^m J(f) \sum_{n=0}^{\infty} (\lambda K_q)^n \right) |q\rangle \langle q| \\ &= \int_0^\infty dq \int_0^\infty dq' \, |q'\rangle \langle q'| \left(\sum_{m=0}^{\infty} \sum_{n=0}^{\infty} \lambda^{m+n} (K_{q'}^\dagger)^m J(f) (K_q)^n \right) |q\rangle \langle q| \, , \end{aligned} \tag{5.61}$$

which can be relabeled by setting $m + n \equiv d$ and $m \equiv t$. Hence, we obtain

Proposition 1. *The general interacting current,* $E_+\Omega_V^\dagger J(f)\Omega_V E_+ = J(\lambda)$*, written as a power series in the parameter* λ *is given by the following expression*

$$J(\lambda) = \int_0^\infty dq \int_0^\infty dq' \, |q'\rangle \langle q'| \left[\sum_{d=0}^{\infty} \sum_{t=0}^{d} \lambda^d \left(K_{q'}^\dagger\right)^t J(f) \left(K_q\right)^{d-t} \right] |q\rangle \langle q| \,. \tag{5.62}$$

Note that the projection E_+ is omitted when the limits of integration are restricted to positive momentum values, and the projection-valued measures are crucial elements in the definition of the current operator. From the expression of the operator $J^{(1)}$ and (5.36), the first correction for the lowest eigenvalue of the probability current operator is

$$\mu^{(1)} = \mathrm{Tr}\left(J^{(1)}P\right), \tag{5.63}$$

where P is the eigenprojection associated with the lowest eigenvalue of $J^{(0)}$. In order to take the trace of this operator, let us choose a particular basis, the eigenvectors of the unperturbed operator $J(f)$ denoted by $|\Xi_j\rangle$, for instance. One of these eigenvectors is the lowest eigenvector $|J_{min}^{(0)}\rangle$ whose associated momentum space eigenfunction is denoted by $\tilde{\mathcal{J}}^{(0)}(k)$. Thus, we obtain the first perturbation correction

$$\begin{aligned}
\mu^{(1)} &= \sum_j \langle \Xi_j, \, J^{(1)} P \Xi_j \rangle = \sum_j \langle \Xi_j | \, J^{(1)} \, |J_{min}^{(0)}\rangle \, \langle J_{min}^{(0)}| \, |\Xi_j\rangle = \langle J_{min}^{(0)}| \, J^{(1)} \, |J_{min}^{(0)}\rangle \\
&= \frac{1}{2\pi} \int_0^\infty dk \int_0^\infty dk' \tilde{\mathcal{J}}^{*(0)}(k') \tilde{\mathcal{J}}^{(0)}(k) \left(\int dx \int dx' g_{k'}^\star(x') J(f)(x', x) \right. \\
&\qquad \times \int dy \; G_k(x-y) U(y) g_k(y) \\
&\qquad \left. + \int dx \int dx' \int dy' \; U(y') G_{k'}^\dagger(x'-y') g_k^\star(y') J(f)(x', x) g_k(x) \right).
\end{aligned} \tag{5.64}$$

We remark that the first approximation to the perturbed lowest eigenvalue reads $\mu(\lambda) = \mu + \lambda\mu^{(1)} + \mathcal{O}(\lambda^2)$, with the perturbed eigenvalue $\mu(\lambda) = \beta_V(f)$ and the unperturbed $\mu = \beta_0(f)$. Similarly to the Hamiltonian with a Coulomb potential, for example, the operator $J(f)$ has a mixed spectrum set composed of both pure point spectrum and also continuous spectrum as previously mentioned. In such cases, the expansion of a general state vector of the Hilbert space with respect to a self-adjoint operator is given by a combination of sums over eigenstates and integrals over generalized eigenstates which are not elements of the space or, in other words, the set of eigenvectors will no longer span the whole Hilbert space, see e.g. [30, 142, 143]. In

fact, the justification is provided by the spectral representation of self-adjoint operators. Although the spectrum of the current operator is mixed, we stress that the perturbation is applied to a non-degenerate discrete, therefore, isolated eigenvalue and not to the whole spectrum. For an expository account of the perturbation of continuous Spectra, see [144]. In that manner, taking traces of the combination $J(\lambda)P(\lambda) = P(\lambda)J(\lambda)$ is possible as long as P is an eigenprojection whose range is finite-dimensional. However, in the presence of a mixed spectrum, the reduced resolvent with respect to μ can not be exactly expanded as before in (5.30) with sums over the discrete part of the spectrum, but it has also to include integration over the generalized eigenvectors corresponding to the continuous part of the spectrum. The reduced resolvent of the unperturbed current operator evaluated at $\xi = \mu$ is then

$$S = \sum_{l\neq 0} \frac{P_l}{(\mu_l - \mu)} + \int \frac{1}{(\mu_\nu - \mu)} dE(\nu), \tag{5.65}$$

where $E(\nu)$ denotes orthogonal projection operators associated with the continuous spectrum part and ν takes a continuous range of values. We can now obtain the second perturbation correction for the lowest eigenvalue

$$\begin{aligned}
\mu^{(2)} &= \mathrm{Tr}\left(J^{(2)}P - J^{(1)}SJ^{(1)}P\right) \\
&= \sum_j \langle \Xi_j | \, J^{(2)} \, | J^{(0)}_{min} \rangle \, \langle J^{(0)}_{min} | \, | \Xi_j \rangle \\
&\quad - \sum_j \langle \Xi_j | \, J^{(1)} \left[\sum_{l\neq 0} \frac{P_l}{(\mu_l - \mu)} + \int \frac{1}{(\mu_\nu - \mu)} dE(\nu) \right] J^{(1)} \, | J^{(0)}_{min} \rangle \, \langle J^{(0)}_{min} | \, | \Xi_j \rangle \\
&= \langle J^{(0)}_{min} | \, J^{(2)} \, | J^{(0)}_{min} \rangle - \sum_{l\neq 0} \frac{1}{(\mu_l - \mu)} \, \langle J^{(0)}_{min} | \, J^{(1)} \, | J^{(0)}_l \rangle \, \langle J^{(0)}_l | \, J^{(1)} \, | J^{(0)}_{min} \rangle \\
&\quad - \langle J^{(0)}_{min} | \, J^{(1)} \int \frac{1}{(\mu_\nu - \mu)} dE(\nu) J^{(1)} \, | J^{(0)}_{min} \rangle \\
&= \langle J^{(0)}_{min} | \, J^{(2)} \, | J^{(0)}_{min} \rangle - \sum_{l\neq 0} \frac{\left| \langle J^{(0)}_{min} | \, J^{(1)} \, | J^{(0)}_l \rangle \right|^2}{(\mu_l - \mu)} \\
&\quad - \int \frac{1}{(\mu_\nu - \mu)} d \, \langle J^{(0)}_{min} | \, J^{(1)} E(\nu) J^{(1)} \, | J^{(0)}_{min} \rangle \\
&= J^{(2)}_{00} - \sum_{l\neq 0} \frac{\left| J^{(1)}_{0l} \right|^2}{(\mu_l - \mu)} - \int \frac{1}{(\mu_\nu - \mu)} d \, \langle J^{(0)}_{min} | \, J^{(1)} E(\nu) J^{(1)} \, | J^{(0)}_{min} \rangle \, ,
\end{aligned} \tag{5.66}$$

where, in the last line, we introduced a notation generally used in physics literature for the expectation value of a perturbation to the lowest eigenvalue for the unperturbed energy eigenstates. More specifically, in our case, we are referring to the unperturbed J-eigenstates, and $J^{(2)}_{00}$ denotes the expectation value of $J^{(2)}$ with respect to the lowest eigenvector $|J^{(0)}_{min}\rangle$ of the unperturbed current operator. While both the summation term and the integral above have a negative contribution to $\mu^{(2)}$, because μ is the lowest eigenvalue and $\mu_l - \mu > 0$, the first term $J^{(2)}_{00}$ does not have a definite sign. However, these factors $(\mu_l - \mu)^{-1}$ become smaller for eigenvalues distant from μ and, therefore, less important. As a matter of comparison between the minimum and the maximum eigenvalues, we mention that numerical calculations in the case of a jump-defect for the following parameters: $N = 1000$, $P_{\text{cutoff}} = 100$, $\alpha = 1$, $x_0 = -2$ give the lowest egenvalue $\mu \approx -0.24$ and the maximum eigenvalue $\mu_{1000} \approx 275.21$. That explains the difficulty in the numerical analysis concerning the problem of ill-conditioned matrices [145] as a result of the discretization of an infinite-dimensional operator.

5.3.1 Perturbed and unperturbed lowest eigenvalue

Having found the power series expansion of the lowest eigenvalue of the probability current operator under perturbation

$$\mu(\lambda) = \mu + \sum_{n=1}^{\infty} \lambda^n \mu^{(n)}, \tag{5.67}$$

we gave particular emphasis to the first (5.64) and second (5.37) corrections. Each order contributes with a term which has the form $\left\langle J^{(0)}_{min} \middle| J^{(n)} \middle| J^{(0)}_{min} \right\rangle$, which is the expectation value of the corresponding perturbation in the lowest eigenvector $|J^{(0)}_{min}\rangle$. Particularly, the case $n = 0$ corresponds to the unperturbed μ. Hence, the perturbed eigenvalue can be rewritten in the following alternative form

$$\mu(\lambda) = \sum_{n=0}^{\infty} \lambda^n \left\langle J^{(0)}_{min} \middle| J^{(n)} \middle| J^{(0)}_{min} \right\rangle + \widetilde{\widetilde{\mu}}(\lambda), \tag{5.68}$$

where the term $\widetilde{\widetilde{\mu}}(\lambda)$ represents the sum of all other terms. Note that these other terms are second order in λ at least and all higher orders as well. From (5.35), we can see that is true indeed, because it is always possible to obtain terms similar to the first

order perturbation from the allowed combinations of the indices of the sum. Taking into consideration that the perturbed operator takes the form (5.1), the summation can be included in the definition of $J(\lambda)$ as follows

$$\mu(\lambda) = \underbrace{\left\langle J^{(0)}_{min}\middle| J(\lambda)\middle| J^{(0)}_{min}\right\rangle}_{(A)} + \underbrace{\widetilde{\widetilde{\mu}}(\lambda)}_{(B)}, \tag{5.69}$$

with part (A) representing all the expectation value expressions of the perturbed operator in $|J^{(0)}_{min}\rangle$ and part (B) representing all the other terms. We can make use of the minimax principle for analysing the sign of the (B)-contribution. Given that $\mu(\lambda)$ is the lowest eigenvalue of some operator, namely, the operator $J(\lambda)$ with associated lowest eigenvector $|J_{min}(\lambda)\rangle$, the inequality

$$\min_{|\psi\rangle} \langle\psi|J(\lambda)|\psi\rangle = \mu(\lambda) \leqslant \left\langle J^{(0)}_{min}\middle| J(\lambda)\middle| J^{(0)}_{min}\right\rangle \tag{5.70}$$

holds because $|J^{(0)}_{min}\rangle$ is not the lowest eigenvector of $J(\lambda)$, and that is one formulation of the variational principle [146, 147]. In other words, the expectation value of an operator in a vector which is not its lowest eigenvector gives an upper bound on the lowest eigenvalue of that operator. Hence, we conclude that the (B)-contribution is negative, $\widetilde{\widetilde{\mu}}(\lambda) \leqslant 0$. Furthermore, expression (5.69) can be further decomposed and written in terms of the notation employed in the context of the backflow

$$\beta_V(f) = \underbrace{\beta_0(f) + \left\langle J^{(0)}_{min}\middle|\sum_{n=1}^{\infty}\lambda^n J^{(n)}\middle| J^{(0)}_{min}\right\rangle}_{(A)} + \underbrace{\widetilde{\widetilde{\mu}}(\lambda)}_{(B)}. \tag{5.71}$$

In view of that, the question on whether $\beta_V(f)$ is larger or smaller than $\beta_0(f)$ depends largely on the sign of the $\sum_{n=1}^{\infty}\lambda^n \left\langle J^{(0)}_{min}\middle| J^{(n)}\middle| J^{(0)}_{min}\right\rangle$, and investigations on that directions require a choice of a particular potential function V in order to calculate the first and the second order perturbation approximations, for instance.

Alternatively, considering that the perturbed lowest eigenvalue $\mu(\lambda)$ is an non-degenerate isolated eigenvalue of the probability current operator $J(\lambda)$ with corresponding normalized lowest eigenvector denoted as $|J_{min}(\lambda)\rangle$, it is given by

$$\mu(\lambda) = \langle J_{min}(\lambda)|J(\lambda)|J_{min}(\lambda)\rangle\,. \tag{5.72}$$

Under the appropriate assumptions of differentiability for $J(\lambda)$, $\mu(\lambda)$ and $|J_{min}(\lambda)\rangle$, sufficiently smooth functions of λ, it follows that

$$\left.\frac{d\mu(\lambda)}{d\lambda}\right|_{\lambda=0} = \left\langle J^{(0)}_{min}\right| \left.\frac{dJ(\lambda)}{d\lambda}\right|_{\lambda=0} \left|J^{(0)}_{min}\right\rangle = \left\langle J^{(0)}_{min}\middle|J^{(1)}\middle|J^{(0)}_{min}\right\rangle \tag{5.73}$$

gives the first order approximation $\mu^{(1)}$ to the lowest unperturbed eigenvalue from the first derivative of $\mu(\lambda)$ with respect to λ. That is the equivalent version of the Hellmann-Feynman theorem for the Hamiltonian operator. However, upon taking a second derivative before setting $\lambda = 0$, we can show (see, for instance, the account of [148] in the case of the Hamiltonian operator) that the second derivative is

$$\frac{d^2\mu(\lambda)}{d\lambda^2} = \langle J_{min}(\lambda)|\frac{d^2J(\lambda)}{d\lambda^2}|J_{min}(\lambda)\rangle - 2\left(\langle J'_{min}(\lambda)|J(\lambda)|J'_{min}(\lambda)\rangle - \mu(\lambda)\right), \tag{5.74}$$

where the vector $|J'_{min}(\lambda)\rangle$ denotes the first derivative of $|J_{min}(\lambda)\rangle$ with respect to λ; thus $|J'_{min}(\lambda)\rangle := d\,|J_{min}(\lambda)\rangle\,/d\lambda$. It follows from the variational principle, therefore, that

$$\frac{d^2\mu(\lambda)}{d\lambda^2} \leq \langle J_{min}(\lambda)|\frac{d^2J(\lambda)}{d\lambda^2}|J_{min}(\lambda)\rangle\,, \tag{5.75}$$

which implies that $\mu^{(2)} \leq \left\langle J^{(0)}_{min}\middle|J^{(2)}\middle|J^{(0)}_{min}\right\rangle = J^{(2)}_{00}$ in agreement with expression (5.66). These arguments provide upper bounds on the perturbed lowest eigenvalue and, combined with lower bounds estimates, could narrow $\beta_V(f)$ to certain intervals. As previously mentioned, (2.23) provides lower bounds, but these are rough estimates as shown in [11]. In section 5.4, devoted to present the numerical results in the case of a single δ-defect, the first order approximation perturbation seems to be a much sharper lower bound. The case of a general double δ-defect, which depends on two parameters, namely, λ_1 and λ_2, requires a generalization of the analytic perturbation theory because, even if the operator $J(\lambda_1, \lambda_2)$ is holomorphic in the two variables, total differentiability is a subtle concept, and the eigenvalues might have complicated singularities [50, 149]. As for the jump-defect, it cannot be classified as a potential in $L^1_1(\mathbb{R})$ because it is not even described in terms of an explicit potential function V, and, therefore, there is no lower bound estimate in terms of (2.23). Nonetheless, the first order perturbation results for the jump-defect is presented in section 5.5.

The exact relation between the perturbed and the unperturbed lowest eigenvalue is given in (5.71), and we might check how approximations of low order compare to

the exact calculation when the solutions are explicitly known. For any finite order n, using the general expression for the expansion of the lowest eigenvalue (5.35) together with the general perturbation to the probability current operator (5.62), we have the perturbation corrections to the lowest eigenvalue

$$\mu^{(n)} = \sum_{p=1}^{n} \frac{(-1)^p}{p} \sum_{\substack{\nu_1+\ldots+\nu_p=n \\ \alpha_1+\ldots+\alpha_p=p-1}} \mathrm{Tr}\left(J^{(\nu_1)} S^{(\alpha_1)} J^{(\nu_2)} S^{(\alpha_2)} \ldots J^{(\nu_p)} S^{(\alpha_p)}\right), \tag{5.76}$$

with $\alpha_j \geq 0$ and $\nu_j \geq 1$. We remark that the presence of the Green's function (5.44) in the one-dimensional scattering problem causes an infrared or low-momentum divergence (at $k = 0$) in the perturbations series. It is also worth remarking that the Green's function used before in (2.21) would not have been a more suitable choice because the complementary function in the Lippmann-Schwinger equation (2.20) depends on $T(k)$, which is a power series in λ, and it would be difficult to keep track of the perturbation series in λ. As its known that the exact backflow calculations are not divergent, that divergence is artificially produced by our choice of asymptotics in the scattering analysis. Formally, a small positive constant cutoff ϵ could be used for restricting the limits of integration in momentum space to $k \in (\epsilon, \infty)$. However, a solution to this issue will not be attempted in this thesis. Finally, note that $J^{(\nu_j)}$ in the expression (5.76) are integral operators. The trace operation is evaluated by inserting complete sets of generalized eigenvectors and taking the trace inside the integrals. Now we come to the general expression of the perturbation corrections to the backflow constant $\beta_V(f)$.

Proposition 2. *The nth order perturbation correction $\mu^{(n)}$ in the parameter λ to the*

lowest eigenvalue of the probability current operator in the parameter λ is given by

$$\begin{aligned}\mu^{(n)} = \sum_{p=1}^{n} \frac{(-1)^p}{p} \int_0^\infty dq_1 \int_0^\infty dq_1' \int_0^\infty dq_2 \int_0^\infty dq_2' \dots \int_0^\infty dq_p \int_0^\infty dq_p' \\ \times \sum_{\substack{\nu_1+\dots+\nu_p=n \\ \alpha_1+\dots+\alpha_p=p-1 \\ \alpha_j\geq 0;\, \nu_j\geq 1}} \mathrm{Tr}\Bigg(|q_1'\rangle\langle q_1'| \left[\sum_{t_1=0}^{\nu_1} \left(K_{q_1'}^\dagger\right)^{t_1} J(f) \left(K_{q_1}\right)^{\nu_1-t_1}\right] |q_1\rangle\langle q_1| \\ \times S^{(\alpha_1)}\ |q_2'\rangle\langle q_2'| \left[\sum_{t_2=0}^{\nu_2} \left(K_{q_2'}^\dagger\right)^{t_2} J(f) \left(K_{q_2}\right)^{\nu_2-t_2}\right] |q_2\rangle\langle q_2| \\ \times S^{(\alpha_2)} \dots |q_p'\rangle\langle q_p'| \left[\sum_{t_p=0}^{\nu_p} \left(K_{q_p'}^\dagger\right)^{t_p} J(f) \left(K_{q_p}\right)^{\nu_p-t_p}\right] |q_p\rangle\langle q_p|\ S^{(\alpha_p)}\Bigg).\end{aligned} \tag{5.77}$$

As a matter of reordering the sums, that expression can also be written in the following alternative form

$$\begin{aligned}\mu^{(n)} = \sum_{p=1}^{n} \frac{(-1)^p}{p} \int_0^\infty dq_1 \int_0^\infty dq_1' \int_0^\infty dq_2 \int_0^\infty dq_2' \dots \int_0^\infty dq_p \int_0^\infty dq_p' \\ \times \sum_{\substack{\nu_1+\dots+\nu_p=n \\ \alpha_1+\dots+\alpha_p=p-1 \\ \alpha_j\geq 0;\, \nu_j\geq 1}} \sum_{(0\leq t_j\leq \nu_j)} \mathrm{Tr}\Bigg(|q_1'\rangle\langle q_1'| \left[\left(K_{q_1'}^\dagger\right)^{t_1} J(f) \left(K_{q_1}\right)^{\nu_1-t_1}\right] |q_1\rangle\langle q_1| \\ \times S^{(\alpha_1)}\ |q_2'\rangle\langle q_2'| \left[\left(K_{q_2'}^\dagger\right)^{t_2} J(f) \left(K_{q_2}\right)^{\nu_2-t_2}\right] |q_2\rangle\langle q_2| \\ \times S^{(\alpha_2)}\ \dots |q_p'\rangle\langle q_p'| \left[\left(K_{q_p'}^\dagger\right)^{t_p} J(f) \left(K_{q_p}\right)^{\nu_p-t_p}\right] |q_p\rangle\langle q_p|\ S^{(\alpha_p)}\Bigg).\end{aligned} \tag{5.78}$$

In the next two sections, we will apply that perturbation correction to the cases of the backflow in the presence of δ-defect and in the presence of a jump-defect. More specifically, we will take into account the first order correction for small λ and compare the results to the previous exact calculations depicted in the collection of plots.

5.4 FIRST ORDER APPROXIMATION IN THE PRESENCE OF A δ-DEFECT

Due to the fact that the free resolvent, and consequently the Green's function, has an infrared singularity at $k = 0$, the perturbation terms of orders higher than one present additional difficulty for the numerical calculations. The first order correction is manageable, but the second order is more singular and can radically affect the value of the backflow constant $\beta_V(f)$. For that reason, we will not treat in this thesis the second or any higher order perturbation corrections. However, resolving this issue would certainly be a worthwhile task for the future.

For the calculation of the backflow constant, we shall take the infimum of the expectation value $\langle\psi| E_+\Omega_V^\dagger J(f)\Omega_V E_+ |\psi\rangle$, which is achieved for the lowest eigenfunction associated with the interacting probability current operator. Instead of finding the exact result as we did in previous chapters and as a direct application of the analytic perturbation discussed in the context of the backflow, we can calculate the first order correction to the lowest eigenvalue of the probability current in the presence of the δ-defect using the expression (5.64) to give

$$\begin{aligned}\mu^{(1)} = \frac{1}{2\pi}\int_0^\infty dk \int_0^\infty dk' \tilde{\mathcal{J}}^{*(0)}(k')\tilde{\mathcal{J}}^{(0)}(k)\Bigg(\int dx \int dx' g^\star_{k'}(x')J(f)(x',x) \\ \times \int dy\; G_k(x-y)2\delta(y)g_k(y) \\ + \int dx \int dx' \int dy'\; 2\delta(y')G^\dagger_{k'}(x'-y')g^\star_k(y')J(f)(x',x)g_k(x)\Bigg),\end{aligned} \tag{5.79}$$

where we particularized to our case of interest, namely, the delta impurity $V(x) = \delta(x)$. We stress that the strength λ was conveniently put outside this expression and will appear again when the entire first contribution $\lambda\mu^{(1)}$ is taking into account. Knowing the Green's function (5.44), the following integrals can be easily calculated

$$\int dy\; G_k(x-y)2\delta(y)\exp(iky) = \frac{\exp(ik|x|)}{ik} \tag{5.80}$$

$$\int dy'\; 2\delta(y')G^\dagger_{k'}(x'-y')\exp(-ik'y') = -\frac{\exp(-ik'|x'|)}{ik'}. \tag{5.81}$$

Back to our expression for the first correction, let us denote by $L_1(k',k)$ the kernel of the operator $J^{(1)}$ associated with the first order approximation to the lowest eigenvalue

$$\mu^{(1)} = \frac{1}{2\pi}\int_0^\infty dk \int_0^\infty dk' \tilde{\mathcal{J}}^{*(0)}(k')\tilde{\mathcal{J}}^{(0)}(k)L_1(k',k). \tag{5.82}$$

The first order probability current operator kernel $L_1(k',k)$ in the case of a delta impurity can be obtained after calculating the following expression

$$2iL_1(k',k) = \int dx' f(x') \left(\exp(-ik'x') \frac{\partial}{\partial x'} \frac{\exp(ik|x'|)}{ik} - \frac{\partial}{\partial x'} (\exp(-ik'x')) \frac{\exp(ik|x'|)}{ik} \right) - \int dx' f(x') \left(\frac{\exp(-ik'|x'|)}{ik'} \frac{\partial}{\partial x'} \exp(ikx') - \frac{\partial}{\partial x'} \left(\frac{\exp(-ik'|x'|)}{ik'} \right) \exp(ikx') \right). \tag{5.83}$$

Recall that $\varphi \in H^1(\mathbb{R}) \cap H^2(\mathbb{R} \setminus \{0\})$. The derivatives of φ are piecewise defined, and the integrals on the real line split into two pieces corresponding to the left region $x < 0$ and right region $x > 0$. In fact, we even did not need to use Heaviside functions in the calculations leading to the expression (5.83). It follows that the kernel can be simplified leading to its final form with contributions to the left and right regions as

$$\begin{aligned} 2iL_1(k',k) = {} & \frac{k'}{k} \int_{-\infty}^{0} dx' f(x') \exp(-ix'(k+k')) - \frac{k}{k'} \int_{-\infty}^{0} dx' f(x') \exp(ix'(k+k')) \\ & + \int_{-\infty}^{0} dx' f(x') \exp(ix'(k+k')) - \int_{-\infty}^{0} dx' f(x') \exp(-ix'(k+k')) \\ & + \frac{(k'-k)(k'+k)}{k'k} \int_{0}^{\infty} dx' f(x') \exp(ix'(k-k')). \end{aligned} \tag{5.84}$$

Note that the eigenvalue at first order $\mu^{(1)}$, given by equation (5.82), is calculated in terms of the eigenfunction at zeroth order $\tilde{\mathcal{J}}^{(0)}$, which corresponds to the unperturbed physical system. Now we may use that result to find the backflow constant $\beta_V(f)$ up to the first order approximation in λ given by

$$\beta_V(f) \approx \beta_0(f) + \lambda \mu^{(1)}. \tag{5.85}$$

The following figures show the results for some small values of the potential strength. In fact, the question on how small should be the parameter λ depends on the particular potential in consideration. In figure 5.1, for example, $|\lambda| = 0.3$ and $|\lambda| = 0.05$ are very satisfactory approximations as can be seen in comparison with the exact calculation. For values $|\lambda| > 0.1$, figure 5.2, the results become compromised in the sense that the first order approximation does not seem to be enough. In general, for larger values $|\lambda|$, the first order results for $\beta_V(f)$ become even more negative. It is worth noting that, in contrast to the exact calculations of section 3.2, $k = -i\lambda$ is no longer a pole (and

possibly bound state) of the kernel (5.84), and the first order results do not show the presence of maxima, previously found in the exact calculations, that would peak in the region at the left of the defect.

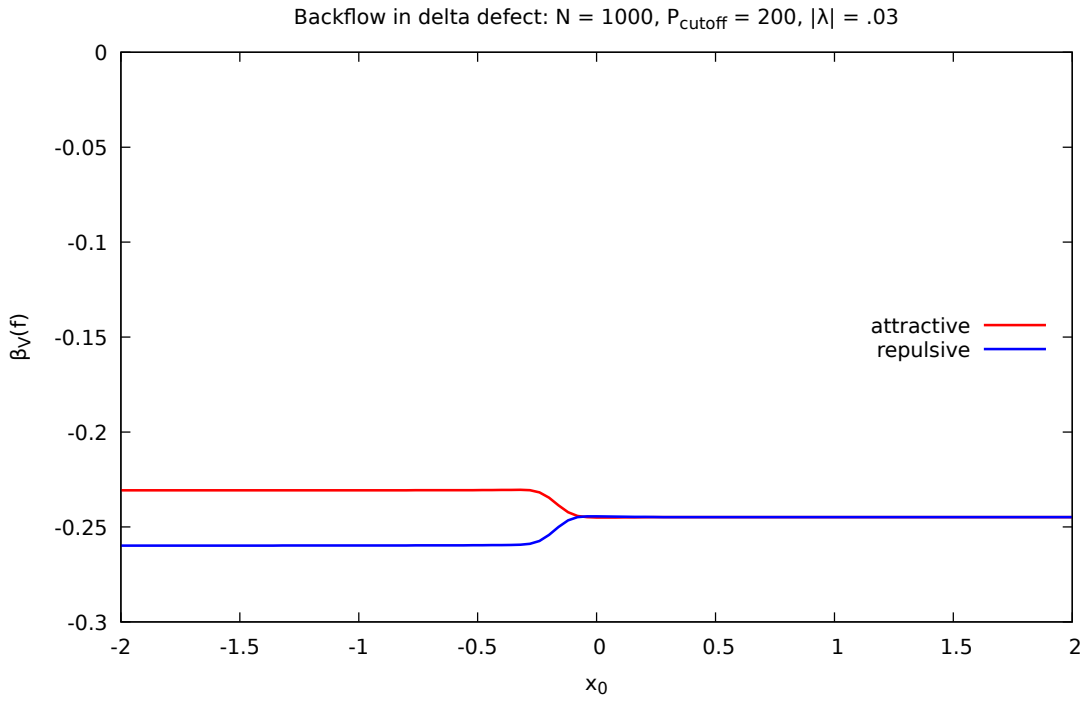

(a) Refer to Figure 3.1 (a) for exact calculation

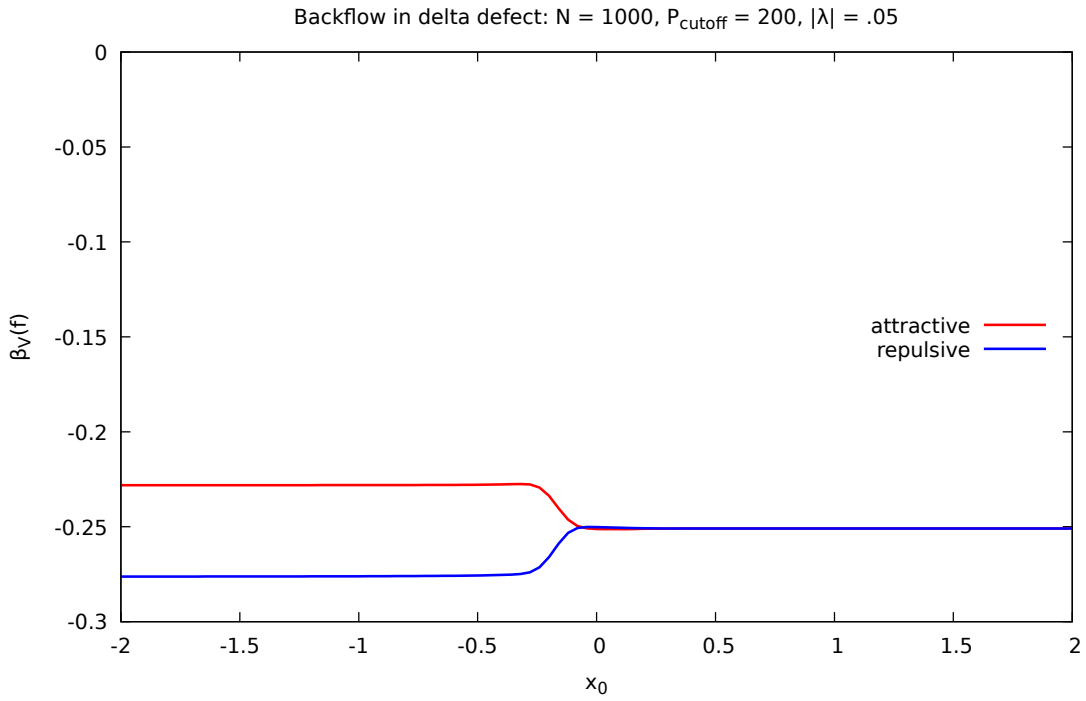

(b)

Figure 5.1: First order approximation - Lowest backflow eigenvalue of the current operator, for which (a) $|\lambda| = 0.03$ (b) $|\lambda| = 0.05$.

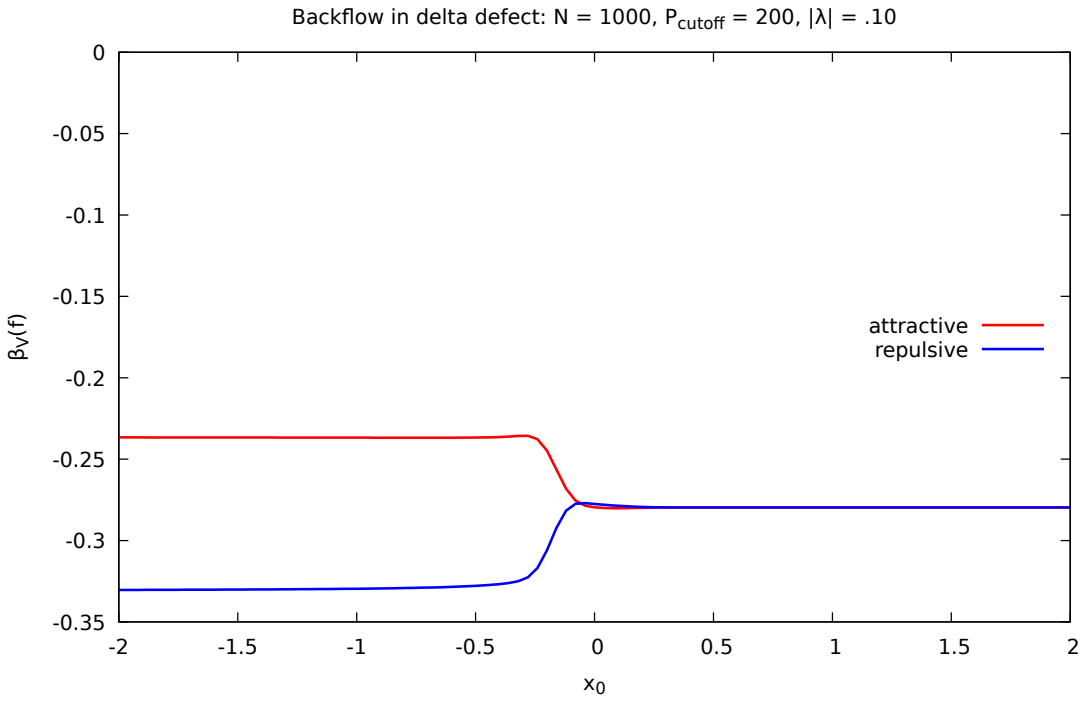

(a) Refer to Figure 3.1 (b) for exact calculation

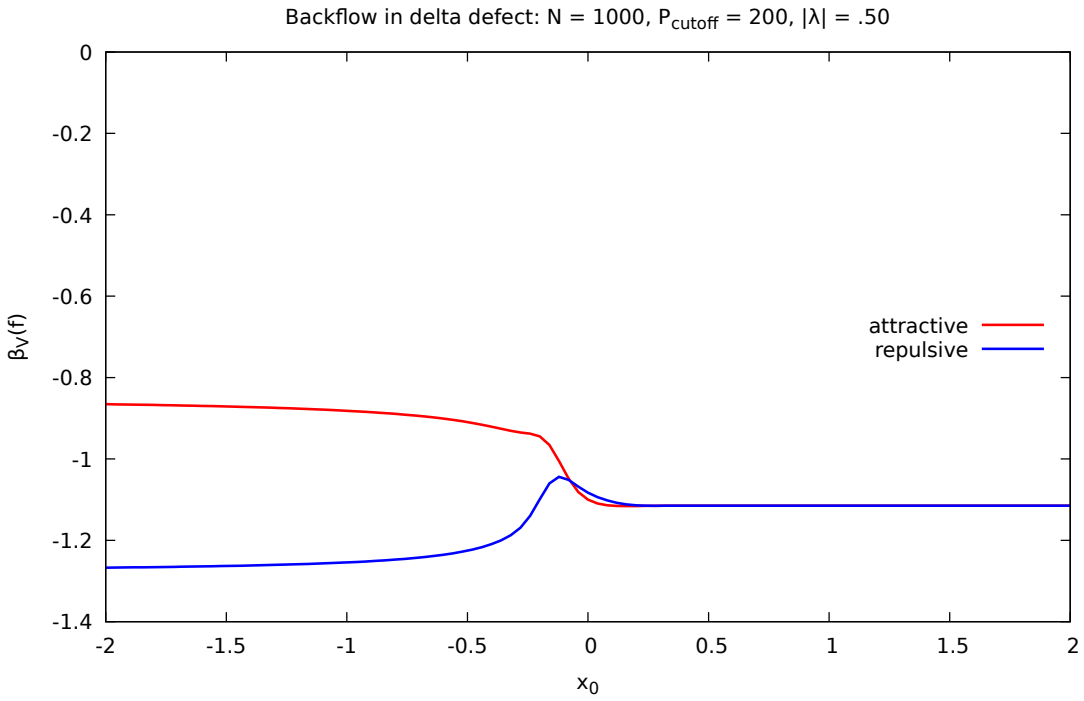

(b) Refer to Figure 3.2 (a) for exact calculation

Figure 5.2: First order approximation - Lowest backflow eigenvalue of the current operator, for which (a) $|\lambda| = 0.03$ (b) $|\lambda| = 0.05$.

5.5 first order approximation in the presence of a jump-defect

In section 5.3, we used the time-independent solution $\varphi_k(x)$ for finding the expressions of the probability interacting current operator. In particular, we can apply our results to the first order approximation in the parameter α.

Although we made a direct use of the Lippmann-Schwinger equation in the analytic perturbation theory for the first order approximation of the lowest eigenvalue $\beta_V(f)$, which has an explicit potential term, we are not able to proceed in exactly the same manner as did in the presence of a δ-defect. Because the jump does not have an explicit potential function to describe it but rather a set of sewing conditions, we will work out an alternative way based on the fact that the jump is a exactly solvable model. That means we shall use the exact scattering solution to provide information on the possible different approximations. Let us combine the scattering solution of the jump-defect (4.24) and the Lippmann-Schwinger equation (5.43) into the following expression

$$\exp(ikx) + \alpha \int dy G_k(x-y)U(y)\varphi_k(y) = \begin{cases} \exp(ikx) & x < 0, \\ \left(\dfrac{k+i\alpha}{k-i\alpha}\right)\exp(ikx) & x > 0, \end{cases} \tag{5.86}$$

which can be equivalently written in the form

$$\alpha \int dy G_k(x-y)U(y)\varphi_k(y) = \begin{cases} 0 & x < 0, \\ \dfrac{2i\alpha}{k-i\alpha}\exp(ikx) & x > 0. \end{cases} \tag{5.87}$$

Similarly, the adjoint part can also be written in the form

$$\alpha \int dy' G^{\dagger}_{k'}(x'-y')U(y')\varphi^{\star}_{k'}(y') = \begin{cases} 0 & x < 0, \\ \dfrac{-2i\alpha}{k'+i\alpha}\exp(-ik'x) & x > 0, \end{cases} \tag{5.88}$$

which makes manifest the dependence on α of the first-order approximation or any order above. To find a linear term in α, we can expand

$$\frac{2i\alpha}{(k-i\alpha)} = \frac{2i\alpha}{k}\left(1 + \frac{i\alpha}{k} + \mathcal{O}(\alpha^2)\right), \tag{5.89}$$

valid only for small values of the defect parameter, $\alpha << k$. The first-order contribution to the scattering solution of the jump-defect can be found using the Born approximation, namely, $\varphi_k(y) = \exp(ikx)$ that results

$$\int dy G_k(x-y)U(y)\varphi_k(y) = \frac{2i}{k}\theta(x)\exp(ikx), \tag{5.90}$$

$$\int dy' G^{\dagger}_{k'}(x'-y')U(y')\varphi^{\star}_{k'}(y') = -\frac{2i}{k'}\theta(x')\exp(-ik'x'). \tag{5.91}$$

As discussed in section 4.2, the wavefunction φ is discontinuous at the origin in the case of a jump-defect. Because the wavefunction has piecewise defined derivatives, the integrals on the entire real line are split into two pieces. Physically, the wavefunction is not being defined at the origin, where the defect is placed, and the sewing conditions determining the physics at this point, rather than the Schrödinger equation. The solution u_k at the left of the defect has zero first-order contribution and, therefore, zero contribution to the first-order kernel $L_1(k',k)$. The contributions associated with the solution v_k at the right of the defect are the combination of the Born approximation, which is a zero-order term in α, with the first-order approximation given by equation (5.90), both restricted to the right region $x > 0$ such that the kernel has the following form

$$\begin{aligned} L_1(k',k) = \frac{1}{k}\int_0^{\infty} dx' f(x')\left(\exp(-ik'x')\frac{\partial}{\partial x'}\exp(ikx') - \frac{\partial}{\partial x'}(\exp(-ik'x'))\exp(ikx')\right) \\ - \frac{1}{k'}\int_0^{\infty} dx' f(x')\left(\exp(-ik'x')\frac{\partial}{\partial x'}\exp(ikx') - \frac{\partial}{\partial x'}(\exp(-ik'x'))\exp(ikx')\right). \end{aligned} \tag{5.92}$$

Note that all the integrals have support in the appropriate right region because there is no contribution from the left region. This can be simplified to a single term. Finally, the contributions sum up to obtain

$$L_1(k',k) = -\frac{i(k^2-k'^2)}{kk'}\int_0^{\infty} dx' f(x')\exp(ix'(k-k')). \tag{5.93}$$

This expression could also be derived by expanding the exact kernel in (4.27), but the idea of this section is to find the results following use of the perturbative method. The backflow constant in the presence of a jump-defect taking into account the first-order perturbation approximation in α is given by

$$\beta_V(f) \approx \beta_0(f) + \alpha\mu^{(1)}, \tag{5.94}$$

with the correction $\mu^{(1)}$ calculated from the integrals

$$\mu^{(1)} = -\frac{i(k^2 - k'^2)}{2\pi kk'} \int_0^\infty dk \int_0^\infty dk' \tilde{\jmath}^{*(0)}(k') \tilde{\jmath}^{(0)}(k) \int_0^\infty dx' f(x') \exp(ix'(k - k')). \tag{5.95}$$

In the case of the conserved probability current, where there is an extra contribution included whose origin is purely from the defect, we shall take into account the first-order approximation from this defect contribution as well. This term, given by (4.31), has support defined only at the origin and can be expanded to first order

$$\left(\frac{2i\alpha(k + k')}{(k - i\alpha)(k' + i\alpha)} \right) f(0) = \frac{2i\alpha(k + k')}{kk'} f(0) + \mathcal{O}(\alpha^2), \tag{5.96}$$

valid for small values of the parameter, $\alpha << k, k'$. The backflow constant in the presence of a jump-defect after considering the conservation of the probability current operator is, up to first-order in α, given by the same expression (5.94) with the difference that now $\mu^{(1)}$ is adjusted taking into account the contribution from the defect itself

$$\begin{aligned} \mu^{(1)} = -\frac{1}{2\pi} \int_0^\infty dk \int_0^\infty dk' \tilde{\jmath}^{*(0)}(k') \tilde{\jmath}^{(0)}(k) \left[\frac{k + k'}{kk'} f(0) \right. \\ \left. + \frac{i(k^2 - k'^2)}{kk'} \int_0^\infty dx' f(x') \exp(ix'(k - k')) \right]. \end{aligned} \tag{5.97}$$

With the first order approximations for both cases, without considering the conservation of the current and after taking it into consideration, numerical calculations are used in order to summarize the results in similar plots to those considered in previous chapters.

The following plots summarize the results for the backflow constant (up to first order) in the presence of a jump-defect. First, figures 5.3 and 5.4 show the case of the non-conserved probability current operator. For very small values, $|\alpha| = 0.01$ in figure 5.3, for example, the result is very satisfactory. However, for larger absolute values of the parameter, the backflow constant is strongly changed at positions $x_0 > 0$, at the right of the defect, as can be seen in figure 5.4. Note that the defect is purely-transmitting and, therefore, there is no reflection term being affected at the left of the defect position, but the first order approximation of the transmission factor is causing this asymmetry in contrast to the exact calculation. Then, we take into account the conservation of the probability current and use (5.97) to produce the next set of plots, figures 5.5, 5.6 and 5.7. In particular, figure 5.5 shows the approximation to the backflow constant

for $|\alpha| = 0.01$ and $|\alpha| = 0.06$, which are again satisfactory. The similar issue that happens in the non-conserved case, where there is an asymmetry with respect to the defect position, is shown for larger values of the parameter, in figure 5.6 and figure 5.7. That was already expected because the distinction between the non-conserved and the conserved probability current is only the extra defect contribution that has compact support in the neighbourhood of $x_0 = 0$. In order to check the first order approximation from the defect contribution only, we adjust the expression (5.97) by removing the second term and keeping only the first term that is proportional to $f(0)$. The results are plotted in figures 5.8, 5.9 and 5.10. From these, it is clear that the decrease in $\beta_V(f)$, as $|\alpha|$ increases, for positions $x_0 > 0$ is an effect with origin in the bulk. Although not included in this thesis, we report that the first order defect contribution for extremely large values of the parameter, $|\alpha| > 100$, becomes progressively negligible in comparison to the interaction-free value $\beta_0(f)$. These are results from the first order perturbation and, therefore, it is a natural step to proceed by looking into the second order perturbation corrections. To satisfactorily succeed on that, we understand that the present scattering analysis of the backflow needs to be modified in the sense of avoiding the infrared divergence previously mentioned. A possible way around that issue is conveniently changing the incoming asymptote. However, that would also change the value of $\beta_0(f)$ for the same test function f. We started to look into this possibility, but did not progress enough in that direction to give a report in this thesis.

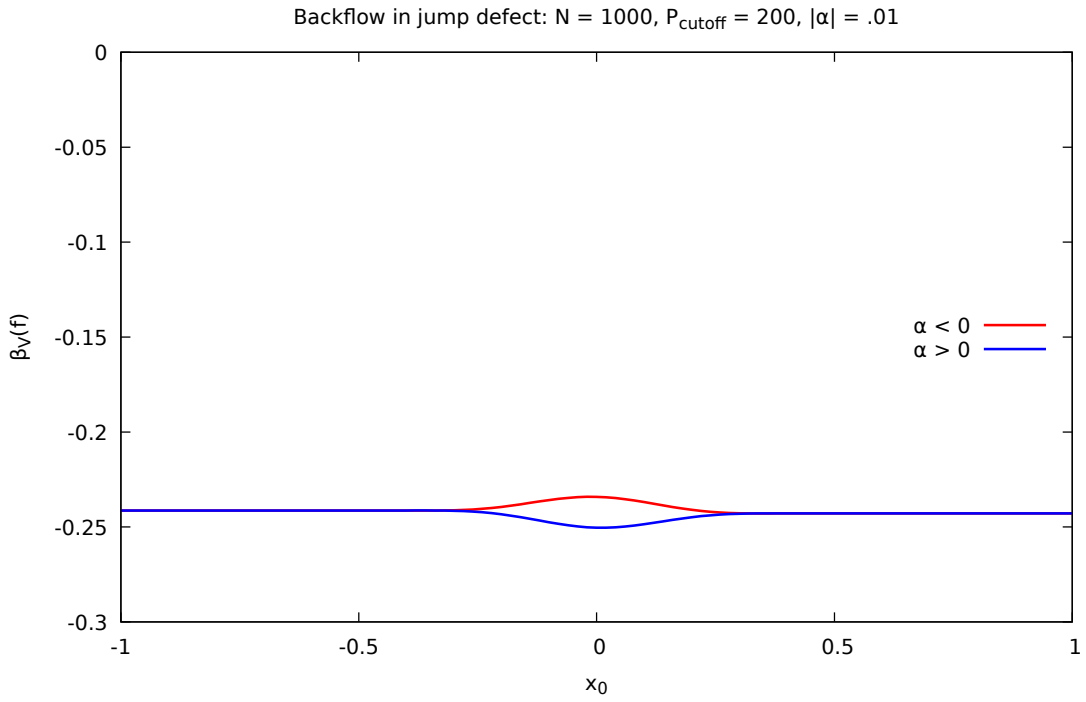

(a) Refer to Figure 4.2 (a) for exact calculation

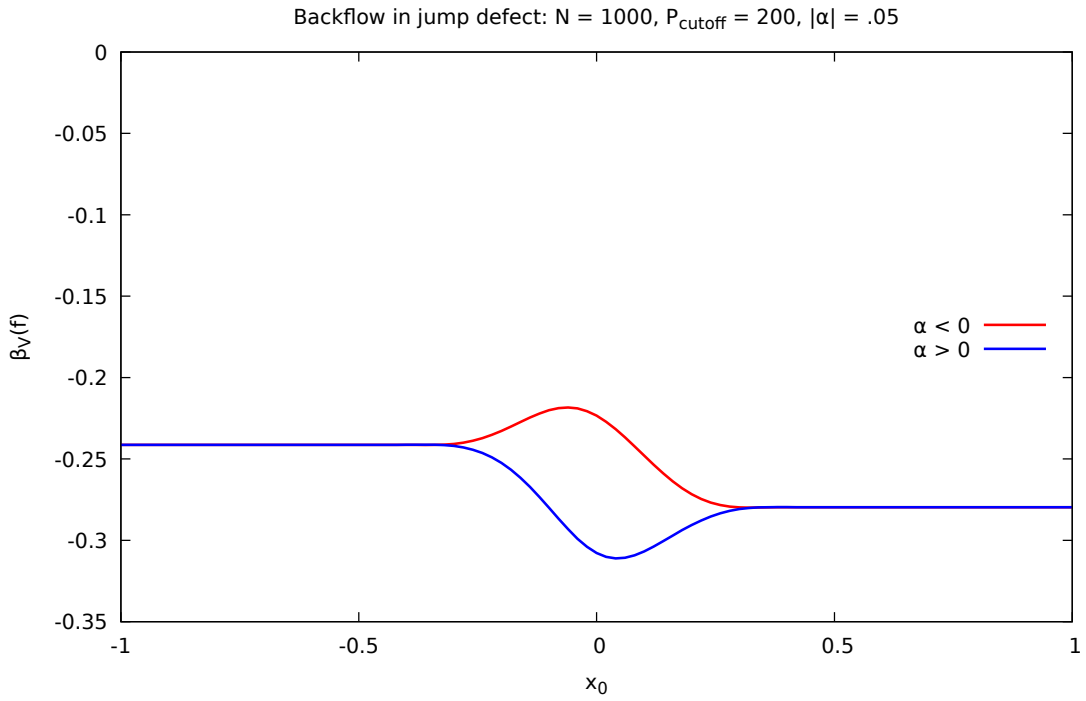

(b) Refer to Figure 4.2 (b) for exact calculation

Figure 5.3: First order approximation - Lowest backflow eigenvalue of the current operator, for which (a) $|\alpha| = 0.01$ (b) $|\alpha| = 0.05$.

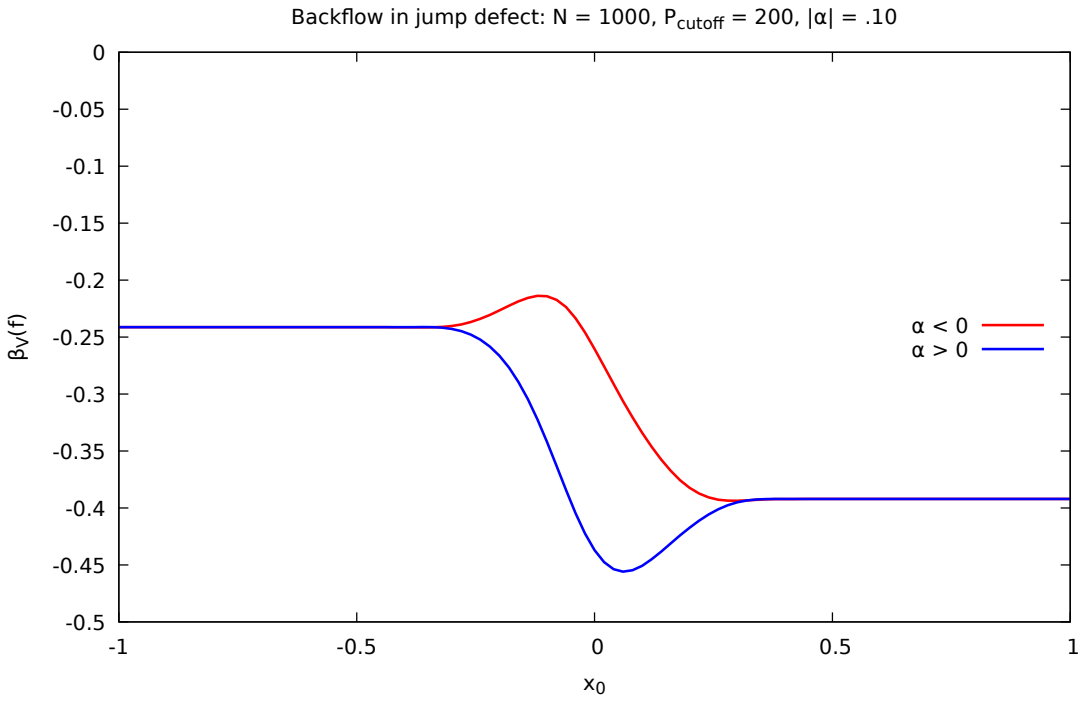

(a) Refer to Figure 4.3 (b) for exact calculation

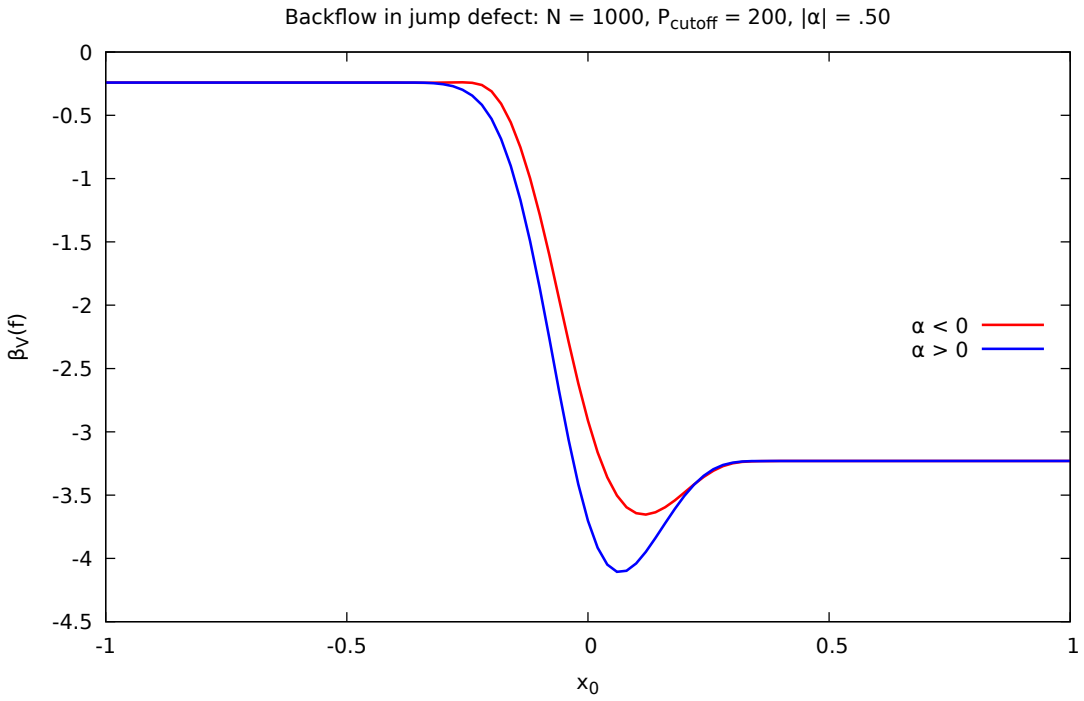

(b) Refer to Figure 4.4 (b) for exact calculation

Figure 5.4: First order approximation - Lowest backflow eigenvalue of the current operator, for which (a) $|\alpha| = 0.1$ (b) $|\alpha| = 0.5$.

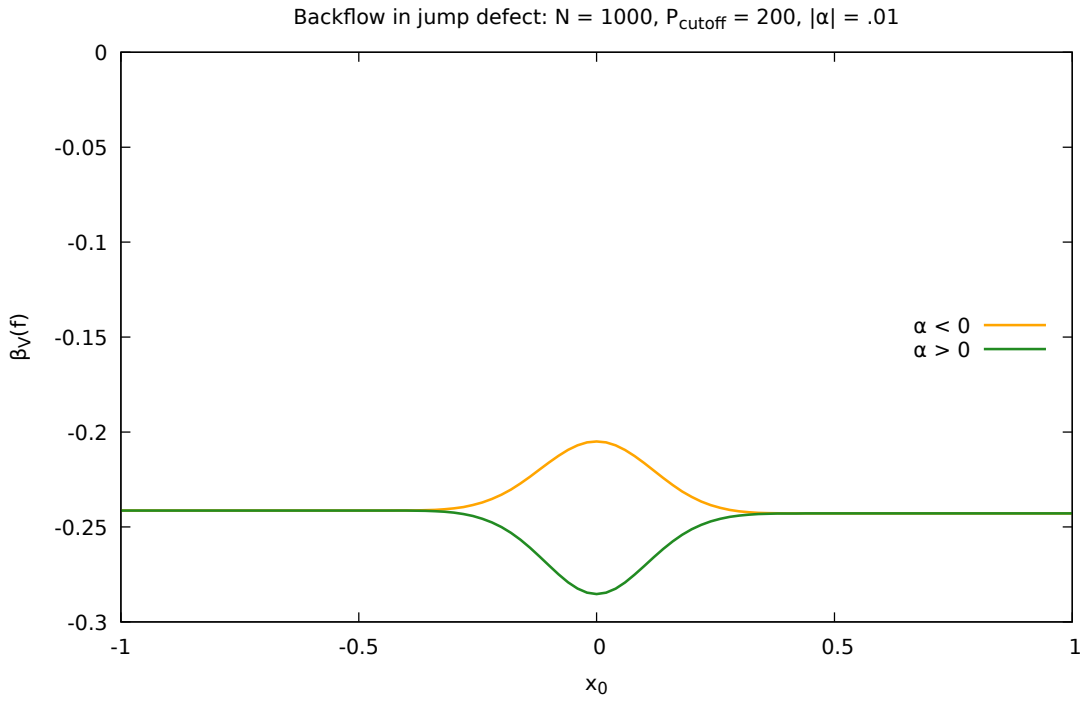

(a) Refer to Figure 4.2 (a) for the exact calculation

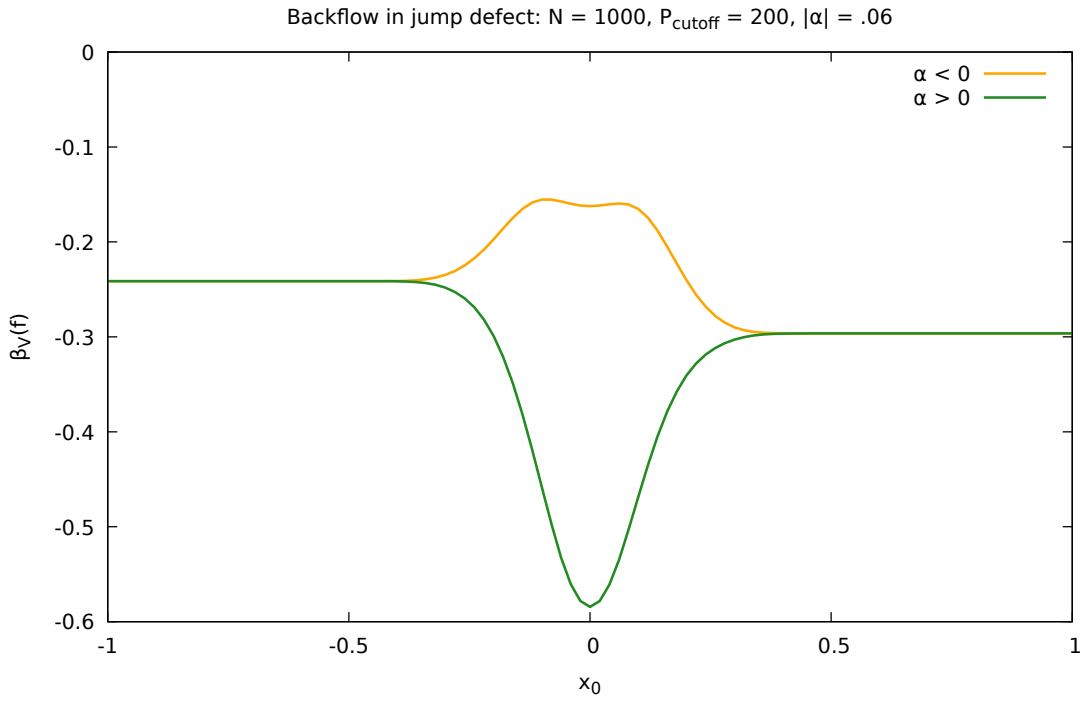

(b) Refer to Figure 4.3 (a) for the exact calculation

Figure 5.5: First order approximation - Lowest backflow eigenvalue of the conserved current operator, for which (a) $|\alpha| = 0.01$ (b) $|\alpha| = 0.05$.

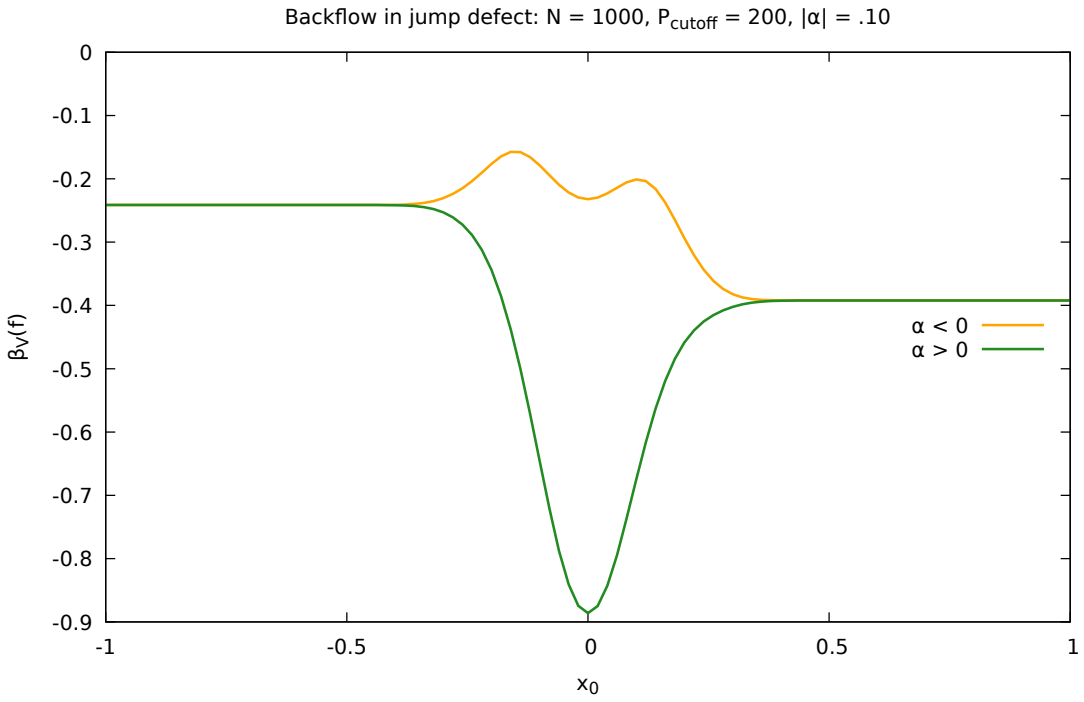

(a) Refer to Figure 4.3 (b) for the exact calculation

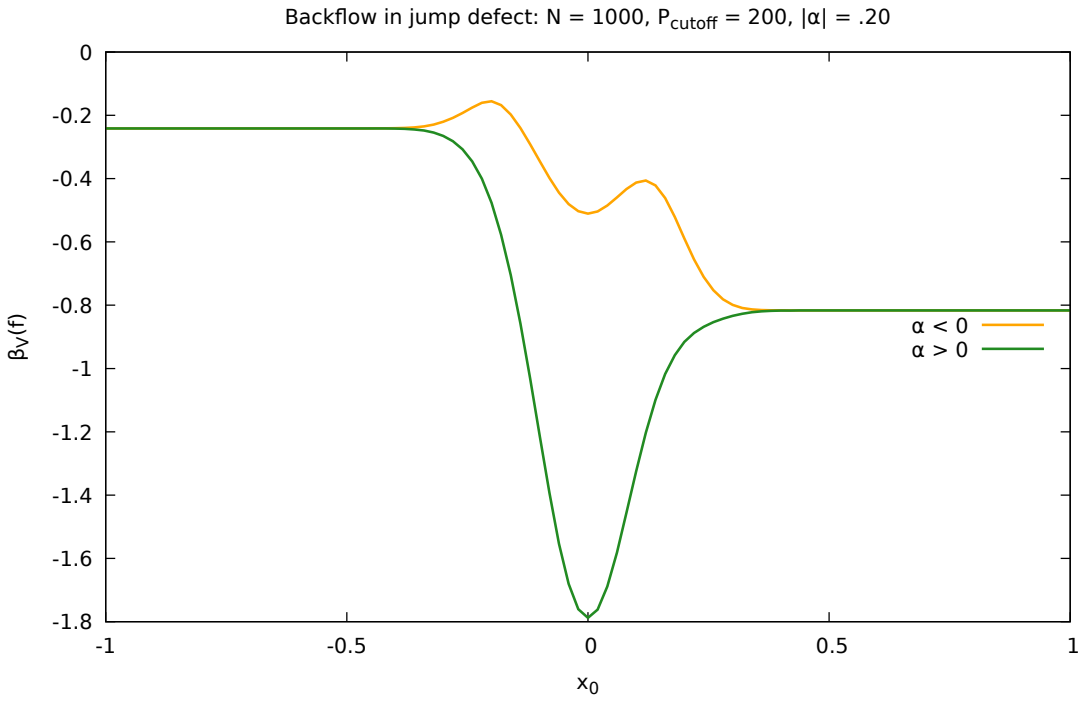

(b) Refer to Figure 4.4 (a) for the exact calculation

Figure 5.6: First order approximation - Lowest backflow eigenvalue of the conserved current operator, for which (a) $|\alpha| = 0.01$ (b) $|\alpha| = 0.05$.

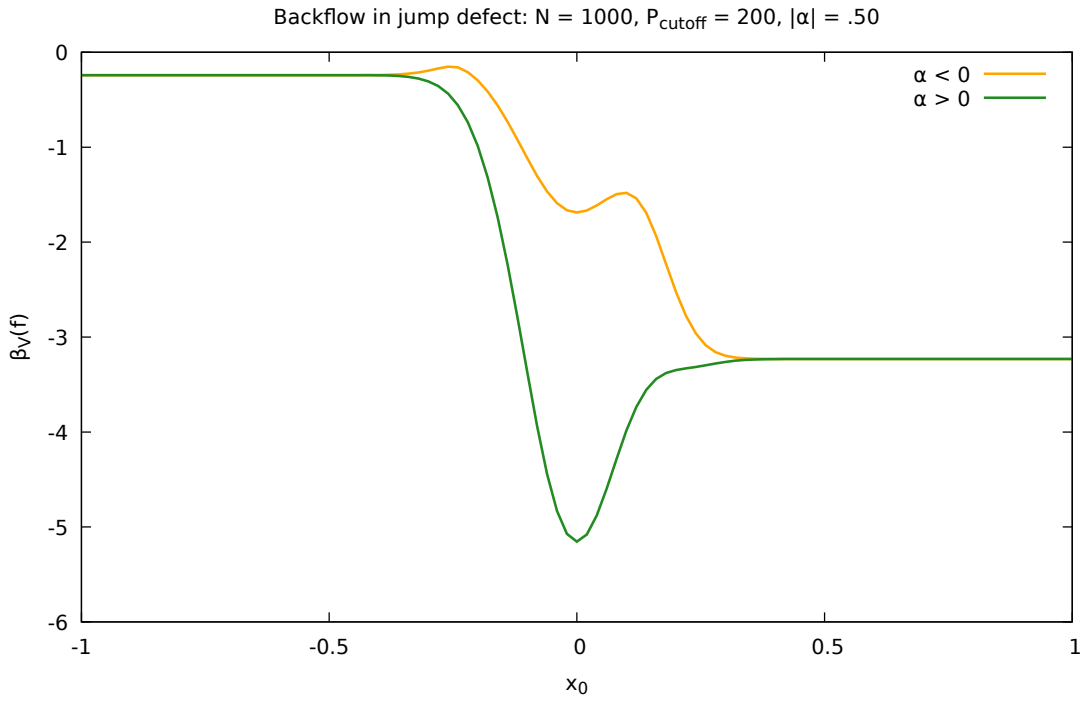

(a) Refer to Figure 4.4 (b) for the exact calculation

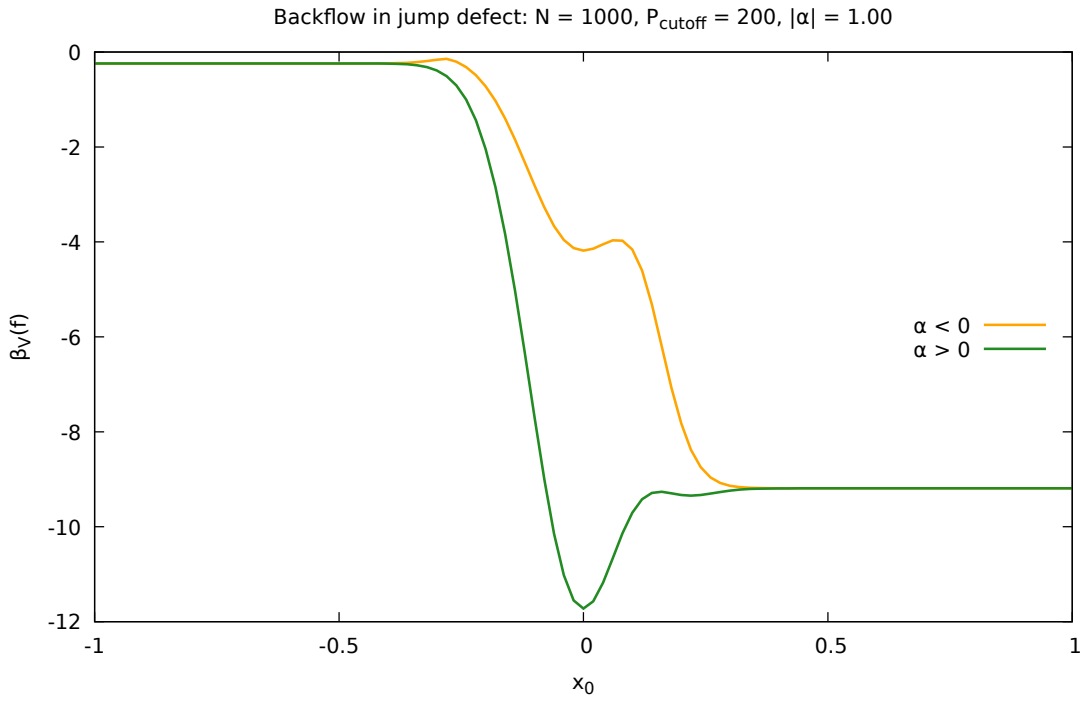

(b) Refer to Figure 4.5 (a) for the exact calculation

Figure 5.7: First order approximation - Lowest backflow eigenvalue of the conserved current operator, for which (a) $|\alpha| = 0.5$ (b) $|\alpha| = 1.0$.

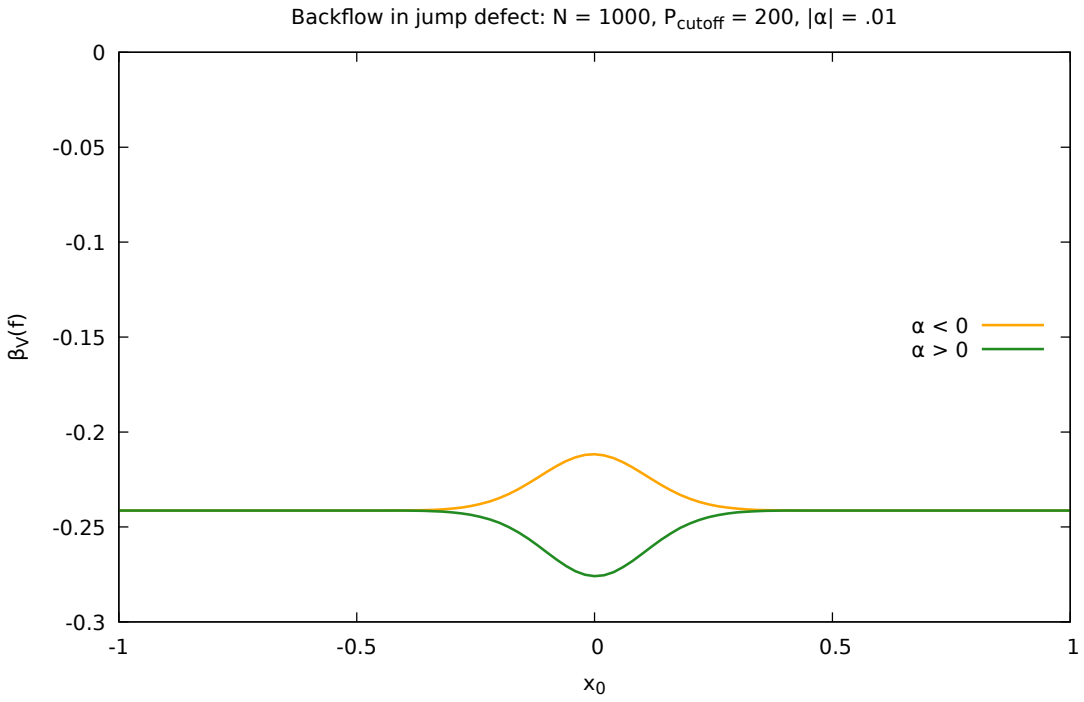

(a)

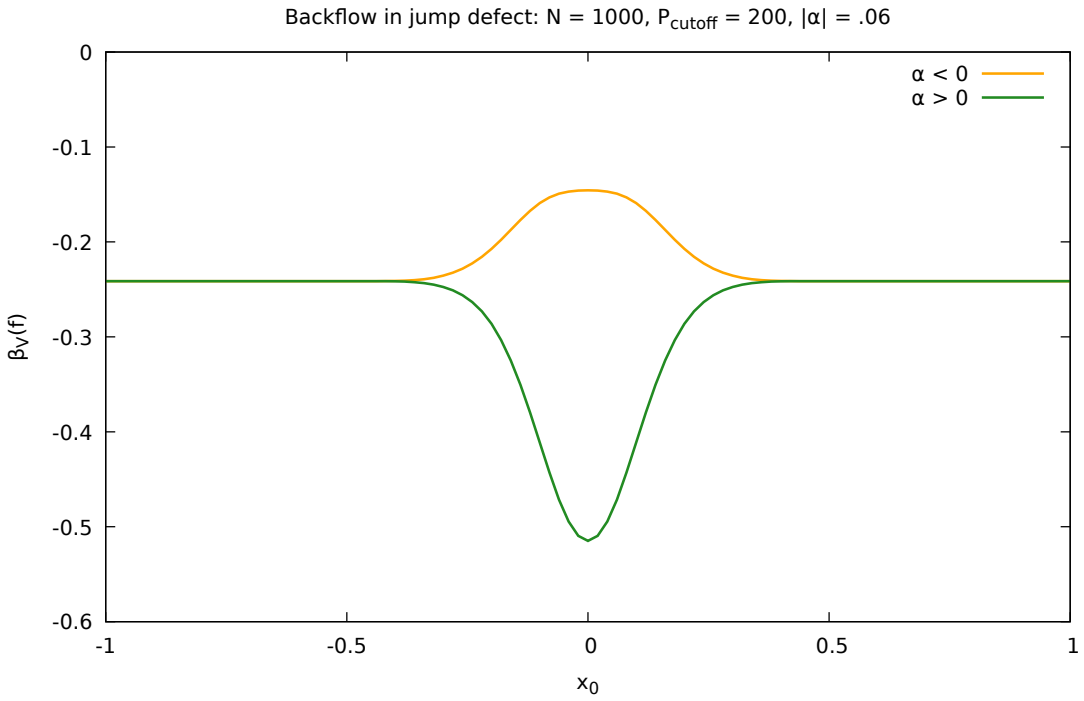

(b)

Figure 5.8: First order approximation - defect contribution to the lowest backflow eigenvalue of the conserved current operator, for which (a) $|\alpha| = 0.01$ (b) $|\alpha| = 0.05$.

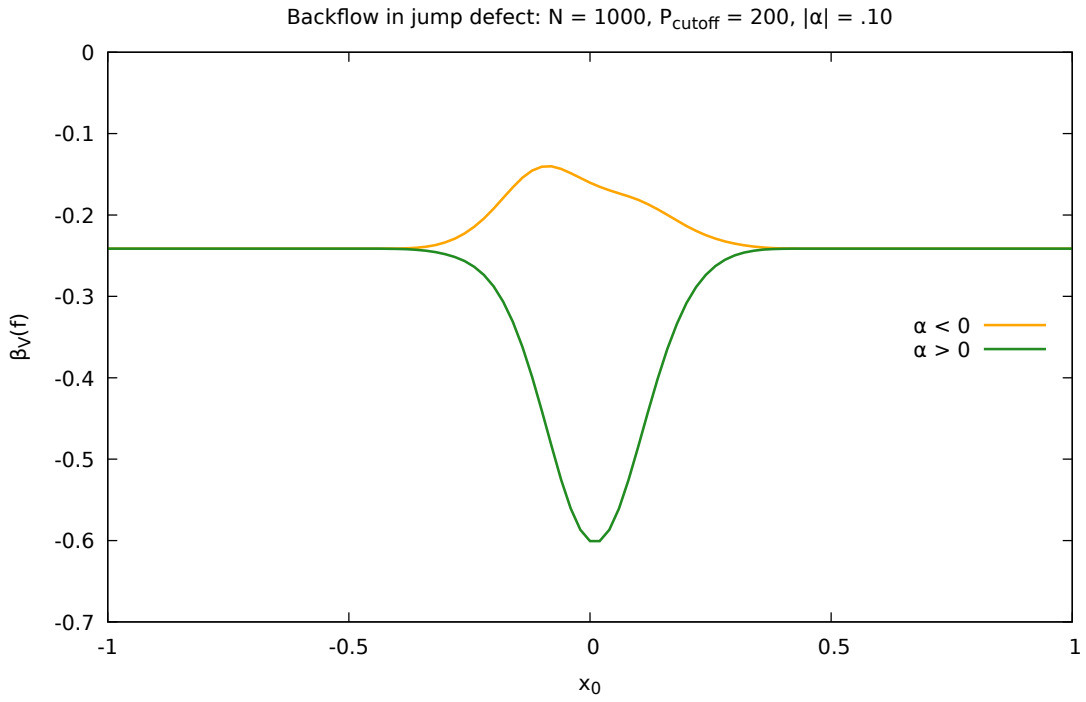

(a)

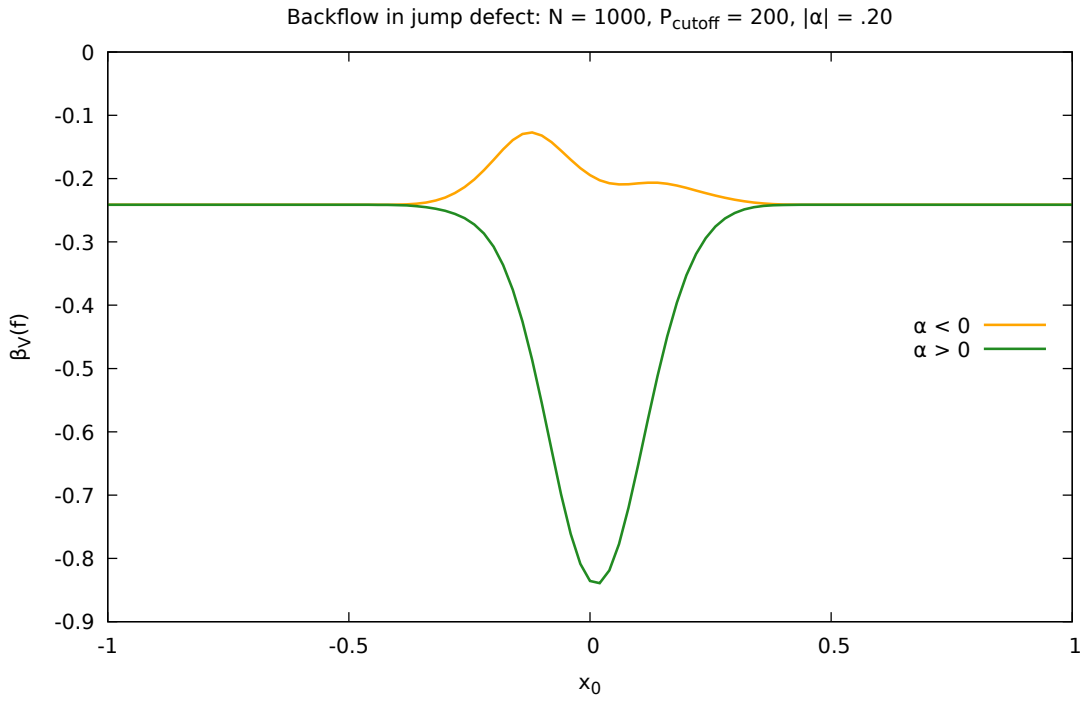

(b)

Figure 5.9: First order approximation - defect contribution to the lowest backflow eigenvalue of the conserved current operator, for which (a) $|\alpha| = 0.1$ (b) $|\alpha| = 0.2$.

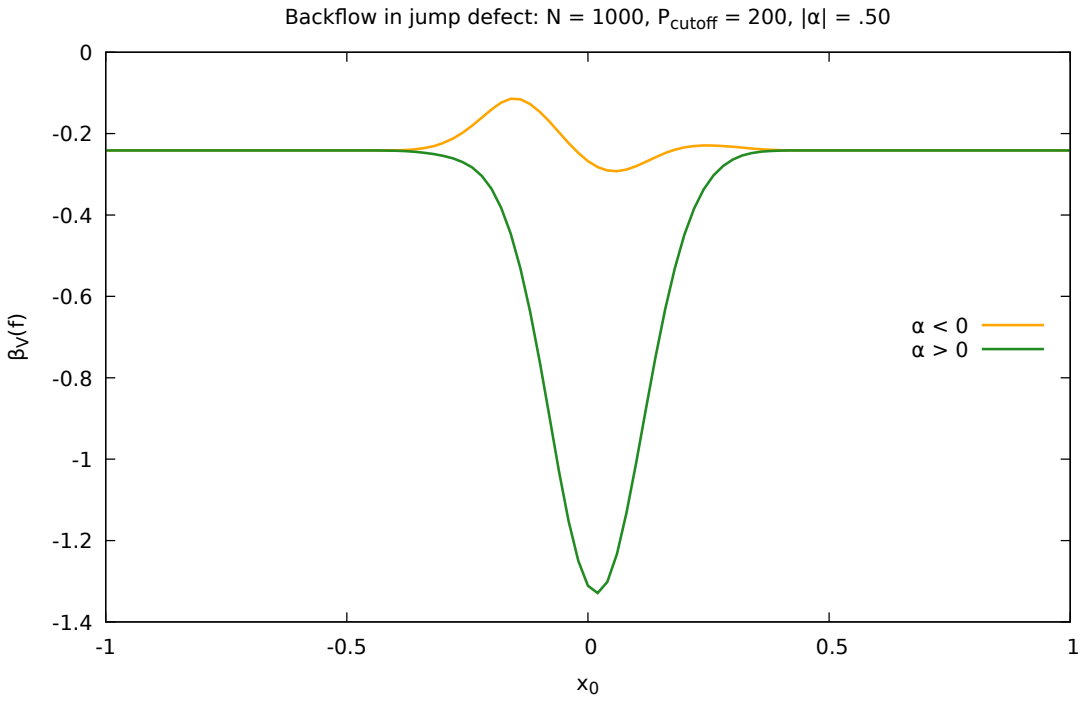

(a)

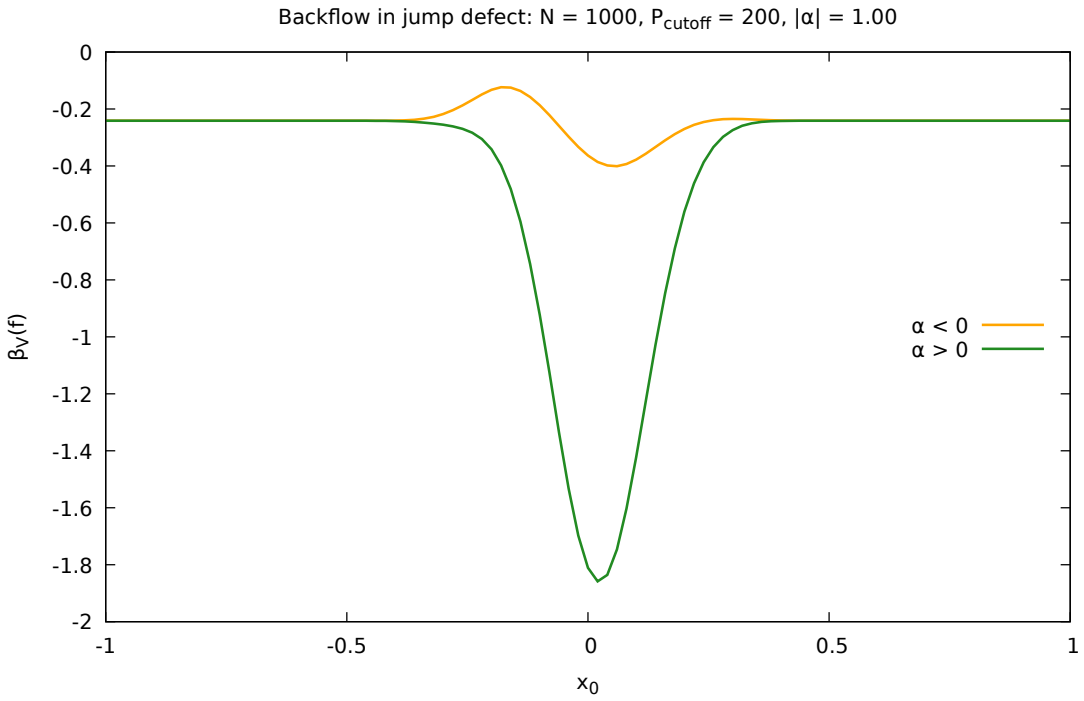

(b)

Figure 5.10: First order approximation - defect contribution to the lowest backflow eigenvalue of the conserved current operator, for which (a) $|\alpha| = 0.5$ (b) $|\alpha| = 1.0$.

— 6 —

Backflow and defects for the Dirac equation

When the quantum backflow effect was first discussed in Chapter 2, the discussion was restricted to situations described by the Schrödinger equation. After that, in Chapter 3 we considered the backflow in the presence of δ-defects, but again without including the spin of the particles. Here we devote the discussion to situations described by the Dirac equation. The free case was firstly and previously considered in [10], and we extend that introducing interactions with the view that a point interaction can be defined by a set of sewing conditions at that point. In particular, we discuss the introduction of a point defect in the Dirac equation, a first-order differential equation, how the conservation laws are modified and the quantum backflow effect.

6.1 INTRODUCING A δ-DEFECT

The δ-defect in the Dirac equation was previously studied in the context of solid-state physics as the relativistic Kronig-Penney model, see [150] and references therein. However, the presence of discontinuities lead to confusion and incorrect results in the literature [151]. This section presents a brief summary of the Dirac equation and review the proper treatment of a δ-defect in the one-dimensional Dirac equation. We consider Dirac particles in one dimension and start from the interaction-free case. For the quantum mechanical interpretation of the theory, we need a Hilbert space to accommodate the action of 2x2-matrix differential operators. These operators act on $\mathbb{C}^2$-valued functions of $x \in \mathbb{R}$. We take the Hilbert space $\mathcal{H} = L^2(\mathbb{R})^2 = L^2(\mathbb{R}) \otimes \mathbb{C}^2$. Because now we have 2-component column vectors ψ, with complex valued functions ψ_i

as components, the inner product is

$$\langle \psi,\, \phi \rangle = \int_{\mathbb{R}} \sum_{i=1}^{2} \psi_i^{\star}(x)\phi_i(x)\, dx = \int_{\mathbb{R}} \psi^{\dagger}(x)\phi(x)dx. \tag{6.1}$$

The Dirac equation for a spinor ψ exhibits its relativistic covariance properties when it takes the form

$$(i\hbar\gamma^{\mu}\partial_{\mu} - mc)\psi(x) = 0, \tag{6.2}$$

for a particle of mass $m > 0$ and where the gamma γ^{μ} matrices obey the Clifford relations

$$\gamma^{\mu}\gamma^{\nu} + \gamma^{\nu}\gamma^{\mu} = 2g^{\mu\nu},$$

where the metric tensor $g^{\mu\nu}$ on $\mathbb{R}^{1,1}$ has signature $(+-)$, of the associated Clifford algebra $Cl_{1,1}(\mathbb{R})$. The Dirac equation can be written in terms of the Dirac adjoint $\bar{\psi} = \psi^{\dagger}\gamma^{0}$, associated to the fermionic anti-particle, as

$$i\hbar\partial_{\mu}\bar{\psi}\gamma^{\mu} + m\bar{\psi} = 0. \tag{6.3}$$

We continue adopting the choice of units such that, effectively, $\hbar = c = 1$. The free Dirac equation in $(1+1)$ dimensions, choosing the Dirac representation of the gamma matrices,

$$\gamma^{0} = \sigma_3, \quad \gamma^{1} = i\sigma_2,$$

in terms of the Hermitian Pauli matrices, reads

$$(i\sigma_3\partial_t - \sigma_2\partial_x - m)\psi(x) = 0, \tag{6.4}$$

which can be cast into a Hamiltonian form

$$i\partial_t\psi = (-i\sigma_1\partial_x + m\sigma_3)\psi.$$

Because it is the free Dirac equation, we call the matrix operator

$$H_0 = -i\sigma_1\partial_x + m\sigma_3 \tag{6.5}$$

the free Dirac Hamiltonian in the Hilbert space $\mathcal{H}$. H_0 is an Hermitian (symmetric) operator, and we also require it to be self-adjoint in order to have a unitary dynamics described by the time evolution operator $\exp(-iH_0t)$, which leaves the inner product

(6.1) invariant. Thus, by Stone's theorem, we have a well posed initial value problem in the Hilbert space $\mathcal{H}$. For that, one needs H_0 to be defined on a dense domain of $\mathcal{H}$, usually taken to be the space of test functions $C_0^\infty(\mathbb{R})^2$, where H_0 is essentially self-adjoint. From where one takes an extension that is self-adjoint on the Sobolev space $W^{1,2}(\mathbb{R})^2 = H^1(\mathbb{R})^2$, the space of all $\psi \in L^2(\mathbb{R})^2$ whose first order (distribution) derivatives belong to $L^2(\mathbb{R})^2$

$$H^1(\mathbb{R})^2 = \left\{\psi \in L^2(\mathbb{R})^2 |\ \partial\psi \in L^2(\mathbb{R})^2\right\}. \tag{6.6}$$

In particular, we have the following sequence of inclusions

$$C_0^\infty(\mathbb{R}^n) \subset H^1(\mathbb{R}^n) \subset L^2(\mathbb{R}^n).$$

Hence, a suitable domain of H_0 is

$$\mathcal{D}(H_0) = H^1(\mathbb{R})^2 \subset \mathcal{H}. \tag{6.7}$$

Although the present work is not focused on self-adjointness issues, it is important to stress that discontinuous wave functions naturally appear in boundary-value problems for differential operators, and Sobolev spaces, having a Hilbert space structure, can include these by considering relativistic point interactions in terms of wavefunctions in the Sobolev space $H^1(\mathbb{R} \setminus \{0\})^2$, that is, allowing a wavefunction to have a finite jump discontinuity at the origin. That is similar to the treatment given to discontinuous wavefunctions in the domain of Schrödinger operators. The key difference is that Schrödinger operators are second order in space derivatives, and Dirac operators are first order. Thus, the appropriate Sobolev space in the case of the Dirac equation is larger than the one required in the case of the Schrödinger equation. It is worth remarking that introducing a δ-defect in the Schrödinger equation does not cause a discontinuous wavefunction solution at the origin, and the weak and strong derivatives coincide in the sense explained in (3.6). From that perspective, introducing a δ-defect in the Dirac equation is more similar to the previous case of a discontinuous jump-defect, and the derivatives can also be understood in the strong sense for functions in the Sobolev space $H^1(\mathbb{R} \setminus \{0\})^2$, where the two notions of derivative coincide. Moreover, the analysis of conserved quantities will follow the previous procedure done in section 4.1.2, where the integrals can appropriately be split into left ($x < 0$) and right ($x > 0$) regions, and the fields u and v are evaluated at the origin in a limiting sense.

The Dirac operator H_0 is also commonly described in momentum space $L^2(\mathbb{R}, dp)^2$. The Fourier transformation

$$(\mathcal{F}\psi)(p) = \tilde{\psi}(p) = \frac{1}{\sqrt{2\pi}} \int \exp(-ipx)\psi(x)\, dx \tag{6.8}$$

and its inverse $\mathcal{F}^{-1}$ allow us to switch between the Hilbert spaces $L^2(\mathbb{R}, dp)^2$ and $L^2(\mathbb{R}, dx)^2$, transforming the matrix differential operator H_0 into a matrix multiplication operator in momentum space

$$(\mathcal{F}H_0\mathcal{F}^{-1})(p) = \begin{pmatrix} m & \hat{P} \\ \hat{P} & -m \end{pmatrix}, \tag{6.9}$$

with momentum operator $\hat{P} = -i\partial_x$. The eigenvalues of this Hermitian 2x2-matrix are $E = \pm\sqrt{p^2 + m^2}$, corresponding to the positive and negative energy frequencies. From this free theory, we consider the perturbation of the self-adjoint Hamiltonian by introducing an interaction at a point of the real line.

There are a couple of ways to introduce an external potential in the Dirac equation: an "electrostatic" potential or a "mass-like" potential, for example. More generally, the external potential can be expressed [152] as a combination

$$V(x) = V_0(x)\mathbb{1} + V_1(x)\sigma_1 + V_2(x)\sigma_3 + V_3(x)\sigma_1\sigma_3,$$

which will be simplified here by taking $V_3 = 0$ and further reduced to a simpler linear combination of the identity matrix and σ_3 only

$$V(x) = V_e(x)\mathbb{1} + V_m(x)\sigma_3,$$

based on considerations of gauge symmetry: the potential is a function of the position only, and V_1 can be removed by a gauge transformation of the spinor ψ. We used the terms V_e and V_m to emphasize their physical significance as a electrostatic term and mass-like term, respectively. Let us introduce an electrostatic potential function V into the Dirac equation, we write

$$(i\partial_t - V)\psi = (-i\sigma_1\partial_x + \sigma_3 m)\psi, \tag{6.10}$$

and we take $V(x) = \lambda\delta(x)\mathbb{1}$, corresponding to the electrostatic Dirac potential function, namely a δ-defect located at the origin with real parameter λ that will be called δ_e-defect.

The usual procedure of integrating both sides of the equation, as it is done in the Schrödinger equation, is followed

$$-i\sigma_1\int_{-\varepsilon}^{\varepsilon}\psi_x dx+\sigma_3 m\int_{-\varepsilon}^{\varepsilon}\psi dx=\int_{-\varepsilon}^{\varepsilon}E\psi dx-\lambda\int_{-\varepsilon}^{\varepsilon}\delta(x)\psi(x)dx, \tag{6.11}$$

and we take the limit $\varepsilon\to 0$ to consider the integration in the neighbourhood of the defect's location at $x=0$

$$-i\sigma_1(\psi(0^+)-\psi(0^-))=-\lambda\int_{-\varepsilon}^{\varepsilon}\delta(x)\psi(x)dx. \tag{6.12}$$

An important difference from the same situation in the case of a Schrödinger equation being integrated over the range $(-\varepsilon,\varepsilon)$ is that the solution ψ to the Dirac equation, in the presence of a δ potential function, is discontinuous. The ψ-discontinuity does not allow one to take the common arbitrary choice of using the mean value as

$$\int_{-\varepsilon}^{\varepsilon}\delta(x)\psi(x)dx=\frac{1}{2}(\psi(0^+)+\psi(0^-)), \tag{6.13}$$

which is a wrong choice. That integral expression is equivalent to use that $\delta(x)\theta(x)=(1/2)\delta(x)$, taking $\theta(0)=1/2$. However, the product $\delta(x)\theta(x)$ is ill-defined accordingly to the Hörmander's criterion [153] on the product of distributions. In a nutshell, the criterion requires that, given two distributions for which a product may be defined, the sum of the two wave front sets does not intersect the zero section, that is, their sum cannot contain zero covectors. In particular, these two distributions share the same singular support ($x=0$), both the $\delta(x)$ and the $\theta(x)$ have the same wave front set ($WF(\theta)=WF(\delta)=\{(0,k),k\neq 0\}$) and, therefore, Hörmander's criterion fails. Moreover, even if their product can be defined by other means, it may be that the Leibniz rule fails. Instead, as presented in [151, 154], one needs to make sure that the differential equation is respected. For that, we take a particular model for the δ in the sense that it has the same properties of the δ in a suitable limiting process such as the limit of the rectangular pulses

$$\delta(x)=\lim_{\varepsilon\to 0}\left(\frac{1-\theta(|x|-\varepsilon)}{2\varepsilon}\right), \tag{6.14}$$

with positive ε. In fact, any other choice of function, as the Gaussian, for example, will lead to the same result, and the limit is independent of the particular model chosen.

Back to the equation (6.11), it simplifies to

$$\lim_{\varepsilon\to 0}\int_{-\varepsilon}^{\varepsilon}\left[-i\begin{pmatrix}0&1\\1&0\end{pmatrix}\begin{pmatrix}\psi_1\\\psi_2\end{pmatrix}_x+\left(\frac{\lambda}{2\varepsilon}\right)\begin{pmatrix}\psi_1\\\psi_2\end{pmatrix}\right]dx=0, \tag{6.15}$$

and the first-order matrix differential equation

$$\begin{pmatrix}\psi_1\\\psi_2\end{pmatrix}_x=-\frac{i\lambda}{2\varepsilon}\begin{pmatrix}0&1\\1&0\end{pmatrix}\begin{pmatrix}\psi_1\\\psi_2\end{pmatrix}, \tag{6.16}$$

valid for $-\varepsilon<x<\varepsilon$, has the following solution

$$\begin{pmatrix}\psi_1\\\psi_2\end{pmatrix}=\exp\left(-\frac{i\lambda x}{2\varepsilon}\sigma_1\right)\begin{pmatrix}\eta_1\\\eta_2\end{pmatrix}, \tag{6.17}$$

with η_1 and η_2 constants. The continuity of the solution at $x=-\varepsilon$

$$\begin{pmatrix}\psi_1(-\varepsilon)\\\psi_2(-\varepsilon)\end{pmatrix}=\exp\left(\frac{i\lambda\sigma_1}{2}\right)\begin{pmatrix}\eta_1\\\eta_2\end{pmatrix}, \tag{6.18}$$

and the continuity of the solution at $x=\varepsilon$

$$\begin{pmatrix}\psi_1(+\varepsilon)\\\psi_2(+\varepsilon)\end{pmatrix}=\exp\left(-\frac{i\lambda\sigma_1}{2}\right)\begin{pmatrix}\eta_1\\\eta_2\end{pmatrix}, \tag{6.19}$$

and taking the appropriate limit ($\varepsilon\to 0$), allow us to relate the solution at the left of the real interval $(-\varepsilon,\varepsilon)$, that is for $x<-\varepsilon$, to its right side $x>\varepsilon$. For that, we remember the result

$$e^{i\alpha\sigma_k}=(\cos\alpha)\mathbb{1}+i(\sin\alpha)\sigma_k, \tag{6.20}$$

where α is a complex number and σ_k is any one of the three Pauli matrices, and rewrite the left continuity condition as

$$\begin{pmatrix}\psi_1(0^-)\\\psi_2(0^-)\end{pmatrix}=\left[\cos\left(\frac{\lambda}{2}\right)\mathbb{1}+i\sin\left(\frac{\lambda}{2}\right)\sigma_1\right]\begin{pmatrix}\eta_1\\\eta_2\end{pmatrix}, \tag{6.21}$$

and the right continuity condition as

$$\begin{pmatrix}\psi_1(0^+)\\\psi_2(0^+)\end{pmatrix}=\left[\cos\left(\frac{\lambda}{2}\right)\mathbb{1}-i\sin\left(\frac{\lambda}{2}\right)\sigma_1\right]\begin{pmatrix}\eta_1\\\eta_2\end{pmatrix}. \tag{6.22}$$

From these expressions (6.21) and (6.22), it follows that

$$\begin{pmatrix}\psi_1(0^+)\\ \psi_2(0^+)\end{pmatrix} = \begin{pmatrix}\cos\lambda & -i\sin\lambda\\ -i\sin\lambda & \cos\lambda\end{pmatrix}\begin{pmatrix}\psi_1(0^-)\\ \psi_2(0^-)\end{pmatrix}, \tag{6.23}$$

the sewing condition for a δ-defect relating the solutions at the left of the defect's location ($x = 0$) and at the right of it.

We want to analyse the scattering of a positive energy electron in the presence of a δ_e-defect. For that, we restrict our analysis to the one-particle theory of the Dirac equation and work with the positive energy monochromatic plane wave solution of the free Dirac equation

$$\Phi_k(x,t) = \begin{pmatrix}\phi_1(k)\\ \phi_2(k)\end{pmatrix} e^{i(kx-Et)}, \tag{6.24}$$

meaning that $E = \sqrt{k^2+m^2}$. In components, the Dirac equation splits into

$$\begin{aligned}(\psi_1)_t &= -(\psi_2)_x - im\psi_1,\\ (\psi_2)_t &= -(\psi_1)_x + im\psi_2,\end{aligned} \tag{6.25}$$

from where the following relation, using that $k^2 = E^2 - m^2$, holds true for the plane wave solution (6.24)

$$\phi_1 = \frac{ik}{i(E-m)}\phi_2 = \frac{k(E+m)}{(E^2-m^2)}\phi_2 = \frac{(E+m)}{k}\phi_2. \tag{6.26}$$

One possible choice is to take

$$\Phi_k(x,t) = e^{-iEt}\Phi_k(x) = \begin{pmatrix}m+E\\ k\end{pmatrix} e^{i(kx-Et)}. \tag{6.27}$$

A free particle wave packet solution $\psi \in L^2(\mathbb{R})\otimes\mathbb{C}^2$ with positive energy can be constructed

$$\psi(x,t) = \frac{1}{\sqrt{2\pi}}\int_{-\infty}^{\infty} dk \frac{\tilde{g}(k)}{\sqrt{2E(E+m)}}\exp(-iEt)\Phi_k(x), \tag{6.28}$$

with $\tilde{g} \in C_0^\infty(\mathbb{R})$ an arbitrary non-zero smoothly varying function normalized by

$$\int_{-\infty}^{\infty} dk\ \tilde{g}^\star(k)\tilde{g}(k) = 1, \tag{6.29}$$

and $\left(\sqrt{2E(E+m)}\right)^{-1}$ is a convenient normalization factor. When convenient, we will write it in terms of a function $\mathbb{E}$ and denote $\mathbb{E}(k) = \sqrt{2E(k)(E(k)+m)}$.

Having the backflow analysis in mind, we are interested in considering the Dirac δ_e-defect in a scattering situation described as follows. An incoming particle, with positive momentum, comes from the left of the δ_e-defect and scatters off at the defect's position. In the stationary picture of the scattering theory, we consider the solutions $x \mapsto \varphi_k(x)$ with $k > 0$, and the asymptotics described by the functions u_k and v_k. Specifically, we denote the full solution at the left of the defect by u and at the right by v, exactly as before when considering the Scrödinger equation. The time-independent scattering states are then

$$\varphi_k(x) = \begin{cases} u_k(x) &= \begin{pmatrix} m+E \\ k \end{pmatrix} \exp(ikx) + \begin{pmatrix} m+E \\ -k \end{pmatrix} R(k) \exp(-ikx), \quad x < 0 \\ \\ v_k(x) &= \begin{pmatrix} m+E \\ k \end{pmatrix} T(k) \exp(ikx), \quad x > 0, \end{cases} \tag{6.30}$$

where $R(k)$ and $T(k)$ are the reflection and the transmission coefficients for the δ_e-defect located at the origin. They were not specified yet. By using the sewing condition (6.23) together with the solution (6.30), we can obtain these coefficients from the relation

$$T(k) \begin{pmatrix} m+E \\ k \end{pmatrix} \exp(ikx - Et)\Big|_{x=0} = \begin{pmatrix} \cos\lambda & -i\sin\lambda \\ -i\sin\lambda & \cos\lambda \end{pmatrix} u_k(x,t)\Big|_{x=0}. \tag{6.31}$$

Because the time-dependence is the same for the entire equation, it simplifies to

$$T(k) \begin{pmatrix} m+E \\ k \end{pmatrix} = \begin{pmatrix} \cos\lambda & -i\sin\lambda \\ -i\sin\lambda & \cos\lambda \end{pmatrix} \left[\begin{pmatrix} m+E \\ k \end{pmatrix} + \begin{pmatrix} m+E \\ -k \end{pmatrix} R(k) \right], \tag{6.32}$$

which can equivalently be written as

$$R(k) \begin{pmatrix} m+E \\ -k \end{pmatrix} = \left[T(k) \begin{pmatrix} \cos\lambda & i\sin\lambda \\ i\sin\lambda & \cos\lambda \end{pmatrix} - 1 \right] \begin{pmatrix} m+E \\ k \end{pmatrix}. \tag{6.33}$$

Equation (6.32) splits, after rearrangement, into two relations denoted by

$$(m+E)T(k) = (m+E)(1+R(k))\cos\lambda - ik(1-R(k))\sin\lambda, \tag{6.34}$$

$$kT(k) = -i(m+E)(1+R(k))\sin\lambda + k(1-R(k))\cos\lambda. \tag{6.35}$$

Isolating $R(k)$ from (6.34) and substituting into (6.35) gives the transmission coefficient

$$T(k) = \frac{k}{k\cos\lambda + iE\sin\lambda}. \tag{6.36}$$

For the reflection coefficient $R(k)$, substitute the transmission coefficient $T(k)$ back into the (6.33), for example, to obtain

$$R(k) = -\frac{im\sin\lambda}{k\cos\lambda + iE\sin\lambda}. \tag{6.37}$$

Note, in particular, these are related by

$$|R(k)|^2 + |T(k)|^2 = 1, \tag{6.38}$$

which will ensure the conservation of probability.

A wave packet solution, taking into account the presence of a δ_e-defect at the origin, $\psi \in H^1(\mathbb{R}\setminus\{0\}) \otimes \mathbb{C}^2 \subset \mathcal{H} = L^2(\mathbb{R}) \otimes \mathbb{C}^2$ with positive energy can be constructed by

$$\psi(x,t) = \frac{1}{\sqrt{2\pi}} \int_0^\infty dk \frac{\tilde{g}(k)}{\sqrt{2E(E+m)}} \exp(-iEt)\varphi_k(x), \tag{6.39}$$

with scattering states φ_k determined by (6.30) and $\tilde{g}$, an arbitrary non-zero smoothly varying function, normalized by

$$\int_0^\infty dk\ \tilde{g}^\star(k)\tilde{g}(k) = 1, \tag{6.40}$$

together with the sewing condition (6.23) relating the right solution to the left solution

$$\begin{aligned} v_1(0^+) &= \cos\lambda\ u_1(0^-) - i\sin\lambda\ u_2(0^-), \\ v_2(0^+) &= -i\sin\lambda\ u_1(0^-) + \cos\lambda\ u_2(0^-), \end{aligned}$$

where u_i (v_i) denotes the two components of u (v) for $i = 1, 2$. As in the previous Schrödinger case, the Hamiltonian for the Dirac equation, with deficiency indices $(2, 2)$, has a four-parameter family of self-adjoint extensions [155] that are represented by sets of sewing conditions. A defect connects the field u in the left region $x < 0$ to the field v in the right region $x > 0$ by the sewing conditions at the defect's location.

6.2 CONSERVATION LAWS FOR THE δ-DEFECT

In the section 4.1.2, when we discussed the presence of defects in the Schrödinger equation, we checked how a point-defect can modify the conservation laws by means of using their sewing conditions. Here again we analyse some conserved quantities of physical importance after the introduction of a δ-defect, but in the case of a system described by the Dirac equation. In particular, the δ_e-defect, defined in (6.10) with $V(x) = \lambda\delta(x)\mathbb{1}$, will be used as a calculation model in this section, but the analysis is essentially the same for a mass-like δ-defect or any combination of them, for instance.

Starting with the total contribution of the fields to the probability

$$N = \int \psi^\dagger \psi \, dx. \tag{6.41}$$

For checking whether it is conserved, we take its time derivative

$$\begin{aligned} N_t &= \int (\psi_t^\dagger \psi + \psi^\dagger \psi_t) dx \\ &= \int \left(-\psi_x^\dagger \sigma_1 \psi + im\psi^\dagger \sigma_3 \psi - \psi^\dagger \sigma_1 \psi_x - im\psi^\dagger \sigma_3 \psi \right) dx \\ &= \int \left(-(\psi^\dagger \sigma_1 \psi)_x \right) dx \\ &= \int_{-\infty}^{0} -(u^\dagger \sigma_1 u)_x dx + \int_0^{\infty} -(v^\dagger \sigma_1 v)_x dx \\ &= -(u^\dagger \sigma_1 u)|_{x=0} + (v^\dagger \sigma_1 v)|_{x=0}, \end{aligned} \tag{6.42}$$

where we used the Dirac equation and ignored the zero contributions at infinities. Now we can make use the sewing condition (6.23) to obtain

$$\begin{aligned} N_t &= \left[-v^\dagger \begin{pmatrix} \cos\lambda & i\sin\lambda \\ i\sin\lambda & \cos\lambda \end{pmatrix} \begin{pmatrix} 0 & 1 \\ 1 & 0 \end{pmatrix} \begin{pmatrix} \cos\lambda & -i\sin\lambda \\ -i\sin\lambda & \cos\lambda \end{pmatrix} v + v^\dagger \sigma_1 v \right]_{x=0} \\ &= 0. \end{aligned} \tag{6.43}$$

Thus, the total probability N (or electric charge) is conserved without any adjustment.

The second quantity we analyse is the energy. The total contribution of the fields to the energy is given by

$$E = \int \frac{i}{2} \left(\psi^\dagger \psi_t - \psi_t^\dagger \psi \right) dx. \tag{6.44}$$

To examine its conservation, we consider

$$E_t = \int \frac{i}{2}\left(\psi_t^\dagger\psi_t + \psi^\dagger\psi_{tt} - \psi_{tt}^\dagger\psi - \psi_t^\dagger\psi_t\right) dx \tag{6.45}$$

and use the Dirac equation as

$$\begin{aligned} E_t = \int \frac{i}{2}\big[&(-\psi_x^\dagger\sigma_1 + im\psi^\dagger\sigma_3)(-\sigma_1\psi_x - im\sigma_3\psi) + \psi^\dagger(-\sigma_1\psi_x - im\sigma_3\psi)_t \\ &- (-\psi_x^\dagger\sigma_1 + im\psi^\dagger\sigma_3)(-\sigma_1\psi_x - im\sigma_3\psi) - (-\psi_x^\dagger\sigma_1 + im\psi^\dagger\sigma_3)_t\psi\big]\, dx, \end{aligned}$$

and use it once again to write that in terms of spatial derivatives

$$\begin{aligned} E_t &= \int \frac{i}{2}\left[\partial_x\left(\psi^\dagger\psi_x - \psi_x^\dagger\psi\right) + im\partial_x(\psi^\dagger\sigma_1\sigma_3\psi) + im\partial_x(\psi^\dagger\sigma_3\sigma_1\psi)\right] dx \\ &= \frac{i}{2}\int_{-\infty}^{0}\partial_x\left(u^\dagger u_x - u_x^\dagger u\right) dx + \frac{i}{2}\int_0^\infty \partial_x\left(v^\dagger v_x - v_x^\dagger v\right) dx \\ &= \frac{i}{2}\left[u^\dagger u_x - u_x^\dagger u\right]_{x=0} - \frac{i}{2}\left[v^\dagger v_x - v_x^\dagger v\right]_{x=0}, \end{aligned}$$

ignoring the zero contributions at infinities. Now we use the sewing condition (6.23) to rewrite the previous expression

$$E_t = \frac{i}{2}\left[v^\dagger\left(\begin{pmatrix}\cos\lambda & i\sin\lambda\\ i\sin\lambda & \cos\lambda\end{pmatrix}u_x - v_x\right) - \left(u_x^\dagger\begin{pmatrix}\cos\lambda & -i\sin\lambda\\ -i\sin\lambda & \cos\lambda\end{pmatrix} - v_x^\dagger\right)v\right]_{x=0}$$

and use again the Dirac equation to substitute u_x and v_x as

$$\begin{aligned} E_t = \frac{i}{2}\Bigg[v^\dagger\Bigg(&-\begin{pmatrix}\cos\lambda & i\sin\lambda\\ i\sin\lambda & \cos\lambda\end{pmatrix}\begin{pmatrix}0 & 1\\ 1 & 0\end{pmatrix}u_t - m\begin{pmatrix}\cos\lambda & i\sin\lambda\\ i\sin\lambda & \cos\lambda\end{pmatrix}\begin{pmatrix}0 & -i\\ i & 0\end{pmatrix}u\Bigg) \\ &- \Bigg(\left(-u_t^\dagger\sigma_1 - mu^\dagger\sigma_2\right)\begin{pmatrix}\cos\lambda & -i\sin\lambda\\ -i\sin\lambda & \cos\lambda\end{pmatrix}v + v_t^\dagger\sigma_1 v + mv^\dagger\sigma_2 v\Bigg) \\ &+ v^\dagger\sigma_1 v_t + v^\dagger\sigma_1 v_t + mv^\dagger\sigma_2 v\Bigg]_{x=0}. \end{aligned} \tag{6.46}$$

Because the sewing relation

$$u(x,t)|_{x=0} = \begin{pmatrix}\cos\lambda & -i\sin\lambda\\ -i\sin\lambda & \cos\lambda\end{pmatrix}v(x,t)\Big|_{x=0}$$

holds true for all time t, we can finally obtain, after simplification, the result

$$\frac{dE}{dt} = 0.$$

Thus, the energy is conserved, as expected from a self-adjoint Hamiltonian.

Lastly, for the total contribution of the fields to the momentum, we know that

$$P = -\int_{-\infty}^{0} \frac{i}{2}\left(u^\dagger u_x - u_x^\dagger u\right) dx - \int_{0}^{\infty} \frac{i}{2}\left(v^\dagger v_x - v_x^\dagger v\right) dx, \tag{6.47}$$

and its time derivative

$$\begin{aligned} P_t = -\frac{i}{2}\int_{-\infty}^{0} &\left(u_t^\dagger u_x + u^\dagger u_{xt} - u_{xt}^\dagger u - u_x^\dagger u_t\right) \\ &- \frac{i}{2}\int_{0}^{\infty} \left(v_t^\dagger v_x + v^\dagger v_{xt} - v_{xt}^\dagger v - v_x^\dagger v_t\right). \end{aligned} \tag{6.48}$$

The Dirac equation can be used in each domain to write that as a total spatial derivative

$$\begin{aligned} P_t &= -\frac{i}{2}\int_{-\infty}^{0} \partial_x\left(u_x^\dagger \sigma_1 u - u^\dagger \sigma_1 u_x\right) - \frac{i}{2}\int_{0}^{\infty} \partial_x\left(v_x^\dagger \sigma_1 v - v^\dagger \sigma_1 v_x\right) \\ &= -\frac{i}{2}\left[u_x^\dagger \sigma_1 u - u^\dagger \sigma_1 u_x\right]_{x=0} + \frac{i}{2}\left[v_x^\dagger \sigma_1 v - v^\dagger \sigma_1 v_x\right]_{x=0}. \end{aligned} \tag{6.49}$$

The next step is to use the sewing condition (6.23) where possible

$$\begin{aligned} P_t = -\frac{i}{2}\Bigg[u_x^\dagger &\begin{pmatrix} -i\sin\lambda & \cos\lambda \\ \cos\lambda & -i\sin\lambda \end{pmatrix} v - v^\dagger \begin{pmatrix} i\sin\lambda & \cos\lambda \\ \cos\lambda & i\sin\lambda \end{pmatrix} u_x \\ &- v_x^\dagger \sigma_1 v + v^\dagger \sigma_1 v_x \Bigg]_{x=0}, \end{aligned} \tag{6.50}$$

and rewrite u_x and v_x in terms of u, v, u_t and v_t with the use of the Dirac equation. Note that the Dirac equation is not being used to relate u and v and, therefore, brings no incompatibility with the sewing condition. Thus,

$$\begin{aligned} P_t = -\frac{i}{2}\Bigg[u_t^\dagger \sigma_1 &\begin{pmatrix} -i\sin\lambda & \cos\lambda \\ \cos\lambda & -i\sin\lambda \end{pmatrix} v - m u^\dagger \sigma_2 \begin{pmatrix} -i\sin\lambda & \cos\lambda \\ \cos\lambda & -i\sin\lambda \end{pmatrix} v \\ &+ v^\dagger \begin{pmatrix} i\sin\lambda & \cos\lambda \\ \cos\lambda & i\sin\lambda \end{pmatrix} \sigma_1 u_t + m v^\dagger \begin{pmatrix} i\sin\lambda & \cos\lambda \\ \cos\lambda & i\sin\lambda \end{pmatrix} \sigma_2 u \\ &- v_t^\dagger v + m v^\dagger \sigma_2 \sigma_1 v - v^\dagger v_t - m v^\dagger \sigma_1 \sigma_2 v \Bigg]_{x=0}, \end{aligned} \tag{6.51}$$

and because the sewing condition holds true for all time t, we can relate u_t to v_t as follows

$$P_t = -\frac{i}{2}\left[v_t^\dagger \begin{pmatrix} 1-\cos\lambda & i\sin\lambda \\ i\sin\lambda & 1-\cos\lambda \end{pmatrix} v + v^\dagger \begin{pmatrix} \cos\lambda - 1 & i\sin\lambda \\ i\sin\lambda & \cos\lambda - 1 \end{pmatrix} v_t \right. \\ \left. + 2mv^\dagger \begin{pmatrix} i\cos(2\lambda) - i & \sin(2\lambda) \\ -\sin(2\lambda) & i - i\cos(2\lambda) \end{pmatrix} v \right]_{x=0}, \tag{6.52}$$

and notice that one is not able to write the result as a total time derivative. The same also happened when we tried to conserve the total momentum of a system described by a δ-defect in the Schrödinger equation in section 4.1.2. In fact, we expect that a defect breaks the spatial translation symmetry causing the total momentum not to be conserved. Moreover, in this case, it does not seem to allow an adjustment either.

6.3 BACKFLOW IN THE PRESENCE OF A δ-DEFECT

As a consequence of the Dirac equation (6.2) and (6.3), the conserved current is

$$j^\mu = \bar{\psi}\gamma^\mu\psi, \tag{6.53}$$

with continuity equation

$$\partial_t\rho + \partial_x j = 0, \tag{6.54}$$

where the non-negative 0-component is $j^0 = \rho = \psi^\dagger\psi$ and the probability current density j is denoted by

$$j_\psi(x,t) = \psi^\dagger(x,t)\sigma_1\psi(x,t) = \psi_1^\star(x,t)\psi_2(x,t) + \psi_2^\star(x,t)\psi_1(x,t), \tag{6.55}$$

where we have explicitly indicated the ψ-dependence. Our backflow analysis will concentrate on spatial averages, and we can leave the time-dependence out of discussion. As before, our probability current operator is constructed from the smearing with $\mathbb{R}$-supported positive test function f. Our expectation value of interest is

$$j_\psi(f) = \langle\psi,\, J(f)\psi\rangle = \int dx\, f(x)\, j_\psi(x)\,, \tag{6.56}$$

with the probability current operator, in terms of the position operator, given by

$$J(f) = f(\hat{X})\sigma_1 = \begin{pmatrix} 0 & f(\hat{X}) \\ f(\hat{X}) & 0 \end{pmatrix}, \tag{6.57}$$

a 2x2-matrix differential operator. Following the same idea presented in Chapter 2, the right-mover states are replaced by asymptotic right-movers in the scattering theory setting. The relation between the full solution ψ and the freely moving asymptotic right-moving incoming configuration Ψ is simply that

$$\psi \to \Psi, \quad t \to -\infty \, .$$

The correspondence is made by the Møller wave operator (2.15), i.e., $\Omega_V \Psi = \psi$. Let us write the incoming configuration in terms of (6.27) as

$$\Psi(x) = \frac{1}{\sqrt{2\pi}} \int_0^\infty dk \, \frac{\tilde{g}(k)}{\mathbb{E}(k)} \Phi_k(x). \tag{6.58}$$

Because of the inverse Fourier transformation, Ψ can be written in momentum space

$$(\mathcal{F}\Psi)(k) = \tilde{\Psi}(k) = \frac{\tilde{g}(k)}{\mathbb{E}(k)} \begin{pmatrix} E(k) + m \\ k \end{pmatrix}. \tag{6.59}$$

Moreover, the expression (6.39) is a result of applying the wave operator as follows

$$(\Omega_V E_+ \Psi)(x) = \frac{1}{\sqrt{2\pi}} \int_0^\infty dk \, \mathbb{M}_k(x) \tilde{\Psi}(k), \tag{6.60}$$

where the diagonal matrix $\mathbb{M}_k(x)$ is defined by

$$\mathbb{M}_k(x) = \begin{cases} \exp(ikx)\mathbb{1} + \sigma_3 R(k) \exp(-ikx), & x < 0 \\ T(k) \exp(ikx)\mathbb{1}, & x > 0 \end{cases} \tag{6.61}$$

We can now consider the expectation value of interest for the backflow. Similarly to (2.24), the expectation value of the probability current operator in terms of the asymptotic state Ψ is

$$\langle J_V(f) \rangle_\Psi \coloneqq \langle \Psi | \, E_+ \Omega_V^\dagger J(f) \Omega_V E_+ \, | \Psi \rangle \, , \tag{6.62}$$

with the positive momentum projection E_+ to ensure a right-moving incoming. In particular, the scattering state ψ shall be kept normalized, and the asymptotic incoming Ψ is normalized and a right-mover. This expectation value can be expressed, including the suitable normalization factors, in terms of integral kernel

$$\begin{aligned} \langle \Psi | \, J_V(f) \, | \Psi \rangle = \frac{1}{2\pi} \int_0^\infty dk \int_0^\infty dk' \int dx \int dx' \\ \times \tilde{\Psi}^\dagger(k') \left(\mathbb{M}_{k'}^\dagger(x') J(f)(x', x) \mathbb{M}_k(x) \right) \tilde{\Psi}(k), \end{aligned}$$

where the probability current integral kernel is

$$J(f)(x',x) = \delta(x'-x)\begin{pmatrix} 0 & f(x) \\ f(x) & 0 \end{pmatrix}. \tag{6.63}$$

Previously, when we analysed the quantum backflow effect in the Schrödinger equation in Chapter 3, our expectation value expression for the probability current operator was given by expression (2.35). Because we will focus here on the solvable δ_e-defect case, without recurring to the analytical perturbation theory, we do not need to make use of expansions and Green's functions. As we will not expand the plane wave solutions φ_k as power series terms, the expectation value is better written in a simplified manner after integrating out the Dirac delta

$$\langle\Psi|\, J_V(f)\,|\Psi\rangle = \frac{1}{2\pi}\int_0^\infty dk \int_0^\infty dk' \int dx\; f(x)\tilde{\Psi}^\dagger(k')\left(\mathbb{M}^\dagger_{k'}(x)\sigma_1\mathbb{M}_k(x)\right)\tilde{\Psi}(k). \tag{6.64}$$

Alternatively, that can also be expressed in the form

$$\begin{aligned}\langle\Psi|\, J_V(f)\,|\Psi\rangle = \frac{1}{2\pi}\int_0^\infty dk \int_0^\infty dk' \int dx\; f(x)\frac{\tilde{g}^\star(k')\tilde{g}(k)}{\mathbb{E}(k')\mathbb{E}(k)} \\ \times\begin{pmatrix} E(k')+m, & k' \end{pmatrix}\left(\mathbb{M}^\dagger_{k'}(x)\sigma_1\mathbb{M}_k(x)\right)\begin{pmatrix} E(k)+m \\ k \end{pmatrix}.\end{aligned} \tag{6.65}$$

The asymptotic backflow constant is given by the minimum eigenvalue of the probability current operator

$$\beta_V(f) = \frac{1}{2\pi}\int_0^\infty dk \int_0^\infty dk'\; \tilde{\mathcal{J}}^*(k')\tilde{\mathcal{J}}(k)L(k',k), \tag{6.66}$$

where the inner kernel reads

$$L(k',k) = \int \frac{dx\; f(x)}{\mathbb{E}(k')\mathbb{E}(k)}\begin{pmatrix} E(k')+m, & k' \end{pmatrix}\left(\mathbb{M}^\dagger_{k'}(x)\sigma_1\mathbb{M}_k(x)\right)\begin{pmatrix} E(k)+m \\ k \end{pmatrix}, \tag{6.67}$$

and, as before, we assume the existence of the wavefunction $\tilde{\mathcal{J}}(k)$ associated with the lowest eigenvector of the operator $J_V(f)$, but its analytical expression is currently unknown. We can, however, simplify the analytical expression of the inner kernel

$L(k',k)$ using the definition (6.61) of the matrix $\mathbb{M}$ to obtain the following

$$\begin{aligned}
L(k',k) = &\frac{(m+E(k'))k+(m+E(k))k'}{\mathbb{E}(k')\mathbb{E}(k)}\int_{-\infty}^{0} dx\ f(x)\exp(ix(k-k')) \\
&- \frac{(m+E(k'))k-(m+E(k))k'}{\mathbb{E}(k')\mathbb{E}(k)}R(k)\int_{-\infty}^{0} dx\ f(x)\exp(-ix(k+k')) \\
&+ \frac{(m+E(k'))k-(m+E(k))k'}{\mathbb{E}(k')\mathbb{E}(k)}R^{\star}(k')\int_{-\infty}^{0} dx\ f(x)\exp(ix(k+k')) \\
&- \frac{(m+E(k'))k+(m+E(k))k'}{\mathbb{E}(k')\mathbb{E}(k)}R^{\star}(k')R(k)\int_{-\infty}^{0} dx\ f(x)\exp(-ix(k-k')) \\
&+ \frac{(m+E(k'))k+(m+E(k))k'}{\mathbb{E}(k')\mathbb{E}(k)}T^{\star}(k')T(k)\int_{0}^{\infty} dx\ f(x)\exp(ix(k-k')),
\end{aligned} \tag{6.68}$$

where the transmission $T(k)$ and the reflection $R(k)$ factors are given by (6.36) and (6.37), respectively. This can be compared to the situation described by the Schrödinger equation in equation (3.9). The results are presented in the next section, where, for all practical numerical calculations, the mass will be effectively set to $m = 1$.

6.4 NUMERICAL RESULTS FOR THE δ_e-DEFECT

In [10], the authors showed that, in the interaction-free situation, the temporal extent of backflow for Dirac particles is smaller if compared to the same interaction-free situation in the non-relativistic Schrödinger equation. Our results show that the spatial average backflow for Dirac particles is also smaller if compared to the non-relativistic case. In particular, in the non-relativistic Schrödinger case, the asymptotic backflow constant is $\beta_0(f) \approx -0.24$ while, in the relativistic Dirac case, it is even smaller approaching the constant $\beta_0(f) \approx -0.02$. The results obtained in this section show quantitative and qualitative differences in the quantum backflow effect upon systems described by a δ-defect when considered in the Dirac equation in contrast to the equivalent situation, when considered in the the Schrödinger equation, of Chapter 3. Moreover, all the results in this section are concerned to the electrostatic δ_e-defect.

First, we note that one can not get rid of the backflow effect by any possible choice of the parameter λ. The lowest eigenvalue of the probability current can be very small at the right side ($x > 0$) of the defect, but it never hits zero. That is different from the results in section 3.2 where the lowest eigenvalue approaches zero very quickly when

$|\lambda|$ increases. This happens because the transmission coefficient (6.36) can never be zero and it is never purely reflecting. Second, the lowest eigenvalue is periodic in the parameter λ with period π coming from the periodicity of the reflection and transmission coefficients, as shown by figure 6.1. Third, considering $\lambda \in S^1$, there can be an electron bound states when the parameter is located in the second quadrant ($\pi/2 < \lambda < \pi$) and a bound state also in the fourth quadrant ($3\pi/2 < \lambda < 2\pi$). These can be seen from the purely imaginary positive poles $k = i\kappa$ of the transmission coefficient $T(k)$ with real $\kappa > 0$. The poles are given by $\kappa = -E\tan\lambda$, hence κ is only positive in the second and fourth quadrants, $\kappa = m\sin\lambda$ and $\kappa = -m\sin\lambda$, respectively. For the energies, $E = -m\cos\lambda$ in the second quadrant and $E = m\cos\lambda$ in the fourth one. It is exactly in these two regions where the backflow effect for negative values of the parameter is smaller (less negative) than for positive values of the parameter, with the negative parameter value determining the quadrant. For example, $-\pi/3$ is in the fourth quadrant, hence it has less backflow if compared to $\pi/3$. As for $-2\pi/3$, it is in the third quadrant and does not have less backflow than $2\pi/3$, see figure 6.1. This was the behaviour encountered in section 3.2, where positive parameters λ are associated with repulsive interactions and negative λ are associated with attractive interactions. Moreover, the values $|\lambda| = \pi/2$ and $|\lambda| = 3\pi/2$ both have $\kappa = m$ and $E = 0$, therefore are associated with zero mode solutions. The backflow effect does not distinguish these values of the parameter, and these parameters set minimum and maximum values of the lowest eigenvalue as can be seen from the figure 6.1. Smaller values of the parameter are displayed in figure 6.2, starting from $|\lambda| = \pi/7$ and showing some intermediate values up to $|\lambda| = \pi/50$. As expected, the lowest eigenvalue $\beta_V(f)$ gets closer to the free backflow eigenvalue $\beta_0(f) \approx -0.02$ as $|\lambda|$ becomes progressively smaller.

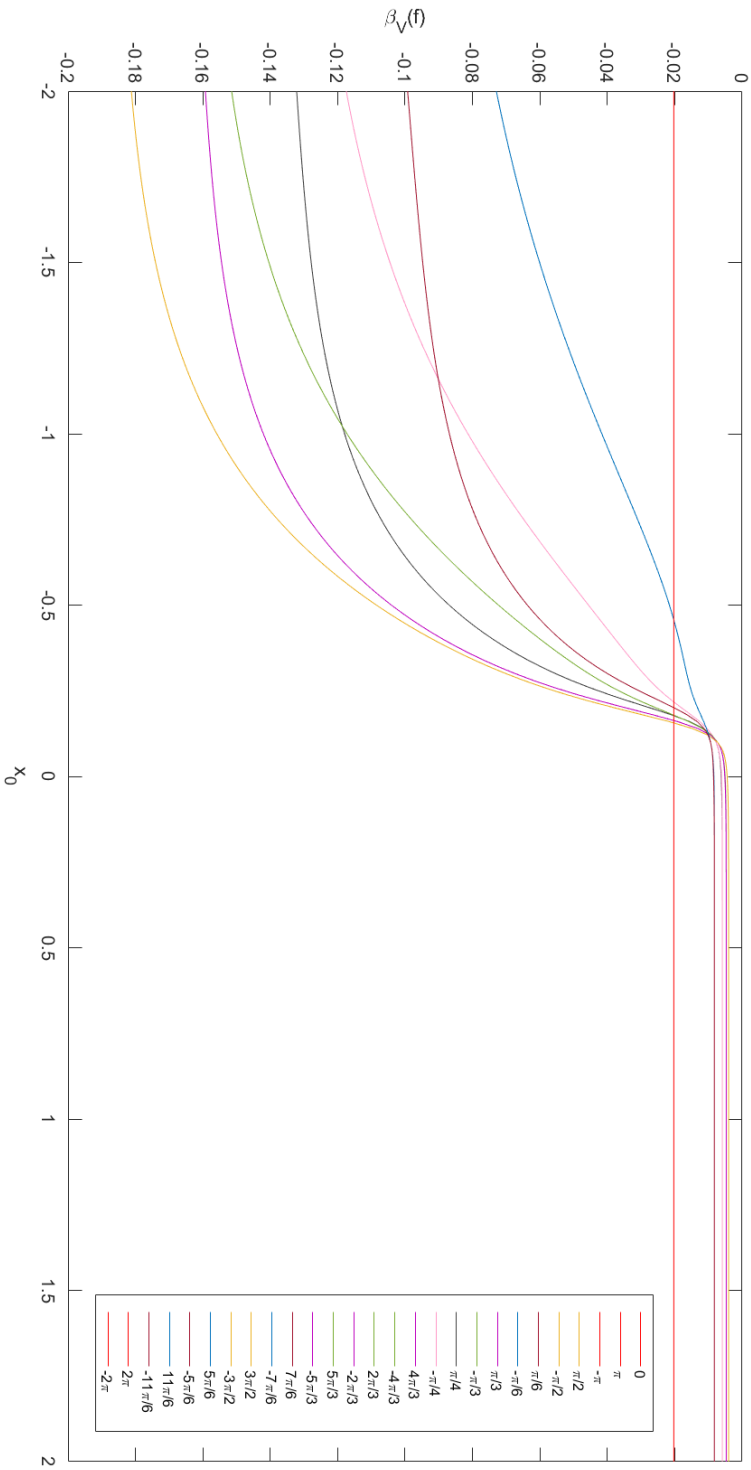

Figure 6.1: Periodicity of the lowest backflow eigenvalue for the δ_e-defect. $P_{\text{cutoff}} = 100$, $N = 1000$.

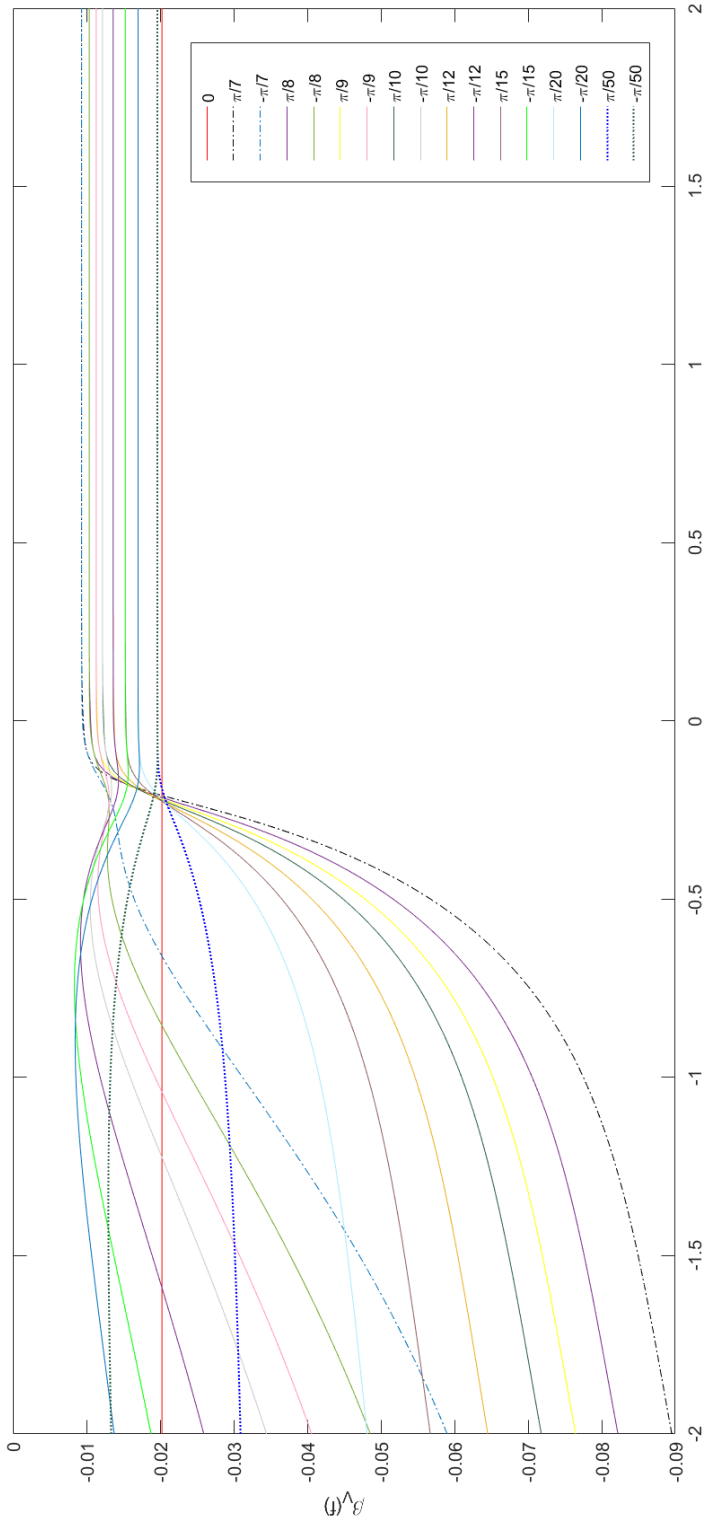

Figure 6.2: Lowest backflow eigenvalue for small parameters of the δ_e-defect. $P_{\text{cutoff}} = 100$, $N = 1000$.

6.5 THE MASS-LIKE δ_m-DEFECT

In the previous section, we considered the introduction of an electrostatic δ_e-defect in the Dirac equation, where the potential was proportional to the identity matrix, $V(x) = \lambda\delta(x)\mathbb{1}$. The present section considers the situation where a mass-spike δ disturbs the Dirac Hamiltonian. For that, the potential is now proportional to the σ_3 as $V(x) = \lambda\delta(x)\sigma_3$. Note that we are using the same notation λ for the potential parameter we used in previous sections. However, this mass-like impurity, denoted δ_m-defect, has the effect of effectively changing the mass term m in the Dirac equation

$$i\partial_t\psi = (-i\sigma_1\partial_x + \sigma_3 M(x))\psi, \tag{6.69}$$

where $M(x) = m + \lambda\delta(x)$ corresponds to an effective position-dependent mass.

Once again, we need to work out the sewing conditions that can describe this defect, but we can take the advantage of using some results from the previous section. For that, we follow the usual procedure of integrating the differential equation

$$-i\sigma_1\int_{-\varepsilon}^{\varepsilon}\psi_x dx + \sigma_3 m\int_{-\varepsilon}^{\varepsilon}\psi dx + \sigma_3\lambda\int_{-\varepsilon}^{\varepsilon}\delta(x)\psi(x)dx = \int_{-\varepsilon}^{\varepsilon}E\psi dx, \tag{6.70}$$

taking the limit $\varepsilon \to 0$ to consider the integration in the neighbourhood of the defect location at $x = 0$

$$-i\sigma_1(\psi(0^+) - \psi(0^-)) + \sigma_3\lambda\int_{-\varepsilon}^{\varepsilon}\delta(x)\psi(x)dx = 0. \tag{6.71}$$

As we have already discussed the implications of a discontinuity in ψ, our next step is to make use of a model for the δ, which we adopted the sequence of rectangular pulses in (6.14), and consider the following

$$\lim_{\varepsilon\to 0}\int_{-\varepsilon}^{\varepsilon}\left[-i\begin{pmatrix}0 & 1\\ 1 & 0\end{pmatrix}\begin{pmatrix}\psi_1\\ \psi_2\end{pmatrix}_x + \left(\frac{\lambda}{2\varepsilon}\right)\begin{pmatrix}1 & 0\\ 0 & -1\end{pmatrix}\begin{pmatrix}\psi_1\\ \psi_2\end{pmatrix}\right] dx = 0, \tag{6.72}$$

which comes from the first-order matrix differential equation

$$\begin{pmatrix}\psi_1\\ \psi_2\end{pmatrix}_x = -\frac{i\lambda}{2\varepsilon}\begin{pmatrix}0 & 1\\ 1 & 0\end{pmatrix}\begin{pmatrix}1 & 0\\ 0 & -1\end{pmatrix}\begin{pmatrix}\psi_1\\ \psi_2\end{pmatrix}, \tag{6.73}$$

valid for $-\varepsilon < x < \varepsilon$. This differential equation has the following solution

$$\begin{pmatrix}\psi_1\\ \psi_2\end{pmatrix} = \exp\left(-\frac{\lambda x}{2\varepsilon}\sigma_2\right)\begin{pmatrix}\eta_1\\ \eta_2\end{pmatrix}, \tag{6.74}$$

with η_1 and η_2 constants. The continuity of the solution at $x = -\varepsilon$ implies

$$\begin{pmatrix}\psi_1(-\varepsilon)\\ \psi_2(-\varepsilon)\end{pmatrix} = \exp\left(\frac{\lambda\sigma_2}{2}\right)\begin{pmatrix}\eta_1\\ \eta_2\end{pmatrix}, \tag{6.75}$$

and the continuity of the solution at $x = \varepsilon$ implies

$$\begin{pmatrix}\psi_1(+\varepsilon)\\ \psi_2(+\varepsilon)\end{pmatrix} = \exp\left(-\frac{\lambda\sigma_2}{2}\right)\begin{pmatrix}\eta_1\\ \eta_2\end{pmatrix}, \tag{6.76}$$

where we take the appropriate limit ($\varepsilon \to 0$) allowing us to relate the solution at the left of the real interval $(-\varepsilon, \varepsilon)$, that is for $x < -\varepsilon$, to its right side $x > \varepsilon$. It is known that the relation

$$e^{\alpha\sigma_k} = (\cosh\alpha)\mathbb{1} + (\sinh\alpha)\sigma_k \tag{6.77}$$

holds true for any complex number α and any one of the three Pauli matrices denoted by σ_k. Thus, we rewrite the left continuity condition as

$$\begin{pmatrix}\psi_1(0^-)\\ \psi_2(0^-)\end{pmatrix} = \left[\cosh\left(\frac{\lambda}{2}\right)\mathbb{1} + \sinh\left(\frac{\lambda}{2}\right)\sigma_2\right]\begin{pmatrix}\eta_1\\ \eta_2\end{pmatrix}, \tag{6.78}$$

and the right continuity condition as

$$\begin{pmatrix}\psi_1(0^+)\\ \psi_2(0^+)\end{pmatrix} = \left[\cosh\left(\frac{\lambda}{2}\right)\mathbb{1} - \sinh\left(\frac{\lambda}{2}\right)\sigma_2\right]\begin{pmatrix}\eta_1\\ \eta_2\end{pmatrix}. \tag{6.79}$$

From these expressions (6.78) and (6.79), it follows that

$$\begin{pmatrix}\psi_1(0^+)\\ \psi_2(0^+)\end{pmatrix} = \begin{pmatrix}\cosh\lambda & i\sinh\lambda\\ -i\sinh\lambda & \cosh\lambda\end{pmatrix}\begin{pmatrix}\psi_1(0^-)\\ \psi_2(0^-)\end{pmatrix}, \tag{6.80}$$

the sewing condition for a mass-like δ_m-defect relating the solutions at the left of the defect's location ($x = 0$) and at the right of it. The knowledge of the sewing condition

together with the time-independent scattering states (6.30) will determine the reflection and transmission as follows. Starting from the general condition

$$T(k)\begin{pmatrix} m+E \\ k \end{pmatrix}\exp(ikx-Et)\Big|_{x=0} = \begin{pmatrix} \cosh\lambda & i\sinh\lambda \\ -i\sinh\lambda & \cosh\lambda \end{pmatrix} u_k(x,t)\Big|_{x=0}, \tag{6.81}$$

and because the time-dependence is the same for the entire equation, it reads

$$T(k)\begin{pmatrix} m+E \\ k \end{pmatrix} = \begin{pmatrix} \cosh\lambda & i\sinh\lambda \\ -i\sinh\lambda & \cosh\lambda \end{pmatrix}\left[\begin{pmatrix} m+E \\ k \end{pmatrix} + \begin{pmatrix} m+E \\ -k \end{pmatrix} R(k)\right], \tag{6.82}$$

which can be rewritten in a more convenient form

$$R(k)\begin{pmatrix} m+E \\ -k \end{pmatrix} = \left[T(k)\begin{pmatrix} \cosh\lambda & -i\sinh\lambda \\ i\sinh\lambda & \cosh\lambda \end{pmatrix} - 1\right]\begin{pmatrix} m+E \\ k \end{pmatrix}. \tag{6.83}$$

Upon solving the system of linear equations, one obtains the transmission coefficient

$$T(k) = \frac{k}{k\cosh\lambda + im\sinh\lambda} \tag{6.84}$$

and the reflection coefficient

$$R(k) = -\frac{iE\sinh\lambda}{k\cosh\lambda + im\sinh\lambda}. \tag{6.85}$$

Note, in particular, these are related by

$$|R(k)|^2 + |T(k)|^2 = 1, \tag{6.86}$$

which will ensure the conservation of probability as before. A wave packet solution for the δ_m-defect is the same as in the previous electrostatic case, solution (6.39). However, the difference is only that the new set of sewing conditions reads

$$\begin{aligned} v_1(0^+) &= \cosh\lambda\ u_1(0^-) + i\sinh\lambda\ u_2(0^-), \\ v_2(0^+) &= -i\sinh\lambda\ u_1(0^-) + \cosh\lambda\ u_2(0^-), \end{aligned}$$

where u_i (v_i) denotes the two components of u (v) for $i = 1, 2$.

The backflow analysis will rigorously follow the same process of the previous section. In particular, equations (6.66) and (6.66) are equally valid for obtaining the minimum eigenvalue of the probability current operator with the inner kernel (6.68) using, however, the correct expressions of the transmission $T(k)$ and reflection coefficients $R(k)$ given by (6.84) and (6.85), respectively.

6.6 NUMERICAL RESULTS FOR THE δ_m-DEFECT

Here the results for the mass-like δ_m-defect are presented alongside the relevant plots. The interaction-free situation, represented by setting $\lambda = 0$, is evidently the same as in the electrostatic case, with the free asymptotic backflow constant $\beta_0(f) \approx -0.02$.

First, contrary to the δ_e-defect case, the δ_m-defect accommodates a purely reflecting situation for sufficiently large values of the parameter λ, when $T(k)$ approaches zero. This can be seen from figure 6.3, for $|\lambda| = 100$ or $|\lambda| = 10$, for example. The same happens in section 3.2 as mentioned before. Second, there is no periodicity in λ as the coefficients (6.84) and (6.85) depend on hyperbolic functions rather than trigonometric ones. Third, the bound states can be found again by looking at the purely-imaginary poles with positive imaginary part of the transmission $T(k)$, setting $k = i\kappa$ with real and positive κ. For the bound states, $\kappa = -m \tanh \lambda$ and only negative values of λ, with energy given by $E = m \operatorname{sech} \lambda$, are allowed. Hence, for each $\lambda < 0$, there is an electron bound state. In particular, for these negative values of λ, there are maxima (one for each attractive strength) of $\beta_V(f)$ that peak on the left of the defect, that is, in the region $x_0 < 0$. For sufficiently negative values of λ, however, the maxima become less noticeable. That feature is also present in the previous case of a single δ-defect in the Schrödinger equation. It is worth noting that the δ_m-defect has a backflow constant more negative for the attractive case than for the corresponding repulsive case in most of the negative positions x_0, expect for a limited region close to the defect location where the maxima occur.

Because the δ_m-defect shows more structure around the defect's location at the origin when compared to the δ_e-defect, figure 6.4 was plotted for a smaller range of the position x_0 in order to better display its behaviour around the origin. Note that the number of bumps in the graphs, for certain values of λ, makes the result very distinct from those in the δ_e-defect case. Moreover, as expected, sufficiently small values of the parameter cause the lowest backflow eigenvalue to approach the free backflow eigenvalue for the Dirac equation that is $\beta_0(f) \approx -0.02$.

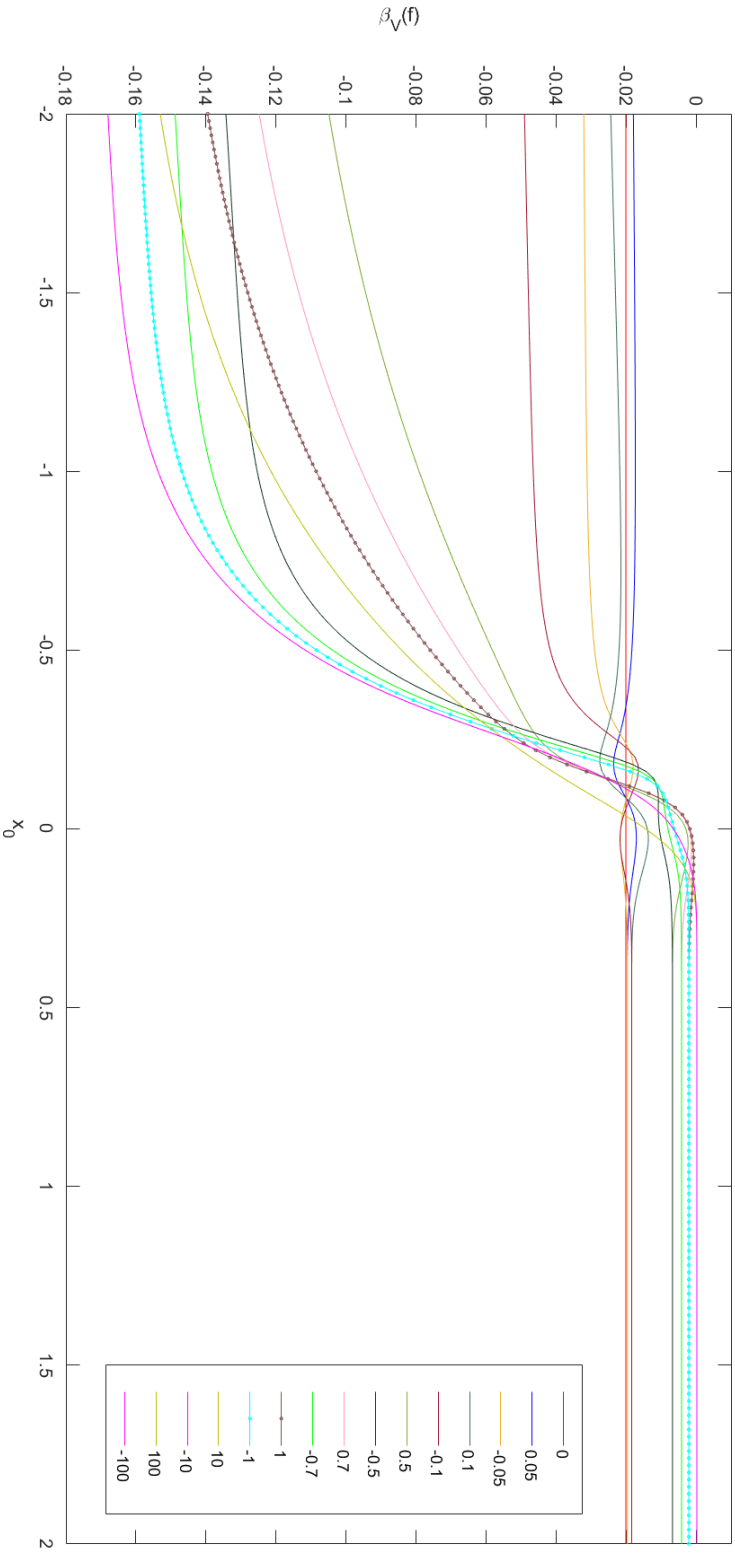

Figure 6.3: Lowest backflow eigenvalue for the δ_m-defect. $P_{\text{cutoff}} = 100$, $N = 1000$

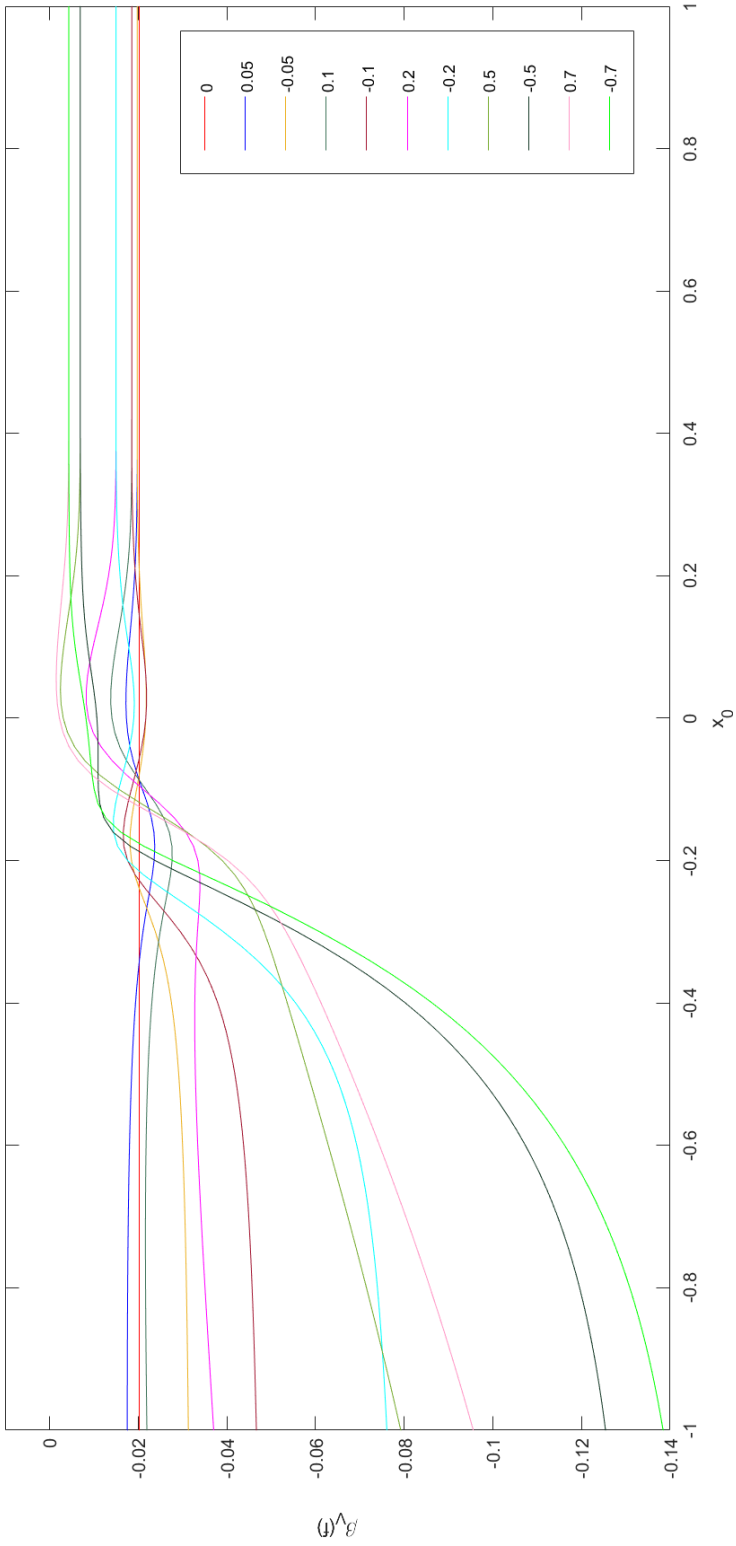

Figure 6.4: Lowest backflow eigenvalue for small parameters of the δ_m-defect. $P_{\text{cutoff}} = 100$, $N = 1000$

6.7 3D PLOTS FOR THE DIRAC EQUATION

This section presents three-dimensional plots, in situations described by the δ_e-defect and by the δ_m-defect in the Dirac equation, displaying the lowest eigenvalue $\beta_V(f)$ of the corresponding probability current operator as the defect parameter λ and the position of measurement x_0, which is the center of the averaging Gaussian function f, change. The plots of this section are also to be compared to figure 3.4, which corresponds to the δ-defect in the Schrödinger equation. In order to better show some of the details involved in the shape of the surface, each situation was plotted twice with the first plot varying the defect parameter up to $|\lambda| = 10$ and the second up to $|\lambda| = 50$. The range of the position of measurement x_0 was kept unchanged.

While in the Schrödinger case the free backflow constant is $\beta_0(f) \approx -0.24$, in the relativistic Dirac case the constant is smaller $\beta_0(f) \approx -0.02$. All situations described by a δ-defect have the presence of reflection in the process of scattering and, therefore, backscattering is inevitable. There is, however, a difference between the δ_e-defect and the δ_m-defect regarding the backflow eigenvalue at positions on the left of the defect's location. Exactly as previously shown in figure 3.4, the results for the mass-like defect, figure 6.7 and figure 6.8, show an increasingly backflow effect as $|\lambda|$ increases. In the electrostatic case, figure 6.5 and figure 6.6, because of the periodicity in the parameter λ, increasing the strength of the interaction does not always cause the increase of the backflow effect. The δ_m-defect is more similar to the δ-defect in the Schrödinger case as for the lack of periodicity in λ and for achieving the value zero for the lowest eigenvalue of the probability current, effectively becoming a potential wall, but there are notable differences for small absolute values of the parameter λ that can be observed specially in figure 6.7 in contrast to figure 3.4. With regard to the presence of electron bound states, the δ_e-defect can have one bound state whenever the parameter λ is located in the second trigonometric quadrant or in the fourth quadrant, independently of its sign. From zero to 2π, for example, the presence or not of bound state alternates as the parameter increases. Note that, in figure 6.5, there are two maximum cusps and two minimum cusps in the range $(0, 2\pi)$. Differently, the δ_m-defect has one electron bound state for negative values of the parameter, $\lambda < 0$. Thus, the presence or not of bound state is changed at $\lambda = 0$, where its sign changes. Note that, in figure 6.7, there is a maximum cusp at $\lambda = 0$, where the number of bound states change.

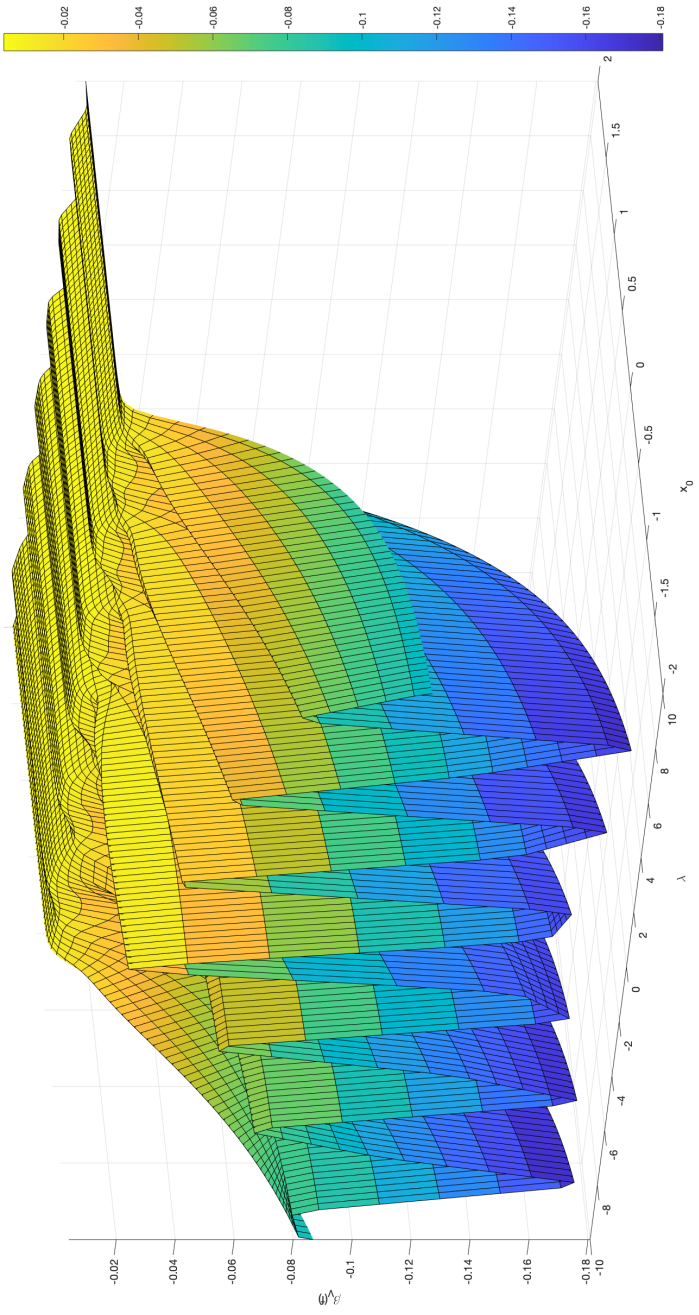

Figure 6.5: Probability current lowest eigenvalue for the δ_e-defect, $P_{\text{cutoff}} = 100$, $N = 1000$.

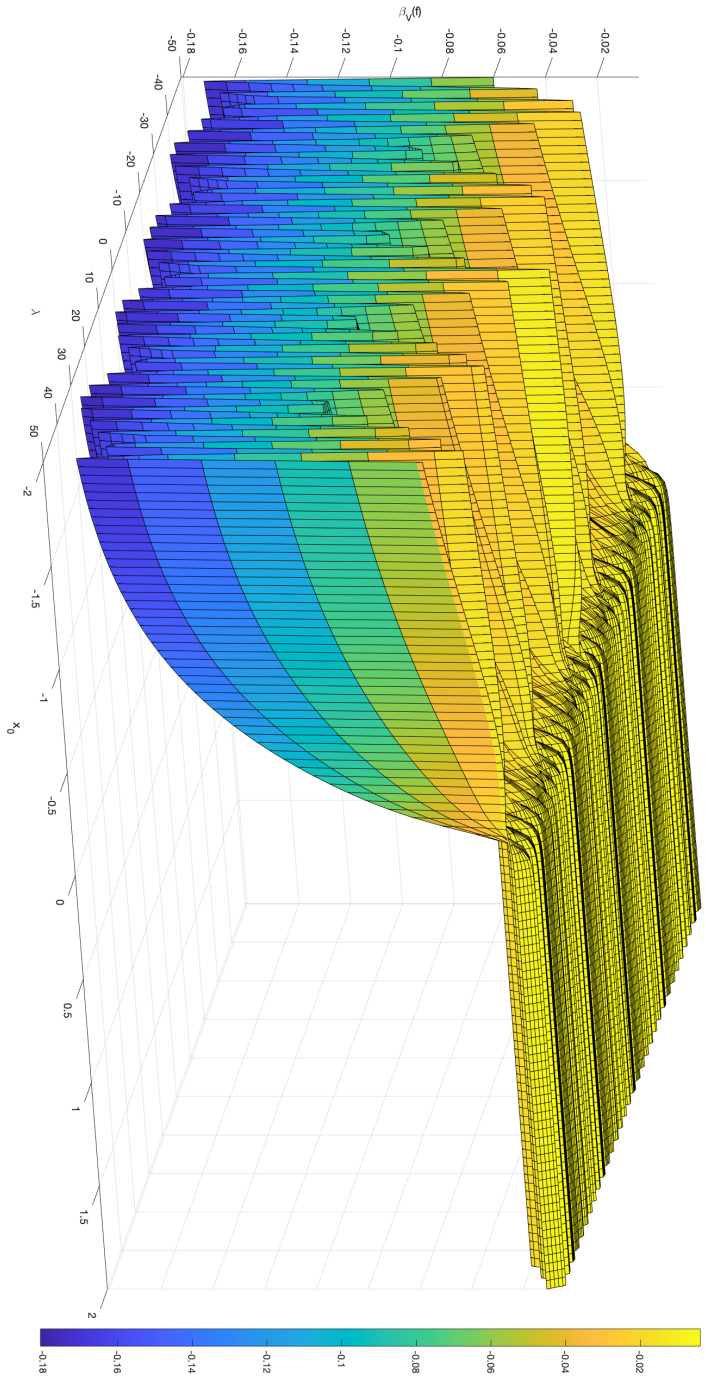

Figure 6.6: Probability current lowest eigenvalue for the δ_e-defect, $P_{\text{cutoff}} = 100$, $N = 1000$.

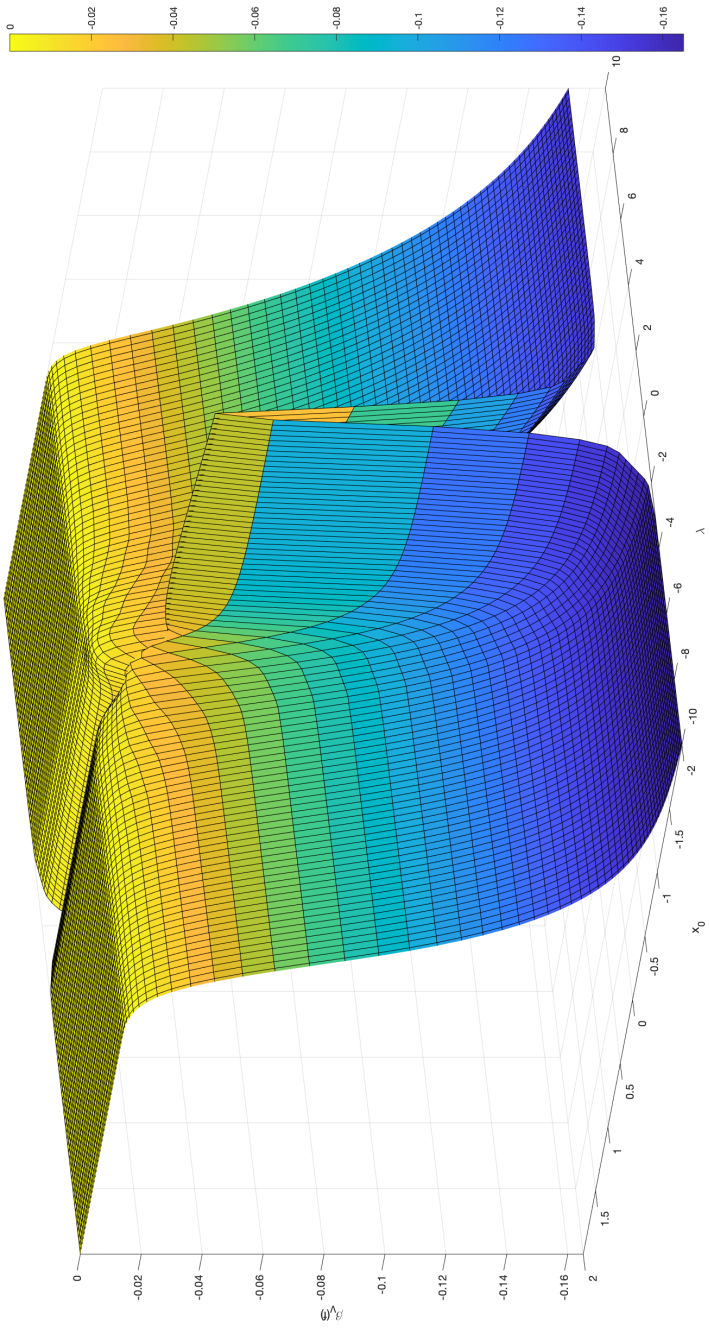

Figure 6.7: Probability current lowest eigenvalue for the mass-like δ_m-defect, $P_{\text{cutoff}} = 100$, $N = 1000$.

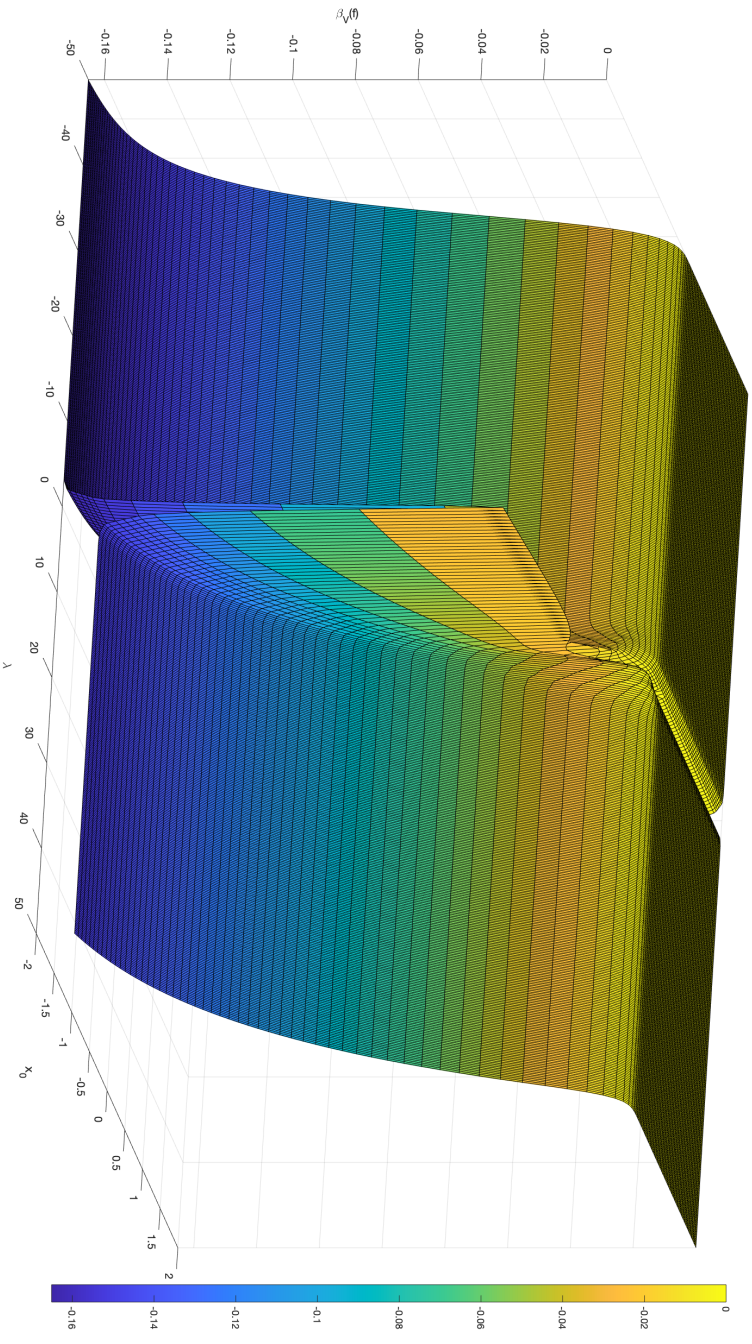

Figure 6.8: Probability current lowest eigenvalue for the mass-like δ_m-defect, $P_{\text{cutoff}} = 100$, $N = 1000$.

6.8 brief comments on the dirac conserved current

Some comments are in order about the one-particle probability density ρ and the probability current density j in the Dirac equation. The probabilistic interpretation has a direct connection with the problem of localization in quantum theory [156, 157, 158]. In quantum field theory, however, it is known that $j^\mu = (c\rho, j)$ is interpreted as the source of the electromagnetic interaction.

There are two different notions of localization in quantum theory [2], the first, called Born localization, is about position operators and projectors and is a concept from quantum mechanics. The other one, called modular localization, underlying the causal locality notion in quantum field theory, relates fields to local observables. Newton and Wigner [159] adapted the Born probabilistic localization to relativistic quantum mechanics, seeking self-adjoint position operators for elementary particles of any spin leaving positive energy Hilbert subspaces invariant. However, not being covariant, the Newton-Wigner position is plagued with superluminal effects when considered at finite times rather than in the asymptotic limit of large times, where exact covariance is valid.

Any relativistic quantum mechanical notion of strict localisation in terms of particle positions suffer difficulties with relativistic covariance and positivity of the energy combined [160, 161, 162]. The notion of localization in local quantum theory field, modular localization, is relativistic covariant. It is not about positions of particles, but about local measurements of observables [163]. Even within this setting of local algebra of observables $\mathcal{A}(\mathcal{O})$, attached to a space-time region $\mathcal{O}$, it is accepted the existence of objects localized on a semi-infinite space-like line, hence non-compact region, if one takes the Wigner's particle classification seriously [164]. Modular localization does not exclude the Born localization for particle's wavefunction, as quantum field theory actually requires both notions for its physical significance [2].

The authors of [165, 166] use a notion of localization that is not an exact localization in a region of compact support with positive energy generalized position eigenstates, but an arbitrarily precise localization in terms of probability density and probability flux of positive-energy state vectors in the Dirac one-particle theory. More precisely, a sequence of positive energy state vectors $(\psi_n)_{n\in\mathbb{N}}$ of the electron is constructed such that the associated sequences of probability densities $\psi_n^\dagger(x)\psi_n(x)$ and currents approach, in the limit that $n \to \infty$, $\delta(x-a)$ and $v\delta(x-a)$, respectively, where a is the prescribed position

of localization and v is the mean value of the velocity operator. In that sense, although there is no strictly localized states with positive energy (generalized eigenstates) and, therefore, no self-adjoint position operator in the positive Hilbert subspace, arbitrary small standard deviations of the Dirac position operator

$$\Delta\hat{X} = \sqrt{\left\langle \hat{X}^2 \right\rangle - \left\langle \hat{X} \right\rangle^2}$$

can be obtained for "localizing" states [167]. This is of course not a strict localization in a compact region.

In relativistic theories, it is generally accepted that strict localization involves arbitrarily high energies that can be accompanied by the creation of particles and, therefore, invalidating the description in terms of one-particle theory. Because we are analysing backflow in the relativistic one-particle Dirac theory, we adopt the view that a quantum observable is associated with a more general positive operator valued measure instead of a projection valued measure. The former corresponds to unsharp observables [168, 169, 170], and the latter corresponds to sharp observables. In this regard, by making use of observables smeared with a positive test function f when analysing the spatial averaged backflow, we are working with unsharp measurements and employing the interpretation of $\rho(x)$ as a position probability density restricted to positive energy one-particle systems. In summary, the one-particle interpretation of the Dirac equation can be made physically sensible by considering unsharp observables and smearing physical quantities with a suitable test function.

6.9 JUMP-DEFECT FOR THE DIRAC EQUATION

In Chapter 4, we considered the jump-defect in the non-relativistic setting. It is natural to ask whether it is possible to construct the equivalent in the relativistic setting of the Dirac equation. In a very particular sense, the δ-defect discussed here in this chapter is already a jump. More specifically, the sewing conditions (6.23) and (6.80) for the δ_e-defect and δ_m-defect, respectively, represent a jump discontinuity in the spinor solution of the Dirac equation at the defect's location. However, the jump-defect in Chapter 4 has a key feature not shared with any of these δ-defects: it is a purely transmitting point defect. The search for transparent potentials in the one-dimensional Dirac equations is not a new one. In [171, 172, 173], the authors, inspired by Kay and

Moses [174], constructed static scalar and pseudo-scalar transparent potentials for the Dirac equation exploring the relation between the Dirac equation and the Schrödinger equation via supersymmetric quantum mechanics. More recently, time-dependent transparent potentials were constructed for a combination of scalar and pseudoscalar Dirac potentials [175], but they are not point defect as in the case of the δ-defect and the jump-defect. Moreover, these transparent potentials are really constructed as functions of fermionic state vectors and are related to nonlinear Dirac equations. Hence, we would like to construct a type I jump-defect for the Dirac equation and consider its backflow similarly to what was done for the Schrödinger equation.

Furthermore, in Chapter 4, the sewing conditions for the jump-defect were noted as a frozen Bäcklund transformation for the Schrödinger equation at the defect's location. Similarly, we would like to construct the sewing conditions for the $(1+1)$ Dirac equation (6.2). The Dirac equation for a massive particle, however, is already an auto-Bäcklund transformation for the second-order Klein-Gordon equation. It turns out that the Dirac equation is a first-order differential equation and does not have an obvious Bäcklund transformation to guide us on how to construct the set of sewing conditions corresponding to a purely transmitting defect. Nevertheless, the jump-defect was shown to conserve total momentum, together with energy and probability (or total number of species in fields settings), in all previously studied cases. The first strategy is, therefore, to force the conservation of these quantities and identify what are the requirements on the set of sewing conditions that follow from the conservation laws. For that, we make use of some expressions derived in section 6.2, starting from the probability conservation.

The total contribution of the fields to the probability is again calculated by splitting the limits of integration into two domains, and its time derivative

$$\begin{aligned} N_t &= \int (\psi_t^\dagger \psi + \psi^\dagger \psi_t) dx \\ &= -(u^\dagger \sigma_1 u)|_{x=0} + (v^\dagger \sigma_1 v)|_{x=0} \end{aligned}$$

needs to be zero in order to have probability conserved or a total time-derivative that can be used for defining an adjusted probability conserved. The Gordon decomposition, see, for example, [176, 26] for details,

$$\bar{\psi}\gamma^\mu\psi = \frac{i}{2m}\left(\bar{\psi}\partial^\mu\psi - (\partial^\mu\bar{\psi})\psi) + \frac{1}{m}\partial_\nu\left(\bar{\psi}\Sigma^{\mu\nu}\psi\right)\right) \tag{6.87}$$

of the Dirac current can be used to rewrite the above expression in a more convenient form. The matrices $\Sigma^{\mu\nu}$ represents generators of the Lorentz group and are given in terms of the commutator

$$\Sigma^{\mu\nu} = \frac{1}{4}\left[\gamma^{\mu}, \gamma^{\nu}\right].$$

In particular, for the one-dimensional spatial component ($\mu = 1$), N_t reads

$$\begin{aligned} N_t = \frac{i}{2m}\left[u^{\dagger}\sigma_3 u_x - u_x^{\dagger}\sigma_3 u - v^{\dagger}\sigma_3 v_x + v_x^{\dagger}\sigma_3 v\right]_{x=0} \\ + \frac{i}{4m}\left[\partial_t(u^{\dagger} i\sigma_2 u - v^{\dagger} i\sigma_2 v)\right]_{x=0}. \end{aligned} \tag{6.88}$$

One possible attempt is to write the sewing conditions as a general combination, similar to (4.8) in the Schrödinger case, as

$$\begin{aligned} u_x|_{x=0} &= au_t + bv_t + cu + dv|_{x=0}, \\ v_x|_{x=0} &= eu_t + fv_t + gu + hv|_{x=0}, \end{aligned} \tag{6.89}$$

with arbitrary constant matrices a, b, c, d, e, f, g, h as coefficients. Substituting these into expression (6.88) gives, after some simplification,

$$\begin{aligned} N_t = \frac{i}{2m}\Big[&\partial_t(u^{\dagger}\sigma_3 a u) - u_t^{\dagger}\sigma_3 a u - u_t^{\dagger}a^{\dagger}\sigma_3 u + u^{\dagger}\sigma_3 c u - u^{\dagger}c^{\dagger}\sigma_3 u \\ &+ \partial_t(u^{\dagger}\sigma_3 b v) - u_t^{\dagger}\sigma_3 b v + u_t^{\dagger}e^{\dagger}\sigma_3 v + u^{\dagger}\sigma_3 d v + u^{\dagger}g^{\dagger}\sigma_3 v \\ &- \partial_t(v^{\dagger}\sigma_3 e u) + v_t^{\dagger}\sigma_3 e u - v_t^{\dagger}b^{\dagger}\sigma_3 u - v^{\dagger}d^{\dagger}\sigma_3 u - v^{\dagger}\sigma_3 g u \\ &+ \partial_t(v^{\dagger}f^{\dagger}\sigma_3 v) - v^{\dagger}f^{\dagger}\sigma_3 v_t - v^{\dagger}\sigma_3 f v_t + v^{\dagger}h^{\dagger}\sigma_3 v - v^{\dagger}\sigma_3 h v\Big]_{x=0} \\ &+ \frac{i}{4m}\left[\partial_t(u^{\dagger} i\sigma_2 u - v^{\dagger} i\sigma_2 v)\right]_{x=0}, \end{aligned} \tag{6.90}$$

which can be reduced to a total time derivative

$$\begin{aligned} N_t = \frac{i}{4m}\big[&\partial_t(2u^{\dagger}\sigma_3 a u + 2u^{\dagger}\sigma_3 b v - 2v^{\dagger}\sigma_3 e u \\ &+ 2v^{\dagger}f^{\dagger}\sigma_3 v + u^{\dagger} i\sigma_2 u - v^{\dagger} i\sigma_2 v)\big]_{x=0}, \end{aligned} \tag{6.91}$$

provided that $a = -a^{\dagger}, c = c^{\dagger}, e = b^{\dagger}, g = -d^{\dagger}, f = -f^{\dagger}, h = h^{\dagger}$ and that they commute with σ_3, that is, $[a, \sigma_3] = [b, \sigma_3] = [c, \sigma_3] = [d, \sigma_3] = [f, \sigma_3] = [h, \sigma_3] = 0$. These are conditions that must be met in order to obtain an adjusted total probability quantity N_c that is conserved and given by

$$\begin{aligned} N_c := N - \frac{i}{4m}\big[&2u^{\dagger}\sigma_3 a u + 2u^{\dagger}\sigma_3 b v - 2v^{\dagger}\sigma_3 e u \\ &+ 2v^{\dagger}f^{\dagger}\sigma_3 v + u^{\dagger} i\sigma_2 u - v^{\dagger} i\sigma_2 v\big]_{x=0}. \end{aligned} \tag{6.92}$$

The next step is to impose conservation of energy and obtain new constraints on the sewing condition's parameters as a way of narrowing them down. For that, we recall that the time derivative of the energy is

$$E_t = \frac{i}{2}\left[u^\dagger u_x - u_x^\dagger u\right]_{x=0} - \frac{i}{2}\left[v^\dagger v_x - v_x^\dagger v\right]_{x=0},$$

and the substitution of the sewing conditions (6.89) into this expression will give

$$\begin{aligned} E_t = \frac{i}{2}\Big[&\partial_t(u^\dagger a u) - u_t^\dagger a u - u_t^\dagger a^\dagger u + \partial_t(v^\dagger f^\dagger v) - v^\dagger f^\dagger v_t - v^\dagger f v_t \\ &+ \partial_t(u^\dagger b v) - u^\dagger b v - u_t^\dagger e^\dagger v + u^\dagger c u - u^\dagger c^\dagger u - v^\dagger h v + v^\dagger h^\dagger v \\ &+ u^\dagger d v + u^\dagger g^\dagger v - \partial_t(v^\dagger b^\dagger u) + v^\dagger b^\dagger u_t - v^\dagger e u_t - v^\dagger d^\dagger u - v^\dagger g u\Big]_{x=0}, \end{aligned} \tag{6.93}$$

which can be reduced to a total time derivative

$$E_t = \frac{i}{2}\left[\partial_t\left(u^\dagger a u + v^\dagger f^\dagger v + u^\dagger b v - v^\dagger b^\dagger u\right)\right]_{x=0},$$

provided that $a^\dagger = -a, c^\dagger = c, f^\dagger = -f, h^\dagger = h, b^\dagger = e, d^\dagger = -g$. These conditions are compatible with the ones just found with the conservation of probability. Thus, the following adjusted total energy E_c is conserved and given by

$$E_c := E - \frac{i}{2}\left[u^\dagger a u + v^\dagger f^\dagger v + u^\dagger b v - v^\dagger b^\dagger u\right]_{x=0}. \tag{6.94}$$

Lastly, the time derivative of the momentum in the presence of a defect located at the origin was shown to be

$$P_t = -\frac{i}{2}\left[u_x^\dagger \sigma_1 u - u^\dagger \sigma_1 u_x\right]_{x=0} + \frac{i}{2}\left[v_x^\dagger \sigma_1 v - v^\dagger \sigma_1 v_x\right]_{x=0},$$

which, upon using the sewing conditions (6.89), can be written as

$$\begin{aligned} P_t = -\frac{i}{2}\Big[&\partial_t(u^\dagger a^\dagger \sigma_1 u) - u^\dagger a^\dagger \sigma_1 u_t - u_t^\dagger \sigma_1 a u_t + \partial_t(v^\dagger b^\dagger \sigma_1 u) - v^\dagger b^\dagger \sigma_1 u_t \\ &+ v^\dagger \sigma_1 e u_t + u^\dagger c^\dagger \sigma_1 u - u^\dagger \sigma_1 c u - v^\dagger h^\dagger \sigma_1 v + v^\dagger \sigma_1 h v + v^\dagger d^\dagger \sigma_1 u \\ &+ v^\dagger \sigma_1 g u - \partial_t(u^\dagger \sigma_1 b v) + u_t^\dagger \sigma_1 b v - u^\dagger \sigma_1 d v \\ &- \partial_t(v^\dagger f^\dagger \sigma_1 v) + v^\dagger f^\dagger \sigma_1 v_t + v^\dagger \sigma_1 f v_t - u_t^\dagger e^\dagger \sigma_1 v - u^\dagger g^\dagger \sigma_1 v\Big]_{x=0}, \end{aligned} \tag{6.95}$$

which can be reduced to a total derivative

$$P_t = -\frac{i}{2}\left[\partial_t\left(u^\dagger a^\dagger \sigma_1 u + v^\dagger b^\dagger \sigma_1 u - u^\dagger \sigma_1 b v - v^\dagger f^\dagger \sigma_1 v\right)\right]_{x=0}, \tag{6.96}$$

provided that $a^\dagger = -a, c^\dagger = c, f^\dagger = -f, h^\dagger = h, e^\dagger = b, g^\dagger = -d$ and that they commute with σ_1, that is, $[a,\sigma_1] = [b,\sigma_1] = [c,\sigma_1] = [d,\sigma_1] = [f,\sigma_1] = [h,\sigma_1] = 0$. With these, the adjusted total momentum P_c is conserved and given by

$$P_c = P + \frac{i}{2}\left[u^\dagger a^\dagger \sigma_1 u + v^\dagger b^\dagger \sigma_1 u - u^\dagger \sigma_1 b v - v^\dagger f^\dagger \sigma_1 v\right]_{x=0}. \tag{6.97}$$

As before, all the adjustment terms are contributions evaluated at the origin and, therefore, coming from the defect. However, the required conditions for conserving the probability are in discordance with the required conditions for keeping the momentum conserved. Imposing a matrix to commute with both σ_3 and σ_1 causes the matrix to be proportional to the 2x2-identity matrix. Hence, the choice of (6.89) as sewing conditions does not work to describe the proposed situation of a jump-defect in the Dirac equation. Based on the case of the δ-defects, either (6.23) or (6.80), a second attempt would be to consider that the following sewing condition

$$u|_{x=0} = Mv|_{x=0}\ , \tag{6.98}$$

with M a 2x2-matrix depending on a single real parameter α. Upon checking the conserved quantities as done before, we find the corresponding conditions restricting M. For the total probability N, it is easy to show that

$$N_t = 0, \tag{6.99}$$

provided that $M^\dagger \sigma_1 M = \sigma_1$. While for the energy, one finds that

$$\begin{aligned} E_t = \frac{i}{2}\big[&-v^\dagger M^\dagger \sigma_1 M v_t + v^\dagger \sigma_1 v_t - v^\dagger M^\dagger m \sigma_2 M v + m v^\dagger \sigma_2 v \\ &+ v_t^\dagger M^\dagger \sigma_1 M v - v_t^\dagger \sigma_1 v + m v^\dagger M^\dagger \sigma_2 M v - m v^\dagger \sigma_2 v\Big], \end{aligned} \tag{6.100}$$

which is equal to zero provided that $M^\dagger \sigma_1 M = \sigma_1$. Hence, conservation of energy and probability once again are compatible with each other. As for the total contribution of the fields to the momentum, its time derivative is

$$\begin{aligned} P_t = -\frac{i}{2}\big[&-v_t^\dagger \sigma_1 M^\dagger \sigma_1 M v + v_t^\dagger \sigma_1^2 v - m v^\dagger \sigma_2 M^\dagger \sigma_1 M v + m v^\dagger \sigma_2 \sigma_1 v \\ &+ v^\dagger M^\dagger \sigma_1^2 M v_t + m v^\dagger M^\dagger \sigma_1 \sigma_2 M v - v^\dagger \sigma_1^2 v_t - m v^\dagger \sigma_1 \sigma_2 v\big]_{x=0}\ . \end{aligned} \tag{6.101}$$

Now, if we use that $M^\dagger\sigma_1 M = \sigma_1$, this expression is simplified to

$$\begin{aligned} P_t = -\frac{i}{2}\Big[&\partial_t(v^\dagger M^\dagger M v - v^\dagger v) - v_t^\dagger M^\dagger M v + v_t^\dagger v \\ &+ m v^\dagger(M^\dagger\sigma_1\sigma_2 M - \sigma_1\sigma_2)v\Big]_{x=0}, \end{aligned} \tag{6.102}$$

that can be set to zero for the conservation of the momentum provided that $M^\dagger M = \mathbb{1}$ and that $M^\dagger\sigma_2 M = \sigma_1$. That is again an unfavourable conclusion as we are left with a trivial sewing condition in the sense that the matrix M is defined as a global phase such as $M = e^{i\alpha}\mathbb{1}$. Evidently, that would not represent a jump-defect, and the particular choice (6.98) of sewing condition is not suitable for our purposes.

Additionally to the type I defects, one could consider a type II jump-defect, which includes an extra degree of freedom characterized by a dynamics determined by the defect. For that, Bäcklund transformations involving an auxiliary variable seem to provide the ideal setting for that kind of construction. This Bäcklund transformation was, in fact, constructed in [177] for the massive Thirring model with field values in a Grassmannian algebra and also for commuting field values in [178]. Based on that, a jump-defect was obtained in [179, 180, 181] for the Grassmannian Thirring model and in the context of the supersymmetric sinh-Gordon equation. The Thirring model reduces to the Dirac equation when the coupling constant of the self-interaction term in the model is set equal to zero. Thus, one could explore the quantum backflow in the presence of that jump-defect in the Grassmannian Thirring model in the particular situation describing the Dirac equation. However, any attempt in that direction is out of the scope of the present work because the implementation of Grassmanian variables would have to be carried over into the numerical analysis with Fortran. We considered the possibility of taking the Bäcklund transformation for the Thirring model with commuting field values [178, 182] as a guide to construct a type II jump-defect. For that, we set the sewing condition defined at the defect's location, chosen to be zero,

$$\begin{aligned} u_1 &= a v_1 + c\chi \quad x = 0, \\ u_2 &= b v_2 + d\chi \quad x = 0, \end{aligned} \tag{6.103}$$

with a, b, c, d nonzero complex constants, u_1, u_2, v_1, v_2 components of the spinors u and v, respectively, and χ an auxiliary variable with dynamics. More specifically, choosing the Weyl basis for the gamma matrices, $\gamma^0 = \sigma_1$ and $\gamma^1 = i\sigma_2$, the Dirac equation for a

generic spinor ψ with components ψ_1 and ψ_2 reads

$$\begin{aligned} i(\partial_t + \partial_x)\psi_1 &= m\psi_2, \\ i(\partial_t - \partial_x)\psi_2 &= m\psi_1. \end{aligned} \tag{6.104}$$

Then, the following additional sewing condition determining the dynamics of the auxiliary variable and defined only at the defect's location

$$\begin{aligned} \partial_t\chi &= -c^\star\left(u_1 + \frac{v_1}{a^\star}\right) + d^\star\left(u_2 + \frac{v_2}{b^\star}\right) \quad x = 0, \\ \partial_t\chi^\star &= -c\left(u_1^\star + \frac{v_1^\star}{a}\right) + d\left(u_2^\star + \frac{v_2^\star}{b}\right) \quad x = 0, \end{aligned} \tag{6.105}$$

would allow the modified quantity

$$N_c := N + \frac{1}{2}(\chi^\star\chi) \tag{6.106}$$

to be conserved, provided that $a^\star a = b^\star b = 1$. For a modified momentum P_c to be conserved, we could have a compatible choice of parameters such that $a^\star a = b^\star b = 1$, $a^\star b = -1$ and $cd^\star = -dc^\star$, but the dynamics described by the defect would need to be slightly changed to

$$\begin{aligned} \partial_t\chi &= c^\star\left(u_1 + \frac{v_1}{a^\star}\right) + d^\star\left(u_2 + \frac{v_2}{b^\star}\right) \quad x = 0, \\ \partial_t\chi^\star &= c\left(u_1^\star + \frac{v_1^\star}{a}\right) + d\left(u_2^\star + \frac{v_2^\star}{b}\right) \quad x = 0. \end{aligned} \tag{6.107}$$

As for the energy, the condition $a^\star a = b^\star b = 1$ is incompatible with the conservation of a modified total energy E_c term in light of the aforementioned sewing conditions. The result is that does not seem possible to have one single dynamics for χ that keeps conserved the probability, total energy and total momentum altogether as requirement for constructing a purely transmitting jump-defect in the Dirac equation.

— 7 —

Discussion and outlook

7.1 PART 1: FINAL REMARKS

Even in the interaction-free situation, the required restriction of the wavefunction with positive momenta, right-moving states, in the study of the quantum backflow effect causes a dramatic change in the analysis of the probability current operator. Note that the corresponding operator $E_+ J(f) E_+$ with the spectral projection E_+ is much less trivial than the more usual $J(f)$. In fact, suppose that $|J\rangle$ is an eigenvector of $J(f)$ allowing both positive and negative momenta with associated eigenfunction $\mathcal{J}$ in position space, then the eigenvalue equation would be

$$\frac{\hat{P} f(\hat{X}) + f(\hat{X})\hat{P}}{2} |J\rangle = \mu |J\rangle, \tag{7.1}$$

where μ is an eigenvalue of the probability current operator which depends on the choice of the positive test function f. However, taking into account the restriction to right-moving states only, the lowest eigenvalue equation in terms of the unbounded integral operator on $L^2(\mathbb{R}_+, dk')$ is given by

$$\int_0^\infty dk' \, \frac{(k'+k)}{2\sqrt{2\pi}} \tilde{f}(k'-k) \tilde{\mathcal{J}}(k') = \mu \, \tilde{\mathcal{J}}(k), \tag{7.2}$$

where μ now represents the lowest eigenvalue of the operator $E_+ J(f) E_+$, and the projection E_+ is used to constrain the range of integration to $k' > 0$.

Different from the energy, which has a global energy condition where the expectation value of the Hamiltonian in any state $\psi \in \mathcal{H}$ obeys $\langle H \rangle_\psi \geq 0$, the expectation value of the momentum operator $\langle \hat{P} \rangle_\psi$ has no a priori global condition upon it. The fact

that the total energy is non-negative and $\langle H \rangle_\psi = 0$ when ψ is the vacuum state of the theory, despite the possibility of negative energy density in localized regions, has the physical importance of supporting stable quantum systems, but an equivalent condition for the momentum, in general, lacks the same physical significance. However, there are situations where the system may be restricted to positive momenta only, and the most obvious is the interaction-free case where the particle moves with positive momentum. Beyond a free theory, an asymptotic right-mover will have positive momentum until it finds a region with a potential, or a defect, and undergoes scattering with reflection and transmission. Evidently, the asymptotic right-mover is, in general, not a right-mover after the scattering because the interaction with the scattering center. In that sense, the asymptotic backflow constant $\beta_V(f)$ is associated with a mixture of contributions from the backflow effect and backscattering as well unless there is no reflection as a result of the scattering process. Although that is not the case for the δ-defect, the jump-defect is precisely the example where total transmission is always possible without any restriction upon the defect parameter or the incident energy.

For all interactions that are not purely transmitting, it would be very useful to distinguish between negative probability fluxes due to backscattering and genuine backflow from superposition of right-moving states. A very recent work [183] proposed an "experiment-friendly" formulation of quantum backflow modifying the standard criterion that asserts the existence of backflow, namely, $j_\psi(x) < 0$ for right-moving states. The authors of the work claim that measuring a particular phase-space distribution gives an equivalent criterion to the standard one while also more suitable for experimental verification of the backflow effect. Instead of measuring $j_\psi(a)$, their criterion uses a lower bound estimation for the backflow at a particular point $x = a$ as

$$j_\psi(a) - \frac{1}{m}\int_{-\infty}^{0} dk\ k\,|W_{\psi,\phi}(a,k)|^2 < 0, \tag{7.3}$$

where $W_{\psi,\phi}$ is a Wigner-Moyal transform [184] (also known as Fourier-Wigner transform [185]) of functions $\psi, \phi \in L^2(\mathbb{R})$ defined on phase space by

$$\begin{aligned} W_{\psi,\phi}(x,k) &= \frac{1}{\sqrt{2\pi}}\int_{-\infty}^{\infty} dy\ e^{-iky}\phi^\star(y - \frac{x}{2})\psi(y + \frac{x}{2}) \\ &= \frac{1}{\sqrt{2\pi}}\int_{-\infty}^{\infty} dp\ e^{ixp}\phi^\star(p - \frac{k}{2})\psi(p + \frac{k}{2}) \end{aligned} \tag{7.4}$$

with ϕ representing the precision function of a measurement apparatus that has normalization $\int_{-\infty}^{\infty} dx|\phi(x)|^2 = 1$. The Wigner function W_ψ is (up to scaling factors) simply $W_{\psi,\psi}$. Let us take ϕ to be a Gaussian function with a fixed width σ and given by

$$\phi(x) = \frac{1}{\pi^{1/4}\sqrt{\sigma}} \exp\left(-\frac{x^2}{2\sigma^2}\right), \tag{7.5}$$

which has the following Fourier transform

$$\tilde{\phi}(k) = \frac{1}{\pi^{1/4}\sqrt{\tilde{\sigma}}} \exp\left(-\frac{k^2}{2\tilde{\sigma}^2}\right), \tag{7.6}$$

where the width $\tilde{\sigma}$ is related to σ by $\sigma\tilde{\sigma} = 1$. Upon setting ϕ to be a Gaussian function, $|W_{\psi,\phi}(x,k)|^2$ becomes a Gaussian smoothing of the Wigner function W_ψ, that is, a function given by W_ψ smoothed with a phase-space Gaussian. Such averages of the Wigner function over phase-space are non-negative and denoted Husimi distribution function H_ψ on phase-space [186, 187]

$$H_\psi(x,k) = \frac{1}{2\pi} \left|\langle \phi_{xk}|\psi\rangle\right|^2, \tag{7.7}$$

where $|\phi_{xk}\rangle$ is a coherent state with squeezing represented by $\tilde{\sigma}$ with momentum space wavefunction [188, 189]

$$\langle p'|\phi_{xk}\rangle = \frac{1}{\pi^{1/4}\sqrt{\tilde{\sigma}}} \exp\left(-\frac{(k-p')^2}{2\tilde{\sigma}^2} - ixp'\right). \tag{7.8}$$

Moreover, the proposed criterion (7.3) in [183] is discussed for the temporal extent of the backflow, and the right-moving state ψ in momentum space has time-dependence

$$\tilde{\psi}(p,t) = e^{-ip^2t/2}\tilde{\psi}(p), \tag{7.9}$$

and the corresponding position space wavefunction

$$\psi(x,t) = \frac{1}{\sqrt{2\pi}} \int_0^\infty dp\ \tilde{\psi}(p)\ e^{i(xp-p^2t/2)}. \tag{7.10}$$

In [190], Barbier and Goussev made a numerical comparison of the criterion (7.3) with the standard criterion in the situation of a free particle described by a right-moving state that was first introduced by Bracken and Melloy in [6]. Their result shows that the experiment-friendly criterion may fail to indicate the presence of backflow if the

measurement apparatus is not sufficiently precise in momentum space. More specifically, $\tilde{\sigma}$ has to be sufficiently small such that the experiment-friendly criterion can be in agreement with the standard criterion. The reason for that can be seen from (2.9), where the first estimation comes from the integration in the interval $k \in (-\infty, 0)$. Note that the convolution with the test function g in (2.10) is related to the overlap between ψ and the squeezed coherent state in (7.7), and both g and ϕ have same normalization. Coherent states saturate the uncertainty principle $\Delta\hat{X}\Delta\hat{P} = 1/2$, but squeezed coherent states saturate the uncertainty relation while reducing the uncertainty in momentum and increasing the uncertainty in position. In fact, criterion (7.3) is using the estimation obtained in (2.11) to reduce the negativity of the backflow. In both cases, the inequalities involve the estimation of the portion of an integral arising from $k < 0$. Specifically, the spatial smearing with the Gaussian function $f = g^2$ plays the role, in momentum space, of the overlap (7.7) between ψ and a coherent state with squeezing represented by $\tilde{\sigma}$ and centered on x, k. As an illustrative example, we can consider the particular right-moving state introduced in [6]

$$\tilde{\psi}(p) = \begin{cases} 0 & p < 0, \\ \\ \dfrac{18p}{\sqrt{35K}}\left(e^{-p/K} - \frac{1}{6}e^{-p/2K}\right) & p > 0, \end{cases} \tag{7.11}$$

where K is a positive constant that has physical dimension of momentum. The corresponding wavefunction, at time $t = 0$, in position space is given by

$$\psi(x, 0) = 18\sqrt{\frac{K}{70\pi}}\left(\frac{1}{(1 - iKx)^2} - \frac{2}{3(1 - 2iKx)^2}\right), \tag{7.12}$$

and the probability current density at the origin

$$j_\psi(0, 0) = -\frac{36K^2}{35\pi} < 0, \tag{7.13}$$

all in natural units such that $\hbar = m = 1$. The probability flux can be made arbitrarily negative at a particular point by suitably choosing the constant K. In a region of backflow, it is, therefore, expected that $j_\psi(a) < \int dx f(x) j_\psi(x)$ with the spatial Gaussian test function centered at $x_0 = a$ and width σ. Using the first estimation (2.11), the inequality, at $t = 0$, can be written in the following form

$$j_\psi(a) < \int_{-\infty}^{0} \frac{dk}{2\pi} k \ \left|\widetilde{(M_g\psi)}(k)\right|^2 \leq \int dx \ f(x) j_\psi(x). \tag{7.14}$$

In particular, setting $a = 0$ and noting that g is related to ϕ in (7.5) by a simple substitution $\sigma \mapsto \sigma/\sqrt{2}$, the term $\left|(\widetilde{M_g\psi})(k)\right|^2$ is essentially the Husimi function (7.7) $H_\psi(0,k)$ with the squeezed coherent state centered on $0, k$. Thus, the above inequality has an equivalent form in terms of the non-negative Husimi function

$$j_\psi(0) - \int_{-\infty}^{0} dk\ kH_\psi(0,k) < 0 \leq \int dx\ f(x)j_\psi(x) - \int_{-\infty}^{0} dk\ kH_\psi(0,k), \tag{7.15}$$

where the first part of the inequality corresponds to the criterion (7.3). In the extreme limiting case in which $\tilde{\sigma} \to 0$, the integral involving the Husimi function tends to zero, and the experiment-friendly formulation reduces to the standard formulation in which $j_\psi(0) < 0$. Note that, if $\tilde{\sigma}$ is not small enough, the proposed criterion can fail to identify the presence of backflow for a given right-moving state ψ because the integral becomes very negative. Nevertheless, the negativity of the probability flux (7.13) could compensate the effect of $\tilde{\sigma}$ by choosing sufficiently large K such that $j_\psi(0)$ is even more negative. That is in agreement with the fact that $\beta_V(f) \approx 0$ when the test function f has a sufficiently large width σ. Equivalently, as showed in [190], in the limit that $\tilde{\sigma} \to 0$, the Bracken-Melloy bound $\Delta_{BM} \approx 0.038$ is obtained because the experiment-friendly criterion reduces to the standard criterion. Thereby, the issue with (7.3) is that, although it can remove negative fluxes from backscattering, it also removes genuine backflow from the superposition of right-moving states. In the scattering situations in the presence of defects located at the origin, one can restrict ψ to the wavefunction u because the backscattering is limited to the region $x < 0$, and the region $x > 0$ has only right-moving states represented by wavefunction v. However, u is composed of an (right-moving) incoming asymptote and a reflection part as well. At the defect position, all contributions overlap, and it is not clear how to isolate the genuine backflow contribution.

Let us take the example of a single δ-defect with kernel given by (3.9). The kernel has five terms where just the last term, the fifth term, has support at the right of the defect, $x' \in (0, \infty)$, and the other terms have support at the left of the defect. In particular, the first term is a contribution purely from the incoming asymptote that is a right-mover. Hence, second, third and fourth contributions involve a reflection coefficient. If we deliberately[1] remove contributions from the backscattering, we can have a rough idea

[1]That could be represented by a complex potential function or an absorbing boundary. See [191, 44, 45] in connection with arrival times and backflow.

on how the contributions are summed up together. For instance, for the case of a δ-defect with $\lambda = -0.5$, we remove the fourth contribution, which arises entirely from the reflection coefficient, to the Kernel and, separately, we remove the second and third contributions that involve reflection and the right-mover incoming. The results for $\beta_V(f)$ against the position of measurement x_0 are plotted in figure 7.1 below. Note that

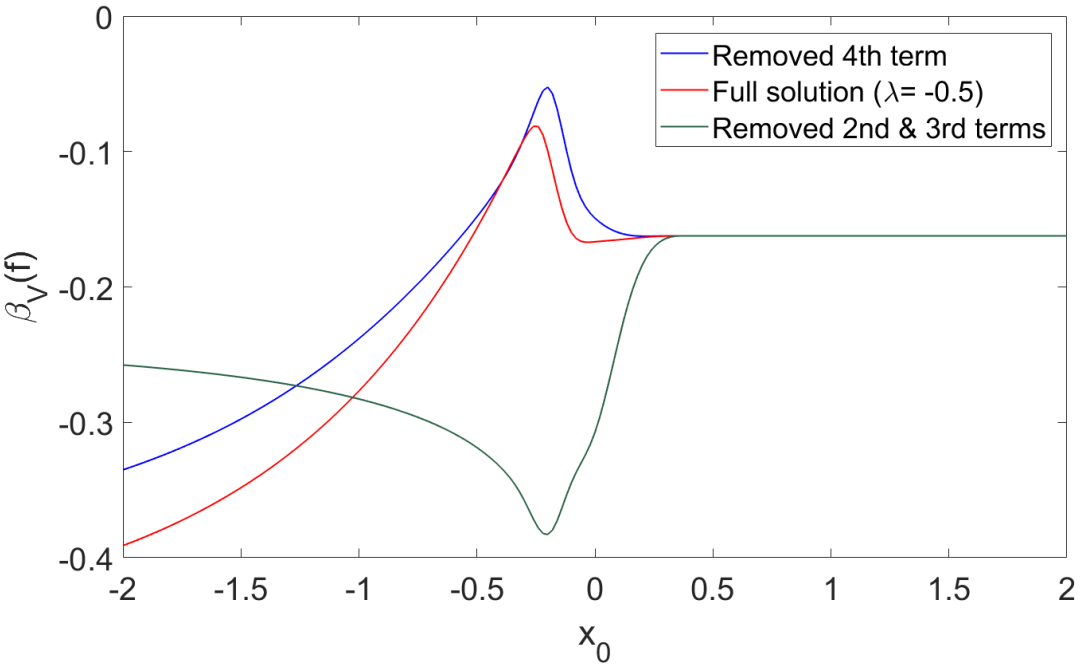

Figure 7.1: Lowest backflow eigenvalue of the current operator for the δ-defect. **Red** refers to the full calculation without subtracting any term, **blue** refers to the result without the fourth contribution, and **green** refer to the result without second and third contributions. Parameters: $P_{\text{cutoff}} = 60$, $N = 600$, $\lambda = -0.5$.

the fourth contribution composed entirely from the reflection coefficient has a negative contribution and it makes the backflow constant less negative when it is removed, while the second and third terms in (3.9) can have a positive contribution to the probability current. Clearly, in general scattering situations with reflection, adjusting the backflow criterion so that it could be possible to distinguish backscattering contributions from the (right-movers) backflow would be a primary goal of future work in this direction.

7.2 PART 2: CONCLUSIONS

This thesis has explored the quantum backflow effect in the presence of defects. These two topics were not previously examined in combination. For that, we mainly focused on two point defects describing different situations: the δ-defect and the jump-defect.

Quantum backflow is an effect that was first discovered as a constraint on the temporal extent of the probability current in interaction-free situations described by the Schrödinger equation. Later, it was also shown to have bounded spatial extent. Specifically, there are lower bounds on the temporal and spatial averages of the probability fluxes. The existence of lower bounds was extended to include backflow in scattering situations with short-range potential functions $V \in L^1_1(\mathbb{R})$ in the Schrödinger equation. While this phenomenon has origin in the context of wavefunctions from quantum mechanics, its formulation in terms of time or space-averages with a non-negative weight function is closely related to quantum energy inequalities in quantum field theory that were established for several theories including scalar, spin-$\frac{1}{2}$ and spin-1 free fields in globally hyperbolic spacetimes. Nonetheless, for interacting theories, these state-independent inequalities may not hold. More generally, all quantum inequalities (backflow included) may well have origin in common grounds, such as the uncertainty principle, and be related. Thus, understanding on the behaviour of the lower bounds in interacting theories is certainly needed at the level of quantum fields and wavefunctions as well. A general type of interaction that can possibly be implemented in any field theory is a defect, which is a kind of internal boundary at a particular point x_D linking a field in the region $x_D < 0$ with a field in the region $x_D > 0$.

The main feature of any defect is the presence of a discontinuity that can be less or more severe depending on the case of interest. In electromagnetism, for instance, the normal component of the electric field has a jump discontinuity across a surface charge. Discontinuities are ubiquitous in physical applications, and their inclusion into mathematical models constitutes a vast arena for the discussion of many important questions such as conservation laws.

δ-defects are very well-known as an interaction whose potential function V is given in terms of Dirac δ-distributions although it has the alternative formulation in terms of sewing conditions at a point. While equivalent, this formulation allows the inclusion of more general interactions that are not described by an explicit potential function and is

closely related to other structures such as boundaries and more general defects. In an integrable model, the introduction of these additional structures will, in general, spoil the integrability of the theory. That is the case of the δ-defect when considered, for example, in the non-linear integrable sine-Gordon equation. Integrability is usually associated with the existence of infinitely many conserved charges and it is trivial for linear theories, such as the linear Schrödinger equation. However, even in linear theories, defects may cause the breakdown of one or more conservation laws indicating that it is not an integrable defect in the sense of preserving integrability. In particular, conservation of total energy and momentum work as a good indicator of that. Requiring conservation of momentum in the presence of a defect places strong constraints on the defect conditions that are relatively equivalent to the restrictions imposed by integrability [116]. If momentum and energy cannot be conserved in the presence of a defect, we expect that it will generally spoil the integrability of a theory. In the case of the δ-defect, momentum cannot be conserved neither in the Schrödinger equation nor in the Dirac equation, as shown in previous chapters. In fact, the requirement of integrability for interacting field theories poses strong constraints on the existence of such defects, and it was shown that, when they exist, they are either purely reflecting (an integrable boundary) or purely transmitting [12, 112]. The δ-defect, which is largely used to describe numerous physical situations, has a mixture of reflection and transmission and also serves as a model for other distinct defects that are constructed upon it, the Dirac-Kronig-Penney model and the δ'-defect, for instance. An interesting new observation for the backflow in the presence of a δ-defect is the existence of a maximum of the lowest backflow eigenvalue $\beta_V(f)$ that seems to peak for the defect parameter $\lambda = -1/2$, figure 3.5 has a clear illustration of this behaviour. That indicates how the presence of bound states may affect the backflow constant, and it is worth seeking an explanation behind the existence and the location of maxima. Although bound states are very different from scattering states, there are some connections. Levinson's theorem, for example, relates the number of bound states to the number of positive energy states lost in the presence of interaction when compared to the free case, and to time delay [192]. The other examples of defects analysed in this thesis give indeed more insight into that matter. However, the absence of reflection makes it much clearer.

We also investigated the double δ-defect for distinct situations corresponding to the symmetric ($\lambda_1 = \lambda_2$), anti-symmetric ($\lambda_1 = -\lambda_2$) and the more general asymmetric

($|\lambda_1| \neq |\lambda_2|$) case, where λ_1 refers to the first defect parameter associated with the first delta and λ_2 refers to the second defect parameter. Double δ-defects support resonances and total transmission, although the total transmission does not occur for all energies. In fact, the results (see chapter 3) for the backflow constant in the presence of double δ-defects are more intricate. Firstly, we mention the case of a pair of identical deltas in figure 3.11. Note that the the result in the region $x_0 > 0.5$ is very similar to the case of a single delta in the corresponding region $x_0 > 0$, but there are two maxima in the region $x_0 < 0.5$ in correspondence with the possible existence of two bound states. Secondly, the pair of opposite deltas depicted in figure 3.23 shows a very distinct behaviour in the region between the defects ($-0.5 < x_0 < 0.5$). Decreasing the distance between the deltas, which can be seen in figure 3.24, suppress the complicated behaviour of the backflow constant in the middle region whilst connecting the outer regions. We expect that these are scattering effects interfering with the negative backflow currents. In order to further explore that in section 3.4.3, we considered a general general asymmetric pair of deltas when the second defect is stronger than the first ($|\lambda_2| = 2|\lambda_1|$) and when the second dect is much stronger than the first ($|\lambda_2| = 10|\lambda_1|$). The results suggest that strong effects from scattering can greatly change the behaviour one might expect solely based on whether the interaction is attractive or repulsive. Also, very small or very large values of the defect parameter do not result in very intricate behaviours. That can be expected from the fact that very small values of the defect parameter are small perturbations of the free case, and very large values become perfectly reflecting walls.

From a pair of deltas, we also discussed the δ'-defect as a point dipole interaction and found, for small values of $|\lambda|$, a similar bell-shape, figure 3.16, of the backflow constant to the case of a jump-defect with small $|\alpha|$ in figure 4.2. Moreover, despite the discordance between the definitions of that interaction in the literature, we remarked in section 3.4.2 that the backflow results do indicate a situation where partial transmission is possible, rather than only a perfectly reflecting wall corresponding to a boundary.

The jump-defect, in contrast to the δ-defect, is a purely transmitting integrable defect that allows the conservation of momentum and energy. In the context of quantum mechanics, it does, after suitable modification, preserve the conservation of the probability current, total energy and total probability. It is a topological defect in the sense that it can be placed at any point of the real line and, when taking its contribution into account, will neither cause a breakdown of the space-translation symmetry nor

the time-translation symmetry. Nevertheless, jump-defects are not characterized by any explicit known potential function term that can be added to the Hamiltonian of a physical system, but they are described by a set of sewing conditions defined at a point instead. An interesting fact is that these conditions have the form of frozen Bäcklund transformations. While, at the moment, there is no known physical system described by this set of conditions, the jump-defect has a very physical motivation as a guiding principle, namely, the conservation of momentum, energy and probability. Generalized point defects described by (2.27) can be obtained by considering self-adjoint extensions of the Hamiltonian operator or, equivalently, the enforcement of probability conservation. For the jump-defect, that is not enough, and the probability current has also to be adjusted for the purpose of being conserved. We obtained the analytical expression for the integral kernel of the operator current used for the numerical analysis in the jump-defect and in the δ-defect as well, but the origin ($x = 0$) is a special point where distinct discontinuities are represented by also distinct sets of sewing conditions, and that was properly taken into account when the full real line was split into a pair of domains. Moreover, the backflow effect is spatially constrained in the presence of a jump-defect due to the existence of the lowest eigenvalue associated with the probability current operator, even though a jump-defect has no explicit potential function to be classified in the $L_1^1(\mathbb{R})$-class. Because jump-defects are purely-transmitting, there is no backscattering contribution to the backflow and, therefore, they provide an ideal interacting model to isolate the backflow effect in contrast to the δ-defect, which has an unavoidable backscattering contribution to the backflow constant $\beta_V(f)$. Indeed, we explored in details the effect of a reflection term for the backflow constant in the case of the δ-defect. Observe that $\beta_V(f)$ for $x_0 < 0$ becomes increasingly more negative as $|\lambda|$ increases. In other words, $\beta_V(f)$ becomes progressively smaller than $\beta_0(f)$. In the case of the jump-defect, for either the non-conserved current or the conserved current, $\beta_V(f)$ is never very small for large values of $|\alpha|$ in comparison with the δ-defect case, but becomes less negative when $|\alpha|$ is large enough. A surprising result is that the backflow effect can be larger than in the free case at the defect location, even though the jump-defect behaves similarly to an attractive potential (presence of bound states) for both positive and negative values of α, while the (attractive) Pöschl-Teller has a smaller backflow effect inside the interaction region. It is worth remarking that, for all sets of parameters explored in section 4.3, the non-conserved probability current

in the presence of a jump-defect has lowest eigenvalue bounded below by the bound proved [7] in the interaction-free situation, namely, $\beta_0(f) \geq -0.995$ when weighted with a Gaussian function f given by (4.43) with $\sigma = 0.1$. Although we do not expect this to hold true for all possible sets of parameters in the numerical analysis, it shows that the backflow in the case of the jump-defect does not deviate much from the interaction-free case, yet it is non-trivial. In fact, even taking into account the contribution from the defect for the conserved probability current, $\beta_V(f)$ does not become very negative regardless of the value $|\alpha|$. For making possible the comparison of our numerical results of the non-conserved probability current with the case where its conserved, we modified the integral kernel of the probability current operator by adding the contribution purely from the defect, which has support only at the defect location. Although it does not drastically change the magnitude of the backflow constant, it has the effect of developing pronounced bumps in comparison to the non-conserved case, which can be seen, for example, in the result illustrated by figure 4.6. Observe that a defect connects a field in $x < 0$ (considering a defect located at the origin) to its Bäcklund transformed field in $x > 0$. The adjustment term, which is proportional to the test function evaluated at the defect location, in (4.31) is responsible for the conservation of the probability current and it seems to be connecting the two bound state solutions at the origin. The pair of bound states (4.40) is disconnected (either on the left or on the right of the defect) at the origin, but the defect contribution to the total momentum of the system is responsible for the extra term in (4.31), which has both poles and is proportional to $f(0) \neq 0$.

Another interaction that is reflectionless for all values of the incident energy is given by the Pöschl-Teller potential (1.2) with integer μ, which is similar to the jump-defect in this respect, although the former is extended and the latter is a point defect. Note that the (transparent) Pöschl-Teller has its parameter μ constrained to be a positive integer, whereas the jump-defect parameter α assumes positive and negative real values. Pöschl-Teller has a finite number of bound states given by μ with energy $E_n = -(\mu - n)^2/2$, $n \in \mathbb{N},\ 0 \leq n < \mu$. From our observations on both the δ-defect and the jump-defect, we can conjecture that the number of maxima in the backflow constant is less or equal to the maximum number of bound states supported in the corresponding interacting theory. In particular, that conjecture is supported by the cases investigated in this thesis. While the presence of backscattering can make the analysis more complicated,

reflectionless interactions provide better examples to illustrate the point. To show some further evidence for that, we look at the backflow constant averaged with the same Gaussian function f against the position x_0 of measurement for the Pöschl-Teller potential, and these can be found in the Appendix A. Note that the plots are symmetric with respect to x_0 due to the total transmission for integer values of μ, and $\beta_V(f)$ approaches $\beta_0(f)$ far away from the interaction region. For comparison, the non-integer cases where $\mu = 1.5$ and $\mu = 2.5$ are provided as well. We remark that there is one maximum for $\mu = 1$ and two maxima for $\mu = 2$. We show that the pattern repeats for larger integer values of μ in figure A.3, where the number of maxima increase with the number of possible bound states. However, as μ increases, two of these maxima are distorted becoming more distant from the others that approach the value zero for the backflow constant (more on that in Appendix A). Note that similar effect happens in the case of the δ-defect, supporting a single bound state with energy $E = -\lambda^2/2$, when $|\lambda|$ increases, and the single maximum becomes progressively less noticeable as the backflow constant approaches zero for $x_0 > 0$. In fact, the modified Pöschl-Teller potential [30, 193, 194] given by $V = -\alpha^2\mu(\mu+1)/2\cosh^2(\alpha x)$ is related to the Dirac delta in the limit $\alpha \to \infty$, where the bound state energy for a Dirac delta potential is obtained from the ground state of the modified Pöschl-Teller potential [195].

To look into more details in regard to the behaviour of $\beta_V(f)$ in relation to the value of $\beta_0(f)$, analytic perturbation theory was applied in chapter 5 considering the interaction as a perturbation in formal power series of the potential strength, λ in the case of the δ-defect and α in the case of the jump-defect. In particular, the first order perturbation correction to the backflow constant was calculated for small values of the potential strength and compared to the exact calculation, which does not involve any perturbation methods. As for the δ-defect, the result of the first order approximation is very satisfactory for very small values of $|\lambda|$ although it was not possible to reproduce the maximum value of $\beta_V(f)$ that occurs in the attractive case, for example at $\lambda = -1/2$. Despite the fact that the first order perturbation for very small values of $|\alpha|$ satisfactorily reproduced the results of the jump-defect, the backflow constant rapidly becomes negative when $|\alpha|$ increases in the region $x_0 > 0$. The same does not happen in the region $x_0 < 0$ as there is no reflection coefficient to be approximated by means of a perturbation method. The contribution term from the defect was analysed separately in figures 5.8, 5.9 and 5.10 where this issue does not

occur, and, therefore, the approximation of the term coming from the bulk $x_0 > 0$ and involving the transmission coefficient is responsible for causing that.

We restricted our analysis to the first order perturbation, but considering the second order requires addressing an issue with the power series expansions in low-energy scattering because the Born approximation is not reliable at low energies. More precisely, the free resolvent of the Hamiltonian operator in one dimension has a singularity at $k = 0$. This infrared divergence is not present in the exact calculation for the examples explored in this thesis. The δ-defect has a transmission coefficient $T(k) \to 0$ as $k \to 0$, and the jump-defect has $T(k) \to -1$ as $k \to 0$. Hence, this topic requires a proper treatment. Some Hilbert space analysis of low-energy scattering was studied in [196, 197, 198, 199, 200] for short-range and medium-range real potentials in the Schrödinger equation. More recently, an alternative treatment for low-energy scattering with short-range potentials in one dimension was elaborated in [201]. However, these are Laurent expansions around $k = 0$ for the transition operator and the scattering amplitude, and the perturbation series aims at expanding a perturbation in terms of the potential strength λ instead. Further work in this direction would be more enlightening in establishing a relation between $\beta_0(f)$ and $\beta_V(f)$ by means of taking into account second order perturbation terms. In practice, that could be helpful in optimizing lower bounds.

Another question examined in this thesis was how a particle with an internal degree of freedom is affected with regard to the backflow effect in the presence of defects. The backflow for a Dirac current was analysed before, but only in the free case and for its temporal extent. More specifically, in chapter 6, we considered the Dirac equation for a spin-$\frac{1}{2}$ particle with an electrostatic δ_e-defect and with a mass-like δ_m-defect. As consequence of that, we found that a fermionic spin, understanding the Dirac equation as the description of a massive particle of spin-1/2, reduced the negativity of the backflow constant in interaction-free situations from $\beta_0(f) \approx -0.24$ to the value $\beta_0(f) \approx -0.02$ with the same choice of test function f. Moreover, taking a very small width $\sigma = 0.001$ increased the amount of backflow to $\beta_0(f) \approx -0.06$, but that is still very limited, and it has to do with the fact that the speed of light is constant. Note that $|j_\psi(x,t)| \leq c\rho_\psi(x,t)$, and we effectively set $c = 1$. The opposite, taking a larger width $\sigma = 1.0$, decreased the amount of backflow to $\beta_0(f) \approx -0.001$, as expected. The results for an electrostatic δ_e-defect, which is never purely reflecting, point to a periodic probability current lowest eigenvalue in the defect parameter λ and can be seen in

figure 6.5. The mass-like δ_m-defect shares more similarities with the single δ-defect in the Schröndinger equation although a very distinct behaviour is worth noting: the backflow constant $\beta_V(f)$ for the attractive case is, in general, more negative than the $\beta_V(f)$ for the repulsive case in the left region $x_0 < 0$, expect for negative values of x_0 that are close enough to the defect location, where the attractive case rapidly becomes less negative than the repulsive case as one would expect, see figures 6.4 and 6.7.

Despite our attempt in section 6.9, it was not possible to include a jump-defect in the Dirac equation in order to compare with the results of a jump-defect in the Schrödinger equation. The reason lies in the fact that it might be possible that the jump conditions are too stringent on a first-order differential equation with commuting field variables. Note that the Dirac equation is already a Bäcklund transformation for the Klein-Gordon equation [202]. Considering the Grassmanian case is certainly a possibility for future work, but that is perhaps more interesting in the context of supersymmetric quantum mechanics. Other than a defect, transparent potentials constructed by means of an inverse scattering problem [173] present a possible alternative way, beyond a free theory, to enforce right-moving states in the Dirac equation .

There are several avenue for future work following the results discussed in this thesis. Some are straightforward as including a double δ-defect in the Dirac equation and, even more interesting, including a double jump-defect in the Schrödinger equation. We investigated a type I jump-defect, constructing a type II jump-defect gives one more parameter accounting for an internal degree of freedom of the defect and could bring different aspects to the results on backflow. A combination of the double δ-defect with a Pöschl-Teller potential in the middle would be very interesting as well, specially in the regime of impenetrable walls represented by Dirichlet boundary conditions. Another avenue would be the implementation of a jump-defect with Grassmannian variables in the Dirac equation as we did not find a suitable set of sewing conditions with commuting variables. That would provide a purely reflecting situation in the Dirac equation to have its backflow analysed and compared to the results in the Schrödinger equation.

There are new directions as well to be considered. The probability current in quantum mechanics with finite-dimensional Hilbert spaces was previously studied in the context of the thermodynamics of open quantum system in [203]. It would be useful to investigate the appearance of backflow in the discrete space setting and understand how it relates to thermodynamic heat and work. Also, one can take this same direction

further by making time discrete [204] and understanding how the phenomenon of backflow changes with the structure of space and time.

The lack of optimal bounds, even in interaction-free situations, is an invitation to the very useful task of finding optimal bounds for the backflow constant. If that could be achieved with the analytic perturbation method applied in chapter 5, it is unclear how bound state contributions would be accounted for. Nevertheless, the issue of low-energy divergences in the perturbation power series has to be addressed in order to properly characterize higher orders of approximation beyond that of a first order. An experimental scheme to detect backflow was proposed in [205], yet it was not observed experimentally. Lower bounds restricting the temporal and spatial extent of the effect are known, at least in the free case, but a possible relation between them is missing.

Ultimately, the discovery of deeper connections between the different quantum inequalities would be an ambitious achievement leading to a much clearer understanding on the existence of negative lower bounds on classically positive physical observables.

— A —

Results in the Pöschl-Teller case

Plots of the backflow constant averaged with a Gaussian function against the position of measurement x_0 in the case of a Pöschl-Teller potential (1.2)

$$V(x) = -\frac{\mu(\mu+1)}{2\cosh^2 x}, \quad \mu > 0,$$

commonly used in molecular and solid-state physics, are provided below. For reference, we reproduce the result from [11] corresponding to the value $\mu = 1$ but also include other values not previously published. All these can be calculated by numerically solving the Schrödinger equation using their Java code. In all plots of this appendix, $N = 1000$ and $P_{\text{cutoff}} = 100$. Also, the Gaussian has a fixed width $\sigma = 0.1$. In the last chapter, it was said that, as μ increases, two maxima are distorted moving away from the others maxima. It is perhaps worth remarking that increasing the momentum cutoff P_{cutoff} slightly moves these two distorted maxima towards the others. This observation was not investigated enough and requires more data to be checked.

It is well-known that the Pöschl-Teller potential corresponds [206, 207] to multi-soliton solutions of the Korteweg–de Vries equation (KdV) and that it is reflectionless for integer values of the parameter $\mu > 0$. It also has a finite number μ of bound states with negative energy and a critically bound state [208, 209] with zero energy for positive integer μ. See [210] for an interesting connection of group theory with both its scattering and bound states.

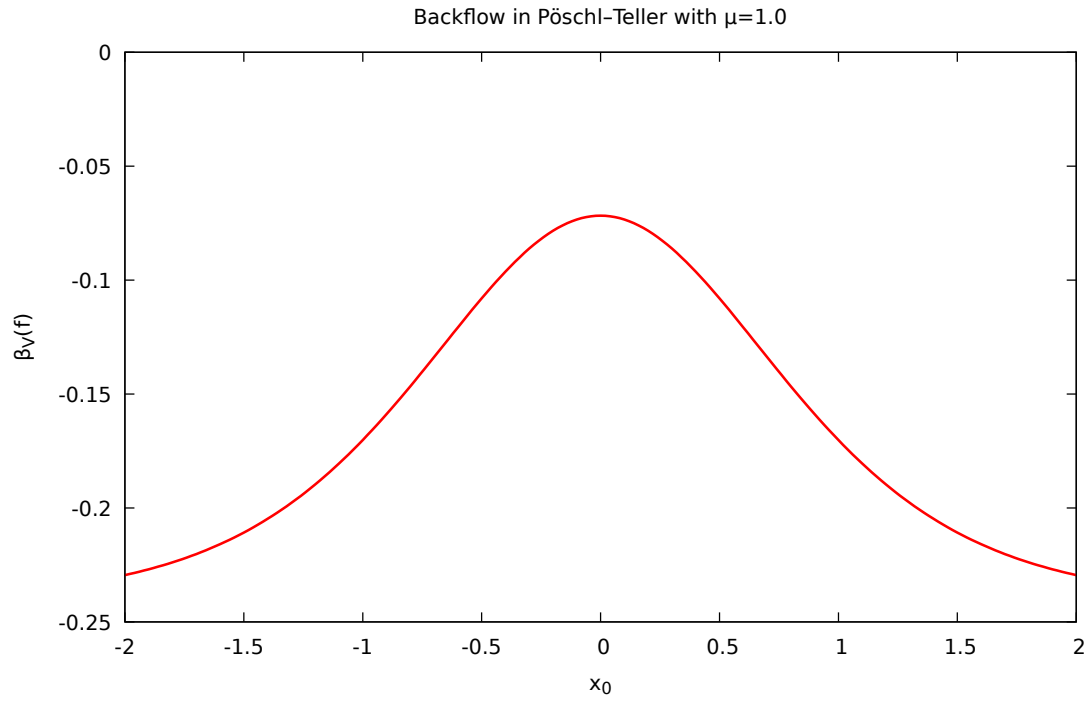

(a)

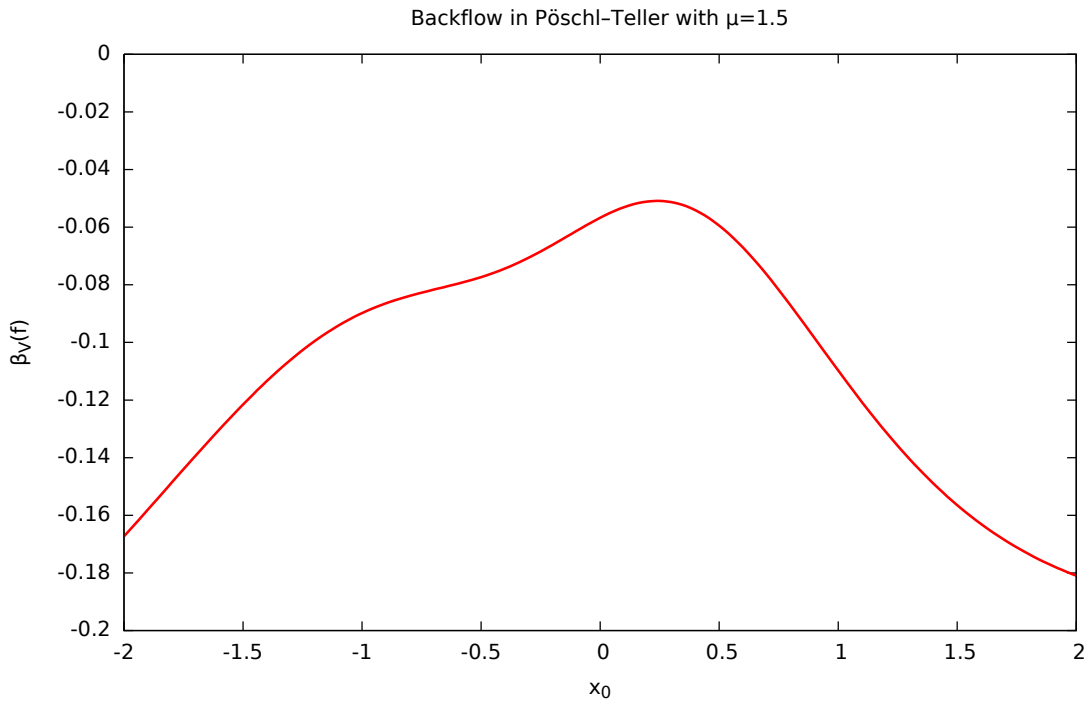

(b)

Figure A.1: Lowest backflow eigenvalue of the current operator (a) $\mu = 1.0$ (b) $\mu = 1.5$.

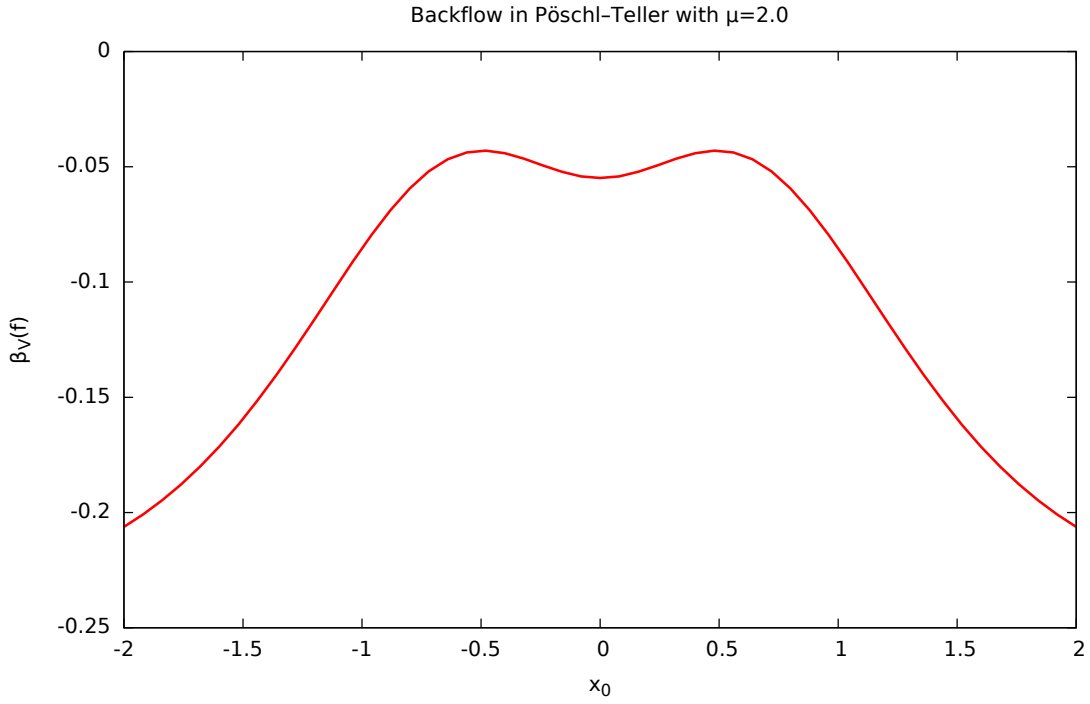

(a)

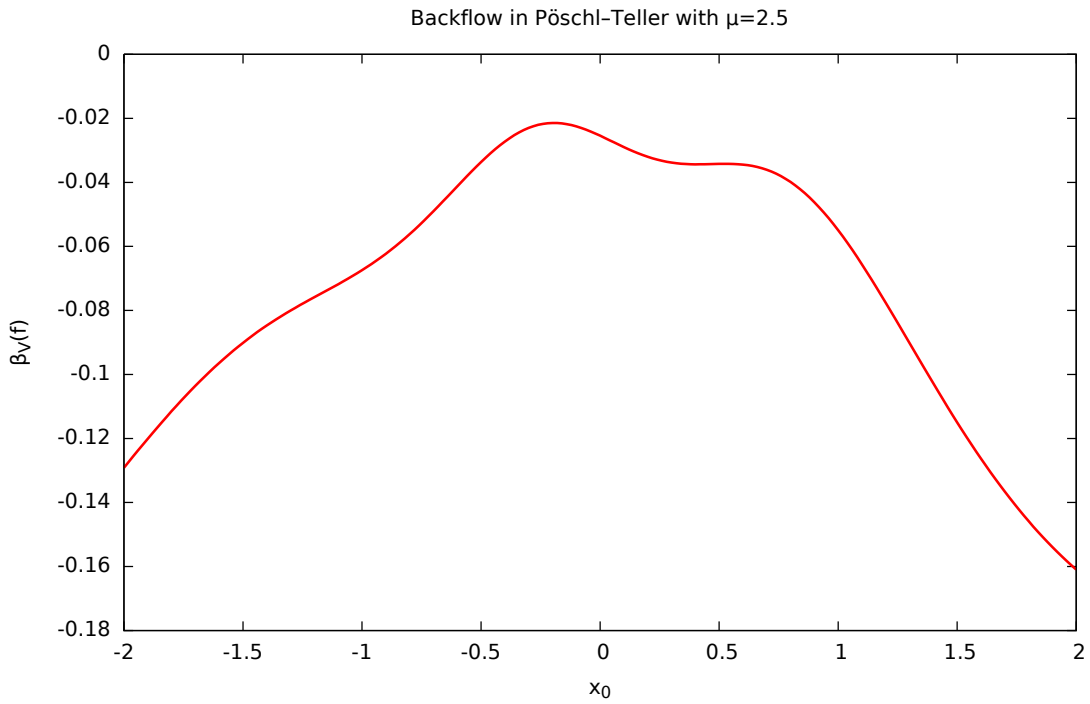

(b)

Figure A.2: Lowest backflow eigenvalue of the current operator (a) $\mu = 2.0$ (b) $\mu = 2.5$.

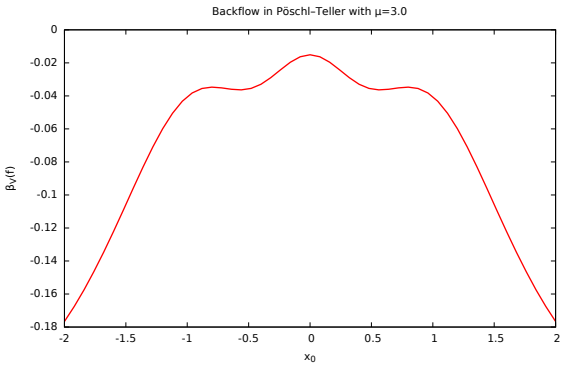

(a) $\mu = 3$

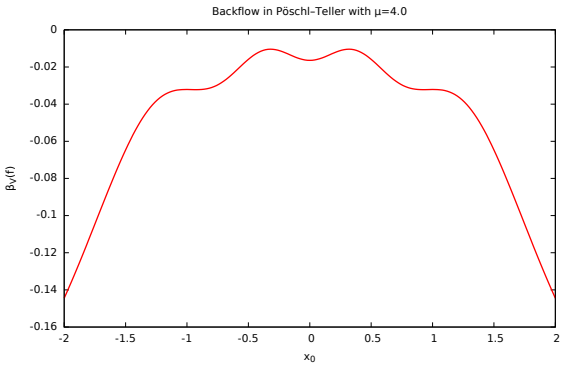

(b) $\mu = 4$

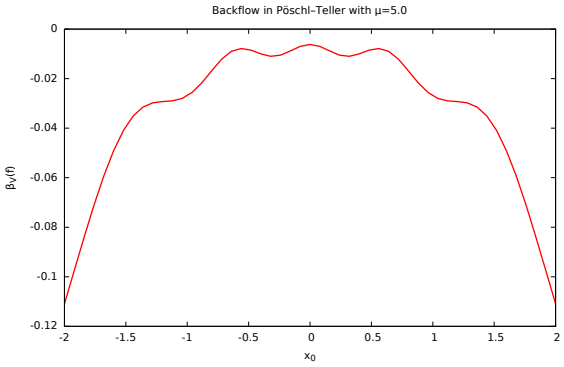

(c) $\mu = 5$

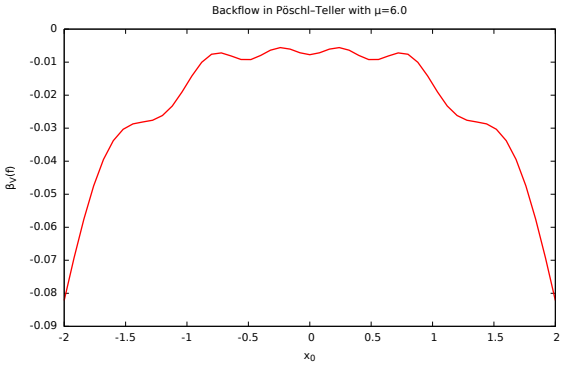

(d) $\mu = 6$

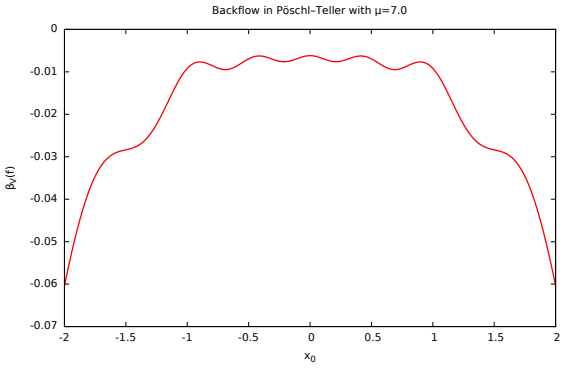

(e) $\mu = 7$

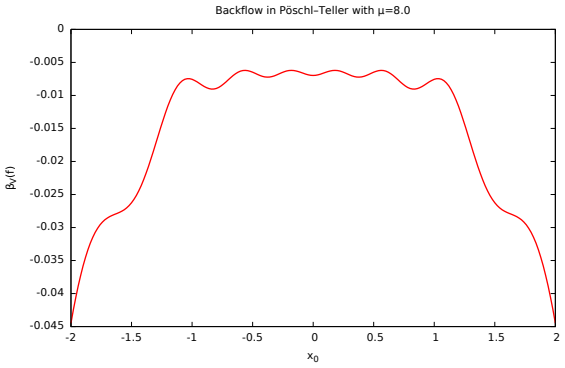

(f) $\mu = 8$

Figure A.3: Lowest backflow eigenvalue of the current operator from $\mu = 3$ to $\mu = 8$.

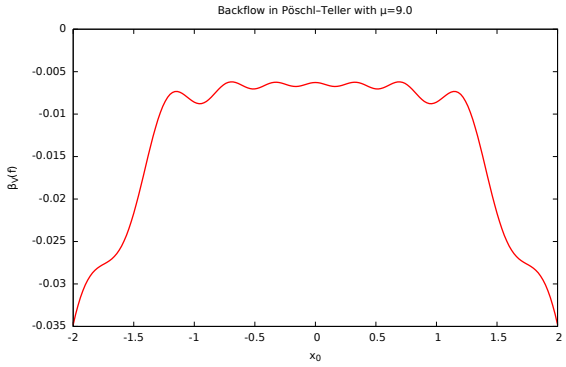

(a) $\mu = 9$

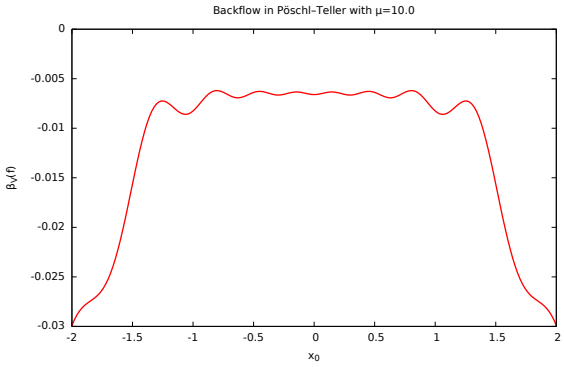

(b) $\mu = 10$

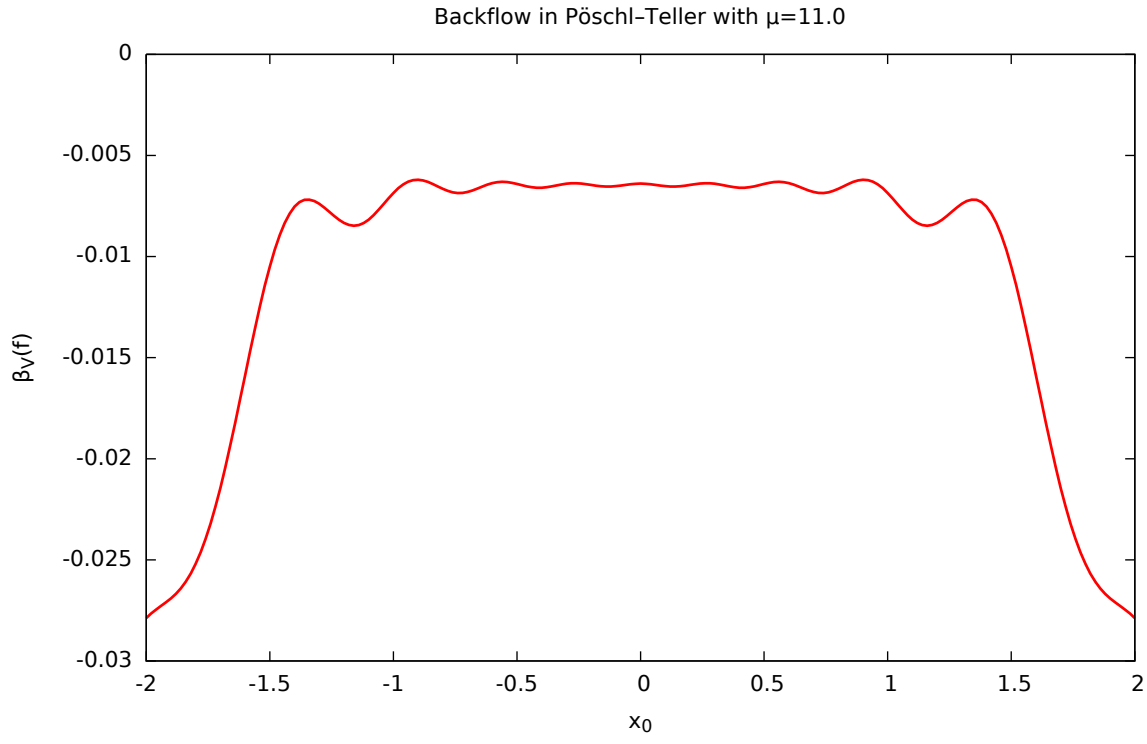

(c) $\mu = 11$

Figure A.4: Lowest backflow eigenvalue of the current operator from $\mu = 9$ to $\mu = 11$.

— B —

Different choices of weight functions

We also illustrate the backflow constant in the presence of a jump-defect with different choices of weight functions other than a Gaussian, which is given here again for convenience of the reader. Specifically, our choices for the Gaussian, the squared Lorentzian and the rectangular function are, respectively,

$$f(x) = \frac{1}{\sigma\sqrt{2\pi}} \exp\left(-\frac{(x-x_0)^2}{2\sigma^2}\right), \tag{B.1}$$

$$f(x) = \frac{2\sigma^3}{\pi((x-x_0)^2+\sigma^2)^2}, \tag{B.2}$$

$$f(x) = \frac{[\theta(x-x_0+a)-\theta(x-x_0-a)]}{2a}, \tag{B.3}$$

with widths $a = 0.5$, $\sigma = 0.1$ and center x_0. Note that each of these functions has unit integral, and we integrate the Gaussian and the squared Lorentzian in the interval $x \in [x_0 - 8\sigma, x_0 + 8\sigma]$. The rectangular function is compactly supported, but it is not C^∞ (it is even not in the Sobolev space $H^1(\mathbb{R})$), therefore, it is not really a test function. Nonetheless, it corresponds to the uniform distribution and is considered in the numerical analysis for comparison with the other weight functions.

The backflow constant averaged with the squared Lorentzian function has results, figure B.1(a), B.2(a), B.3(a) and B.4(a), that are qualitatively similar to those obtained in the case of averaging with a Gaussian without any change in the number of bumps. In particular, the free value decreased to $\beta_0(f) \approx -0.30$, but this is to be expected

with a different choice of test function. The squared Lorentzian centered at the origin ($x_0 = 0$) has Fourier transform

$$\tilde{f}(k) = \frac{1}{\sqrt{2\pi}}(1 + \sigma|k|)\exp(-\sigma|k|), \tag{B.4}$$

in contrast to the Fourier transform of a Gaussian centered at the origin

$$\tilde{f}(k) = \frac{1}{\sqrt{2\pi}}\exp\left(-\frac{1}{2}k^2\sigma^2\right). \tag{B.5}$$

For the rectangular function, figures B.1(b), B.2(b), B.3(b) and B.4(b), it is quite noticeable the presence of some ripples, specially for higher values of $|\alpha|$, in the graphs depicting the behaviour of the backflow constant. In fact, these are consequence of choosing a weight function f that is not continuous. Lorentz spatial averaging produces similar results with steplike form in the context of electromagnetism [211]. In the case of the conserved probability current, it does not seem to have the ripples, and the reason may be that the extra contribution from the jump-defect, a term proportional to $f(0)$, counterbalance the discontinuities of f. Nonetheless, these edge effects are unavoidable at $|x_0| = a = 0.5$. The backflow constant in the free case was further reduced in comparison with previous examples to $\beta_0(f) \approx -0.63$. The rectangular function centered at the origin has Fourier transform

$$\tilde{f}(k) = \frac{1}{\sqrt{2\pi}}\frac{\sin(ka)}{ka}. \tag{B.6}$$

In all examples provided, the momentum cutoff was set to $P_{\text{cutoff}} = 200$, but we have to mention that the backflow constant spatially averaged with a rectangular function further decreased when the cutoff was increased ($P_{\text{cutoff}} = 250$, $P_{\text{cutoff}} = 300$ and $P_{\text{cutoff}} = 500$) in numerical results not included in this thesis. Hence, the results are not stable, and the rectangular function is not a satisfactory weight function as expected from its smoothness properties. It is known that the smoothness of a function is related to the decay properties of its Fourier transform.

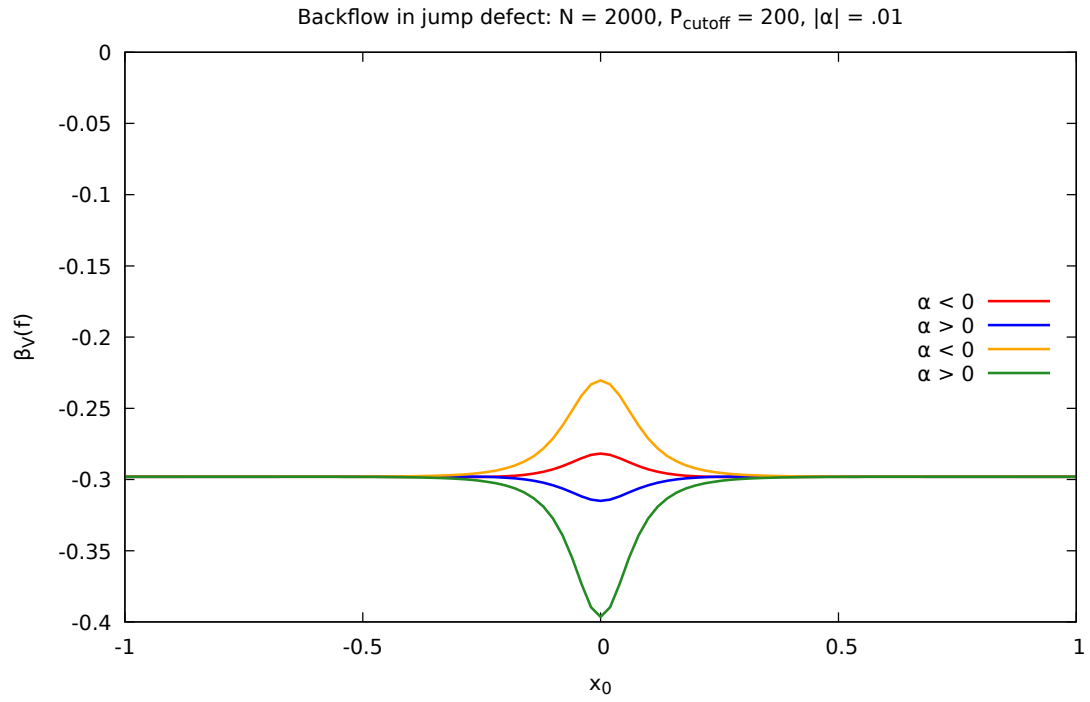

(a)

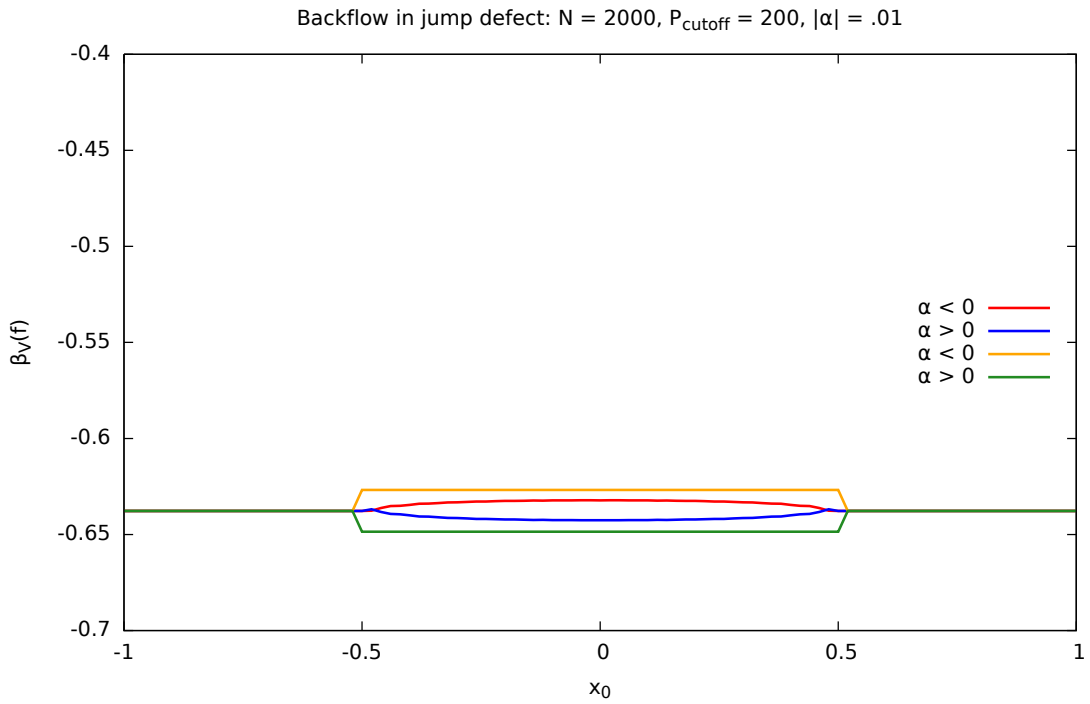

(b)

Figure B.1: Lowest backflow eigenvalue of the current operator with weight function f (a) Squared Lorentzian (b) Rectangular. **Red**/**blue** refer to the non-conserved probability current. **Yellow**/**green** refer to the conserved one.

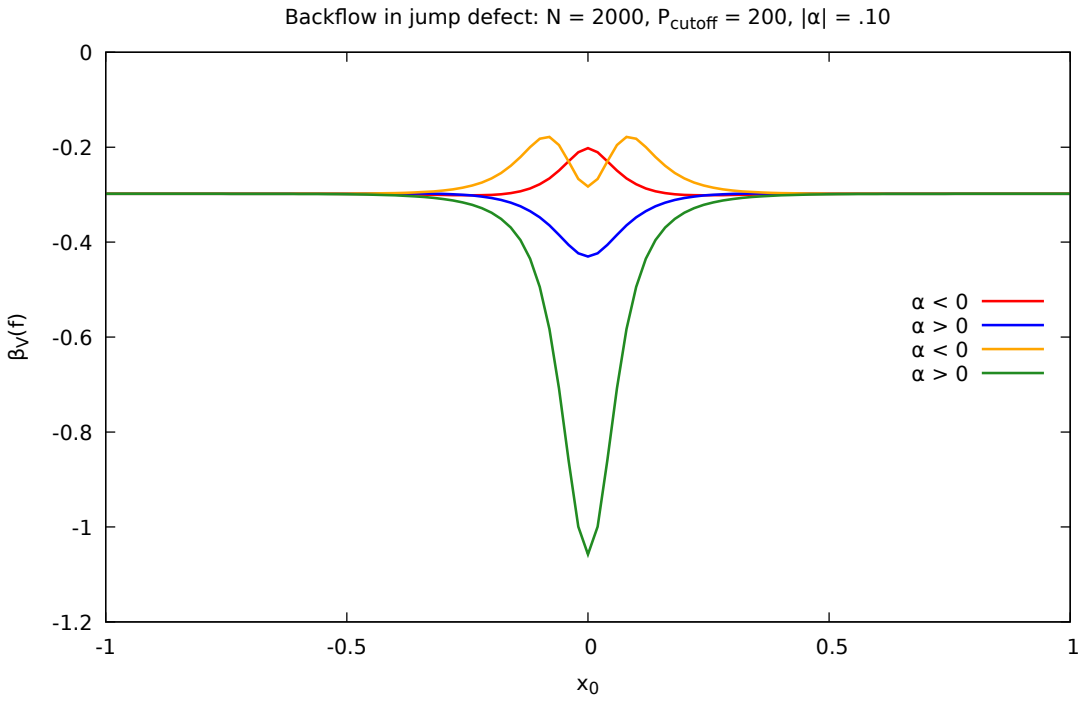

(a)

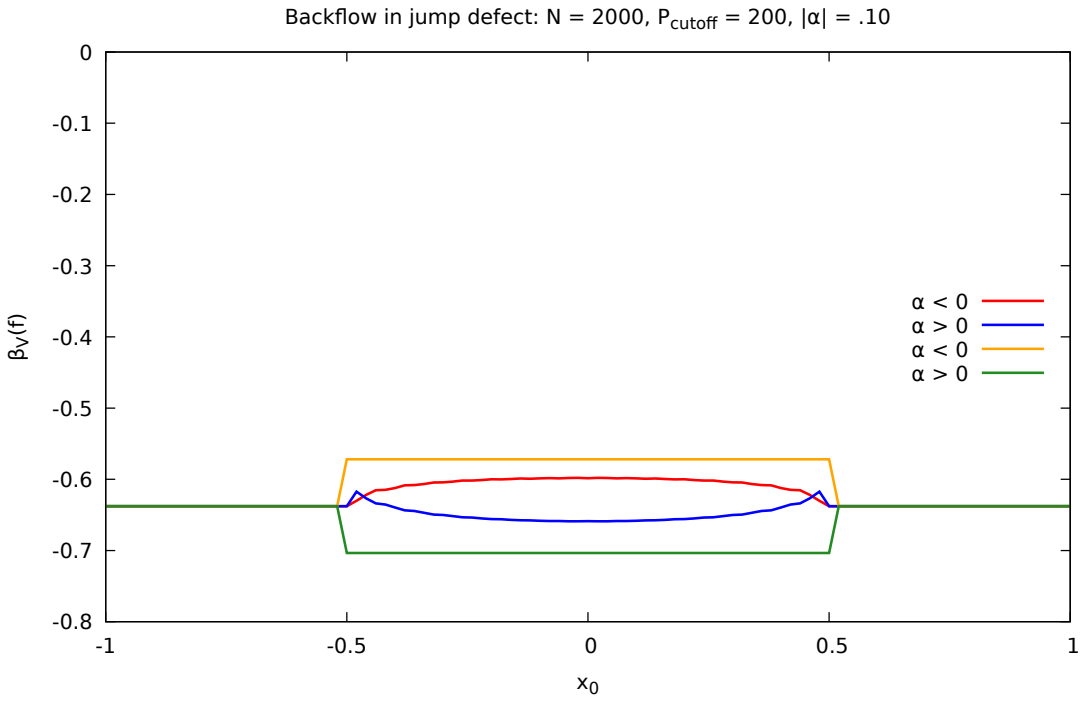

(b)

Figure B.2: Lowest backflow eigenvalue of the current operator with weight function f (a) Squared Lorentzian (b) Rectangular. **Red**/**blue** refer to the non-conserved probability current. **Yellow**/**green** refer to the conserved one.

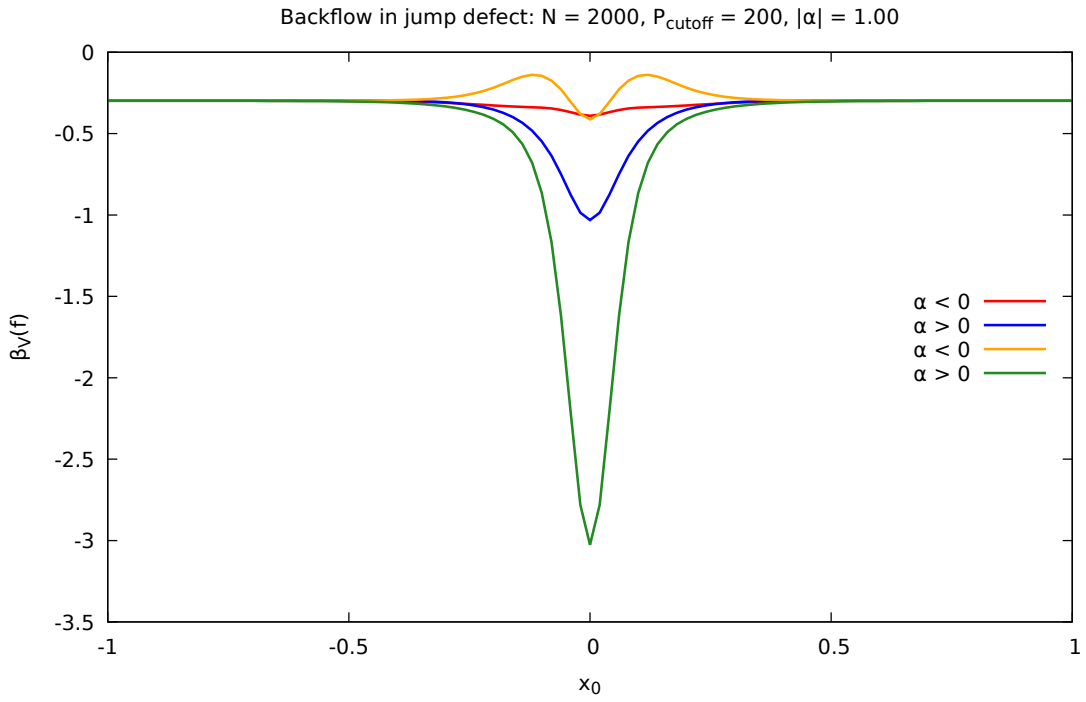

(a)

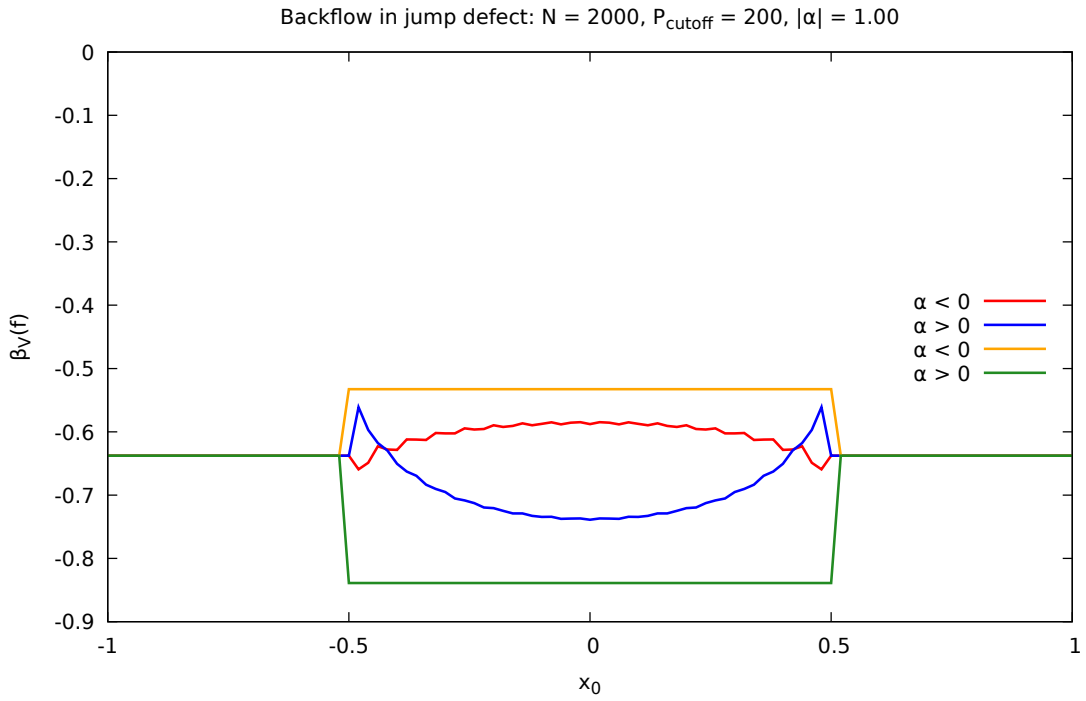

(b)

Figure B.3: Lowest backflow eigenvalue of the current operator with weight function f (a) Squared Lorentzian (b) Rectangular. **Red**/**blue** refer to the non-conserved probability current. **Yellow**/**green** refer to the conserved one.

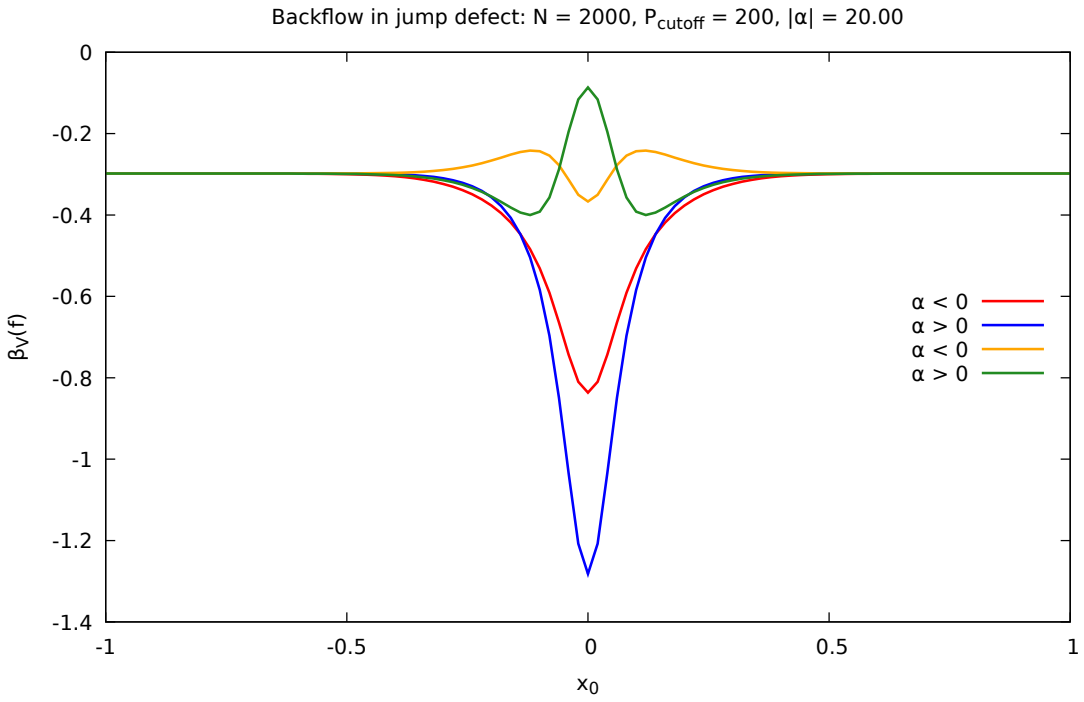

(a)

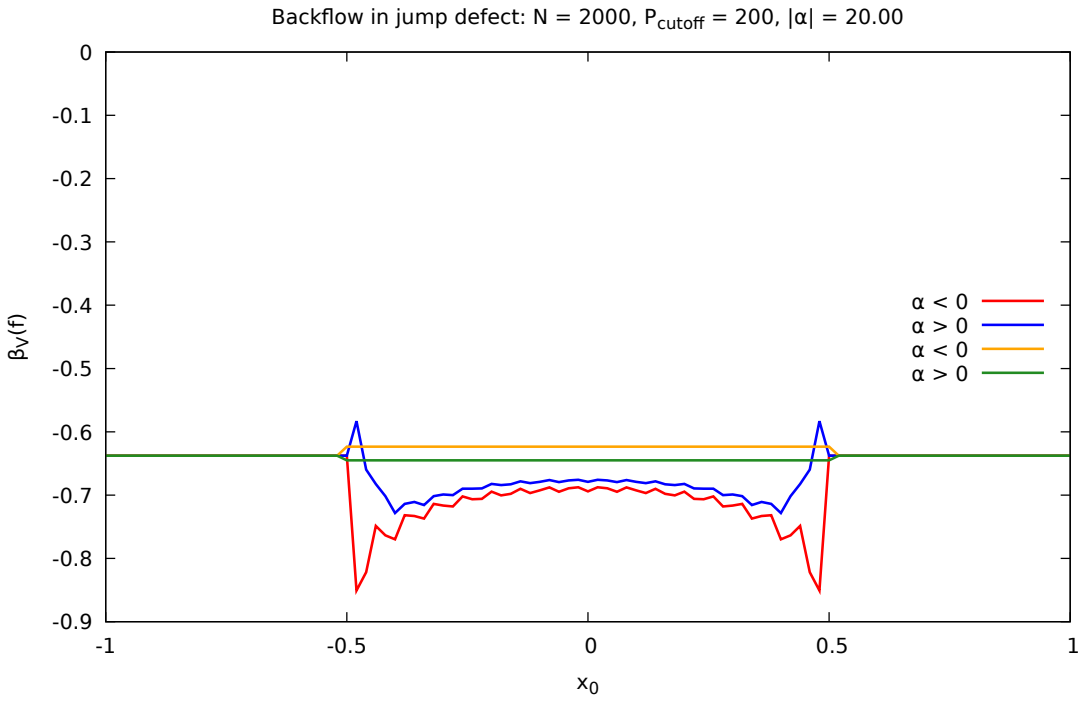

(b)

Figure B.4: Lowest backflow eigenvalue of the current operator with weight function f (a) Squared Lorentzian (b) Rectangular. **Red**/**blue** refer to the non-conserved probability current. **Yellow**/**green** refer to the conserved one.

References

[1] A. H. de Vasconcelos Jr. "Quantum backflow in the presence of a purely transmitting defect". In: *arXiv preprint arXiv:2007.07393* (2020).

[2] B. Schroer. "Localization and the interface between quantum mechanics, quantum field theory and quantum gravity I: the two antagonistic localizations and their asymptotic compatibility". In: *Studies in History and Philosophy of Science Part B: Studies in History and Philosophy of Modern Physics* 41.2 (2010), pp. 104–127.

[3] L. Ford. "Quantum coherence effects and the second law of thermodynamics". In: *Proceedings of the Royal Society of London. A. Mathematical and Physical Sciences* 364.1717 (1978), pp. 227–236.

[4] C. J. Fewster. "Lectures on quantum energy inequalities". In: *arXiv preprint arXiv:1208.5399* (2012).

[5] G. R. Allcock. "The time of arrival in quantum mechanics III. The measurement ensemble". In: *Annals of physics* 53.2 (1969), 311–348.

[6] A. Bracken and G. Melloy. "Probability backflow and a new dimensionless quantum number". In: *Journal of Physics A: Mathematical and General* 27.6 (1994), p. 2197.

[7] S. P. Eveson, C. J. Fewster, and R. Verch. "Quantum inequalities in quantum mechanics". In: *Annales Henri Poincaré*. Vol. 6. 1. Springer. 2005, pp. 1–30.

[8] M. Penz, G. Grübl, S. Kreidl, and P. Wagner. "A new approach to quantum backflow". In: *Journal of Physics A: Mathematical and General* 39.2 (2005), p. 423.

[9] H. Epstein, V. Glaser, and A. Jaffe. "Nonpositivity of the energy density in quantized field theories". In: *Il Nuovo Cimento (1955-1965)* 36.3 (1965), pp. 1016–1022.

[10] G. Melloy and A. Bracken. "Probability backflow for a Dirac particle". In: *Foundations of physics* 28.3 (1998), pp. 505–514.

[11] H. Bostelmann, D. Cadamuro, and G. Lechner. "Quantum backflow and scattering". In: *Physical Review A* 96.1 (2017), p. 012112.

[12] G. Delfino, G. Mussardo, and P. Simonetti. "Scattering theory and correlation functions in statistical models with a line of defect". In: *Nuclear Physics B* 432.3 (1994), pp. 518–550.

[13] R. Konik and A. LeClair. "Purely transmitting defect field theories". In: *Nuclear Physics B* 538.3 (1999), pp. 587–611.

[14] P. Bowcock, E. Corrigan, and C. Zambon. "Classically integrable field theories with defects". In: *International Journal of Modern Physics A* 19.supp02 (2004), pp. 82–91.

[15] P. Bowcock, E. Corrigan, and C. Zambon. "Some aspects of jump-defects in the quantum sine-Gordon model". In: *Journal of High Energy Physics* 2005.08 (2005), p. 023.

[16] G. Pöschl and E. Teller. "Bemerkungen zur Quantenmechanik des anharmonischen Oszillators". In: *Zeitschrift für Physik* 83.3-4 (1933), pp. 143–151.

[17] E. Corrigan and C. Zambon. "Integrable defects at junctions within a network". In: *Journal of Physics A: Mathematical and Theoretical* 53.48 (2020), p. 484001.

[18] R. d. L. Kronig and W. G. Penney. "Quantum mechanics of electrons in crystal lattices". In: *Proceedings of the Royal Society of London. Series A, Containing Papers of a Mathematical and Physical Character* 130.814 (1931), pp. 499–513.

[19] E. H. Lieb and W. Liniger. "Exact analysis of an interacting Bose gas. I. The general solution and the ground state". In: *Physical Review* 130.4 (1963), p. 1605.

[20] C.-N. Yang. "Some exact results for the many-body problem in one dimension with repulsive delta-function interaction". In: *Physical Review Letters* 19.23 (1967), p. 1312.

[21] I. R. Lapidus. "Resonance scattering from a double δ-function potential". In: *American Journal of Physics* 50.7 (1982), pp. 663–664.

[22] M. Takahashi. "One-dimensional electron gas with delta-function interaction at finite temperature". In: *Exactly Solvable Models Of Strongly Correlated Electrons*. World Scientific, 1994, pp. 388–406.

[23] C. J. Fewster and E. Teo. "Quantum inequalities and "quantum interest" as eigenvalue problems". In: *Physical Review D* 61.8 (2000), p. 084012.

[24] L. H. Ford and T. A. Roman. "The quantum interest conjecture". In: *Physical Review D* 60.10 (1999), p. 104018.

[25] L. Ford, A. D. Helfer, and T. A. Roman. "Spatially averaged quantum inequalities do not exist in four-dimensional spacetime". In: *Physical Review D* 66.12 (2002), p. 124012.

[26] G. Grensing. *Structural Aspects of Quantum Field Theory and Noncommutative Geometry: (In 2 Volumes)*. 2013.

[27] P. A. M. Dirac. "Bakerian lecture-the physical interpretation of quantum mechanics". In: *Proceedings of the Royal Society of London. Series A. Mathematical and Physical Sciences* 180.980 (1942), pp. 1–40.

[28] R. P. Feynman. "Negative probability". In: *Quantum implications: essays in honour of David Bohm* (1987), pp. 235–248.

[29] W. Hodge, S. Migirditch, and W. C. Kerr. "Electron spin and probability current density in quantum mechanics". In: *American Journal of Physics* 82.7 (2014), pp. 681–690.

[30] L. D. Landau and E. M. Lifshitz. *Quantum mechanics: non-relativistic theory*. Vol. 3. Elsevier, 2013.

[31] G. Melloy and A. Bracken. "The velocity of probability transport in quantum mechanics". In: *Annalen der Physik* 7.7-8 (1998), pp. 726–731.

[32] A. A. D. Villanueva. "The negative flow of probability". In: *American Journal of Physics* 88.4 (2020), pp. 325–333.

[33] A. Goussev. "Comment on "The negative flow of probability" [Am. J. Phys. 88, 325–333 (2020)]". In: *American Journal of Physics* 88.11 (2020), pp. 1023–1028.

[34] J. Yearsley, J. Halliwell, R. Hartshorn, and A. Whitby. "Analytical examples, measurement models, and classical limit of quantum backflow". In: *Physical Review A* 86.4 (2012), p. 042116.

[35] A. Goussev. "Equivalence between quantum backflow and classically forbidden probability flow in a diffraction-in-time problem". In: *Physical Review A* 99.4 (2019), p. 043626.

[36] A. Goussev. "Probability backflow for correlated quantum states". In: *Physical Review Research* 2.3 (2020), p. 033206.

[37] W. van Dijk and F. M. Toyama. "Decay of a quasistable quantum system and quantum backflow". In: *Physical Review A* 100.5 (2019), p. 052101.

[38] S. Mardonov, M. Palmero, M. Modugno, E. Y. Sherman, and J. Muga. "Interference of spin-orbit–coupled Bose-Einstein condensates". In: *EPL (Europhysics Letters)* 106.6 (2014), p. 60004.

[39] A. Goussev. "Quantum backflow in a ring". In: *Physical Review A* 103.2 (2021), p. 022217.

[40] H.-Y. Su and J.-L. Chen. "Quantum backflow in solutions to the Dirac equation of the spin-1 2 free particle". In: *Modern Physics Letters A* 33.32 (2018), p. 1850186.

[41] J. Ashfaque, J. Lynch, and P. Strange. "Relativistic quantum backflow". In: *Physica Scripta* 94.12 (2019), p. 125107.

[42] J. Halliwell, E. Gillman, O. Lennon, M. Patel, and I. Ramirez. "Quantum backflow states from eigenstates of the regularized current operator". In: *Journal of Physics A: Mathematical and Theoretical* 46.47 (2013), p. 475303.

[43] F. Albarelli, T. Guaita, and M. G. Paris. "Quantum backflow effect and nonclassicality". In: *International Journal of Quantum Information* 14.07 (2016), p. 1650032.

[44] J. Muga, J. Palao, and C. Leavens. "Arrival time distributions and perfect absorption in classical and quantum mechanics". In: *Physics Letters A* 253.1-2 (1999), pp. 21–27.

[45] J. G. Muga and C. R. Leavens. "Arrival time in quantum mechanics". In: *Physics Reports* 338.4 (2000), pp. 353–438.

[46] M. Berry. "Quantum backflow, negative kinetic energy, and optical retro propagation". In: *Journal of Physics A: Mathematical and Theoretical* 43.41 (2010), p. 415302.

[47] P. Strange. "Large quantum probability backflow and the azimuthal angle–angular momentum uncertainty relation for an electron in a constant magnetic field". In: *European journal of physics* 33.5 (2012), p. 1147.

[48] V. D. Paccoia, O. Panella, and P. Roy. "Angular momentum quantum backflow in the noncommutative plane". In: *Physical Review A* 102.6 (2020), p. 062218.

[49] Y. Eliezer, T. Zacharias, and A. Bahabad. "Observation of optical backflow". In: *Optica* 7.1 (2020), pp. 72–76.

[50] T. Kato. *Perturbation theory for linear operators*. Vol. 132. Springer Science & Business Media, 2013.

[51] M. Taylor. *Partial differential equations II: Qualitative studies of linear equations*. Vol. 116. Springer Science & Business Media, 2013.

[52] C. Fefferman and D. H. Phong. "The uncertainty principle and sharp Gårding inequalities". In: *Communications on Pure and Applied Mathematics* 34.3 (1981), pp. 285–331.

[53] C. L. Fefferman. "The uncertainty principle". In: *Bulletin (New Series) of the American Mathematical Society* 9.2 (1983), pp. 129–206.

[54] L. D. Faddeev. "Properties of the S-matrix of the one-dimensional Schrödinger equation". In: *Trudy Matematicheskogo Instituta imeni VA Steklova* 73 (1964), pp. 314–336.

[55] R. G. Newton. *Scattering theory of waves and particles*. Springer Science & Business Media, 2013.

[56] D. R. Yafaev. *Mathematical scattering theory: analytic theory*. 158. American Mathematical Soc., 2010.

[57] P. Deift and E. Trubowitz. "Inverse scattering on the line". In: (1979).

[58] M. Reed and B. Simon. *II: Fourier Analysis, Self-Adjointness*. Vol. 2. Elsevier, 1975.

[59] F. A. Berezin and L. D. Faddeev. "Remark on the Schrödinger equation with singular potential". In: *Doklady Akademii Nauk*. Vol. 137. 5. Russian Academy of Sciences. 1961, pp. 1011–1014.

[60] H. Weyl. "Über gewöhnliche Differentialgleichungen mit Singularitäten und die zugehörigen Entwicklungen willkürlicher Funktionen". In: *Mathematische Annalen* 68.2 (1910), pp. 220–269.

[61] J. v. Neumann. "Allgemeine eigenwerttheorie hermitescher funktionaloperatoren". In: *Mathematische Annalen* 102.1 (1930), pp. 49–131.

[62] M. H. Stone. *Linear transformations in Hilbert space and their applications to analysis*. Vol. 15. American Mathematical Soc., 1932.

[63] K. Friedrichs. "Spektraltheorie halbbeschränkter Operatoren und Anwendung auf die Spektralzerlegung von Differentialoperatoren". In: *Mathematische Annalen* 109.1 (1934), pp. 465–487.

[64] J. Calkin. "Abstract symmetric boundary conditions". In: *Transactions of the American Mathematical Society* 45.3 (1939), pp. 369–442.

[65] M. Krein. "The theory of self-adjoint extensions of somi-bcunded Hermitian transformations and its applications. I". In: *Matematicheskii Sbornik* 62.3 (1947), pp. 431–495.

[66] B. S. Pavlov. "Model of a zero-range potential with internal structure". In: *Teoreticheskaya i Matematicheskaya Fizika* 59.3 (1984), pp. 345–353.

[67] S. Albeverio, F. Gesztesy, R. Hoegh-Krohn, and H. Holden. *Solvable models in quantum mechanics*. Springer Science & Business Media, 2012.

[68] R. A. Adams and J. J. Fournier. *Sobolev spaces*. Elsevier, 2003.

[69] T. Cheon and T. Shigehara. "Realizing discontinuous wave functions with renormalized short-range potentials". In: *Physics Letters A* 243.3 (1998), pp. 111–116.

[70] T. Cheon and T. Shigehara. "Fermion-boson duality of one-dimensional quantum particles with generalized contact interactions". In: *Physical review letters* 82.12 (1999), p. 2536.

[71] Q.-G. Zhu and H. Kroemer. "Interface connection rules for effective-mass wave functions at an abrupt heterojunction between two different semiconductors". In: *Physical Review B* 27.6 (1983), p. 3519.

[72] V. Kulinskii and D. Y. Panchenko. "Physical structure of point-like interactions for one-dimensional Schrödinger operator and the gauge symmetry". In: *Physica B: Condensed Matter* 472 (2015), pp. 78–83.

[73] M. Gadella, Ş. Kuru, and J. Negro. "Self-adjoint Hamiltonians with a mass jump: General matching conditions". In: *Physics Letters A* 362.4 (2007), pp. 265–268.

[74] M. Gadella, F. Heras, J. Negro, and L. Nieto. "A delta well with a mass jump". In: *Journal of Physics A: Mathematical and Theoretical* 42.46 (2009), p. 465207.

[75] P. Šeba. "The generalized point interaction in one dimension". In: *Czechoslovak Journal of Physics B* 36.6 (1986), pp. 667–673.

[76] S. Albeverio, Z. Brzezniak, and L. Dabrowski. "Time-dependent propagator with point interaction". In: *Journal of Physics A: Mathematical and General* 27.14 (1994), p. 4933.

[77] P. Exner and H. Grosse. "Some properties of the one-dimensional generalized point interactions (a torso)". In: *arXiv preprint math-ph/9910029* (1999).

[78] Z. Brzezniak and B. Jefferies. "Characterization of one-dimensional point interactions for the Schrödinger operator by means of boundary conditions". In: *Journal of Physics A: Mathematical and General* 34.14 (2001), p. 2977.

[79] J. Kuhn, F. Zanetti, A. Azevedo, A. Schmidt, B. K. Cheng, and M. da Luz. "Time-dependent point interactions and infinite walls: some results for wavepacket scattering". In: *Journal of Optics B: Quantum and Semiclassical Optics* 7.3 (2005), S77.

[80] S. Albeverio, L. Dabrowski, and P. Kurasov. "Symmetries of Schrödinger operator with point interactions". In: *Letters in Mathematical Physics* 45.1 (1998), pp. 33–47.

[81] M. Carreau, E. Farhi, and S. Gutmann. "Functional integral for a free particle in a box". In: *Physical Review D* 42.4 (1990), p. 1194.

[82] P. Exner. "Lattice kronig-penney models". In: *Physical review letters* 74.18 (1995), p. 3503.

[83] L. J. Boya and E. Sudarshan. "Point interactions from flux conservation". In: *International Journal of Theoretical Physics* 35.6 (1996), pp. 1063–1068.

[84] P. Exner and P. Šeba. "A simple model of thin-film point contact in two and three dimensions". In: *Czechoslovak Journal of Physics B* 38.10 (1988), pp. 1095–1110.

[85] S. Albeverio, Z. Brzezniak, and L. Dabrowski. "Fundamental solution of the heat and Schrödinger equations with point interaction". In: *Journal of Functional Analysis* 130.1 (1995), pp. 220–254.

[86] T. Fülöp and I. Tsutsui. "A free particle on a circle with point interaction". In: *Physics Letters A* 264.5 (2000), pp. 366–374.

[87] I. Tsutsui, T. Fülöp, and T. Cheon. "Möbius structure of the spectral space of Schrödinger operators with point interaction". In: *Journal of Mathematical Physics* 42.12 (2001), pp. 5687–5697.

[88] D. R. Herschbach, J. S. Avery, and O. Goscinski. *Dimensional scaling in chemical physics*. Springer Science & Business Media, 2012.

[89] M. Bordag, D. Hennig, and D. Robaschik. "Vacuum energy in quantum field theory with external potentials concentrated on planes". In: *Journal of Physics A: Mathematical and General* 25.16 (1992), p. 4483.

[90] K. A. Milton. "Casimir energies and pressures for δ-function potentials". In: *Journal of Physics A: Mathematical and General* 37.24 (2004), p. 6391.

[91] J. M. Guilarte and J. M. Munoz-Castaneda. "Double-Delta Potentials: One Dimensional Scattering". In: *International Journal of Theoretical Physics* 50.7 (2011), pp. 2227–2241.

[92] J. M. Muñoz-Castañeda and J. M. Guilarte. "δ- δ' generalized Robin boundary conditions and quantum vacuum fluctuations". In: *Physical Review D* 91.2 (2015), p. 025028.

[93] L. M. Nieto, M. Gadella, J. Mateos-Guilarte, J. M. Munoz-Castaneda, and C. Romaniega. "Some recent results on contact or point supported potentials". In: *Geometric Methods in Physics XXXVIII*. Springer, 2020, pp. 197–219.

[94] P. Šeba. "Some remarks on the δ'-interaction in one dimension". In: *Reports on mathematical physics* 24.1 (1986), pp. 111–120.

[95] F. Gesztesy and H. Holden. "A new class of solvable models in quantum mechanics describing point interactions on the line". In: *Journal of Physics A: Mathematical and General* 20.15 (1987), p. 5157.

[96] S. Albeverio, F. Gesztesy, and H. Holden. "Comments on a recent note on the Schrödinger equation with a delta'-interaction". In: *Journal of Physics A: Mathematical and General* 26.15 (1993), p. 3903.

[97] M. Carreau. "Four-parameter point-interaction in 1D quantum systems". In: *Journal of Physics A: Mathematical and General* 26.2 (1993), p. 427.

[98] P. Kurasov. "Distribution theory for discontinuous test functions and differential operators with generalized coefficients". In: *Journal of mathematical analysis and applications* 201.1 (1996), pp. 297–323.

[99] P. Exner. "Contact interactions on graph superlattices". In: *Journal of Physics A: Mathematical and General* 29.1 (1996), p. 87.

[100] J. Behrndt, M. Langer, and V. Lotoreichik. "Schrödinger operators with δ and δ'-potentials supported on hypersurfaces". In: *Annales Henri Poincaré*. Vol. 14. 2. Springer. 2013, pp. 385–423.

[101] F. Coutinho, Y. Nogami, and J. F. Perez. "Generalized point interactions in one-dimensional quantum mechanics". In: *Journal of Physics A: Mathematical and General* 30.11 (1997), p. 3937.

[102] P. L. Christiansen, H. Arnbak, A. V. Zolotaryuk, V. Ermakov, and Y. B. Gaididei. "On the existence of resonances in the transmission probability for interactions arising from derivatives of Dirac's delta function". In: *Journal of Physics A: Mathematical and General* 36.27 (2003), p. 7589.

[103] A. Zolotaryuk, P. L. Christiansen, and S. Iermakova. "Resonant tunnelling through short-range singular potentials". In: *Journal of Physics A: Mathematical and Theoretical* 40.20 (2007), p. 5443.

[104] F. Toyama and Y. Nogami. "Transmission–reflection problem with a potential of the form of the derivative of the delta function". In: *Journal of Physics A: Mathematical and Theoretical* 40.29 (2007), F685.

[105] M. Gadella, J. Negro, and L. Nieto. "Bound states and scattering coefficients of the- aδ(x)+ bδ'(x) potential". In: *Physics Letters A* 373.15 (2009), pp. 1310–1313.

[106] A. Zolotaryuk. "Boundary conditions for the states with resonant tunnelling across the δ'-potential". In: *Physics Letters A* 374.15-16 (2010), pp. 1636–1641.

[107] Y. D. Golovaty and S. S. Man'ko. "Solvable models for the Schrödinger operators with δ'-like potentials". In: *Ukrainian Mathematical Bulletin 6 (2), 169-203; arXiv:0909.1034* (2009).

[108] Y. D. Golovaty and R. Hryniv. "On norm resolvent convergence of Schrödinger operators with δ'-like potentials". In: *Journal of Physics A: Mathematical and Theoretical* 43.15 (2010), p. 155204.

[109] A. Zolotaryuk and Y. Zolotaryuk. "A zero-thickness limit of multilayer structures: a resonant-tunnelling δ'-potential". In: *Journal of Physics A: Mathematical and Theoretical* 48.3 (2014), p. 035302.

[110] G. Delfino, G. Mussardo, and P. Simonetti. "Statistical models with a line of defect". In: *Physics Letters B* 328.1-2 (1994), pp. 123–129.

[111] M. Mintchev, E. Ragoucy, and P. Sorba. "Scattering in the presence of a reflecting and transmitting impurity". In: *Physics Letters B* 547.3-4 (2002), pp. 313–320.

[112] O. Castro-Alvaredo, A. Fring, and F. Göhmann. "On the absence of simultaneous reflection and transmission in integrable impurity systems". In: *arXiv preprint hep-th/0201142* (2002).

[113] Z. Bajnok and A. George. "From defects to boundaries". In: *International Journal of Modern Physics A* 21.05 (2006), pp. 1063–1077.

[114] E. Corrigan and C. Zambon. "Jump-defects in the nonlinear Schrödinger model and other non-relativistic field theories". In: *Nonlinearity* 19.6 (2006), p. 1447.

[115] V. Caudrelier. "On a systematic approach to defects in classical integrable field theories". In: *International Journal of Geometric Methods in Modern Physics* 5.07 (2008), pp. 1085–1108.

[116] E. Corrigan and C. Zambon. "A new class of integrable defects". In: *Journal of Physics A: Mathematical and Theoretical* 42.47 (2009), p. 475203.

[117] R. H. Goodman, P. J. Holmes, and M. I. Weinstein. "Interaction of sine-Gordon kinks with defects: phase space transport in a two-mode model". In: *Physica D: Nonlinear Phenomena* 161.1-2 (2002), pp. 21–44.

[118] E. Corrigan and C. Zambon. "Type II defects revisited". In: *Journal of High Energy Physics* 2018.9 (2018), pp. 1–23.

[119] W. J. M. Rankine. "XV. On the thermodynamic theory of waves of finite longitudinal disturbance". In: *Philosophical Transactions of the Royal Society of London* 160 (1870), pp. 277–288.

[120] N. Doughty. *Lagrangian interaction: an introduction to relativistic symmetry in electrodynamics and gravitation*. CRC Press, 2018.

[121] G. Lamb Jr. "Bäcklund transformations for certain nonlinear evolution equations". In: *Journal of Mathematical Physics* 15.12 (1974), pp. 2157–2165.

[122] K. Brownstein. "Calculation of a bound state wavefunction using free state wavefunctions only". In: *American Journal of Physics* 43.2 (1975), pp. 173–176.

[123] M. Reed and B. Simon. *III: Scattering Theory*. Vol. 3. Elsevier, 1979.

[124] S. Albeverio and P. Kurasov. *Singular perturbations of differential operators: solvable Schrödinger-type operators*. Vol. 271. Cambridge University Press, 2000.

[125] M. S. Birman and M. Z. Solomjak. *Spectral theory of self-adjoint operators in Hilbert space*. Vol. 5. Springer Science & Business Media, 2012.

[126] S. Albeverio, R. Høegh-Krohn, and L. Streit. "Energy forms, Hamiltonians, and distorted Brownian paths". In: *Journal of Mathematical Physics* 18.5 (1977), pp. 907–917.

[127] L. Streit. "Energy forms: Schrödinger theory, processes". In: *Physics reports* 77.3 (1981), pp. 363–375.

[128] S. Albeverio, F. Gesztesy, W. Karwowski, and L. Streit. "On the connection between Schrödinger and Dirichlet forms". In: *Journal of mathematical physics* 26.10 (1985), pp. 2546–2553.

[129] M. Reed. *Methods of modern mathematical physics: Functional analysis*. Elsevier, 2012.

[130] G. Bonneau, J. Faraut, and G. Valent. "Self-adjoint extensions of operators and the teaching of quantum mechanics". In: *American Journal of physics* 69.3 (2001), pp. 322–331.

[131] Y. Shikano and A. Hosoya. "Optimal covariant measurement of momentum on a half line in quantum mechanics". In: *Journal of mathematical physics* 49.5 (2008), p. 052104.

[132] R. Piessens, E. de Doncker-Kapenga, C. W. Überhuber, and D. K. Kahaner. *QUADPACK: A subroutine package for automatic integration*. Vol. 1. Springer Science & Business Media, 2012.

[133] B. T. Smith, J. M. Boyle, B. Garbow, Y. Ikebe, V. Klema, and C. Moler. *Matrix eigensystem routines-EISPACK guide*. Vol. 6. Springer, 2013.

[134] J. H. Wilkinson and C. Reinsch. *Handbook for Automatic Computation: Volume II: Linear Algebra*. Vol. 186. Springer Science & Business Media, 2012.

[135] K. O. Friedrichs. *Perturbation of spectra in Hilbert space*. Vol. 3. American Mathematical Soc., 1965.

[136] W. Thirring. *A course in mathematical physics 3: Quantum mechanics of atoms and molecules*. Springer Science & Business Media, 2013.

[137] N. Dunford and J. T. Schwartz. *Linear operators, part 1: general theory*. Vol. 10. John Wiley & Sons, 1988.

[138] M. Reed and B. Simon. *IV: Analysis of Operators*. Vol. 4. Elsevier, 1978.

[139] P. M. Morse and H. Feshbach. "Methods of theoretical physics". In: *American Journal of Physics* 22.6 (1954), pp. 410–413.

[140] A. Sommerfeld. *Partial differential equations in physics*. Academic press, 1949.

[141] J. R. Taylor. *Scattering theory: the quantum theory of nonrelativistic collisions*. Courier Corporation, 2006.

[142] A. Galindo and P. Pascual. *Quantum mechanics I*. Springer Science & Business Media, 2012.

[143] S. Weinberg. *Lectures on quantum mechanics*. Cambridge University Press, 2015.

[144] K. Friedrichs. "On the perturbation of continuous spectra". In: *Communications on Pure and Applied Mathematics* 1.4 (1948), pp. 361–406.

[145] W. H. Press, H. William, S. A. Teukolsky, W. T. Vetterling, A. Saul, and B. P. Flannery. *Numerical Recipes 3rd Edition: The Art of Scientific Computing*. Cambridge University Press, 2007.

[146] L. D. Faddeev and O. A. Yakubovskiĭ. *Lectures on quantum mechanics for mathematics students*. Vol. 47. American Mathematical Soc., 2009.

[147] B. Schumacher and M. Westmoreland. *Quantum processes systems, and information*. Cambridge University Press, 2010.

[148] K. Hirao. "Analytic derivative theory based on the Hellmann–Feynman theorem". In: *Canadian Journal of Chemistry* 70.2 (1992), pp. 434–442.

[149] F. Rellich and J. Berkowitz. *Perturbation theory of eigenvalue problems*. CRC Press, 1969.

[150] R. Subramanian and K. Bhagwat. "Relativistic generalization of the Saxon-Hutner theorem". In: *physica status solidi (b)* 48.1 (1971), pp. 399–406.

[151] M. Calkin, D. Kiang, and Y. Nogami. "Proper treatment of the delta function potential in the one-dimensional Dirac equation". In: *American Journal of Physics* 55.8 (1987), pp. 737–739.

[152] P. Sundberg and R. Jaffe. "The Casimir effect for fermions in one dimension". In: *Annals of Physics* 309.2 (2004), pp. 442–458.

[153] L. Hörmander et al. "On the theory of general partial differential operators". In: *Acta mathematica* 94 (1955), pp. 161–248.

[154] B. H. McKellar and G. Stephenson Jr. "Relativistic quarks in one-dimensional periodic structures". In: *Physical Review C* 35.6 (1987), p. 2262.

[155] F. Gesztesy and P. Šeba. "New analytically solvable models of relativistic point interactions". In: *Letters in Mathematical Physics* 13.4 (1987), pp. 345–358.

[156] E. Schrödinger. "Sitzungsber". In: *Preuss. Akad. Wiss. Phys. Math. Kl* 24 (1930), p. 418.

[157] L. Landau and R. Peierls. "Erweiterung des Unbestimmtheitsprinzips für die relativistische Quantentheorie". In: *Zeitschrift für Physik* 69.1-2 (1931), pp. 56–69.

[158] M. H. L. Pryce. "The mass-centre in the restricted theory of relativity and its connexion with the quantum theory of elementary particles". In: *Proceedings of the Royal Society of London. Series A. Mathematical and Physical Sciences* 195.1040 (1948), pp. 62–81.

[159] T. D. Newton and E. P. Wigner. "Localized states for elementary systems". In: *Reviews of Modern Physics* 21.3 (1949), p. 400.

[160] G. C. Hegerfeldt. "Remark on causality and particle localization". In: *Physical Review D* 10.10 (1974), p. 3320.

[161] J. F. Perez and I. F. Wilde. "Localization and causality in relativistic quantum mechanics". In: *Physical Review D* 16.2 (1977), p. 315.

[162] G. C. Hegerfeldt. "Instantaneous spreading and Einstein causality in quantum theory". In: *Annalen der Physik* 7.7-8 (1998), pp. 716–725.

[163] J. Mund, B. Schroer, and J. Yngvason. "String-localized quantum fields and modular localization". In: *Communications in mathematical physics* 268.3 (2006), pp. 621–672.

[164] J. Mund, B. Schroer, and J. Yngvason. "String-localized quantum fields from Wigner representations". In: *Physics Letters B* 596.1-2 (2004), pp. 156–162.

[165] A. Bracken, J. Flohr, and G. Melloy. "Time-evolution of highly localized positive-energy states of the free Dirac electron". In: *Proceedings of the Royal Society A: Mathematical, Physical and Engineering Sciences* 461.2063 (2005), pp. 3633–3645.

[166] A. Bracken and G. Melloy. "Localizing the relativistic electron". In: *Journal of Physics A: Mathematical and General* 32.34 (1999), p. 6127.

[167] G. Melloy. "The generalized representation of particle localization in quantum mechanics". In: *Foundations of Physics* 32.4 (2002), pp. 503–530.

[168] P. Busch. "Unsharp localization and causality in relativistic quantum theory". In: *Journal of Physics A: Mathematical and General* 32.37 (1999), p. 6535.

[169] P. Busch, M. Grabowski, and P. J. Lahti. *Operational quantum physics*. Vol. 31. Springer Science & Business Media, 1997.

[170] P. Busch and G. Jaeger. "Unsharp quantum reality". In: *Foundations of Physics* 40.9 (2010), pp. 1341–1367.

[171] Y. Nogami and F. Toyama. "Reflectionless potentials for the one-dimensional Dirac equation: Pseudoscalar potentials". In: *Physical Review A* 57.1 (1998), p. 93.

[172] Y. Nogami and F. Toyama. "Supersymmetry aspects of the Dirac equation in one dimension with a Lorentz scalar potential". In: *Physical Review A* 47.3 (1993), p. 1708.

[173] Y. Nogami and F. Toyama. "Transparent potential for the one-dimensional Dirac equation". In: *Physical Review A* 45.7 (1992), p. 5258.

[174] I. Kay and H. Moses. "Reflectionless transmission through dielectrics and scattering potentials". In: *Journal of Applied Physics* 27.12 (1956), pp. 1503–1508.

[175] G. V. Dunne and M. Thies. "Transparent Dirac potentials in one dimension: The time-dependent case". In: *Physical Review A* 88.6 (2013), p. 062115.

[176] J. J. Sakurai. *Advanced quantum mechanics*. Pearson Education India, 2006.

[177] A. Izergin and J. Stehr. *A Bäcklund transformation for the classical anticommuting massive Thirring model in one space dimension*. Tech. rep. Deutsches Elektronen-Synchrotron (DESY), 1976.

[178] E. R. Nissimov, N. ER, and P. SJ. "Backlund transformation in the classical massive Thirring model". In: (1979).

[179] A. R. Aguirre. "Inverse scattering approach for massive Thirring models with integrable type-II defects". In: *Journal of Physics A: Mathematical and Theoretical* 45.20 (2012), p. 205205.

[180] A. Aguirre, J. Gomes, L. Ymai, and A. H. Zimerman. "Grassmannian and bosonic Thirring models with jump defects". In: *Journal of High Energy Physics* 2011.2 (2011), pp. 1–21.

[181] J. Gomes, L. Ymai, and A. Zimerman. "Classical integrable super sinh-Gordon equation with defects". In: *Journal of Physics A: Mathematical and General* 39.23 (2006), p. 7471.

[182] A. G. Izergin and P. P. Kulish. "Massive Thirring model with field values in a Grassmann algebra". In: *Zapiski Nauchnykh Seminarov POMI* 77 (1978), pp. 76–83.

[183] M. Miller, W. C. Yuan, R. Dumke, and T. Paterek. "Experiment-friendly formulation of quantum backflow". In: *Quantum* 5 (2021), p. 379.

[184] M. A. De Gosson. *Symplectic geometry and quantum mechanics*. Vol. 166. Springer Science & Business Media, 2006.

[185] G. B. Folland. *Harmonic Analysis in Phase Space.(AM-122), Volume 122*. Princeton university press, 2016.

[186] K. Takahashi. "Wigner and Husimi functions in quantum mechanics". In: *Journal of the Physical Society of Japan* 55.3 (1986), pp. 762–779.

[187] H.-W. Lee. "Theory and application of the quantum phase-space distribution functions". In: *Physics Reports* 259.3 (1995), pp. 147–211.

[188] V. Dodonov. "'Nonclassical' states in quantum optics: a 'squeezed' review of the first 75 years". In: *Journal of Optics B: Quantum and Semiclassical Optics* 4.1 (2002), R1.

[189] M. Berry and N. Moiseyev. "Superoscillations and supershifts in phase space: Wigner and Husimi function interpretations". In: *Journal of Physics A: Mathematical and Theoretical* 47.31 (2014), p. 315203.

[190] M. Barbier and A. Goussev. "On the experiment-friendly formulation of quantum backflow". In: *arXiv preprint arXiv:2103.06728* (2021).

[191] J. Muga, S. Brouard, and D. Macias. "Time of arrival in quantum mechanics". In: *Annals of Physics* 240.2 (1995), pp. 351–366.

[192] M. Sassoli de Bianchi. "Levinson's theorem, zero-energy resonances, and time delay in one-dimensional scattering systems". In: *Journal of Mathematical Physics* 35.6 (1994), pp. 2719–2733.

[193] S. Flügge. *Practical quantum mechanics*. Springer Science & Business Media, 2012.

[194] A. Barut, A. Inomata, and R. Wilson. "Algebraic treatment of second poschl-teller, morse-rosen and eckart equations". In: *Journal of Physics A: Mathematical and General* 20.13 (1987), p. 4083.

[195] J. Diaz, J. Negro, L. Nieto, and O. Rosas-Ortiz. "The supersymmetric modified Pöschl-Teller and delta well potentials". In: *Journal of Physics A: Mathematical and General* 32.48 (1999), p. 8447.

[196] S. Albeverio, F. Gesztesy, and R. Høegh-Krohn. "The low energy expansion in nonrelativistic scattering theory". In: *Annales de l'IHP Physique théorique*. Vol. 37. 1. 1982, pp. 1–28.

[197] D. Bollé, F. Gesztesy, and S. Wilk. "A complete treatment of low-energy scattering in one dimension". In: *Journal of Operator Theory* (1985), pp. 3–32.

[198] R. G. Newton. "Low-energy scattering for medium-range potentials". In: *Journal of mathematical physics* 27.11 (1986), pp. 2720–2730.

[199] M. Klaus. "Low-energy behaviour of the scattering matrix for the Schrödinger equation on the line". In: *Inverse Problems* 4.2 (1988), p. 505.

[200] T. Aktosun and M. Klaus. "Small-energy asymptotics for the Schrödinger equation on the line". In: *Inverse problems* 17.4 (2001), p. 619.

[201] F. Loran and A. Mostafazadeh. "Dynamical formulation of low-energy scattering in one dimension". In: *Journal of Mathematical Physics* 62.4 (2021), p. 042103.

[202] P. J. McCarthy. "Some linear Bäcklund transformations". In: *Letters in Mathematical Physics* 4.1 (1980), pp. 39–43.

[203] B. Schumacher, M. D. Westmoreland, A. New, and H. Qiao. "Probability current and thermodynamics of open quantum systems". In: *arXiv preprint arXiv:1607.01331* (2016).

[204] S. T. Mister, B. J. Arayathel, and A. J. Short. "Local probability conservation in discrete-time quantum walks". In: *Physical Review A* 103.4 (2021), p. 042220.

[205] M. Palmero, E. Torrontegui, J. G. Muga, and M. Modugno. "Detecting quantum backflow by the density of a Bose-Einstein condensate". In: *Physical Review A* 87.5 (2013), p. 053618.

[206] C. S. Gardner, J. M. Greene, M. D. Kruskal, and R. M. Miura. "Method for solving the Korteweg-deVries equation". In: *Physical review letters* 19.19 (1967), p. 1095.

[207] G. L. Lamb Jr. "Elements of soliton theory". In: *New York* (1980), p. 29.

[208] J. Lekner. "Critical binding of diatomic molecules". In: *Molecular Physics* 23.3 (1972), pp. 619–625.

[209] J. Lekner. "Reflectionless eigenstates of the sech 2 potential". In: *American Journal of Physics* 75.12 (2007), pp. 1151–1157.

[210] Y. Alhassid, F. Gürsey, and F. Iachello. "Potential scattering, transfer matrix, and group theory". In: *Physical Review Letters* 50.12 (1983), p. 873.

[211] G. Russakoff. "A derivation of the macroscopic Maxwell equations". In: *American Journal of Physics* 38.10 (1970), pp. 1188–1195.